PHARMACOGENOMICS OF *ABCB1* IN MAINTENANCE PHARMACOTHERAPIES FOR OPIOID DEPENDENCE

Daniel T Barratt BSc (Hons)

Discipline of Pharmacology

School of Medical Sciences, Faculty of Health Sciences

University of Adelaide

August, 2010

A thesis submitted for the degree of Doctor of Philosophy

Table of contents

List of in-text tables

List of in-text figures

Abstract

Opioid dependence is a significant public health problem. Whilst long-term opioid maintenance is the most cost-effective approach for treating opioid dependence, the safe and effective use of substitution opioids like methadone and buprenorphine is complicated by their narrow therapeutic indices and a considerable, as yet unexplained, interindividual variability in their dose-effect relationships. Since there is evidence that the P-glycoprotein efflux transporter may influence the plasma pharmacokinetics and CNS distribution of opioids, it was hypothesised that genetic variability in the *ABCB1* gene (encoding P-glycoprotein) could play a major role in the interindividual variability in opioid maintenance treatment response. Therefore, the primary aim of this thesis was to investigate *ABCB1* genetic variability as a determinant of opioid requirements during maintenance therapy, as well as treatment outcome. This thesis also set out to identify the relationship between *ABCB1* genetic variability and the risk of illicit opioid use and dependence, as well as develop new methods for investigating the dynamic interactions between *ABCB1* genetic variability, P-glycoprotein expression/function and opioid exposure.

For the first major study of this thesis, opioid-dependent methadone maintenance treatment (MMT, n = 78) and buprenorphine maintenance treatment (BMT, n = 30) subjects, as well as non-opioid-dependent healthy controls (n = 98), were retrospectively genotyped and haplotyped for 5 common single nucleotide polymorphisms (SNPs) of *ABCB1* (A61G, G1199A, C1236T, G2677T and C3435T). Whilst no link was observed between *ABCB1* genetic variability and the risk of opioid dependence, the wild-type AGCGC (61A-1199G-1236C-2677G-3435C) haplotype was associated with significantly higher maintenance opioid requirements among both MMT and BMT subjects. In addition, MMT subjects carrying one of the variant haplotypes, AGCTT, required significantly less methadone, presumably due to a decreased P-gp activity at the blood-brain-barrier. Interestingly, a second retrospective study of a specific cohort of 21 (very) high-dose (≥180 mg/day) MMT subjects could not replicate

these findings, suggesting that dose range and/or clinic policy may be important factors influencing the clinical significance of *ABCB1* genetic variability.

The third major study of this thesis incorporated the development and validation of new methods for quantifying *ex vivo* P-glycoprotein expression (mRNA and protein) and function in specific lymphocyte subsets ($CD4^+$, $CD56^+$ and $CD8^+$) of healthy and opioid-dependent subjects, with the aim of determining the combined effects of *ABCB1* genetic variability and opioid exposure on P-glycoprotein function. Applying these new methods in a pilot study of 6 MMT subjects, $CD4^+$ lymphocyte *ABCB1* mRNA and P-glycoprotein expression were found to be positively associated with methadone requirements, and were lowest in the only subject homozygous for the AGCTT haplotype (providing potential mechanistic support for the link between AGCTT haplotypes and low MMT dose requirements).

Therefore, this thesis provides the first evidence that *ABCB1* haplotypes contribute to variability in substitution opioid requirements. However, *ABCB1* genetic variability should not be considered alone, and a combined interpretation of multiple genetic and environmental factors will be required to provide a more complete picture of the factors governing the successful treatment of opioid dependence.

Declaration

This work contains no material which has been accepted for the award of any other degree or diploma in any University or other tertiary institution and, to the best of my knowledge and belief, contains no material previously published or written by another person, except where due reference has been made in the text.

I give consent to this copy of my thesis, when deposited in the University Library, being made available for loan and photocopying, subject to the provisions of the Copyright Act 1968.

The author acknowledges that copyright of the published work contained within this thesis (Coller JK, Barratt DT, Dahlen K, Loennechen MH, Somogyi AA. (2006) *ABCB1* genetic variability and methadone dosage requirements in opioid-dependent individuals. *Clinical Pharmacology and Therapeutics* **80**:682-90) resides with the copyright holder of this work (see Appendix D, page 321).

I also give permission for the digital version of my thesis to be made available on the web, via the University's digital research repository, the Library catalogue, the Australian Digital Theses Program (ADTP) and also through web search engines, unless permission has been granted by the University to restrict access for a period of time.

Daniel T Barratt

18 August 2010

Acknowledgements

I would sincerely like to thank my supervisors, Professor Andrew Somogyi and Dr Janet Coller, for introducing me to the world of pharmacogenetics as an honours student, and then giving me the opportunity to pursue my newfound passion through this PhD. Your ongoing guidance and encouragement, in and out of the lab, has proved instrumental in my development as both a researcher and a member of the greater pharmacogenetics/genomics community. I greatly appreciate all that you have done for me over the years.

The research presented in this thesis would also not have been possible without funding from the University of Adelaide Faculty of Health Sciences, and a National Health and Medical Research Council of Australia (NHMRC) project grant, as well as financial assistance from a Faculty of Health Sciences (University of Adelaide) / Royal Adelaide Hospital, Institute of Medical and Veterinary Sciences Dawes Divisional Scholarship, and a NHMRC Postgraduate Research Scholarship. I am also extremely grateful for the many travel grants provided by the Australasian Society of Clinical and Experimental Pharmacologists and Toxicologists, as well as a Faculty of Health Sciences (University of Adelaide) Postgraduate travel grant, that, along with the financial support and encouragement from my supervisors, have allowed me to attend and present my research at numerous national and international conferences.

I would also like to acknowledge the work of the following people: Janet Coller, Karianne Dahlen and Morten Loennechen for their work with the *ABCB1* genotyping assays; all those involved in the original clinical studies from which I drew my subjects, in particular Prof Jason White, Peter Athanasos, Andrea Gordon, Richard Hallinan, Justin Hay, Sophie La Vincente, and Erin Morton; Aaron Farquharson for his assistance in obtaining subject samples for the *ex vivo* pilot study; Tanya Lewanowitsch for her generous support and advice with Western blotting; David Foster for his assistance with methadone LCMS detection and his work with Pop-PK analysis; and Andrew Menelaou and Glynn Morrish for their guidance with buprenorphine HPLC assay development. Thanks also to Karen Nunes-Vaz and Gordon

Crabb for their administrative support, as well as other past and present members of the Discipline of Pharmacology, particularly the “Bach Pad” and “Green Room”, whose support and friendship have helped me in many, often less tangible, ways.

To my family, thankyou for your unwavering moral, financial and dietary support that has provided me with a stable foundation from which to conduct my postgraduate studies. Thanks also to the Nicholls family for their constant offers of encouragement, meals and weekends at Tiddy Widdy, which have provided welcome stress relief for both me and Amy.

To the Marryatville boys, thankyou for your unwavering support of fishing, surfing, camping, drinking and numerous other activities aimed at preventing me completing my thesis, but all of which have helped keep me sane.

To Amy, thankyou for your patience, sacrifice, love and understanding. You have been with me every step of the way, and have shared many of the highs and all of the lows, and for that I am forever grateful. At last we can look forward to sharing a new and exciting chapter in our lives together.

Publications in support of this thesis

Original research

Coller JK, Barratt DT, Dahlen K, Loennechen MH, Somogyi AA. (2006) *ABCB1* genetic variability and methadone dosage requirements in opioid-dependent individuals. *Clin Pharmacol Ther* **80**:682-90.

Invited review

Somogyi AA, Barratt DT, Coller JK. (2007) Pharmacogenetics of opioids. *Clin Pharmacol Ther* **81**:429-444.

6-MAM	6-monoacetylmorphine
A>B	Apical-to-basal permeability
A_{260}	Absorbance at 260 nm
A_{280}	Absorbance at 280 nm
AAG	α_1-acid glycoprotein
AUC	Area under the concentration-time curve
B>A	Basal-to-apical permeability
BBB	Blood-brain-barrier
BCA	Bicinchoninic acid
BMT	Buprenorphine maintenance treatment
bp	Base pairs
BSA	Bovine serum albumin
cDNA	Complementary DNA
CI	Confidence interval
CL/F	Oral clearance
CL_R	Renal clearance
C_{max}	Maximum plasma concentration
CNS	Central nervous system
CSF	Cerebrospinal fluid
C_{trough}	Trough plasma concentration
C_{trough}/dose	Dose-adjusted trough plasma concentration
CV	Coefficient of variation
DADLE	[D-Ala^2,D-Leu^5]-enkephalin
DAMGO	[D-Ala^2,N-Me-Phe^4,Gly^5-ol]-enkephalin
DMSO	Dimethylsulfoxide
DNA	Deoxyribonucleic acid
dNTP	Deoxynucleoside triphosphate
DPDE	[D-$Pen^{2,5}$]-enkephalin
DPM	Disintegrations per minute
EDTA	Ethylenediaminetetraacetic acid
FCS	Fetal bovine serum
HBSS	Hank's buffered salt solution
HD	High dose
HPLC	High performance liquid chromatography
IC_{50}	50% inhibitory concentration
IDRS	Australian Illicit Drug Reporting System
IDU	Injecting drug users
kb	kilobases
LAAM	Levo-alpha-acetyl-methadol
LD	Linkage disequilibrium
M-6-G	Morphine-6-glucuronide

MEM	Minimal essential medium with Earl's salts
MMT	Methadone maintenance treatment
mRNA	Messenger RNA
NBD	Nucleotide binding domain
ND	Normal dose
OR	Odds Ratio
P_{app}	Apparent permeability
PBMC	Peripheral blood mononuclear cell
PCR	Polymerase chain reaction
PCR-RFLP	PCR - restriction fragment length polymorphism
P-gp	P-glycoprotein
PK/PD	Pharmacokinetic/pharmacodynamic
Pop-PK	Population-pharmacokinetic
qRT-PCR	Quantitative real time - PCR
RNA	Ribonucleic acid
SD	Standard deviation
SDS-PAGE	Sodium dodecyl sulphate – polyacrylamide gel electrophoresis
SNP	Single nucleotide polymorphism
$T_{1/2}$	Half-life
TDM	Therapeutic drug monitoring
TEER	Transepithelial electrical resistance
T_{max}	Time to maximum plasma concentration
TMD	Transmembrane domain
V	Variant allele or digest fragment
V_d	Volume of distribution
Wt	Wild-type allele or digest fragment

Chapter 1. Introduction

For thousands of years the use of opiates for analgesia has gone hand in hand with their abuse as euphoric agents. Today, opioid abuse remains a significant public health problem. As such, as an adjunct to government control of narcotics and policing of illicit opioid trafficking, numerous treatment strategies have been put in place to aid addicts in their abstinence and recovery from illicit opioid abuse.

So far, substitution therapies aimed at long-term maintenance with prescribed opioids, such as methadone and buprenorphine, have proven to be the most cost effective treatments for opioid dependence. However, despite their success, their safe and effective implementation is often complicated by a combination of the narrow therapeutic indices of substitution opioids, and significant interindividual variability in opioid response. As a result, attrition rates from maintenance therapies remain disturbingly high. Therefore, a better understanding of the factors underlying individuals' responses to opioids, and hence their treatment outcomes, is vitally important.

The P-glycoprotein efflux transporter has the potential to influence the intestinal absorption, tissue distribution and elimination of a broad range of substrates, including opioids such as methadone. As such, the polymorphic *ABCB1* gene, encoding P-gp, provides an attractive potential source of variable opioid response.

Before outlining the aims and hypotheses of the thesis, this introduction will explain why opioids continue to be used and abused, why opioid abuse represents a significant social burden, and thus why we require effective treatments for opioid dependence. Furthermore, background will be given as to the effectiveness and the failures of current opioid substitution treatments, and the potential role of pharmacogenetics in improving treatment individualisation. Finally, it will discuss why *ABCB1* genetic variability is a factor worth considering for the individualisation of opioid dosing based on a patient's genetic makeup.

1.1. Opioid pharmacology

At least since the Sumerian cultivation of the opium poppy as *Hul Gil* (the "joy plant") around 3400 BC, and the Egyptian papyrus records of opium use for pain relief, opioids in their various forms, ranging from basic poppy seed extracts to fully synthetic compounds, have continued to be used and abused.

The term opioid refers to all compounds, natural or synthetic, that exhibit morphine-like activity via opioid receptors. The original opioids consisted of alkaloid compounds, such as morphine, isolated from the opium poppy (*Papaver somniferum*). However, numerous partially and fully synthetic opioids have also been developed. Today opioids are categorized into 3 major groups based on their chemical structure: (1) Phenanthrenes, which are the "classical" opioids possessing the 4,5-epoxymorphinan ring structure (these include opiates such as morphine and heroin, as well as synthetic opioids like buprenorphine and naloxone); (2) Piperidines and phenylpiperidines, such as loperamide and fentanyl; and (3) Diphenylheptylamines, such as methadone. Two other compounds, pentazocine and tramadol, do not fit into any of these standard opioid classes but are still agonists at opioid receptors, and are therefore still classified as opioids (Rang et al., 2003).

1.1.1. Mechanisms of action

The pharmacological effects of all opioid drugs are mediated via opioid receptors. These G-protein coupled receptors are found both pre- and post-synaptically, and directly inhibit cell signalling by reducing both neuronal excitability and neurotransmitter release. Located in various regions of the central nervous system (CNS), and to a lesser extent in the periphery, they have been well characterized as playing roles in antinociception, sedation and drug reward (Mansour et al., 1987; Hawkins et al., 1988; Dhawan et al., 1996; Kitchen et al., 1997). Opioid receptors in the brain are responsible for the analgesia, euphoria (or dysphoria), sedation, respiratory depression, and decreased gastrointestinal motility, commonly associated

with opioid compounds, whilst pre-synaptic opioid receptors on primary afferents located in the dorsal horn of the spinal cord may also mediate analgesia (Besse et al., 1990; Rang et al., 1999). There is some evidence that enteric opioid receptors may also influence gut motility (Sternini, 2001).

Of the three opioid receptor subtypes (mu, delta and kappa) that have been identified in humans, the mu-opioid receptor is the best characterised, and provides the primary target of most opioid therapeutics (Dhawan et al., 1996). The opioids most relevant to this thesis are all primarily mu-opioid receptor agonists, hence they exhibit typical opioid effects such as analgesia and euphoria, as well as common side effects such as constipation, nausea, sedation and respiratory depression.

1.1.1.1. Opioid analgesia

Our current understanding of the opioid pathways involved in pain perception and analgesia are complex and expansive. For the purpose of an introduction to this thesis, which is primarily concerned with the rewarding and addictive properties of opioids, it is sufficient to describe the mechanism of opioid analgesia simply as a direct or indirect inhibition of the nociceptive signalling involved in the perception of pain.

1.1.1.2. Opioid reward

It has long been established that acute administration of many drugs of abuse to animals increases extracellular levels of dopamine in the nucleus accumbens (Pontieri et al., 1995) leading to an activation of the brain limbic system, an area synonymous with emotion, motivation and reward (Koob, 2005). Indeed, this has been demonstrated for heroin, morphine and methadone (Di Chiara & Imperato, 1988; Tanda et al., 1997). Specifically, mu-opioid receptors have been located pre-synaptically on the GABA neurons that tonically inhibit ventral tegmental area dopaminergic neurons extending to the reward centres of the brain (Kreek, 1996). Therefore, mu-opioid receptor activation, by inhibiting GABA signalling,

disinhibits dopaminergic neurons and increases dopamine release in areas such as the nucleus accumbens (Johnson & North, 1992), leading to sensations of reward and euphoria.

In addition to the ventral tegmental area, opioid actions directly at the nucleus accumbens shell (Olds, 1982), lateral hypothalamus (Britt & Wise, 1981), hippocampus (Stevens et al., 1991), and periaqueductal grey (van der Kooy et al., 1982; Corrigall & Vaccarino, 1988) have all also been implicated in opioid reward. Endogenous opioid peptides (see section 1.1.2) and the endocannabinoid system are also thought to be involved in the reinforcing effects of opioids (Koob, 2005), whilst recent studies have indicated that CNS immune cells (glia) may also modulate the rewarding response to opioid drugs (Hutchinson et al., 2007). Therefore, multiple pathways are involved in the modulation of opioid reward and euphoria.

1.1.1.3. Side effects

In addition to the 'desired' effects of opioids, there are a number of adverse effects commonly associated with opioid use. The most common of these is constipation which occurs in around 40 to 95% people receiving opioids, and is believed to be both centrally and peripherally mediated (see above) (Swegle & Logemann, 2006). Other adverse opioid effects that occur with varying frequency include sedation, nausea and vomiting.

A less common but nonetheless important adverse effect is opioid-induced respiratory depression, which is a slowing and irregularity of breathing, resulting in potentially fatal hypercapnia and hypoxia. Whilst a number of mechanisms behind opioid-induced respiratory depression have been proposed, abundant opioid receptors located in the respiratory control centres, in particular the brainstem, appear the most likely effector sites (White & Irvine, 1999; Pattinson, 2008). Although relatively rare in the clinical population, severe opioid-induced respiratory depression is the major cause of death from overdose among opioid addicts (White & Irvine, 1999).

1.1.2. Endogenous opioids

The endogenous ligands for opioid receptors are opioid peptides enzymatically cleaved from three precursor proteins: preproopiomelanocortin, preproenkephalin, and preprodynorphin. The best characterised of the endogenous opioid peptides are β-endorphin (mu = delta = kappa agonist), leu-enkephalin (delta >> mu agonist), met-enkephalin (delta > mu agonist), and dynorphin (kappa > mu > delta agonist). Produced by both neuronal and non-neuronal cells, they are widely distributed in the brain and spinal cord, exhibiting similar opioid actions to their exogenous counterparts (Rang et al., 1999). As such, the opioid neuropeptide system can act as an endogenous mediator of pain response and reward. However, the exact role for endogenous opioids in reward and addiction still remains unclear (Roth-Deri et al., 2008).

1.1.3. Therapeutic use of opioids

At present, opioids are used commonly for the treatment of mild to severe cancer pain, chronic non-cancer pain and post-surgical acute pain. However, more relevant in the context of the following studies is the use of opioids for the treatment of opioid dependence. Both methadone and buprenorphine are currently used in Australia in what is referred to as substitution or maintenance treatment, which is discussed in greater detail in section 1.3. Opioid antagonists such as naloxone and naltrexone are also used therapeutically to block the rewarding effects of any relapse to illicit opioid use following opioid detoxification, whilst intravenous naloxone is used to reverse the respiratory depression caused by opioid overdose. Peripherally acting opioids, such as loperamide, are also used clinically, and are employed to treat diarrhoea, exploiting peripheral opioid-induced constipation, whilst avoiding the risk of other centrally mediated side effects.

1.1.4. Illicit opioid use

Heroin (diacetylmorphine or diamorphine) is the drug most often associated with illicit opioid abuse. It is a particularly effective euphoric agent due to its rapid onset of action, and is most

often taken intravenously (however heroin smoking and intranasal administration are also common). Whilst the lipophilicity of heroin allows it rapid entry across the blood-brain-barrier (BBB) into the CNS (Oldendorf et al., 1972), it is rapidly metabolized in both the blood and in tissues, and has a relatively low mu-opioid receptor affinity compared to its metabolites. As such, it can essentially be considered a pro-drug, with its major opioid-active metabolites, 6-monoacetylmorphine (6-MAM) and (to a lesser extent) morphine, being responsible for its euphoric effects (see section 1.4.1).

Unfortunately, opioids intended for therapeutic use (including both pain and maintenance treatment medications) are often also abused for their euphoric and sedative effects. This abuse of prescription opioids can range from the overuse of medications by pain patients, to the illicit diversion, fraudulent acquisition, theft or trafficking of prescribed opioid medications (Darke et al., 1996; Lintzeris et al., 1999; Darke et al., 2002; Jenkinson et al., 2005; Degenhardt et al., 2006; Stafford & Burns, 2009).

1.1.5. Summary

Opioid actions at CNS mu-opioid receptors drive both their primary clinical use as analgesics, as well as their abuse as euphoric agents. Heroin, acting through its mu-opioid active metabolites 6-MAM and morphine, is the opioid most commonly identified with illicit opioid abuse, whilst prescription opioid misuse is also observed and is gaining increased recognition.

1.2. Opioid dependence

1.2.1. The path to opioid addiction

The American Psychological Association's Diagnostic and Statistical Manual of Mental Disorders (DSM-IV) defines substance dependence as three or more of the following symptoms or behaviours – tolerance; withdrawal; usage of large amounts over a long period;

unsuccessful attempts to reduce use; time spent obtaining the substance replacing social, occupational or recreational activities; and continued drug use despite adverse consequences.

To understand the difficulties faced when attempting to manage and treat opioid dependence and addiction, it is important to clarify both the physiological and psychological changes that occur with chronic opioid abuse. As discussed in section 1.1.1.2, most opioids have the potential to produce at least mild sensations of reward and euphoria, depending on the opioid, dose and route of administration. It is this reward and euphoria that can provide the major drive for continuation of illicit opioid use beyond experimentation, or prescription opioid use beyond therapeutic requirements. This continued abuse and opioid exposure will typically result in cellular and physiological changes manifesting as symptoms of tolerance, dependence and withdrawal (Way et al., 1969; Kreek, 1996; Kreek, 1997).

1.2.1.1. Opioid tolerance

Opioid tolerance is a common complication of most opioid treatments, and is defined as a loss of drug potency over time resulting in ever-increasing dose requirements to maintain treatment effectiveness. The two major facets of this phenomenon are pharmacokinetic tolerance and pharmacodynamic tolerance.

The theory of pharmacokinetic tolerance is derived from the proposed upregulation of drug metabolism or transport in response to single or repeated opioid administration. By decreasing bioavailability and/or increasing drug clearance, these changes could decrease the systemic and/or CNS drug exposure for a given dose, leading to increased dose requirements. Whilst there is little evidence for the induction of metabolising enzymes with chronic opioid treatment, some opioid effects on drug transporter expression have been identified, and are discussed in section 1.5.4.1.

Pharmacodynamic tolerance relates to alterations in receptor availability and activation, as well as changes in the descending signalling pathways, resulting in decreased drug efficacy. The proposed mechanisms behind pharmacodynamic opioid tolerance include alterations in opioid receptor density, desensitisation, and/or (re)cycling (Chang et al., 2007; DuPen et al., 2007). There is also evidence that increased activity of sensory neuropeptides and their downstream signalling messengers at the spinal level, as well as a decrease in brain dopamine D_2 receptors, may also be important in the development of opioid tolerance (Volkow et al., 2003; Trang et al., 2005). Similarly, dysregulation of opioid peptide transduction and GABAergic systems has also been reported with chronic administration of drugs of abuse (Kreek & Koob, 1998). Therefore there is evidence that tolerance to both the analgesic and the rewarding effects of opioids can occur.

In addition to these 'classical' theories of opioid tolerance, increased glial activation with chronic opioid use, resulting in increased release of pronociceptive inflammatory cytokines, now also appears to play some role in the development of opioid tolerance (Hutchinson et al., 2007). Whatever the mechanisms, antinociceptive tolerance provides a significant barrier to the long-term efficacy of opioids for analgesia, whilst tolerance to opioid reward can provide the basis for escalating drug use leading to severe opioid dependence.

1.2.1.2. Physical dependence and withdrawal

Physical opioid dependence, as a result of physiological changes resulting from repeated exposure to opioids, is revealed by a withdrawal syndrome upon cessation of opioid use or the administration of an opioid antagonist. The typical opioid withdrawal symptoms are non-fatal, but can include anxiety, muscle and bone ache, muscle cramps, sleep disturbance, sweating, hot and cold flushes, piloerection, yawning, lacrimation, rhinorrhea, abdominal cramps, nausea, vomiting, diarrhoea, palpitations, elevated blood pressure, elevated pulse, and dilated pupils. Most of these acute withdrawal symptoms have been attributed to homeostatic

changes in neurotransmitter systems (e.g. noradrenaline, dopamine, opioid peptides, serotonin and GABA), as well as brain stress system components (e.g. corticotrophin-releasing factor), as a result of chronic opioid activation/inhibition (Redmond & Krystal, 1984; Heinrichs et al., 1995; Maldonado, 1997; Kreek & Koob, 1998). However, more recently, glia have been implicated in the development of opioid dependence and withdrawal in animals, with inhibition of opioid glial activation found to significantly attenuate opioid withdrawal symptoms (Hutchinson et al., 2007).

Among regular heroin users, withdrawal symptoms generally peak around 2-4 days post-abstinence, with obvious physical signs of withdrawal lasting up to 7 days. It is this sometimes severe abstinence withdrawal syndrome that is one of the major barriers to the cessation of opioid abuse, at least in the initial stages of abstinence.

1.2.1.3. Psychological dependence, craving and relapse

Whilst the physiological manifestations of opioid withdrawal can largely revert back to normal within days or weeks of opioid cessation, these acute withdrawal symptoms are typically followed by a protracted withdrawal syndrome characterised by general feelings of reduced well-being and periodical drug craving (Henry-Edwards et al., 2003). This psychological dimension of opioid addiction is far more insidious, with effects lasting for years after abstinence. Typically revealed as continued drug craving following prolonged abstinence from opioids, this psychological addiction can manifest as a residual state of anxiety and dysphoria, or can be induced by stress or specific stimuli including certain environments, people or situations previously associated with drug use (Koob, 2005).

The mechanisms behind drug craving and relapse following protracted abstinence are complex. However, it has been proposed that, in an attempt to maintain a constant hedonic state during chronic opioid challenge, normal brain homeostasis is abandoned in favour of a new allostatic state. Consequently, there is a persistent deviation from normal brain reward

threshold regulation (Koob, 2005), which can also reduce the saliency of natural rewards. It is this complex psychological component to opioid dependence and addiction that is most often responsible for relapse to drug use following protracted abstinence from opioids.

1.2.1.4. Summary

A distinct path from opioid exposure to severe opioid dependence can be identified. Starting with initial exposure to opioids and potential sensations of euphoria, and transitioning into continued opioid abuse, physiological and psychological changes that occur with chronic opioid exposure can manifest as a syndrome of tolerance, physical dependence and severe psychological addiction.

1.2.2. Burden of opioid dependence

1.2.2.1. Prevalence and demographics of opioid dependence

Globally, it is estimated that approximately 16.5 million people abuse illicit opioids (UNODC, 2008), whilst in Australia, 0.2% of the population older than 14 are believed to be regular opiate users (AIHW, 2007). Similar to the United Kingdom and United States of America, the majority of opioid-dependent Australians are male and unemployed, with long histories of heroin and other drug use (Craddock et al., 1997; Mattick et al., 2001), and whilst the vast majority are injecting users, a surprising new trend has been the increase in heroin smokers (now 1 in 10 of all opioid abusers seeking treatment) (Darke et al., 2004).

As mentioned earlier, prescription opioid injectors form a significant fraction of the overall opioid misusing population. In Australia, almost half (42%) of injecting drug users (IDU) surveyed by the Australian Illicit Drug Reporting System (IDRS) reported illicit morphine use in 2009, the majority of whom took the drug intravenously. The abuse of opioid analgesics other than morphine has also been reported, with 29% of IDU participants in the 2009 IDRS reporting they had injected oxycodone in the previous six months (Stafford & Burns, 2009).

1.2.2.2. Costs of opioid dependence

Whilst the prevalence of heroin use in Australia may appear relatively small when compared to cannabis (9.1%), ecstasy (3.5%) and cocaine (1.6%), it carries with it disproportionately large detrimental effects on both users and society (ABCI, 1997; AIHW, 2007).

1.2.2.2.1. Morbidity and mortality

In general, mortality rates among opioid-dependent Australians are reported to be 13-fold higher than the general population (Hulse et al., 1999), with opioid-induced respiratory depression the major cause of death among Australian opioid addicts (White & Irvine, 1999). To put this into perspective, in 1992, opioid abuse was responsible for 21,690 years of life lost, almost 10 times that of tobacco related mortality (2,877 years of life lost) (Hulse et al., 1999). In terms of morbidity, bacterial infection is a very common cause of clinical presentation among opioid abusers, whilst the transmission of blood-borne viruses and their management is also a major concern (Theodorou & Haber, 2005).

1.2.2.2.2. Economic costs

In Australia, the treatment of heroin overdose and associated medical conditions, the spread of diseases such as hepatitis and HIV, drug prevention and law enforcement activities, judicial costs, crime, and loss of productivity, cost the nation hundreds of millions of dollars each year (DASC, 2002). For example, hospital separations related to illicit opioids were greater than any other illicit drug in the 12-months spanning 2004/2005, with an estimated cost of more than $16 million. Therefore, since serious opioid overdose is a diagnosis associated with significantly greater cost per treatment episode (5- to 6-fold greater than ‘drug induced’ psychosis admissions), any reduction in opioid overdose can be expected to have a “substantial impact” (Riddell et al., 2008) on drug related hospital costs.

1.2.3. Summary

In summary, public health costs, as well as other factors associated with illicit opioid abuse (such as increased crime), provide considerable burdens on society. As such, significant economic and public health benefits could be achieved by the effective treatment of opioid dependence and subsequent reductions in illicit opioid abuse.

1.3. Opioid substitution therapy

Whilst the principles of opioid substitution therapy are largely the same when comparing Australian treatment centres with those of other countries, variations in treatment protocols, treatment philosophies, as well as cultural pressures, can impact on the implementation and success of treatments in specific settings. As such, this brief review of opioid substitution therapy will concentrate on recent findings in Australian treatment settings, as these are the most relevant for the opioid-dependent populations being studied in this thesis.

The major pharmacotherapies recognised by the Australian Government's Intergovernmental Committee on Drugs for the treatment of opioid dependence include: opioid maintenance treatment (also termed opioid substitution therapy); buprenorphine-assisted withdrawal and detoxification; and naltrexone for relapse prevention following opioid detoxification. Of these major options, opioid maintenance is the most cost-effective treatment for opioid dependence (Mattick et al., 2001) and provides significant cost benefit over residential rehabilitation and prison ($5000 versus $11,000 and $52,000 per year, respectively) (Moore et al., 2007).

1.3.1. Treatment goals and outcomes

Opioid substitution treatment programs in Australia employ a philosophy of harm minimization directed toward replacing dangerous illicit opioid use with controlled administration of a legally available, affordable opioid that does not require injection. Whilst the primary aim of treatment is to allow patients to decrease their use of illicit opioids, other

outcomes sought include a reduction in morbidity and mortality, reduction in criminal activity and the rehabilitation and socialization of the patient. These outcomes are often heavily reliant on long-term retention of the patient within the program (Zhang et al., 2003b), and thus while some individuals may achieve eventual abstinence from opioids, the majority of substitution treatment programs in Australia are aimed at indefinite maintenance rather than complete opioid detoxification. Currently in Australia, the two major substitution therapies employed for the treatment of opioid dependence are methadone maintenance treatment and buprenorphine maintenance treatment.

1.3.2. Methadone maintenance treatment

Methadone maintenance therapy (MMT) was first trialled in Australia in 1969 and has since become the primary pharmacotherapy for the treatment of opioid dependence. Indeed, as of June 2008, over 28,000 Australians were receiving methadone maintenance treatment (AIHW, 2009).

1.3.2.1. Methadone pharmacology

Methadone is administered as a racemic mixture of its two stereoisomers, (R)- and (S)-methadone. However, the (R)-enantiomer has a 10-fold higher affinity at the mu-opioid receptor than (S)-methadone (Kristensen et al., 1995), and is the only enantiomer effective in suppressing opioid withdrawal (Isbell & Eisenman, 1948).

Typically given as a syrup, methadone and has an oral bioavailability ranging from 40-100%, but is generally around 80% (Meresaar et al., 1981; Nilsson et al., 1982). An advantage of oral administration is that methadone is relatively slowly absorbed, taking around 2-2.5 hours to reach maximum opioid effect (Foster et al., 2004). Therefore, it does not give an initial rush or feeling of euphoria, allowing for a reversal of the euphoric conditioning associated with illicit intravenous opioid abuse.

The major metabolic pathway for methadone is N-demethylation to its inactive metabolite, EDDP, predominantly by hepatic CYP3A enzymes. Other enzymes also believed to play a role in methadone metabolism include CYP2B6, CYP2D6, CYP2C9 and CYP2C19 (Iribarne et al., 1996), and up to 9 different metabolites of methadone have been identified, albeit in clinically irrelevant quantities (Sullivan et al., 1972; Sullivan & Due, 1973).

In MMT patients, renal clearance over the 24-hour dosing interval accounts for around 36% of the total dose, with approximately equal proportions of methadone and EDDP excreted in urine (Foster et al., 2004). A further 6-18% of the dose is excreted as EDDP in bile, whilst biliary excretion of unchanged methadone accounts for less than 1% of the total dose (Verebely et al., 1975; Kreek et al., 1983). The average steady state apparent plasma clearance of methadone is around 140-160 mL/minute, and the plasma half-life ($T_{1/2}$) is around 40 hours (Foster et al., 2000; Foster et al., 2004).

Stereoselectivity in methadone pharmacokinetics has been reported, with (R)-methadone reported to be more slowly absorbed from the intestine, resulting in a longer time to reach peak plasma concentrations (T_{max}) than (S)-methadone. In addition, due to stereoselectivity in plasma protein and tissue binding, (R)-methadone displays a 1.5- to 1.8-fold increased volume of distribution (V_d), resulting in around 15% lower peak plasma concentrations (C_{max}) and a longer $T_{1/2}$ (51 versus 31 hours) than (S)-methadone. Urinary excretion has also been found to be decreased for (R)-methadone and (R)-EDDP, however, despite these differences, no stereoselectivity in the steady-state total oral clearance of methadone is observed in MMT (Kristensen et al., 1996; Foster et al., 2000; Foster et al., 2004).

In addition to hepatic metabolism, the plasma pharmacokinetics of methadone may also be influenced by the activity of drug transporters in the intestine, liver and kidney, which may modulate its absorption and excretion. Furthermore, since its primary site of action is in the CNS, a very important, but often overlooked facet of methadone pharmacokinetics is its brain

distribution. Therefore, whilst CNS concentrations of methadone are generally believed to closely reflect those in the plasma, drug transporters located in the BBB may also have the ability to modulate brain exposure to methadone, and thus modulate its therapeutic effect. The role for drug transporters in methadone absorption, distribution and elimination is discussed in more detail in section 1.5.

1.3.2.2. General treatment protocol

At entry to MMT, patients are typically started on a low (20-30 mg) oral dose of methadone, with the long $T_{1/2}$ of methadone allowing for once daily dosing. Doses are gradually increased over an induction period of around 3-10 days to reach an eventual stabilisation dose, which is generally defined as a dose capable of eliminating withdrawal over the 24-hour dosing period without causing adverse opioid side effects. Higher doses of methadone (60-100 mg) that are able to block the effects of illicit opioids, as well as prevent withdrawal, have generally been found to produce significantly better treatment outcomes than lower doses of methadone (Ling et al., 1996; Faggiano et al., 2003), however, dose requirements can vary significantly between patients.

1.3.2.3. Treatment effectiveness

Methadone maintenance has been shown to be effective in reducing drug craving, alleviating opiate withdrawal, blocking and deconditioning heroin's euphoric effects, and normalising some physiological systems disrupted by chronic heroin administration (Dole & Nyswander, 1965; Tennant et al., 1991; Kreek, 1997). Consequently, evaluations of methadone substitution treatment have revealed it is successful in significantly reducing heroin use, criminal activity, mortality and behaviours associated with a high risk of viral transmission, whilst improving the mental health of patients, particularly when coupled with social services (Bament et al., 2004; Teesson et al., 2006).

1.3.3. Buprenorphine maintenance treatment

Buprenorphine is the main alternative to methadone for the treatment of opioid dependence. Buprenorphine maintenance therapy (BMT) has been available in Australia since 2000, and in June 2008, over 12,000 Australians were receiving this treatment (AIHW, 2009).

1.3.3.1. Buprenorphine pharmacology

Buprenorphine exhibits low oral bioavailability due to extensive first-pass metabolism and as such is administered in the form of a sublingual tablet. Its T_{max} is anywhere between 40 minutes and 3.5 hours after administration with an onset of effects at around 30-60 minutes. Unlike the pure agonist (R)-methadone, buprenorphine is considered a partial agonist for the mu-opioid receptor and an antagonist at the kappa-opioid receptor. Despite its partial agonist profile, buprenorphine has high affinity for, and is slow in dissociating from, the mu-opioid receptors, and thus has high potency at low doses (Jasinski et al., 1978; Cowan et al., 2005).

In terms of metabolism, buprenorphine undergoes *N*-dealkylation by CYP3A4 to an active metabolite norbuprenorphine, as well as glucuronidation, with most of the drug excreted in faeces. With a $T_{1/2}$ of around 24-37 hours, it exhibits a very long duration of opioid action, ranging from 12 hours at low doses (2 mg), to 24-72 hours at higher doses (>16 mg) (Ohtani et al., 1995; Lintzeris et al., 2006).

1.3.3.2. General treatment protocol

Due to its longer duration of action than methadone, buprenorphine can be administered every second day or even longer if needed, but is still most often administered daily, with a recommended starting dose of around 4-8 mg, and a dose of around 12-16 mg/day during steady state maintenance. Apart from the dose ranges employed, the clinical management of opioid dependence with buprenorphine is largely the same as for methadone (see above).

1.3.3.3. Treatment effectiveness

When given at sufficient doses, buprenorphine's high receptor affinity also allows it to block the effects of other opioid agonists, reducing the likelihood of a positive response to illicit opioid use (Schuh et al., 1999). In addition, buprenorphine does not produce significant physical dependence and consequently withdrawal from treatment is less severe than that for methadone, facilitating an easier transition from opioid maintenance to opioid abstinence if desired. Buprenorphine also appears to have a ceiling on its respiratory depressive effects (Walsh et al., 1995; Dahan et al., 2005), and therefore presents a lower risk of fatal overdose than methadone (Umbricht et al., 2004). However, due to its partial agonist profile, buprenorphine may have limited clinical efficacy for patients with high levels of opioid tolerance and, due to its high receptor affinity, may have the potential to precipitate withdrawal in these individuals. Therefore, caution is required when administering buprenorphine to patients with high levels of recent opioid use, or during the transition from MMT to BMT (Lintzeris et al., 2006).

Recent comparisons of the effectiveness of MMT and BMT have revealed methadone patients generally exhibit slightly higher retention rates during the first few weeks of treatment, and equivalent or slightly less illicit opioid use than buprenorphine patients (Mattick et al., 2003; Mattick et al., 2004; Amato et al., 2005). However, comparisons of BMT and MMT in Australian treatment settings have found that, despite the small differences in treatment efficacies, there are no significant differences in the overall cost-effectiveness of the two treatments (Doran et al., 2003). As such, buprenorphine provides a viable and increasingly employed alternative to methadone for the treatment of opioid dependence.

1.3.4. Barriers to effective opioid substitution therapy

The risk of death for opioid-dependent individuals who remain in treatment is 4 times lower than those not in treatment (Caplehorn et al., 1996), with positive treatment outcomes

correlating strongly with treatment retention. Therefore, it is highly important to retain patients in treatment for as long as possible. Unfortunately, the yearly retention rates for opioid substitution therapies are only approximately 50-60% (Amato et al., 2005), indicating that many patients respond poorly to methadone or buprenorphine, particularly during the induction phase of treatment.

Numerous patient characteristics have been identified as general risk factors for poor treatment outcome, including young age, poly-drug use, criminal activity, severe alcohol abuse, severe opioid dependence, and psychiatric comorbidities (Darke et al., 1992; Magura et al., 1998; Ward et al., 1998; Bell et al., 2006). Conversely, patients with pre-treatment employment, family support, high motivation, and prior history of opioid substitution treatment, tend to have a better prognosis for treatment retention (Gaughwin et al., 1998; Rhoades et al., 1998; Ward et al., 1998). Clinic policies can also have a significant impact on treatment retention. For example, a clinic policy and staff mentality in favour of opioid maintenance, rather than complete opioid abstinence, has been found to be more successful in retaining patients and reducing illicit drug use (Caplehorn et al., 1994; Caplehorn et al., 1998; Magura et al., 1998; Ward et al., 1998). The provision of counselling and other ancillary services like medical care and vocational training, and a clinic that is accessible in terms of operating hours and location, are also more conducive to positive treatment outcomes (Ward et al., 1998), as is the implementation of takeaway doses (Henry-Edwards et al., 2003).

Unfortunately, whilst these patient demographic and clinic factors may help predict a patient's risk of poor treatment outcome, it is how a patient responds to their maintenance dose that has the most significant impact on their chances of success. Indeed, one of the major clinical predictors of treatment response is methadone dose, which has consistently shown to have a positive relationship with treatment retention, and a negative relationship with heroin use (Ward et al., 1998; Ganapathy & Miyauchi, 2005; Hallinan et al., 2006). However, individual

dose requirements are highly variable and, like most opioid agonists, the safe and effective use of substitution opioids is complicated by their narrow therapeutic index. As such, there is a real risk of opioid adverse effects or opioid withdrawal during the course of treatment.

One of the most important considerations when discussing opioid substitution therapies, is that the patient is still dependent on opioids. Therefore, a decrease in opioid intake (deliberate or otherwise) represents a real potential for precipitating opioid withdrawal (see section 1.2.1.2). As such, if a dose is missed, or the maintenance dose prescribed is insufficient, patients will experience possibly severe opioid withdrawal symptoms.

Conversely, if the dose is too high, patients are at risk of adverse opioid effects. In addition to those discussed in section 1.1.1.3, other common adverse symptoms experienced by opioid substitution patients include sleep disturbances, reduced libido, sexual dysfunction, sweating, and dry mouth. Whilst some of these symptoms are easily managed (e.g. chewing gum for dry mouth), others may only be alleviated by a dose decrease, which must be balanced with the risk of precipitating withdrawal. Whilst deaths by methadone overdose do occur, the risk of respiratory depression and death purely as result of methadone over-prescription is quite low (Bell et al., 2009). In addition, few, if any, deaths among buprenorphine maintenance patients are attributed to buprenorphine overdose (Bell et al., 2009).

Both side effects as a result of overdosing, and withdrawal as a result of underdosing, can result in the patient dropping out of treatment and potentially returning to opioid abuse. Therefore, determining the appropriate dose that prevents withdrawal, whilst minimising adverse opioid effects, is a critical issue in the treatment of opioid dependence. Unfortunately, the establishment of individualized dosing regimens for the effective use of substitution opioids is complicated not only by their narrow therapeutic range, but also a considerable and as yet unexplained interindividual variability in opioid response.

1.4. Variability in opioid response

Significant interindividual variability in the dose-response relationship is typical of opioid therapies. For example, in heterogenous populations such as cancer patients, morphine doses for the relief of cancer pain can range up to 1000-fold (EWGEAPC, 1996). Even in relatively homogenous populations, such as patients receiving morphine for post-surgical pain, there is still a 40-fold variability in analgesic dose requirements (Aubrun et al., 2003). Therefore, a dose that may be effective for one patient, may be ineffective, or deleterious, for another.

Two different facets of variability in opioid response are relevant for the opioid substitution treatment patients investigated in this thesis. Firstly, those factors related to variability either in response to illicit opioids, or in endogenous opioid peptide systems, that could potentially influence an individual's risk or severity of opioid abuse and dependence. Secondly, those factors directly affecting a patient's treatment response, through changes to the pharmacokinetics and/or pharmacodynamics of substitution opioids.

These two categories are not mutually exclusive, but are intertwined, with the aetiology and severity of dependence likely to play an important role in influencing treatment response. Therefore, whilst this thesis concentrates mostly on in-treatment variability in methadone and buprenorphine response, a brief understanding of the factors that influence the acute and chronic response to heroin is also important, as they may in some way determine susceptibility to dependence, levels of opioid abuse and dependence prior to entering treatment, and risk of relapse to drug seeking when in treatment.

1.4.1. Variability in response to heroin

Heroin's clearance pathway (shown in Figure 1-1) provides important clues as to the potential sources for variability in heroin response. As mentioned previously, heroin's opioid effects are primarily mediated by its opioid-active metabolites, 6-MAM and morphine. As such, the

experience of reward and euphoria is reliant on heroin's rapid hydrolysis (deacetylation), in the CNS and in the blood, to 6-MAM, and the further hydrolysis of 6-MAM to morphine. It makes sense then that interindividual variability in the esterases or glucuronidases responsible for the formation and elimination of 6-MAM and morphine could have the potential to modulate the intensity and duration of heroin's effects. Indeed, significant *in vivo* drug-drug interactions in humans have been confirmed for ethanol (induction of heroin hydrolysis resulting in increased 6-MAM levels and increased risk of heroin overdose), acetaminophen (induction of morphine glucuronidation) and ranitidine (inhibition of glucuronidation resulting in increased morphine opioid effects) (Rook et al., 2006).

In addition to these drug-drug interactions, genetic variability in metabolising enzymes may also impact on heroin clearance. However, whilst at least one plasma cholinesterase genetic variant has been associated with a lack of heroin hydrolysis *in vitro* (Lockridge et al., 1980), the *in vivo* significance of this is unknown. Furthermore, investigations of *UGT2B7* and *UGT1A1* genetic polymorphisms have failed to identify a consistent link with morphine: morphine glucuronide ratios or clinical responses to morphine (Somogyi et al., 2007).

The brain distribution of heroin and its metabolites may also be an important determinant of heroin response. Since heroin and 6-MAM are both highly lipophilic, they possess high passive permeability across membranes, and therefore, their brain distribution is not limited by the BBB. However, as will be discussed in section 1.5, CNS exposure to morphine, which crosses the BBB much less efficiently, may be influenced by drug transporters, and could provide a source of variability in the duration and intensity of heroin's effects. Transporters involved in the biliary excretion and enteric reabsorption of morphine (see Figure 1-1) may also be relevant for its plasma pharmacokinetics.

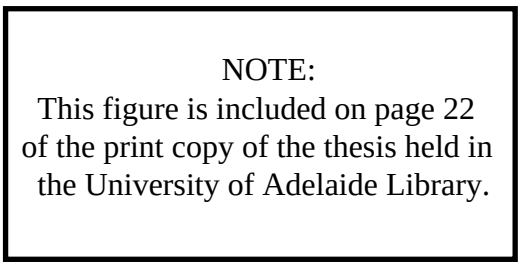

Figure 1-1. Heroin metabolism (adapted from Rook et al. (2006)).

Apart from factors influencing the pharmacokinetics of heroin and its metabolites, variability in more generalised mechanisms of reward (such as in dopamine or serotonin pathways, or the endogenous opioid system), leading to more global addictive personality traits, may affect the development and severity of the psychological dimension of heroin dependence. Therefore, by influencing the distribution of opioid peptides (see section 1.5.3), drug transporters may also play an important role in modulating the endogenous opioid reward system, thus potentially influencing both the physiological and psychological facets of heroin addiction.

As such, drug transporters provide a previously uninvestigated source of variability in morphine and endogenous opioid distribution following heroin administration, potentially influencing the degree of euphoric conditioning, tolerance and dependence, with possible implications for treatment response.

1.4.2. Variability in response to methadone

Whilst methadone in the range of 60-100 mg/day is generally recommended as a safe and effective dose for opioid substitution therapy (Ling et al., 1996; Faggiano et al., 2003), in reality, there is a significant interindividual variability in the actual maintenance doses required by patients. For example, in European treatment settings, a 140-fold variability (3-430 mg/day) in daily dose requirements for MMT has been described (Crettol et al., 2005), whereas a lesser, but still substantial, 40-fold variability (7.5-300 mg/day) in maintenance doses has been observed among South Australian MMT patients (Foster et al., 2000; Mitchell et al., 2004; Hanna et al., 2005).

Over the past decade or so, our Discipline of Pharmacology has conducted numerous studies investigating the pharmacokinetics and pharmacodynamics of methadone in opioid substitution treatment. These studies have highlighted a significant interindividual variability in both the pharmacokinetics and the pharmacokinetic/pharmacodynamic (PK/PD) relationship of methadone among MMT patients. For example, an investigation of MMT symptom complaints revealed that approximately 34% of the subject population report their dose as "not holding" and thus experience withdrawal symptoms over the dosing interval. Furthermore, those who report their doses as "not holding", do not differ from other subjects in terms of age, time in treatment or methadone dose received, thus indicating a legitimate variability in methadone response (Dyer & White, 1997).

1.4.2.1. Variability in methadone pharmacokinetics

At steady-state, methadone dose has been found to predict only around 68% of variability in total (bound and unbound) plasma (R)-methadone concentrations (Foster et al., 2000). As such, significant interindividual variability is observed in dose-normalised plasma concentrations (3- to 6-fold), apparent plasma clearance (7-fold, ~60-400 mL/min), V_d (up to 7-fold) and $T_{1/2}$ (over 9-fold, 15-140 hours) (Dyer et al., 1999; Foster et al., 2000).

Interestingly, unlike many other drugs, body weight does not appear to influence the V_d or clearance of methadone (Foster et al., 2004). However, methadone in plasma is extensively bound to plasma proteins (primarily α_1-acid glycoprotein, AAG), with the fraction of unbound methadone varying 2.7-fold (1.8-4.8%) between patients (Foster et al., 2000). As such, plasma AAG levels, determining the ratio of bound/unbound methadone, have been identified as a significant determinant of V_d in population-pharmacokinetic (Pop-PK) analysis (Foster et al., 2000; Foster et al., 2004). Pop-PK analysis also indicates that sex can have a significant effect on methadone distribution, with V_d in the central compartment greater in males (although this may be simply related to sex differences in percentage body fat) (Foster et al., 2004). Despite the identification of these factors, adjustments for plasma AAG and sex decrease the interindividual variability in methadone distribution by only around 20%. Therefore, significant unexplained variability in methadone distribution still exists.

With regard to the oral clearance of methadone, it is not associated with demographic variables such as age, sex or AAG levels, but may be modulated by significant interindividual variability in the expression of CYP3A4 (Thummel et al., 1994a; Thummel et al., 1994b; Lown et al., 1995; Thummel et al., 1996), the major CYP isoform mediating the metabolic clearance of methadone by N-dealkylation to EDDP (Foster et al., 1999). Indeed, CYP3A4 metabolism of methadone has been found to vary significantly between individuals, and is determined partially by genetics (see section 1.4.2.3), but also by numerous environmental factors, particularly drug-drug interactions (see Appendix A: Table A-1) (Moody et al., 1997; Boulton et al., 2001; Eap et al., 2001; Calvo et al., 2002; Wojnowski & Kamdem, 2006). Despite this, recent studies aimed at investigating the correlation between CYP3A4 activity and methadone clearance have failed to demonstrate a clear relationship between the two, casting doubt as to the utility of CYP3A4 activity alone as a predictive factor of methadone pharmacokinetics (Kharasch et al., 2004b; Morton, 2007). Alternatively, whilst only functional in 10-20% of Caucasians (Xie et al., 2004), CYP3A5 can account for around 50%

of the total hepatic CYP3A activity when expressed (Wojnowski, 2004), and has substantial overlapping substrate affinities with CYP3A4. As such, it can be proposed that variability in CYP3A5 activity may also account for some of individual differences in methadone clearance. However, prior to this thesis, this had yet to be investigated.

It has also been proposed that variability in the activity of other CYP enzymes implicated in methadone metabolism, such as CYP2B6, CYP2D6, CYP2C19 and CYP2C9, may also contribute to individual differences in methadone clearance (Eap et al., 2002; Kharasch et al., 2004b), and whilst there is a lack of a clear correlation between any single enzyme's activity and variability in methadone pharmacokinetics, clinically relevant pharmacokinetic drug-drug interactions involving CYP2B6 and CYP2D6 have been observed (see Appendix A: Table A-1) (Trescot et al., 2008). Case reports, animal studies and/or *in vitro* experiments have also indicated pharmacokinetic interactions with methadone for recreational and illicit drugs such as cocaine (Moolchan et al. 2001) and alcohol (Kreek et al., 1976b; Borowsky & Lieber, 1978; Kreek, 1984; Quinn et al., 1997) via induction of CYP450 metabolism.

In addition to drug-drug interactions, other factors such as disease, diet, and patient genetics, can also interact to determine CYP expression and function. Therefore, an individual's CYP activity, and hence variability in methadone pharmacokinetics, is difficult to predict.

Whilst an understanding of the mechanisms behind variability in the plasma pharmacokinetics of methadone is important, mass spectrometry and Pop-PK modelling methods have recently been developed that allow for the determination an individual's plasma concentration and clearance from only one or two blood samples (Foster et al., 2004). Therefore, variability in methadone plasma pharmacokinetics can be relatively easily accounted for using these techniques. Indeed, this method has been proposed as the basis for the application of therapeutic drug monitoring (TDM) for targeting plasma concentrations in MMT. However,

these TDM protocols are developed on the premise that a specific target plasma concentration will work for all patients, which may not necessarily be the case for methadone (see below).

As will be discussed in section 1.5, drug transporters may also influence the absorption, distribution and elimination of methadone, and as such may also provide a largely uninvestigated source of variability in methadone pharmacokinetics.

1.4.2.2. Variability in methadone plasma PK/PD relationship

A 10- to 18-fold variability in (R)-methadone plasma concentrations has been reported among South Australian MMT subjects (Foster et al., 2000; Mitchell et al., 2004), suggesting vastly different plasma methadone requirements. In addition, further investigations of the "not holding" MMT patients described previously, have revealed that their mean methadone plasma area under the concentration-time curve (AUC) is not significantly different from "holders" (Dyer et al., 1999). Within the same study, substantial inter-subject variability in the plasma methadone concentration-response relationship was also observed (5-fold in just 9 subjects) (Dyer et al., 1999). Therefore, there is clear clinical evidence that significant interindividual variability in methadone's PK/PD relationship exists among MMT patients.

Poly-drug use culminating in pharmacodynamic drug-drug interactions is one of the more obvious casues of methadone PK/PD variability, and can compromise the safety of MMT. For example, most CNS depressant drugs like alcohol and benzodiazepines have the ability to enhance methadone's sedative and respiratory depressive effects, whilst co-administration of full mu-opioid agonists may also enhance methadone's opioid effects, depending on the level of cross-tolerance. Alternatively, partial agonists (such as buprenorphine and pentazocine) have the potential to antagonise methadone and possibly precipitate withdrawal, whilst genetic variability influencing opioid receptors and other signalling pathways may also affect methadone pharmacodynamics (see section 1.4.2.3).

In addition to pharmacodynamic variables, the CNS distribution of methadone is also likely to influence its PK/PD. As such, another potential source of interindividual variability in methadone's plasma concentration-effect relationship is drug transporters. As will be discussed in section 1.5, their ability to control the passage of drugs, particularly from the blood into the CNS via the BBB, means they can alter the balance between plasma concentrations and actual CNS drug exposure. Therefore, variability in drug transport at the BBB may be an additional significant factor determining an individual's response to a given plasma concentration of methadone.

1.4.2.3. Genetic variability influencing methadone response

Any genetic factor influencing the pharmacokinetic or pharmacodynamic pathways of methadone has the potential to affect a patient's response to methadone treatment. Prior to commencing this PhD, the majority of research into the pharmacogenetics of MMT had concentrated on genetic variability affecting methadone metabolism. However, *CYP3A4* genetic polymorphisms have generally been found to be poor predictors of activity (Zanger et al., 2008), whilst studies investigating the effects of *CYP2D6* polymorphisms on methadone clearance have been conflicting (Somogyi et al., 2007). Alternatively, there is some evidence that *CYP2B6* genetic variants influence (S)- and, to a lesser extent, (R)-methadone plasma concentrations (Crettol et al., 2005), however these findings have yet to be replicated. Finally, whilst *CYP3A5* genotypes correlate well with activity (effectively differentiating expressors from non-expressors) (Lamba et al., 2002), their influence on methadone pharmacokinetics remains to be determined.

As discussed previously, relatively simple methods are available for determination of methadone concentrations in plasma, therefore determining what genetic factors influence variability in methadone pharmacodynamics may prove more useful than trying to genetically predict methadone plasma pharmacokinetics. In terms of the gene encoding the mu-opioid

receptor, *OPRM1*, the A118G polymorphism has been linked to reduced effect of opioid agonists (Somogyi et al., 2007). However, at the time of commencement of this project, studies into the role of the *OPRM1* A118G variant in opioid dependence and MMT were ongoing in our Discipline, with initial experiments indicating that the A118G polymorphism did not impact on methadone dosage requirements in MMT, or the risk of opioid dependence (Somogyi et al., 2007). More recent findings on the impact of the *OPRM1* A118G SNP in MMT are discussed in Chapter 4, section 4.4.

Genetic variants of the *DRD2* gene, encoding the dopamine D_2 receptor involved in opioid signalling and drug reward (see section 1.1.1.2), have also been investigated previously. The most studied *DRD2* SNP, rs1800497C>T (previously termed *DRD2* Taq1A but recently found to belong to the *ANKK1* gene) has previously been linked with poor MMT treatment outcomes (Lawford et al., 2000). More recent studies have observed no effect of this variant (Barratt et al., 2006; Crettol et al., 2008a; Doehring et al., 2009), but have implicated other *DRD2* SNPs as potential factors influencing MMT treatment response and/or dose requirements (Crettol et al., 2008a; Doehring et al., 2009).

Prior to commencing this PhD, drug transporter genetic polymorphisms influencing methadone response had not been previously investigated.

1.4.3. Variability in response to buprenorphine

Based largely on government clinical guidelines, patients in Australia generally receive buprenorphine doses of 1-16 mg/day for opioid substitution treatment (Mattick et al., 2003), indicating some degree of variation between patients.

Apart from one study (in 5 patients receiving 8 mg/day) reporting a 2.6-fold variability in buprenorphine's $T_{1/2}$ (23.9-62.5 hours), there are very little data on interindividual variability in buprenorphine pharmacokinetics. Although, since buprenorphine is predominantly

metabolised by CYP3A4 (see section 1.3.3.1), those factors that affect methadone pharmacokinetics through CYP3A4 modulation (see above, section 1.4.2.1), would be expected to have a similar influence on buprenorphine pharmacokinetics. Indeed, HIV protease inhibitors have been shown to inhibit CYP3A4 metabolism of buprenorphine *in vitro* (Iribarne et al., 1998), whilst ketoconazole is reported to up to double buprenorphine's plasma concentrations *in vivo* (Reckitt-Benckiser, 2005).

In terms of variability in buprenorphine's plasma PK/PD relationship, due to the apparent ceiling on buprenorphine's adverse opioid effects, serious adverse events due to supraoptimal dosing would be unlikely at typical doses (see section 1.3.3.3). However, whilst plasma concentrations appear to correlate reasonably well with indicators of treatment efficacy (e.g. suppression of withdrawal and craving) and receptor occupancy (Kuhlman et al., 1998; Greenwald et al., 2003), at 16 mg/day a small subset of BMT patients still experience significant withdrawal symptoms towards the end of their dosing interval. Furthermore, in a situation analogous to "non-holders" in MMT (Dyer & White, 1997; Dyer et al., 1999), these subjects that experience withdrawal do not have significantly different plasma concentrations of buprenorphine over the 24 hour period (Lopatko et al., 2003). Therefore, there also appears to be interindividual variability in buprenorphine's plasma PK/PD relationship. Environmental and genetic factors influencing this relationship are likely to be similar to those discussed for methadone. However, to my knowledge, genetic determinants of buprenorphine dose requirements and BMT response have not yet been investigated.

1.4.4. Summary

In summary, there is significant interindividual variability in the pharmacokinetics and the plasma PK/PD relationships of heroin (and its metabolites), methadone and buprenorphine, which may have clinically relevant impacts on opioid maintenance treatment response. Despite extensive research into the roles of genetically variable metabolic enzymes (such as

the Cytochrome P450s) in drug clearance, interindividual differences in plasma pharmacokinetics are still difficult to predict, but can be accounted for by directly measuring opioid plasma concentrations. Alternatively, investigations into genetic polymorphisms affecting the plasma PK/PD of these opioids have been scarce, and a large portion of variability in methadone and buprenorphine plasma PK/PD relationship remains unexplained.

As mentioned briefly, drug transporters may have the ability to alter both the pharmacokinetics and the plasma PK/PD relationship of morphine, methadone and buprenorphine. Therefore, at the time of commencing this PhD, they represented a previously unexplored contributing factor to the interindividual variability in opioid substitution treatment response.

1.5. P-glycoprotein efflux transporter

Of the known human drug transporters, the efflux transporter P-glycoprotein (P-gp), encoded by the *ABCB1* gene, appears the most likely source of variability in opioid pharmacokinetics.

P-gp first came to the attention of pharmacologists as an overexpressed glycosylated protein isolated from multi-drug resistant tumour cells. Since then, P-gp in cancer tumour cells has been extensively investigated regarding its role in resistance to chemotherapeutic drugs, but is now also well recognized for its expression in normal tissue and its effect on the distribution of a wide range of medications.

1.5.1. P-glycoprotein structure

P-gp belongs to the ATP-binding cassette membrane transporter superfamily that consists of nearly 50 known human members divided into 7 sub-families, all of which transport their substrates in an ATP-dependent manner. As shown in Figure 1-3 (page 49), this 170 kDa transporter resides in the lipid bilayer of the cell membrane and consists of two homologous halves, each of which contains 6 transmembrane spanning regions and an intracellular

nucleotide binding domain (NBD). The NBDs are known to be essential for the utilisation of ATP for the active transport process. In addition, the flexible linker region located between the homologous halves of P-gp is necessary for their interaction, as well as the communication between the two NBDs (Ambudkar et al., 2003).

The transmembrane domains (TMDs) of P-gp are proposed as the likely sites of substrate recognition, with TMD sites 5 and 6, and TMD sites 11 and 12 identified as the two possible major substrate binding regions (Wang et al., 2003). However, the mechanisms by which P-gp recognizes and transports its substrates are still to be fully characterised. In addition, the size and structure of P-gp substrates varies significantly, ranging from small organic cations, carbohydrates and amino acids, to large molecules such as polysaccharides and proteins (Zhou, 2008). As such, P-gp exhibits very broad substrate specificity and is known to transport many different classes of structurally diverse drugs, with over 480 substrates currently reported in the TP-Search Transporter Database established by the University of Tokyo (http://www.tp-search.jp, last accessed April 2010). Numerous P-gp inducers and inhibitors have also been identified, and can provide the basis for a number of P-gp-centric drug-drug interactions (see sections 1.5.4.1 and 1.5.4.2). Whilst the majority of inhibitors act through competitive binding and transport, there is also evidence that allosteric binding sites exist that may also modify P-gp activity (Martin et al., 1997).

1.5.2. Expression and function

P-gp is expressed in numerous human tissues and is almost exclusively an efflux transporter, actively transporting substrates out of cells and into the extracellular space. It has been found in the apical membranes of epithelial cells of the stomach, small intestine, colon and renal proximal tubule, where it plays a protective role by reducing the absorption and increasing the elimination of its substrates (Tanigawara, 2000; Bendayan et al., 2006; Takano et al., 2006). In addition, P-gp plays a role in drug distribution into organs such as the testes, placenta,

pancreas, and the CNS (via the BBB), preventing the accumulation of substrates within these tissues. P-gp also has a high expression in liver hepatocytes (Fojo et al., 1987; Thiebaut et al., 1989; Tanigawara, 2000) and demonstrates an overlapping substrate specificity and colocalization with the CYP3A4 metabolising enzyme, suggesting a coordinated function in tissue protection and elimination of xenobiotics. Variable degrees of expression are also observed among different lineages of leukocytes (Klimecki et al., 1994; Ford et al., 2003). Therefore, P-gp has the ability to limit absorption, facilitate elimination and performs a protective role in specific tissues. Highlighted in Figure 1-2, the most relevant P-gp sites of action for opioid drugs are likely those influencing the intestinal absorption, brain distribution, and elimination pathways.

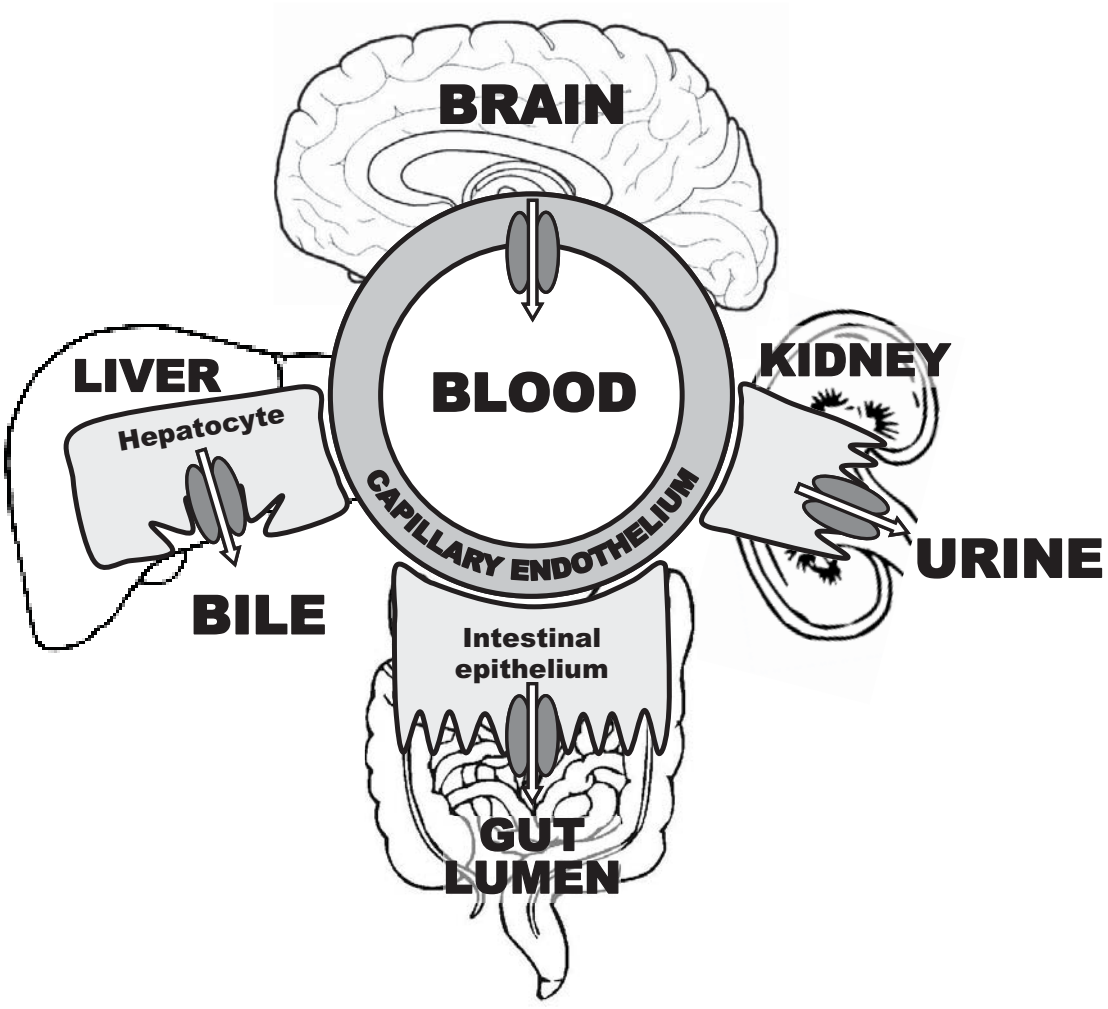

Figure 1-2. P-glycoprotein sites of action important for opioid pharmacokinetics.

1.5.2.1. Intestinal absorption

P-gp is expressed on the luminal/apical membranes of intestinal epithelial cells and transports in a basal to apical direction, extruding substrates from the enterocytes back into the gut (Takano et al., 2006). In this manner, P-gp has the potential to limit the intestinal absorption, and thus bioavailability, of orally administered substrates, as well as actively excrete them from the blood into the small intestine (Gramatte & Oertel, 1999; Drescher et al., 2003). However, there is a dynamic counter-action between P-gp efflux from the cells into the lumen, and passive diffusion across the enterocytes into the mucosal blood circulation. As such, the ability of P-gp to limit the intestinal absorption of a substrate is counteracted by the passive diffusion of that substrate across the enterocytes. Therefore, the bioavailabilities of drugs with slow rates of passive diffusion (such as paclitaxel) are significantly reduced by P-gp (Sparreboom et al., 1997), whereas compounds that are good P-gp substrates but have high rates of passive diffusion (such as digoxin and quinidine), can still exhibit reasonable oral bioavailability (Ueda et al., 1976; Polli et al., 2001; Lin & Yamazaki, 2003b).

In addition to drug lipophilicity, rates of passive diffusion are directly proportional to the concentration gradient between the lumen and mucosal blood, which is typically large for an orally administered drug, and is enhanced by both the sink effect of mucosal blood circulation and the slow transit time in the intestine. Furthermore, there is evidence that intestinal P-gp efflux can be saturated when high oral doses are administered (Wetterich et al., 1996). Therefore, whilst the oral bioavailability of some drugs can be significantly diminished by P-gp actions in the small intestine, the impact of P-gp on the intestinal absorption of many of its substrates is quantitatively less than might be expected from *in vitro* studies, particularly at high oral doses (Lin & Yamazaki, 2003a).

1.5.2.2. Brain distribution

P-gp is located within the apical membranes of the brain capillary endothelial cells that constitute the BBB, and transports its substrates in a basal-apical direction, that is, from the endothelial cells back into the blood. A number of factors combine to make P-gp a significant factor determining substrate passage across the BBB. Firstly, due to the tight junctions between capillary endothelial cells, there is a relative absence of passive paracellular movement and therefore drugs must pass through the cells in order to reach the brain extracellular space. Secondly, the concentration gradient between cerebral blood and brain extracellular fluid remains small (due to the lack of brain 'sink' effect) and is significantly lower than the gradient between the intestinal lumen and mucosal blood. Finally, the rapid transit time of cerebral blood flow, compared to the bulk flow of cerebral fluid, means that extruded drug is quickly removed from the BBB interface and cannot be reabsorbed (Lin & Yamazaki, 2003a). Consequently, studies in mice have demonstrated that genetic or inhibitor knockout of P-gp causes 17- to 83-fold increases in brain distribution of a wide range of P-gp substrates, whilst changes in liver, kidney, small intestine and plasma distribution are altered only 2- to 3-fold (Schinkel et al., 1994; Schinkel et al., 1995; Schinkel et al., 1997; Polli et al., 1999; Yokogawa et al., 1999; Choo et al., 2000; Kusuhara & Sugiyama, 2001). In humans, positron emission tomography has been able to show that co-administration of cyclosporine (a P-gp inhibitor) results in an 87% increase in the brain:blood AUC ratio of the P-gp substrate verapamil (Sasongko et al., 2005). Furthermore, clinical studies measuring cerebrospinal fluid (CSF) concentrations of antiretrovirals have revealed they reach only 6-17% of the unbound concentration in plasma, thus indicating a significant P-gp efflux of these drugs at the BBB (Haas et al., 2000; Khaliq et al., 2000). Therefore, there is good evidence that P-gp has the ability to significantly limit the CNS entry of its substrates

1.5.2.3. Elimination

Hepatic P-gp, located on the canalicular (apical) membrane of hepatocytes, acts in co-operation with other canalicular efflux and basolateral influx hepatic transporters to transport drugs and their metabolites from the blood into the bile (Zhou, 2008). This active canalicular secretion acts against a concentration gradient to concentrate xenobiotics into the bile, and is the rate-limiting step in bile formation (Arrese & Trauner, 2003). Animal studies have demonstrated that P-gp inhibition or genetic knockout decreases biliary excretion of doxorubicin and its metabolite by 62-84% (Booth et al., 1998; van Asperen et al., 2000), whilst P-gp induction results in an 8-51% increase in excretion of tamoxifen (Riley et al., 2000). In humans, quinidine inhibition of P-gp transport decreases the biliary excretion of digoxin by around 42% (Angelin et al., 1987).

In terms of renal elimination, P-gp is expressed at the apical brush-border membranes of the renal proximal tubule cells of the kidney, effluxing from the cell into the renal duct (Thiebaut et al., 1987). As such, substrates of P-gp can be expected to undergo tubular secretion, and will have a rate of renal elimination greater than simple glomerular filtration (unless they also undergo active reabsorption by other transporters).

Therefore, P-gp has the ability to influence the clearance of drugs and their metabolites by facilitating their biliary and/or renal excretion. However, the significance of this influence on drug elimination from liver and kidney in determining the overall clearance and plasma concentrations of substrates is unclear. Indeed, the literature so far has indicated that P-gp tends to have a smaller impact on drug excretion from cells (as in the case of hepatic and renal P-gp), than it does when acting to inhibit drug uptake (as in the case of intestinal and BBB P-gp) (Lin & Yamazaki, 2003a).

1.5.2.4. Summary

In conclusion, P-gp transport has the ability to limit the intestinal absorption and organ distribution of its substrates, and may help facilitate their biliary and renal excretion. However, for opioids, the most clinically important activity of P-gp is likely to be at the BBB, where it has the greatest potential to limit substrate passage, and can directly mediate opioids' access to their CNS site of action.

1.5.3. P-glycoprotein transport of opioids

Quantitative structure-activity relationship analyses have identified chemical moieties important for P-gp transport of neurotransmitters, vasodilators, potassium channel modulators, non-steroidal anti-inflammatories, and anticancer drugs. However, these analyses have not been performed or tested for the opioid class of drugs, and as such, interactions with P-gp are hard to predict based on opioid chemical structure alone. Therefore, the identification of opioid substrates for P-gp has relied on *in vitro* transport and ATPase activity data, as well as animal *in vivo* transport studies.

1.5.3.1. *In vitro* and animal studies

Both *in vitro* and animal *in vivo* studies have identified a number of exogenous and endogenous opioids as P-gp substrates. As shown in Table 1-1, *in vitro* and animal *in vivo* experiments have generally agreed in terms of the substrate status of specific opioid drugs, however some discrepancies between (as well as within) investigative methods have occurred (for example for morphine-6-glucuronide (M-6-G), pethidine (meperidine), and oxycodone).

In these cases, the most reliable conclusions are likely those from *in vivo* gene knockout models as they provide obvious benefits over *in vitro* methods, and rule out problems with poor specificity of the P-gp inhibitors often used in *in vivo* inhibition studies. As such, whilst

in vitro and animal *in vivo* studies agree that morphine and methadone are transported by P-gp, previous studies would suggest that M-6-G is not a substrate.

Table 1-1. Summary of opioid P-gp substrates based on *in vitro*, animal *in vivo* P-gp inhibition, and animal P-gp gene knockout studies. Adapted and updated from Somogyi et al. (2007).

Test Used	*In vitro*	*In vivo* inhibition	*In vivo* knockout
Opioid Medication			
Morphine	Substrate	Substrate	Substrate
Methadone	Substrate/non-substrate[7]	Substrate	Substrate
LAAM	Substrate[4]		
Loperamide	Substrate	Substrate	Substrate
Fentanyl	Substrate	Substrate	Substrate
Alfentanil	-	-	Substrate[3]
Hydrocodone	-	Substrate	-
Pentazocine	Substrate	Substrate	-
Asimadoline	Substrate[1]	-	Substrate
Bremazocine	-	-	Substrate
Naltrindole	-	-	Substrate
M-6-G	Substrate	Substrate	Non-substrate
Meperidine	Substrate	-	Non-substrate
Diprenorphine	Non-substrate[5]	-	Non-substrate[5]
Oxycodone	Substrate[6]	Non-substrate	Substrate[6]
Opioid Peptide			
β-endorphin	-	Substrate	Substrate[9]
DPDPE	-	Substrate	Substrate
Deltorphin II	-	-	Substrate
DAMGO	Substrate	-	-
Endomorphin-1	Non-substrate[8]	-	Non-substrate
Endomorphin-2	Non-substrate[8]	-	Non-substrate
Met-enkephalin	-	-	Non-substrate
DADLE	Non-substrate[2]	-	-
TYR-MIF-1	-	-	Non-substrate

(1) Jonker et al. (1999); (2) Ouyang et al. (2009); (3) Kalvass et al. (2007); (4) Crettol et al. (2007); (5) Hassan et al. (2009); (6) Hassan et al. (2007); (7) Stormer et al. (2001); (8) Somogyvari-Vigh et al. (2004); (9) King et al. (2001). All others are from Somogyi et al. (2007).

In terms of the magnitude of P-gp's effect on morphine transport, inhibition and/or genetic knockout of P-gp has been shown to cause a 5.2-fold increase in the plasma AUC of oral morphine, a 1.2-fold increase in morphine brain uptake (Dagenais et al., 2004), 1.5- to 4.5-fold increase in brain concentrations (2.2- to 4.8-fold increase in brain:blood ratio), 3-fold increased brain half-life, and 2.2- to 4-fold increase in analgesia, with no influence on systemic clearance (Letrent et al., 1998; Letrent et al., 1999a; Letrent et al., 1999b; Xie et al., 1999; Thompson et al., 2000; Hamabe et al., 2006; Okura et al., 2009). Even natural variations in P-gp activity within a population, which are relatively subtle compared to gene knockout, can have relevant impacts on morphine analgesia. For example, examination of individual differences in morphine antinociception (ranging 3- to 10-fold) within a single strain of mice, reveal significant negative correlations with brain P-gp expression and function (Hamabe et al., 2007).

For methadone, P-gp knockout and/or inhibition results in a 1.2-fold increase in oral bioavailability and up to 23-fold higher brain concentrations, equating to a 2.8- to 3.6-fold increase in antinociception (Thompson et al., 2000; Dagenais et al., 2004; Rodriguez et al., 2004; Wang et al., 2004; Ortega et al., 2007). Conversely, induction of P-gp expression in mice results in a 70% decrease in the antinociceptive effects of methadone, without significantly altering methadone plasma concentrations (Bauer et al., 2006). Therefore, at least in rodents, both increases and decreases in P-gp activity have been shown to have significant impacts on the CNS activity of methadone.

Finally, a single study in rats has shown that a 50% lower P-gp expression results in 75% lower brain-to-blood efflux of the endogenous opioid peptide β-endorphin (King et al., 2001).

In summary, previous animal studies suggest that P-gp affects the intestinal absorption and brain distribution (and hence antinociceptive effect), but not the systemic elimination, of both morphine and methadone, but not M-6-G. There is also limited evidence that the distribution

of β-endorphin may too be influenced by P-gp. Prior to commencing this PhD, no study had examined buprenorphine or norbuprenorphine as potential P-gp substrates.

1.5.3.2. Human studies

1.5.3.2.1. Methadone intestinal absorption

As discussed in section 1.5.2.1, P-gp has the potential to influence the intestinal absorption of orally administered substrates. However, studies examining the effects of the P-gp modulators (quinidine, nelfinavir, ritonavir and indinavir) on methadone absorption have suggested a relatively minor role for P-gp (Kharasch et al., 2004a; Kharasch et al., 2009a; Kharasch et al., 2009b). For example, whilst Kharasch and colleagues (2004a) demonstrated that co-administration of the P-gp inhibitor quinidine to healthy controls resulted in significantly increased absorptive phase (30 to 60 minutes post-dose) plasma methadone concentrations, as well as a significant decreases in T_{max} (2.4 ± 0.7 to 1.6 ± 0.9 h), this did not translate to a significant increase in either C_{max} (55.6 ± 10.3 to 59.4 ± 14.1 ng/mL) or plasma AUC (298 ± 46 to 316 ± 74 ng/mL.h). Therefore, it appears that P-gp inhibition may increase the rate of methadone absorption, but not necessarily the amount eventually making it into systemic circulation. As such, the clinical implications of variability in P-gp transport at the intestinal level remains unclear, with any effects likely to be relatively minor.

1.5.3.2.2. Opioid brain distribution

As discussed in section 1.5.2.2, the activity of P-gp in determining CNS exposure to opioids may be of greater importance than its effects on intestinal absorption and elimination (Lin & Yamazaki, 2003a; Lin & Yamazaki, 2003b). Unfortunately it is difficult to directly measure opioid brain concentrations in human subjects, and the relatively small volume of the extravascular brain compartment means that any changes in brain distribution will only have a relatively small effect, if any, on the plasma pharmacokinetics. As such, in humans, investigations into the role of P-gp in the brain distribution of opioids are largely restricted to

comparisons of pharmacodynamic responses following intravenous administration, and/or PK/PD relationships.

The most commonly used example of P-gp's potential to influence brain distribution of opioids is the work of Sadeque and colleagues (2000). They were able to demonstrate that co-administering a P-gp inhibitor (quinidine), with an opioid that does not usually produce central effects (loperamide), results in significant CNS-mediated opioid-induced respiratory depression. Most importantly, CNS effects were observed at time-points prior to any significant changes in plasma pharmacokinetics, strongly implicating P-gp effects at the BBB.

Unfortunately, unlike loperamide, studies investigating the effects of the P-gp inhibitors valspodar (Drewe et al., 2000) and quinidine (Kharasch et al., 2003b; Skarke et al., 2003a) on intravenous morphine response, and oral morphine PK/PD relationships, have failed to demonstrate any significant effect on CNS-mediated pharmacodynamics. However, the findings of Drewe and colleagues are confounded by an observation of significant valspodar pharmacodynamic effects in the absence of morphine, making interpretation of combined morphine/valspodar treatment effects difficult. In addition, the studies employing quinidine recorded pharmacodynamic effects for only 2 (Skarke et al., 2003a) or 8 (Kharasch et al., 2003b) hours post-morphine infusion, thus potentially missing alterations to the end-stage clearance of morphine from the brain (when morphine concentrations are low), and hence changes to the duration of morphine CNS effects.

Studies have also failed to identify an effect of quinidine on intravenous methadone pharmacodynamics or PK/PD relationships following oral administration (Kharasch et al., 2004a). Alternatively, nelfinavir, a potent inhibitor of P-gp in bovine brain microvessel endothelial cells, has been shown to increase the miotic effect / plasma concentration (AUC) ratio of methadone (Kharasch et al., 2009b). These findings with nelfinavir explain, and are supported by, previous clinical reports identifying an absence of withdrawal symptoms among

methadone maintenance patients coadministered nelfinavir, despite 40-50% decreases in plasma methadone concentrations due to CYP450 induction (McCance-Katz et al., 2000; McCance-Katz et al., 2004; Brown et al., 2006; Hsyu et al., 2006; Kharasch et al., 2009b). Also in methadone maintenance patients, the P-gp inducers rifampicin and St John's Wort have been associated with increases in withdrawal symptoms, an effect that could not be solely explained by decreases in plasma concentrations of methadone, thus implicating significant decreases in brain concentrations due to an induction of P-gp activity at the BBB (Kreek et al., 1976a; Eich-Hochli et al., 2003). As such, at least in methadone maintenance patients, P-gp function at the BBB has the ability to influence the brain distribution of methadone, and hence clinical response.

Why distinct effects of P-gp on brain distribution of morphine and methadone are observed in rodents, but not in healthy human controls, is unclear. Whilst the most obvious factor may be species differences in BBB permeability and transporter expression, the BBB efficacy of P-gp inhibitors used in clinical studies has also come under scrutiny. For example, studies using 600-800 mg of oral quinidine typically achieve significantly lower peak plasma quinidine concentrations (6-9 μM) than the IC_{50} determined *in vitro* (2-34 μM) and for mouse brain efflux (36 μM) (Wandel et al., 1999; Dagenais et al., 2001; Kharasch et al., 2003a; Skarke et al., 2003a; Weiss et al., 2003). As such, whether a sufficient level and duration of P-gp inhibition at the BBB was actually achieved in these studies, in order to observe a clinically relevant effect, is questionable. Further to this argument, studies following the distribution of radio-labelled opioid in mice have indicated that P-gp localised at the BBB is more resistant to inhibition than P-gp in other tissues, thus achieving adequate BBB P-gp inhibition may be beyond the therapeutic range of the inhibitors used in previous clinical studies (Choo et al., 2006). As such, the potential impact of P-gp activity at the BBB should not be discounted for either morphine or methadone.

1.5.3.2.3. Opioid elimination

Because quinidine and nelfinavir, the P-gp modulators used in the clinical investigations discussed so far, also cause changes in the activity of hepatic enzymes involved in morphine and methadone metabolism, it is difficult to determine the contribution of P-gp to the biliary excretion of these opioids and their metabolites. However, an estimation of the effect of P-gp modulation on renal excretion of morphine, methadone and their metabolites is possible.

In all studies conducted to date, P-gp inhibition has been found to have no effect on the renal clearance of intravenous morphine (Drewe et al., 2000; Kharasch et al., 2003b; Skarke et al., 2003a). Alternatively, in the only study to investigate the effect of P-gp modulation on intravenous methadone elimination, nelfinavir was found to increase the renal clearance of both methadone enantiomers by 30-50% (Kharasch et al., 2009b). However, whether this can be attributed to an induction of P-gp, or whether another renal transporter sensitive to nelfinavir is involved, is unclear. Therefore, there is only limited evidence to indicate that P-gp may have a clinically significant effect on the renal elimination of methadone.

1.5.3.3. Summary

In summary, the dramatic influence of P-gp transport on morphine and methadone absorption, distribution and elimination seen in rodents has not been observed in all human *in vivo* studies. However, due to the small number of studies and potential issues with inhibitor efficacies, a role for P-gp in determining brain morphine exposure following intravenous heroin use cannot be ruled out. In addition, there is good clinical evidence to suggest that changes in P-gp activity may affect the brain distribution of methadone during the course of opioid substitution treatment. Unfortunately, the role for P-gp in determining endogenous opioid distribution, and hence modulation of their influence on reward and dependence, has yet to be determined *in vivo* in humans.

1.5.4. Variability in P-glycoprotein expression and function

Based upon the existing *in vitro* and *in vivo* evidence describe above, it can be expected that interindividual variability in P-gp expression and function might influence the euphoric/reward response to illicit opioids, and the development of opioid dependence, by modulating morphine exposure, and also possibly the endogenous opioid system (through β-endorphin). In addition, interindividual variability in P-gp may also influence response to opioid substitution therapies by altering methadone or buprenorphine brain distribution. Therefore, identifying the sources of interindividual variability in P-gp activity could be important for understanding and predicting an individual's risk and/or severity of opioid dependence, as well as their opioid substitution treatment dose requirements and/or response.

1.5.4.1. Expression

Significant interindividual variability in P-gp expression has been observed in most, if not all, tissues in which the transporter is found. For example, P-gp protein expression varies 2- to 10-fold in the intestine (Thorn et al., 2005) and 3- to 4-fold in lymphocytes (Becquemont et al., 2000), with a large variability in P-gp expression also described in brain microvessels (Dauchy et al., 2008). Furthermore, in the liver, *ABCB1* messenger ribonucleic acid (mRNA) expression in healthy subjects varies 200-fold, with a corresponding 20- to 50-fold variability in protein levels (Owen et al., 2005; Meier et al., 2006).

In terms of the mechanisms behind this variability, numerous compounds have been shown to induce P-gp expression, the majority of which are P-gp substrates. These P-gp inducers are believed to act at the transcriptional level (Kuwano et al., 2004), increasing *ABCB1* mRNA expression through nuclear receptors like the liver X receptor, farnesoid X receptor, pregnane X receptor, the α and γ peroxisome proliferator-activated receptors, and their co-factors (Borst & Elferink, 2002). As mentioned previously, clinically significant drug-drug interactions have been observed between methadone and P-gp inducers, resulting in opioid withdrawal in MMT

patients (Kreek et al., 1976a; Kreek et al., 1976b; Eich-Hochli et al., 2003). With regard to opioids, oxycodone has been shown to increase P-gp expression in the intestine, liver, kidney and brain of rats by 2.0-, 4.0-, 1.6-, and 1.3-fold, respectively, with corresponding decreases in paclitaxel distribution (Hassan et al., 2007). For morphine, repeated exposure has been associated with increases in P-gp expression of 2-fold in whole brain homogenate, and around 1.4-fold in rat cortex and hippocampus, with a consequent decrease in morphine antinociceptive effect (Aquilante et al., 2000; Yousif et al., 2008).

Apart from the studies discussed above, little research has investigated the effects of other proposed P-gp inducers on opioid distribution *in vivo* in humans. Furthermore, the potential P-gp induction by long-term opioid exposure has yet to be investigated *in vivo* in humans. As such, the direct effects of long-term opioid administration on P-gp expression and/or function, and how they might relate to opioid substitution treatment response, remain to be elucidated.

In addition to pharmacological induction, cell stress and damage (such as exposure to X-rays, heat shock or cytotoxins) are also strong *in vitro* inducers of P-gp expression (Seelig, 1998; Ledoux et al., 2003). *In vivo*, induction of peripheral inflammation in rats results in a significant increase in BBB expression of P-gp, with a corresponding decrease in morphine brain uptake and analgesia, an effect that could be reversed by P-gp inhibition (Seelbach et al., 2007). Immune status also appears to play a role in P-gp regulation, which is of particular relevance to chronic opioid use where there is evidence of immune system modulation (Nair et al., 1986; Vallejo et al., 2004).

1.5.4.2. Function (drug-drug interactions)

In addition to inducing P-gp expression, many medications may inhibit P-gp transport. These P-gp inhibitors tend to be either very high affinity substrates for P-gp that bind non-competitively and prevent binding of other substrates, or are efficient inhibitors of the ATP hydrolysis required for transport (Wang et al., 2003). In addition to the studies in healthy

volunteers discussed so far (see sections 1.5.2.3 and 1.5.3.2.2), co-administration of P-gp inhibitors in treatment settings has been found to result in up to 33-fold increases in the C_{max}, and up to 58-fold increases in the AUC, of numerous medications, with severe drug toxicity in some cases (see Table 1-2). As such, drug-drug interactions with P-gp have been shown to have clinically relevant consequences.

A number of dietary compounds such as flavonoids, as well as numerous pesticides, have also been identified as potential P-gp inhibitors, whilst some excipients found in drug preparations can also inhibit P-gp function (Martin-Facklam et al., 2002).

Table 1-2. Clinically relevant drug-drug interactions due to P-glycoprotein inhibition.

Primary drug	Inhibitor drug	PK	PD	Reference
Digoxin	Erythromycin	2.0-fold ↑ C_{max}		(Maxwell et al., 1989)
	Clarithromycin	↑ [plasma] ↓ CL_R		(Wakasugi et al., 1998)
	Itraconazole	↑ [plasma] ↓ CL_R		(Alderman & Allcroft, 1997)
	Verapamil	1.8-fold ↑ [plasma] 50% ↓ CL_R	↑ cardiac toxicity	(Klein et al., 1982)
	Quinidine	↑ [plasma] ↓ CL_R	↑ cardiac toxicity	(Doering, 1979)
Fexofenadine	Erythromycin	2.9-fold ↑ AUC 1.8-fold ↑ C_{max}		(Davit et al., 1999)
	Ketaconazole	2.6-fold ↑ AUC 2.3-fold ↑ C_{max}		
Ritonavir	Ketaconazole	3-fold ↑ [CSF]/[plasma]		(Khaliq et al., 2000)
Saquinavir	Erythromycin	1.9-fold ↑ AUC 2.1-fold ↑ C_{max}		(Grub et al., 2001)
	Ketaconazole	1.9-fold ↑ AUC 2.7-fold ↑ C_{max} 6-fold ↑ [CSF]/[plasma]		(Khaliq et al., 2000)
	Ritonavir	58-fold ↑ AUC 33-fold ↑ C_{max}		(Merry et al., 1997)
Talinolol	Erythromycin	1.3-fold ↑ AUC		(Schwarz et al., 2000)
Vincristine/ dactinomycin/ cyclophosphamide	Cyclosporine		↑ systemic toxicity	(Theis et al., 1998)
Artorvastatin	Esomeprazole/ clarithromycin		↑ toxicity (rhabdomyolysis)	(Sipe et al., 2003)

Table does not include effects that may have been due to both P-gp and CYP3A4 interactions. PK: pharmacokinetic effects. PD: pharmacodynamic effects. C_{max}: maximum plasma concentration. [plasma]: plasma concentration. CL_R: renal clearance. AUC: area under the plasma concentration-time curve. $T_{1/2}$: half-life. [CSF]/[plasma]: cerebrospinal fluid:unbound plasma concentration ratio.

In terms of opioids, both methadone (IC_{50} = 7.5 uM, (Stormer et al., 2001)) and high concentrations of morphine (IC_{50} > 50 μM, (Schwab et al., 2003)) have been shown to inhibit human P-gp *in vitro*. Whether buprenorphine is a P-gp inhibitor is unknown.

Therefore, numerous environmental factors (such as pharmaceutical/dietary inducers and inhibitors, or cellular stress and inflammation) can combine to determine P-gp expression and/or function. In addition, genetic variability in the *ABCB1* gene encoding P-gp may also be an important factor in determining P-gp expression and function, and hence opioid response.

1.6. *ABCB1* genetic variability

1.6.1. *ABCB1* gene structure

The human ATP-binding cassette transporter B1 gene, *ABCB1* (formerly termed multi-drug resistance protein 1 gene, *MDR1*) is located on chromosome 7 at position q21.1 and is over 120 kilobases (kb) in size (Callen et al., 1987). The gene consists of 29 exons numbered -1 to 28, and has two possible transcription promoter sites, one at the beginning of exon -1 and the other within exon 1, with the latter found to be preferentially expressed in most cells. However, since the ATG translation start site lies within exon 2, the actual protein coding sequence consists of 26 exons, 2 to 28 (Chen et al., 1990; Choudhuri & Klaassen, 2006). In terms of transcription regulation, numerous transcription regulatory elements are located within the first 300 bases upstream of the transcription start sites. Furthermore, there is an *ABCB1* enhancer region located at around 8 kb upstream, which is responsible for modulation by the nuclear receptors described in section 1.5.4.1.

1.6.2. Single nucleotide polymorphisms

Although polymorphisms in the *ABCB1* gene were first identified in 1989 (Kioka et al., 1989), research since had primarily focused on acquired mutations in tumor cells associated with multidrug resistance. It wasn't until 2000 that the first systematic screening for *ABCB1*

genetic variability was conducted by Hoffmeyer and colleagues (2000), which revealed the potential significance of heritable *ABCB1* mutations in influencing drug disposition. This landmark study not only identified 15 naturally occurring single nucleotide polymorphisms (SNPs) in healthy Caucasians, but more significantly found that the variant allele of a synonymous (not resulting in an amino acid change) SNP, C3435T, was associated with decreased duodenal P-gp expression and consequently increased intestinal absorption of the P-gp substrate digoxin. Primarily as a result of this study, the C3435T SNP has been by far the most studied genetic variant of *ABCB1*. However, the *ABCB1* gene has proven to be highly polymorphic, with over 1200 polymorphisms reported within the *ABCB1* gene, and over 60 SNPs currently identified within the transcribed (exonic) sequence (NCBI, 2010). The most common exonic SNPs observed in the Caucasian population are shown in Table 1-3.

Table 1-3. Common *ABCB1* single nucleotide polymorphisms found in Caucasians.

SNP	rs number	Location	Effect	Frequency (%)
A61G	rs9282564	Exon 2	Asn21>Asp	17.6
G1199A	rs2229109	Exon 11	Ser400>Asn	5.5-12.9
C1236T	rs1128503	Exon 12	Synonymous	48.9
G2677T(A)	rs2032582	Exon 21	Ala893>Ser(Thr)	62.0(2)
C3435T	rs1045642	Exon 26	Synonymous	48.3-50.5

Sources: Hoffmeyer et al. (2000); Cascorbi et al. (2001); Kim et al. (2001).

1.6.3. *ABCB1* haplotypes

In Caucasians, the many SNPs have been reported to form around 64 discernable haplotypes. Significant linkage disequilibrium has been reported across the *ABCB1* gene, especially between the three variant alleles of 1236, 2677 and 3435 (Hoffmeyer et al., 2000; Kroetz et al., 2003; Marzolini et al., 2004), as such, the most common haplotypes are those previously termed *MDR1*1* (wild-type) and *MDR1*2* (variant at positions 1236, 2677 and 3435), which account for around 63% of chromosomes (Kim et al., 2001; Kroetz et al., 2003).

It is important to note that substantial inter-ethnic variability is observed in the frequency of various SNPs and haplotypes of the *ABCB1* gene. For example, the frequency of the wild-type C allele at position 3435 ranges from 84% in African American to 34% in South-west Asian populations (Ameyaw et al., 2001), whilst the frequency of the *MDR1*2* haplotype is only around 6-7% in African-Americans as compared to 27% in Caucasians (Kim et al., 2001).

1.6.4. Functional consequences of *ABCB1* genetic variability

Since the discovery by Hoffmeyer and colleagues (2000) of the influence of the C3435T SNP on digoxin pharmacokinetics, there has been a rush to examine the potential of *ABCB1* genotyping in the prediction of other drug response *in vivo*. Parallel to these studies, a need for a better understanding of the mechanistic basis behind SNP effects on expression and function of P-gp has prompted numerous *in vitro* and *ex vivo* investigations.

ABCB1 SNPs and haplotypes have the potential to affect both the expression and function of P-gp, with clinically relevant consequences. The proposed 2D structure and organisation of P-gp provides us with some clues as to the site of mutations that might affect P-gp function. For example, mutations affecting ATP-binding sites (NBDs) will have obvious consequences for the ATP hydrolysis necessary for transport. As mentioned previously (section 1.5.1), the flexible linker region located between the homologous halves of P-gp, as well as the transmembrane domains, may also be important for NBD communication and substrate recognition, respectively, and as such mutations in these areas may result in modulation of transport capacity. Unfortunately, as shown in Figure 1-3, none of the three common non-synonymous SNPs discussed above lie directly within any of these regions, and as such their functional consequences are difficult to predict.

With regards to the common synonymous SNPs of *ABCB1* (C1236T and C3435T), if they were to produce an effect, they would be expected to influence P-gp expression rather than function, however, as will be discussed below, they may in fact play a role in both.

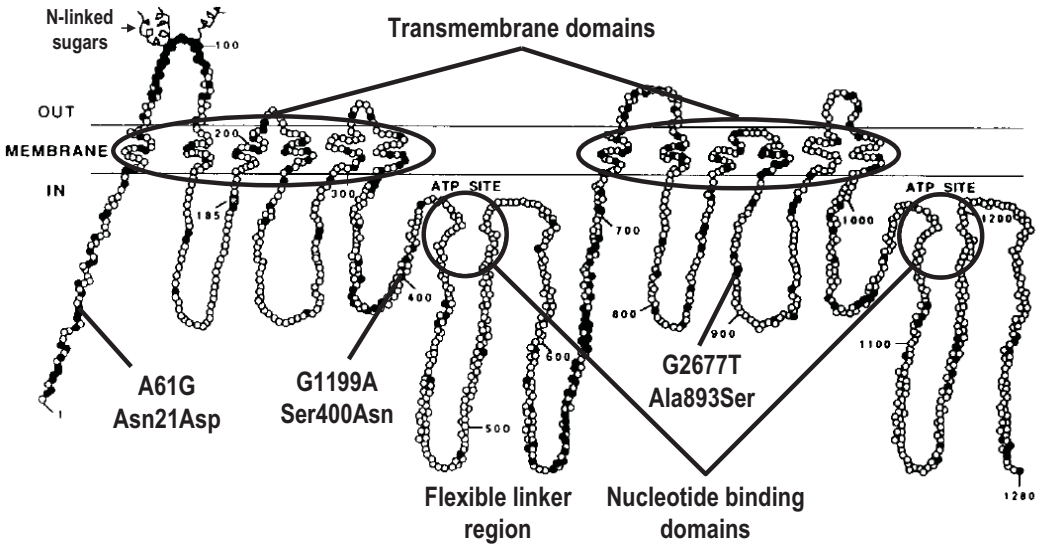

Figure 1-3. Functionally significant regions of P-gp and the location of common *ABCB1* non-synonymous mutations.

Each small circle represents an amino acid (1-1280). Open circles represent conserved amino acid sequences homologous with mouse *mdr1*. Adapted from a figure originally published in Gottesman MM & Pastan I. The multidrug transporter, a double-edged sword. *J Biol Chem*. 1988; 263:pp12164, Figure 1. © the American Society for Biochemistry and Molecular Biology.

The following sections will discuss the research conducted to date, including *in vitro* expression analyses and human *ex vivo* and clinical studies, aimed at elucidating the impact of *ABCB1* genetic variability on P-gp expression and function. As discussed above, there are marked ethnic differences in the frequencies of *ABCB1* mutations, whilst the functional effects of SNPs also appear to differ somewhat between ethnicities. As such, for simplification, the functional significance of *ABCB1* genetic variants will be discussed in the context of Caucasians only, as this is the only ethnic population studied in this thesis.

1.6.4.1. *In vitro* expression and function

Numerous *in vitro* studies have employed cells transfected with wild-type or mutant P-gp to examine their effects on expression and transport. However, despite the application of similar experimental techniques, results have varied significantly, depending on the P-gp substrates tested and the expression systems employed. A complete list of studies and their results are given in Appendix A: Table A-2, and summaries of their findings are given here.

A61G: Of the two studies investigating the synonymous A61G SNP, neither observed an effect on expression, whilst paclitaxel transport was reduced in one study (Kimchi-Sarfaty et al., 2002), but not the other (Gow et al., 2008). There was no effect of the G variant on transport of the other 7 compounds tested.

G1199A: *In vitro* studies have consistently shown that the G1199A SNP does not influence the expression of P-gp, however, reports of its effects on P-gp function have varied considerably. Whilst the majority of results indicate no effect on P-gp function, the variant has shown a decreased transport of some compounds (rhodamine and verapamil), but an increase in transport of others (vinblastine, vincristine, amprenavir, indinavir, lopinavir, ritonavir, saquinavir and doxorubicin). As such, the functional consequences of the G1199A SNP *in vitro* remain unclear, with significant variability both between and within substrates and expression systems.

C1236T: Only two *in vitro* studies have previously examined the functional effects of the C1236T variant on P-gp function. In the first study by Salama and colleagues (2006), variant expressing cells were found to have a diminished transport capacity for rhodamine, vinblastine and vincristine. Alternatively, a more recent investigation by Kimchi-Sarfaty and colleagues (2002) indicated that the T variant alone had no significant effect on expression or function. Interestingly, whilst the C1236T SNP causes a change in mRNA folding (Figure 1-4), it appears to have no significant influence on mRNA stability (Wang & Sadee, 2006).

G2677T: Findings have been relatively consistent for the G2677T SNP, and paclitaxel transport has nearly always been decreased in variant transfected cells. For other compounds, the majority of findings indicated a reduction in transport in variant cells or no effect, depending on the substrate. Nearly all studies have indicated a lack of effect on expression, and (unlike C1236T and C3435T) the G2677T SNP has no significant effect on mRNA folding (Figure 1-4, (Wang & Sadee, 2006)), thus indicating effects are due to a functional

change. In support of this, 3D structural simulations have predicted the conversion of amino acid 893, from alanine to the variant serine, would produce a kink in an important cytoplasmic helical region between transmembrane segments 10 and 11, modifying interactions with the ATP-binding domain, and thus P-gp's transporting capabilities (Sakurai et al., 2007).

C3435T: Given that the C3435T SNP was the first to be identified as a clinically relevant heritable mutation of *ABCB1*, and has been the most extensively studied SNP *in vivo*, there have been surprisingly few *in vitro* functional studies. Those that have been conducted have demonstrated a decrease in the *in vitro* transport of vincristine, but not verapamil, digoxin, paclitaxel, daunorubicin, calcein-AM or cyclosporine, with mixed results for rhodamine and vinblastine. The mechanism behind the C3435T SNP's potential effect on P-gp transport remains debatable, although detailed studies have produced evidence that it may be associated with changes to mRNA secondary structure, resulting in decreased mRNA stability and consequently lower mRNA levels (Figure 1-4) (Wang et al., 2005; Wang & Sadee, 2006).

1.6.4.1.1. Haplotypes

Experiments investigating the variant haplotypes 61G/1199A, 61G/2677T and 1199A/2677T have found that, whilst none were associated with altered P-gp expression, they all displayed decreased transport of paclitaxel (Kimchi-Sarfaty et al., 2002). For 1236T/2677T, 1236T/3435T and 2677T/3435T haplotypes, most studies indicate the variants have decreased transport function, whilst the 1236T/2677T and 2677T/3435T variants were also associated with decreased P-gp expression. Larger haplotypes have also been investigated, with the 1236T/2677T/3435T variant haplotype exhibiting decreased expression and function in some studies, whilst the 61G/1236T/2677T/3435T variant haplotype has been associated with a decreased paclitaxel transport, but no effect on expression.

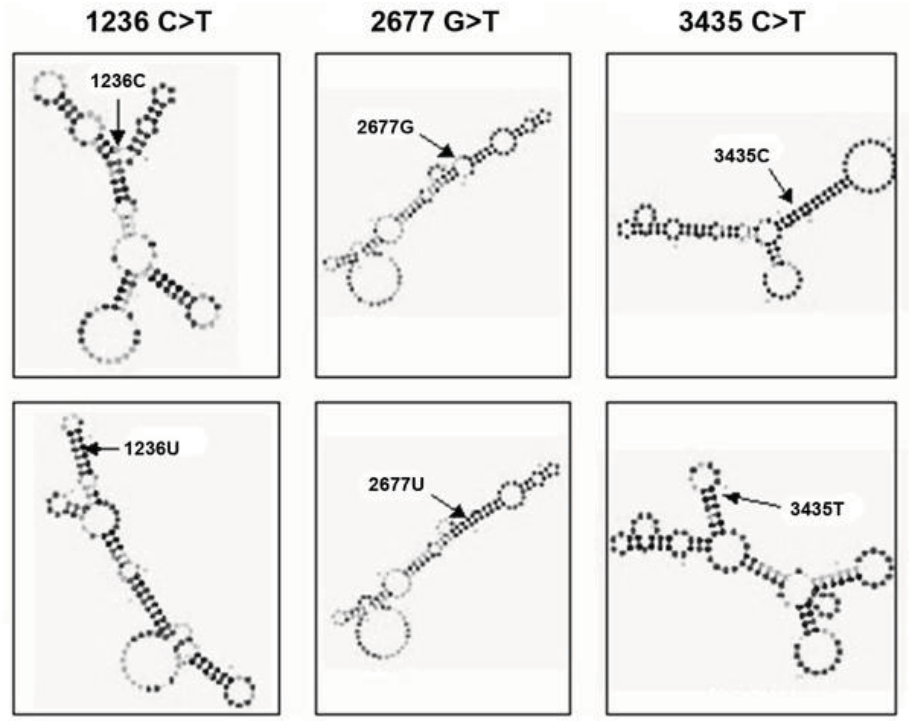

Figure 1-4. Results of mRNA folding predictions (Mfold) displaying how the *ABCB1* genetic variants C1236T (left) and C3435T (right), but not G2677T (middle), can significantly alter the folding and secondary structure of *ABCB1* mRNA.

Top panels are wild-type, bottom panels are variant mRNA. Reprinted with kind permission from Springer Science+Business Media: Wang D & Sadee W (2006) Searching for polymorphisms that affect gene expression and mRNA processing: example *ABCB1* (*MDR1*). *Aaps J* **8:**ppE518, Figure 4.

ABCB1 haplotypes may also affect the efficacy of P-gp inhibitors. For example, whilst Kimchi-Sarfaty and colleagues (2007) found no significant effect of the C1236T, G2667T or C3435T SNPs, or their haplotypes, on P-gp expression or transport, haplotypes containing the 3435T variant along with one or both of the 1236T and 2677T variants (i.e. 1236T/3435T, 2677T/3435T or 1236T/2677T/3435T haplotypes) were associated with significantly decreased P-gp inhibitory efficacy of cyclosporine and verapamil. These findings for the 1236T/3435T haplotype were recently replicated in a study by Hung and colleagues (2008), that found the 2677A/3435T, 1236T/2677A/3435T and 1236T/2677T/3435T haplotypes were also associated with decreased inhibitor efficacy.

Interestingly, Kimchi-Sarfaty and colleagues (2007) were also able to demonstrate that P-gp derived from the 1236T/3435T, 2677T/3435T or 1236T/2677T/3435T haplotypes had a

susceptibility to trypsin degradation different to that of wild-type P-gp, implying these variant haplotype proteins possessed a different tertiary protein structure. Whilst this seems unusual for synonymous SNPs (which do not cause any amino acid change), it has been proposed that mutations, such as the C1236T, G2677T and C3435T SNPs, that encode for rarer codons may cause a translation pause affecting the final folding of the protein (Sauna et al., 2007). As such, there is evidence that, in addition to their potential impact on expression, the C1236T and C3435T SNPs could also cause changes in the tertiary conformation of P-gp affecting its function (Kimchi-Sarfaty et al., 2007).

Finally, the findings of Kimchi-Sarfaty and colleagues (2007) also highlight the importance of examining *ABCB1* haplotypes instead of individual SNPs, as significant effects of the C3435T variant on protein folding were only observed in the presence of at least one other SNP encoding a rare codon (C1236T or G2677T).

In summary, whilst *in vitro* studies can provide some insight into the potential functional significance of *ABCB1* SNPs, the effects observed so far appear to be largely substrate-dependent, with poor agreement between studies. Unfortunately, no *in vitro* studies have examined the impact of *ABCB1* genetic polymorphisms on opioid transport.

1.6.4.2. *Ex vivo* expression and function

One major alternative to *in vitro* studies has been the *ex vivo* analysis of P-gp expression and transport in isolated human tissues. These studies have a distinct advantage over *in vitro* techniques in that the isolated cells and tissues more closely reflect *in vivo* P-gp expression and function. References and details of all the *ex vivo* studies conducted so far are given in Appendix A: Table A-3.

In general, previous *ex vivo* research has found no link between the A61G, G1199A or C1236T SNPs with either P-gp expression or function in duodenal tissue or in peripheral

blood mononuclear cells (PBMCs). Furthermore, findings have consistently indicated a lack of influence of the G2677T SNP on *ex vivo* P-gp expression. There is evidence that G2677T variant genotypes possess diminished transport capacity, although this has not been the case in all studies. For the C3435T SNP, there is also some evidence to suggest an association between variant genotypes and decreased P-gp expression and function, but again results have varied between studies.

In terms of haplotypes, the 2677T/3435T variant haplotype has been associated with decreased transport of certain cytokines, but not cyclosporine, with no effect on P-gp expression. Alternatively, the common variant haplotype, 1236T/2677T/3435T, was found not to effect the *ex vivo* expression or function of P-gp in PBMCs, but has been associated with decreased mRNA and protein expression in the duodenum. It should be noted however that our existing knowledge of the *ex vivo* impact of these haplotypes, as well as of the A61G, G1199A, C1236T SNPs, is restricted to the findings of only one or two studies each, and is therefore far from conclusive.

As discussed previously, the BBB expression and function of P-gp may be just as (if not more) important as intestinal P-gp for opioids such as methadone. Understandably, the BBB expression of P-gp in humans is substantially more difficult to study, however, two post-mortem investigations have indicated that the 3435 C/C genotype may be associated with higher temporal lobe P-gp expression (although neither reached statistical significance) (Vogelgesang et al., 2002; Vogelgesang et al., 2004).

In conclusion, *ex vivo* studies have also been inconclusive, but do suggest that *ABCB1* genetic variants can influence the expression and function of P-gp in humans, with the greatest evidence existing for the G2677T and C3435T SNPs affecting function and expression, respectively. Unfortunately, as with *in vitro* studies, no *ex vivo* studies have investigated the impact of *ABCB1* genetic variability on P-gp transport of opioids.

1.6.4.3. *In vivo* function and clinical significance

A similar picture has arisen from human *in vivo* studies which have also been contradictory, with genetic influences generally dependent on the specific organs and substrates investigated (Gerloff et al., 2002; Johne et al., 2002).

1.6.4.3.1. Function in healthy subjects

Numerous studies have investigated the impact of *ABCB1* genetic variability on the plasma pharmacokinetics of various probe drugs. Possibly as a result of the original study by Hoffmeyer and colleagues (2000) described in section 1.6.2, the most commonly investigated probe drug has been digoxin. Interestingly, a 2005 meta-analysis on the influence of the *ABCB1* C3435T polymorphism on digoxin pharmacokinetics and *ABCB1* gene expression concluded that it affected neither (Chowbay et al., 2005). Alternatively, a more recent analysis by Comets and colleagues (2007) using population pharmacokinetic models concluded that there was a significant effect of C3435T in predicting the digoxin V_d. Therefore, even for this extensively studied P-gp substrate, the findings on the functional effects of *ABCB1* variants in healthy humans remain inconclusive.

A similar discordance between studies has been observed for most other probe substrates, however, these investigations have dealt almost exclusively with the relationship between *ABCB1* genetic variability and plasma pharmacokinetics (for a summary of previous clinical *ABCB1* pharmacogenetic studies in healthy volunteers, see Appendix A: Table A-4). As mentioned earlier, the influence of P-gp activity on BBB permeability may be more important than its influence on intestinal absorption and clearance for opioids such as methadone. Therefore, the effects of *ABCB1* polymorphisms on CNS distribution may be more relevant.

Interestingly, an investigation by Brunner and colleagues (2005) measuring the brain distribution of the P-gp substrate verapamil by positron emission tomography scans, found no

significant differences in the brain AUC between subjects homozygous for variants at 1236, 2677 and 3435, and subjects homozygous wild-type at these positions. However, the functional consequences of *ABCB1* genetic polymorphisms have so far proved largely substrate-dependent, and verapamil transport has not yet been shown to be affected by *ABCB1* variants in human cells *in vitro*, or in human *ex vivo* and *in vivo* studies. Hence, whether verapamil is the best probe to analyse the effects of *ABCB1* variants on brain distribution is questionable. In addition, there is evidence that the 1236T, 2677T and 3435T variant SNPs, as well as the 1236T/2677T/3435T variant haplotype, are associated with increased mefloquine neuropsychiatric side effects in women (Aarnoudse et al., 2006). Therefore, a sex-specific role for *ABCB1* genetic variability in influencing the CNS distribution of P-gp substrates cannot be ruled out.

1.6.4.3.2. Functional effects on opioids

In the case of opioids, studies in healthy subjects investigating the plasma pharmacokinetics and miotic or respiratory depressive effects of oral loperamide have found no significant relationship with the *ABCB1* 3435 variant (Pauli-Magnus et al., 2003; Skarke et al., 2003b). However, there is evidence that morphine brain distribution may be affected by this SNP. For example, pharmacokinetic modelling of morphine in plasma and CSF of neurosurgical patients has revealed a significant association between the homozygous mutant genotype and increased morphine CSF concentrations (Meineke et al., 2002), although the clinical significance of this effect remains less clear. Alternatively, Coulbault and colleagues (2006) found no significant association between the 3435 SNP and post-operative morphine dose requirements in surgery patients, and whilst there was a trend for a decreased requirement of antiemetic treatment among homozygous wild-type patients, this was also not significant.

With regards to morphine for pain relief in cancer pain patients, Campa and colleagues (2008) demonstrated that, during the first 7 days of morphine treatment, the 3435 SNP was

significantly associated with greater pain relief, with the homozygous wild-type (C/C) and homozygous variant (T/T) genotypes predicting 68% of morphine non-responders and 63% of responders, respectively. In fact, 3435 genotype was a better predictor of morphine effects than morphine doses, which were highly variable (10-500 mg/day) and did not correlate whatsoever with changes in pain scores. Therefore, there is strong clinical evidence for a role of *ABCB1* genetic variability in determining the early-stage effectiveness of morphine for cancer pain (i.e. prior to the confounding factor of disease progression (Ross et al., 2008)).

As mentioned previously, the *ABCB1* gene is highly polymorphic, with significant linkage disequilibrium reported between numerous variant loci. Therefore, as previous studies have indicated, consideration of the effect of *ABCB1* haplotypes, in place of individual SNPs, may be more likely to accurately predict P-gp expression and function (Johne et al., 2002). This may also be the case for opioids. For example, whilst Skarke and colleagues (2003b) found that the intestinal absorption and CNS effects of oral loperamide were not significantly associated with the *ABCB1* 3435 variant (as mentioned above), an investigation of haplotypes formed by the 2677 and 3435 SNPs revealed that subjects carrying the *ABCB1* haplotype G2677/T3435, had significantly higher (1.5-fold) plasma loperamide concentrations than non-carriers. Similarly for morphine, Coulbault and colleagues (2006) found that the *ABCB1* GG2677/CC3435 diplotype was a better predictor of morphine side effects (antiemetics for post-operative nausea and vomiting) than either of the two SNPs analysed separately.

As discussed previously, both 2677 and 3435 are in strong linkage disequilibrium with the exon 12 SNP, C1236T, and whilst these three loci account for the majority of the *ABCB1* haplotypes observed in Caucasians, an additional 60 less frequent haplotypes have also been identified (see section 1.6.3). As such, haplotypes extending beyond the 2677 and 3435 SNPs are likely to prove even more informative.

In summary, the functional consequences of common *ABCB1* genetic variants are relatively moderate and substrate-dependent, and do not equate to anything near a loss of function, or the effects seen with pharmacological antagonism. Nonetheless, there is evidence to suggest that polymorphisms at positions 2677 and 3435 may have clinically significant effects on the P-gp transport of opioids, particularly morphine, and controlling for the effect of other common *ABCB1* polymorphisms may also be critical.

As such, *ABCB1* genetic variability may be important in determining morphine exposure during illicit opiate abuse, with *ABCB1* variants expected to increase opioid exposure during the early stages of opioid use and abuse, potentially increasing the risk for, or severity of, opioid dependence. In addition, whilst the potential impact of *ABCB1* genetic variability on methadone or buprenorphine exposure during opioid substitution treatment had not yet been investigated, as potential P-gp substrates, *ABCB1* mutations may be expected to result in reduced maintenance dose requirements and could ultimately influence treatment response. Therefore, based on our current knowledge of the P-gp transport of illicit, endogenous and substitution opioids, the proposed impact of *ABCB1* genetic variability on opioid dependence and substitution treatment response can be summarised as shown in Figure 1-5.

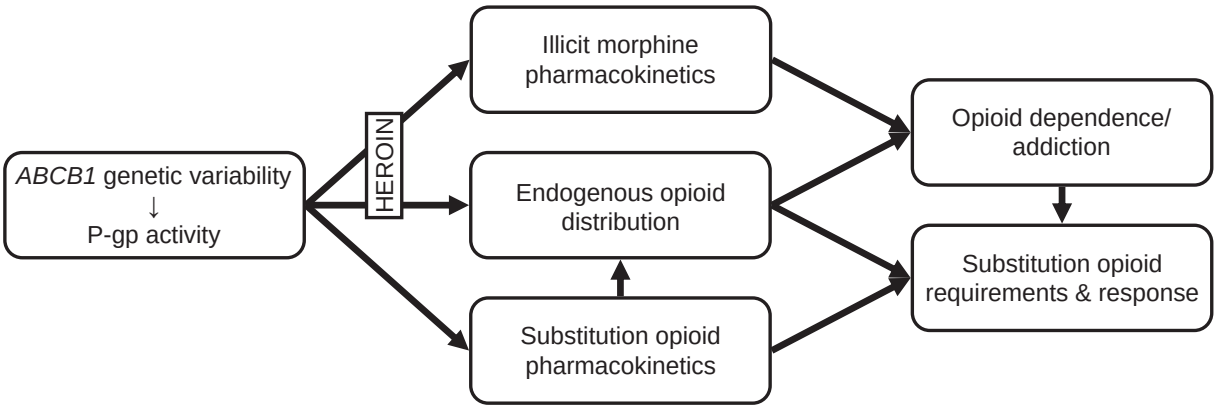

Figure 1-5. The proposed multiple mechanisms by which *ABCB1* genetic variability, affecting P-gp transport, could influence an individual's risk of opioid dependence, severity of addiction and substitution opioid treatment response.

1.7. Summary, aims and hypotheses

The substantial interindividual variability in opioid response necessitates the use of individualized treatment strategies aimed at maximizing patient retention, and hence positive outcomes, in substitution treatment programs. Unfortunately, the existing methods employed for individualizing patient care are only partly successful in retaining patients, with significant treatment drop-out still observed in maintenance programs. In addition, whilst therapeutic drug monitoring of plasma concentrations has been put forward as a solution to many of the problems associated with maintenance dosing (Wolff & Strang, 1999), previous experience has shown that effective target plasma concentrations are still largely variable between individuals (Dyer et al., 1999). Therefore, the application of pharmacogenetic approaches to identify factors that affect the opioid dose-plasma concentration-effect relationship could provide a useful clinical tool for establishing individualized target doses and/or plasma concentrations required for efficacious opioid substitution treatment.

The *ABCB1* gene provides a good candidate for this approach, as its product, the P-glycoprotein efflux transporter, has the ability to limit the intestinal absorption and brain distribution of opioids. In addition, the *ABCB1* gene is highly polymorphic, with some genetic variants associated with clinically relevant changes in opioid response. Ultimately, it is hoped that identification of the role of *ABCB1* genetic variability in opioid response may provide clinicians with a useful dose optimization tool for the successful treatment of opioid dependence. However, at the time of commencing this thesis, several major gaps in the published knowledge of the clinical relevance of *ABCB1* genetic polymorphisms in modulating opioid response were identified;

Firstly, the influence of *ABCB1* genetic variability on patient response to opioid substitution treatments for opioid dependence had not been investigated, nor had the potential relationship between *ABCB1* genetic variability and susceptibility for illicit opioid abuse and dependence.

Secondly, the direct effects of long-term illicit (heroin) or maintenance (methadone or buprenorphine) opioid administration on P-gp expression and/or function in humans, and how they might relate to opioid substitution treatment response, remained to be explored. Furthermore, the effects of *ABCB1* genetic variants on tissue expression and function of P-gp in opioid substitution patients was unknown.

Finally, the *in vitro* transport of methadone and β-endorphin had yet to be confirmed in human P-gp-expressing cell lines, whilst the substrate status of buprenorphine and norbuprenorphine had not been investigated.

Therefore, the main aims of this PhD project were;

Aim 1: To investigate *ABCB1* haplotypes formed by the common A61G, G1199A, C1236T, G2677T and C3435T polymorphisms in opioid-dependent methadone and buprenorphine maintenance treatment patients, as well as in non-opioid-dependent healthy controls, in order to examine the role of *ABCB1* genetic variability in multiple facets of opioid dependence and opioid maintenance treatment response. Having first developed new methods for C1236T SNP genotyping and for the estimation of haplotypes from *ABCB1* genotype data (Chapter 2), this primary aim of the thesis was addressed in retrospective examinations of *ABCB1* genetic variability in opioid-dependent subjects stabilised on standard methadone or buprenorphine doses for opioid maintenance treatment (Chapter 3), opioid-dependent subjects stabilised on substantially higher than standard methadone doses for maintenance treatment (Chapter 4), and in non-opioid-dependent, untreated healthy controls (Chapters 3 and 4).

Aim 2: To develop methods for the *ex vivo* analysis of P-gp expression and function in human lymphocytes, and apply these to a pilot clinical investigation of the influence of *ABCB1* genetic variability, prior illicit opioid use, and opioid substitution treatment, on *ex vivo* P-gp expression and function. The *ex vivo* assay development stage and the pilot study are presented in Chapter 5.

Aim 3: To determine whether various opioids, particularly methadone, buprenorphine, norbuprenorphine and β-endorphin, are substrates and/or inhibitors of human P-gp, by performing *in vitro* P-gp transport experiments across human Caco-2 cell monolayers. This aim is addressed in Chapter 6.

Based on the existing literature, the major hypotheses to be tested for this thesis were;

Hypothesis 1: That *ABCB1* genetic variability is associated with the risk of opioid dependence (by increasing morphine exposure), and as such, the frequency of variant *ABCB1* genotypes and/or haplotypes will be higher in opioid-dependent methadone or buprenorphine maintained patients when compared to a non-opioid-dependent healthy control population.

Hypothesis 2: That variant *ABCB1* genotypes and/or haplotypes will be associated with decreased substitution opioid requirements in maintenance treatments for opioid dependence, with potentially less in-treatment withdrawal, or greater adverse opioid side-effects, particularly for methadone.

Hypothesis 3: That variant *ABCB1* genetic variability and chronic opioid exposure could interact to influence *ex vivo* lymphocyte P-gp expression and function in opioid maintenance patients, and that P-gp expression and function may be related to substitution opioid requirements.

Hypothesis 4: That P-gp transport of methadone, buprenorphine, norbuprenorphine and β-endorphin, at pharmacologically relevant concentrations, can be demonstrated *in vitro* using a human cell line, and that all will also inhibit human P-gp transport in this model.

Chapter 2. Determination of ABCB1 genotypes and haplotypes

2.1. Genotyping

2.1.1. Introduction

Clinical studies conducted as part of this PhD aimed to investigate 5 mutations present in the human *ABCB1* gene, namely the A61G (rs9282564), G1199A (rs2229109), C1236T (rs1128503), G2677T (rs2032582) and C3435T (rs1045642) SNPs. As such, appropriately validated and reliable assays were required in order to accurately genotype study participants.

At the commencement of this PhD, polymerase chain reaction – restriction fragment length polymorphism (PCR-RFLP) assays for the A61G, G1199A and C3435T SNPs had already been developed by Dr Janet Coller, Karianne Dahlen and Morten Loennechen (Discipline of Pharmacology, University of Adelaide) based on the methods of Cascorbi and colleagues (2001) (A61G and G1199A) and Tanabe and colleagues (2001) (C3435T).

For the G2677T variant, both a PCR-RFLP assay based on Cascorbi and colleagues (2001), and an allele-specific PCR assay based on Wilson and colleagues (1995), had also previously been developed. Unfortunately, the allele-specific PCR method for detection of the G2677T SNP was found to be inconsistent in terms of sensitivity and specificity, particularly between investigators. As such, irresolvable problems with non-specific amplification eventually meant that the allele-specific PCR assay was abandoned in favour of the less efficient, but more reliable, PCR-RFLP method.

An allele-specific PCR assay for identification of the C1236T SNP had also been developed by Dr Coller, however, similar to the G2677T allele-specific assay, problems with its consistency and specificity meant that a new PCR-RFLP assay had to be developed for C1236T genotyping.

The PCR-RFLP methods employed in this study centre around the use of polymerase chain reaction (PCR), followed by genotype-specific restriction enzyme digests of PCR products.

2.1.1.1. Polymerase chain reaction

Briefly, PCR is a common technique employed to amplify (i.e. generate multiple copies of) a genomic region of interest, in this case regions of the *ABCB1* gene containing SNP mutations. The region of the genome to be amplified is controlled by a pair of oligonucleotide primers (short single-stranded DNA molecules) that are complementary to genome sequences either side of the mutation site (locus) of interest (one forward primer complementary to one strand of the DNA double helix upstream from the target locus, and one reverse primer complementary to the opposite strand downstream from the target locus). Other core components of the reactions are the genomic DNA template to be amplified (i.e. the subject's DNA), a thermostable DNA polymerase enzyme to synthesise the new strands of DNA, and deoxynucleoside triphosphates (dNTPs) that provide the nucleoside building blocks for synthesis and amplification.

The actual PCR reactions take place by cycling through three steps of varying temperatures: firstly, a denaturation step (~95°C) to separate the two strands of the genomic DNA double helix to allow access for the primers; secondly, an annealing (or hybridization) step (~50-72°C) to allow binding of primers to their specific (complementary) target sequences on the single stranded DNA; and thirdly, an elongation step (~72°C) to allow the DNA polymerase to copy the genomic sequence extending from the 3' end of each primer. By cycling through these temperatures, the region of interest is amplified, with the number of copies doubling with each cycle until there are sufficient quantities to allow detection by simple methods such as gel electrophoresis (see section 2.1.2.3.3). It is important when developing a PCR assay that primer sequences, reagent concentrations and annealing temperatures are carefully

optimised in order to ensure both the specific binding of primers only to their target sequences, and the efficient amplification of the region of interest.

2.1.1.2. Restriction fragment length polymorphism analysis

In the case of PCR-RFLP, PCR products are interrogated by restriction digest using restriction enzymes with recognition sequences complementary to either the wild-type or variant sequences of the polymorphic loci. These digest fragments are then separated by agarose gel electrophoresis according to size, with fragment lengths indicating the genotype.

2.1.2. Methods

2.1.2.1. Materials

Ethanol and sucrose were purchased from Chem-supply (Gillman, Australia). Sodium acetate, ethidium bromide, tris-base, boric acid, ethylenediaminetetraacetic acid (EDTA), and bromophenol blue were purchased from Sigma-Aldrich (Castle Hill, Australia). QIAmp® DNA mini kits were purchased from QIAGEN (Doncaster, Australia). Deoxyribonucleoside triphosphates (dNTPs) were manufactured by Finnzymes (Keilaranta, Finland, distributed by Genesearch, Arundel, Australia). ThermoPol Reaction Buffer, *Taq* DNA Polymerase, bovine serum albumin (BSA), and *Taqα*I, *Acu*I, *Eco*0109I, *Ban*I and *Dpn*II restriction enzymes (with corresponding reaction buffers) were manufactured by New England Biolabs (Beverly, Massachusetts, USA, distributed by Genesearch). *Taq*I, *Eco*57I and *Bsp*143I restriction enzymes (and corresponding reaction buffers), oligonucleotides primers and pUC19/*Hpa*II DNA molecular weight marker were purchased from GeneWorks (Thebarton, Australia). Agarose I was manufactured by AMRESCO (Solon, Ohio, USA, distributed by Astral Scientific, Gymea, NSW, Australia). Omnigel-Sieve Agarose was manufactured by Edwards Instrument Co. (Narellan, Australia, distributed by Adelab Scientific, Thebarton, Australia). BigDye version3.0 sequencing reagents were manufactured by Applied Biosystems (Scoresby, Australia).

2.1.2.2. Genomic DNA isolation, purification and quantification

Genomic DNA was isolated from 200-400 μL of whole blood collected in EDTA tubes, or ≤ 40 mg of liver tissue, using a QIAamp® DNA mini kit according to the manufacturer's protocol. DNA was eluted in 200 μL of autoclaved Milli-Q water and further purified by ethanol precipitation as follows: Firstly, 20 μL of 3 M sodium acetate and 400 μL of ethanol were added to the DNA solution and vortexed. DNA was then precipitated at -80°C for 30 minutes (or -20°C overnight) before being pelleted by centrifugation at full speed (14,000 rpm / 16,000 rcf) for 30 minutes. Supernatants were aspirated and DNA pellets dried at 37°C for 5-10 minutes (or overnight at room temperature) before being resuspended in 30-50 μL of autoclaved milli-Q water. Purified DNA solution (7 μL) was then diluted 1 in 10 with water and the absorbance at 260 (A_{260}) and 280 (A_{280}) nm measured using a spectrophotometer (Hitachi, model U-2000, Hitachi Ltd., Tokyo, Japan) to determine DNA concentration (A_{260} x 50 μg/mL x dilution factor = concentration (ng/μL)) and purity (A_{260}/A_{280}).

For each DNA sample, a working solution of 50 μL of 20 ng/μL DNA was prepared for use in PCR reactions. All DNA samples and working solutions were stored at 4°C.

2.1.2.3. General genotyping protocols

2.1.2.3.1. Polymerase chain reaction setup

To prevent premature polymerization and primer binding, all PCR reactions were prepared on ice. Firstly, master mixes consisting of all reaction components except genomic DNA were prepared in a designated PCR setup area which was kept free from genomic DNA and PCR products at all times. Enough master mix was prepared for all required reactions for a particular run, vortexed briefly to mix, then pulse centrifuged (14,000 rpm for ~5 seconds). Twenty-five microlitre aliquots of master mix were then pipetted into 0.5 or 0.2 mL thin-walled PCR tubes (Bio-rad, Gladesville, NSW, Australia) for each PCR reaction. Genomic DNA was then added to tubes outside of the designated PCR setup area. PCR tubes were

vortexed briefly and pulse spun in a centrifuge before being placed into a PTC-100 or PTC-200 Peltier Thermal Cycler (manufactured by MJ Research, Waltham, Massachusetts, USA, distributed by GeneWorks) and reactions run using a heated lid (to prevent condensation) at optimal temperature programs for the specific assay. PCR products were subjected to agarose gel electrophoresis to confirm amplification of target sequence (see section 2.1.2.3.3).

Primer sequences and expected PCR product sizes for the PCR-RFLP assays are shown in Table 2-1, whilst their specific binding sites and amplification sequences are shown in Appendix C. Optimized master mix and cycling conditions for each assay are shown in Table 2-2.

2.1.2.3.2. Restriction enzyme digest setup

Restriction enzyme digest master mixes (containing all components except PCR product) were prepared on ice, vortexed to mix, then pulse spun. Ten microlitres of digest master mix was then added to 20 μL of PCR product in a 0.5 or 0.2 mL thin-walled PCR tube, vortexed to mix, pulse spun and placed in thermal cycler. Digest reactions were run using a heated lid (to prevent condensation) at optimal temperature programs for the specific digestion enzyme. The digestion enzymes and their optimized digestion conditions for each PCR-RFLP assay are shown in Table 2-3.

Digest products were then subjected to agarose gel electrophoresis for analysis of restriction digest fragments (see section 2.1.2.3.3).

Table 2-1. Primer sequences and expected product size for polymerase chain reaction amplification.

SNP	Name	Sequence	PCR product size
A61G	MDR-1b*	5'-AGG AGC AAA GAA GAA GAA CTT TTT TAA ACT GAT-3'	179 bp
	MDR-6	5'-GAT TCC AAA GGC TAG CTT GC-3'	
G1199A	MDR-24*	5'-CAG CTA TTC GAA GAG TGG GC-3'	258 bp
	MDR-25	5'-CCG TGA GAA AAA AAC TTC AAG G-5'	
C1236T	MDR-24*	5'-CAG CTA TTC GAA GAG TGG GC-3'	527 bp
	C1236-R	5'-ATC CTG TCC ATC AAC ACT GAC-3'	
G2677T	MDR-9*	5'-TGC AGG CTA TAG GTT CCA GG-3'	
	MDR-10a	5'-TTT AGT TTG ACT CAC CTT CCC-3'	224 bp
	G2677RWT	5'-GTT TGA CTC ACC TTC CCA GC-3'	220 bp
	G2677RV	5'-GTT TGA CTC ACC TTC CCA GA-3'	220 bp
C3435T	C3435TF*	5'-TTG ATG GCA AAG AAA TAA AGC-3'	207 bp
	C3435TR	5'-CTT ACA TTA GGC AGC GAC TCG-3'	

*Forward primer, bp = base pairs

2.1.2.3.3. Agarose gel electrophoresis

Electrophoresis through an agarose gel allowed the separation, based on size, of charged molecules such as DNA. Using the intercalating agent ethidium bromide that binds to DNA, PCR or restriction digest bands could then be observed under ultraviolet light (causing intercalated ethidium bromide to fluoresce) and photographed for analysis.

All PCR products were run on 4% 2:1 gels of 3-4 cm in length. These were prepared by dissolving a 2:1 (w:w) mix of Omnigel-Sieve Agarose: Agarose I to a final agarose concentration of 4% (w/v) in TBE buffer (0.09 M Tris-borate, 0.002 M EDTA), before adding ethidium bromide to a final concentration of 0.5 μg/mL. Ten microlitres of each PCR product was combined with 5 μL of 2X gel loading buffer (0.09% bromophenol blue, 13% sucrose) and loaded onto the gel. Gels were then run in TBE buffer at 50-100 milliAmps using specialised gel electrophoresis apparatus (Bio-rad) for 20-60 minutes until the bromophenol blue band reached the end of the gel.

All restriction digest products were run on 4% 3:1 gels of 3-6 cm in length. These were prepared in a similar manner to 4% 2:1 gels except a ratio of 3:1 Omnigel-Sieve Agarose: Agarose I was used, and ethidium bromide was added to a final concentration of 1 μg/mL. Six microlitres of 6X gel loading buffer (0.27% bromophenol blue, 40% sucrose) was combined with 30 μL of digest product and 20-30 μL loaded onto the gel. Gels were then run in TBE buffer at 50-100 milliAmps for 30-60 minutes until the bromophenol blue band reached the end of the gel.

Ten microlitres of pUC19/*Hpa*II DNA size marker (50 μg/mL in 0.03% bromophenol blue, 4% sucrose) was also run with each gel to allow product size determination.

Completed gels were exposed to ultraviolet light using a UV transilluminator and fluorescent bands photographed using a digital camera for analysis.

2.1.2.4. C1236T PCR-RFLP assay development

2.1.2.4.1. Polymerase chain reaction

For C1236T PCR, the close proximity of the G1199A and C1236T SNPs (separated by only 31 base pairs, see Appendix C) allowed the use of the same forward primer (MDR-24, Table 2-1) as for G1199A, with the reverse primer (C1236-R, Table 2-1) the same as a common reverse primer previously designed by Dr Janet Coller for use in the allele-specific PCR assay mentioned previously.

C1236T PCR reactions were prepared using standard procedure (see section 2.1.2.3), and initially tested using the same reaction conditions as for A61G and G1199A PCR (see Table 2-2). C1236T PCR products were run on a 4% 2:1 gel and photographed using standard procedure (see section 2.1.2.3.3). The expected size of the C1236T PCR product is shown in Table 2-1.

2.1.2.4.2. Restriction enzyme digest

For the C1236T restriction digest, two different restriction enzymes were trialed, *Hpy*188I and *Eco*0109I. The recognition sequence of *Hpy*188I is 5'-TCNGA-3' (where N can be any nucleotide), as such, it should recognize and cleave the variant, but not the wild-type, sequence at the C1236T locus. It should also recognize and cleave three other sites within the C1236T PCR product regardless of sequence at the C1236T locus. As such, 4 digest fragments of 302, 93, 76 and 56 bp would be expected to be produced from wild-type PCR product, whilst the variant PCR product should be cleaved to 5 fragments of 170, 132, 93, 76, and 56 bp. The tested digest conditions were: 1X manufacturer's enzyme buffer, 5 Units of *Hpy*188I, and 20 μL of PCR product in a final volume of 30 μL. Digest reactions were tested at 37°C for 2, 4 or 16 hours, followed by 20 minute enzyme deactivation at 65°C and 4°C storage. Digest products were run on a 4% 3:1 gel and photographed using standard procedure (see section 2.1.2.3.3).

For *Eco*0109I, the recognition sequence, 5'-PuGGNCCPy-3' (where Pu is either an A or G, Py is either a C or T, and N can be any nucleotide), recognizes and cleaves the wild-type, but not the variant, sequence at the C1236T locus. As such, wild-type PCR products are cleaved to give two fragments at 251 and 276 bp, whilst variant PCR products are uncleaved and give a single undigested 572 bp product. The tested digest conditions were: 1X manufacturer's enzyme buffer, 0.1 mg/mL BSA, 5 Units of *Eco*0109I, and 20 μL of PCR product in a final volume of 30 μL. Digest reactions were tested at 37°C for 2, 4 or 16 hours, followed by 20 minute enzyme deactivation at 65°C and 4°C storage. Digest products were run on a 4% 3:1 gel and photographed using standard procedure (see section 2.1.2.3.3).

Restriction digests using *Hpy*118I and *Eco*0109I were tested and optimised using control DNA samples of known (sequenced) C1236T genotypes.

2.1.2.5. Assay quality control.

For each run of samples in a PCR or restriction digest reaction, a negative control (no genomic DNA) reaction was performed to confirm that there was no contamination of the master mixes, and hence no non-specific bands. In addition, for each assay a set of control samples of known genotype (a homozygous wild-type, a homozygous variant, and a heterozygote) were also included with each run of samples to confirm correct genotype-specific digestion patterns. The genotype of each control sample had previously been confirmed by sequencing using BigDye v3.0 chemistry analysed on an ABI Prism 7700 sequencer at the sequencing facility of the Institute of Medical and Veterinary Science (Adelaide, South Australia).

SNP genotype frequencies within the study populations described in Chapters 3 and 4 were tested for Hardy-Weinberg Equilibrium by Chi-square test (or Fisher's Exact Test for SNPs with insufficient homozygous variant frequencies) as an additional check for potential genotyping errors.

2.1.3. Results

The optimized PCR and digest conditions for all *ABCB1* PCR-RFLP assays are shown in Table 2-2 and Table 2-3, respectively.

Table 2-2. Optimal polymerase chain reaction conditions.

Assay ►	A61G, G1199A, C1236T	G2677T	C3435T
Master mix (per reaction):			
[PCR reaction buffer]	1X	1X	1X
[dNTPs] (μM each)	50	50	50
[Primers] (μM each)	0.1	0.1	**0.1-0.2***
Taq DNA polymerase (Units)	2.5	2.5	2.5
DNA template (ng)	100	100	100
Final reaction volume (μL)	30	30	30
Cycling conditions:			
Initial denaturation	94°C: 5 min	94°C: 5 min	94°C: 5 min
Denaturing	94°C: 30 sec	94°C: 30 sec	94°C: 30 sec
Annealing	60°C: 30 sec	60°C: 30 sec	60°C: 30 sec
Elongation	72°C: 1.5 min	72°C: 1.5 min	72°C: 1.5 min
Number of cycles	35	**35-45***	**35-45***
Final elongation	72°C: 5 min	72°C: 5 min	72°C: 5 min
Storage	4°C	4°C	4°C

*See section 2.1.3.1.

Table 2-3. Restriction digest enzymes for PCR-RFLP analysis.

SNP	**Enzyme**	**Recognition sequence**	**Reaction conditions**	**Fragment length (bp)**
A61G	TaqI or TaqαI	5'T↓CGA3' 3'AGC↑T5'	1 Unit: 16 h @ 65°C	Wt: 179 V: 146 + 33
G1199A	Eco57I or AcuI	5'CTGAAG$(N)_{16}$↓3' 3'GACTTC$(N)_{14}$↑3'	2.5 Units: 16 h @ 37°C, 20 min @ 65°C	Wt: 206 + 52 V: 258
C1236T	Eco0109I	5'RG↓GNCCY3' 3'YCCNG↑GR5'	5 Units: 16 h @ 37°C, 20 min @ 65°C	Wt: 251 + 276 V: 527
G2677T	BanI	5'G↓GYRCC3' 3'CCRYG↑G5'	4 Units: 16 h @ 37°C, 20 min @ 65°C	Wt: 198 + 26 V: 224
C3435T	Bsp143I or DpnII	5'↓GATC3' 3'CTAG↑5'	5 Units: 16 h @ 37°C, 20 min @ 65°C	Wt: 145 + 62 V: 207

TaqI and TaqαI; Eco57I and AcuI, and; Bsp143I and DpnII, are isoschizomers. ↓ and ↑ indicate cleavage sites, R = A or G, Y = C or T, bp = base pairs, Wt = Wild-type fragment, V = Variant fragment.

2.1.3.1. A61G, G1199A, G2677T, C3435T

The assays for A61G and G1199A remained unchanged from the original protocols, and examples of their restriction digest patterns are shown in Figure 2-1. For the G2677T and C3435T assays, it was occasionally difficult to visualize the digested bands of heterozygous patient samples. As such, primer concentrations were doubled (from 0.1 to 0.2 μM) for the C3435T PCR, and the number of cycles for both G2677T and C3435T PCR increased from 35 to 45 cycles. This resulted in increased PCR product for digestion, and easier detection of bands following digestion (Figure 2-1).

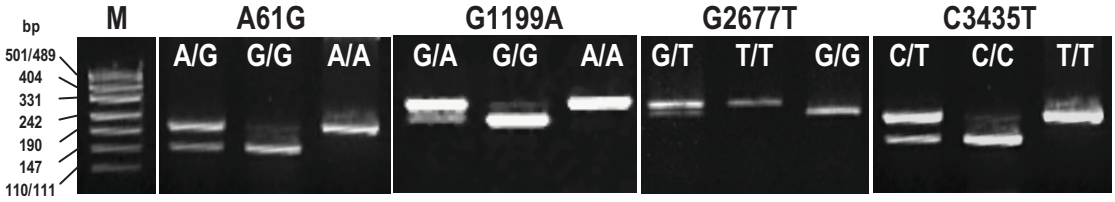

Figure 2-1. Restriction fragment patterns for A61G, G1199A, G2677T and C3435T SNP genotypes.

M: pUC19/*Hpa*II DNA molecular weight marker; bp: size of marker bands in base pairs.

2.1.3.2. C1236T

For the C1236T PCR-RFLP assay, using the same PCR conditions as for A61G and G1199A produced a clear and specific amplified product of 527 bp. Hpy199I digestion failed to distinguish homozygous variant and heterozygous genotypes under all conditions tested. Alternatively, using the optimized conditions shown in Table 2-3, Eco0109I digestion successfully and consistently differentiated between C1236T genotypes (see Figure 2-2).

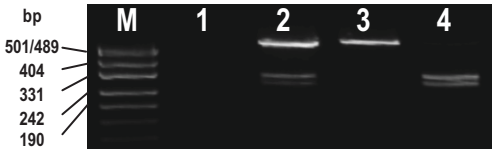

Figure 2-2. Optimised *Eco*0109I restriction fragment patterns for C1236T genotypes.

bp: size of marker bands in base pairs; M: pUC19/*Hpa*II DNA molecular weight marker; 1: no template control; **2:** heterozygous genotype (C/T); **3:** homozygous variant genotype (T/T); **4:** homozygous wild-type genotype (C/C).

2.1.4. Discussion

The PCR-RFLP assays for A61G and G1199A remained the same as those based on the methods described by Cascorbi and colleagues (2001) and previously optimized in our laboratory. Alternatively, whilst allele-specific detection of SNPs is generally more efficient than the PCR-RFLP process, existing allele-specific PCR assays for C1236T and G2677T genotyping were found to be unacceptably prone to non-specific amplification, particularly in the hands of different investigators in the laboratory. As such, because detection of these SNPs was required for other projects, assays more robust to variability between investigators were required. Fortunately, a previously optimised PCR-RFLP assay for G2677T genotyping was already available for use (with minor adjustments), therefore, this more robust method was applied for detection of G2677T SNPs. For C1236T genotyping, a new PCR-RFLP method was successfully developed, optimized and validated. For existing PCR-RFLP assays for G2677T and C3435T SNPs, slight adjustments to the PCR procedures were required in order to increase the amount of PCR products available for digestion, and thus allow improved and consistent visualization of restriction digest fragment patterns. Otherwise, the PCR-RFLP methods for G2677T and C3435T remained largely the same as those previously optimized in our lab.

2.1.5. Conclusion

These optimized PCR-RFLP assays for the detection of A61G, G1199A, C1236T, G2677T and C3435T SNPs of *ABCB1* were robust and reproducible. In addition, the inclusion of sequenced genotype controls in each assay run ensured the accurate determination and interpretation of genotypes, as well as a continuous confirmation of assay accuracy. These assays were employed for the *ABCB1* genotyping of all subjects in the retrospective clinical studies (described in Chapters 3 and 4) and prospective *ex vivo* study (see Chapter 5).

2.2. Estimation of haplotypes and linkage disequilibrium

2.2.1. Introduction

Individual genotypes can prove informative in pharmacogenetic analyses, however, where a gene such as *ABCB1* contains multiple polymorphic loci, a consideration of the combined effects of these mutations may give a more accurate prediction of the overall phenotype. This combination of mutations located on a single chromosome is referred to as a haplotype. In terms of genotypes, an individual possesses two alleles at any one mutation site (locus), one from the mother and one from the father. In a similar manner, each person has two haplotypes (which may be the same or different), consisting of a set of alleles from the mother, and a set of alleles from the father. This pair of haplotypes is an individual's diplotype.

Whilst technologies are available for the direct determination of haplotypes, most studies, including this one, determine genotypes at each locus (i.e. each SNP) separately and, as such, the possible combinations of alleles in haplotypes can be ambiguous. As shown in Figure 2-3, an individual with more than one heterozygous locus can have multiple possible combinations of alleles, each forming different haplotypes and hence diplotypes (haplotype pairs).

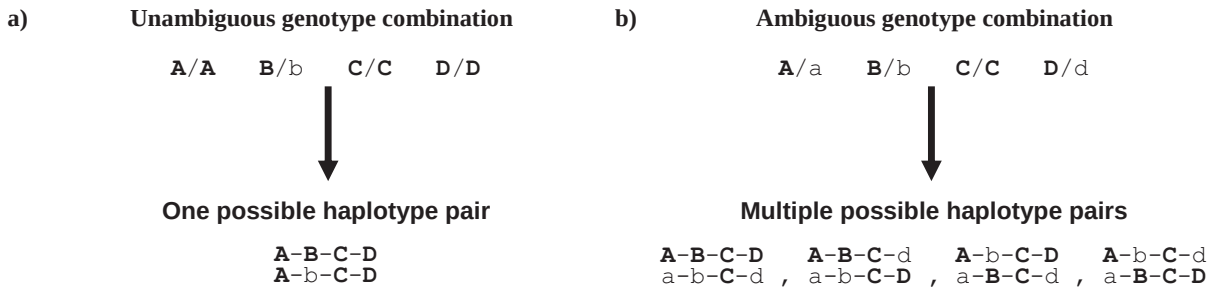

Figure 2-3. Examples of possible haplotype pairs (diplotypes) formed from unambiguous (a) and ambiguous (b) genotype combinations.

Letters (A, B, C, or D) designate different loci. Uppercase bold and lower case letters designate wild-type and variant alleles, respectively, at each locus.

In the absence of familial data, the haplotypes of ambiguous genotype combinations can be estimated using mathematical algorithms. Briefly, these methods employ statistical mathematics to predict the most likely combination of alleles on a chromosome (for a set of given genotypes) based on the observed population distribution and frequency of genotypes, their observed combinations within individuals, and the observed frequency of specific combinations within the population.

Once the haplotype distribution of a population has been determined, it is also possible to determine the linkage disequilibrium (LD) between mutations. That is, the non-random association of two alleles of different loci (mutations) with each other, more or less so than would be expected from a random distribution of alleles based on their individual frequencies. Strong LD can be an indicator of numerous factors such as genetic linkage, recombination and mutation rates, genetic drift and/or population structures, among others (Hedrick, 2005). However, in the case of the studies in this thesis, analysis of LD was employed simply to confirm an accurate haplotype prediction, by replicating previous observations of strong LD between the C1236T, G2677T and C3435T SNPs of *ABCB1* (see Chapter 1, section 1.6.3).

The degree of LD between two loci can be expressed as D, D' or r^2. Lewontin's D is a measure of the difference between the observed haplotype frequency, and the haplotype frequency expected (in the absence of LD) based on the frequency of the alleles at each locus. Alternatively, D' represents the amount of LD (i.e. Lewontin's D) normalized to the maximum LD possible given the allele frequencies at each locus, where D' = 1 indicates complete LD (i.e. no recombination between loci). Care is needed when interpreting D' values as they can be inflated in small sample sizes, or when allele frequencies are low. Alternatively, r^2 is a measure of how well an allele at one locus predicts an allele at the other, where an $r^2 = 1$ indicates that not only does D' = 1 (and hence there is complete LD), but the allele frequencies of the two loci are also equal, meaning that one allele at one loci will

always predict the allele at the other. This also means that where allele frequencies between loci differ, r^2 will be low, even though D' (and thus LD) may be high. Therefore, both D' and r^2 must be interpreted with caution (and preferably together) when assessing the LD between two loci. P-values can also be calculated for measures of LD using chi-square test, however, these also need to be interpreted with caution, as in large sample sizes, statistically significant P-values are often observed even for low LD values (Barnes, 2007).

No methods for estimating haplotype phase and analysing LD had previously been used in our laboratory. Therefore, a protocol for predicting haplotypes and analyzing LD from *ABCB1* SNP data needed to be established and validated, preferably using existing statistical software.

2.2.2. Methods

2.2.2.1. Haplotype estimations

ABCB1 haplotype estimations were performed using PHASE version 2.1 software (Stephens et al., 2001; Stephens & Donnely, 2003) which is freely available for download from http://www.stat.washington.edu/stephens/software.html. Briefly, the PHASE program employs a Bayesian statistical method for the estimation of haplotypes based on population genotype data. The PHASE program was chosen because it can handle small amounts of missing genotype data, as well as perform case-control permutation tests to test for significant differences in haplotype distributions between different populations. PHASE was also chosen because, in simulation experiments, it was found to have half the error rate of other methods employing expectation-maximisation algorithms (Stephens & Donnely, 2003).

Input files were formulated in Microsoft® Notepad according to PHASE program instructions and saved as filename.inp files. Input files specified: the number of individuals to be analysed (n); the number (5), relative position (11612975 11662641 11662849 11681078 11703063) and type (all SNPs = SSSSS) of loci to be analysed; and for each individual, their case-control

status (0 or 1), their subject number (#xxx), and their genotypes. Any missing genotype was denoted with a ? character. An example input file is shown in Figure 2-4.

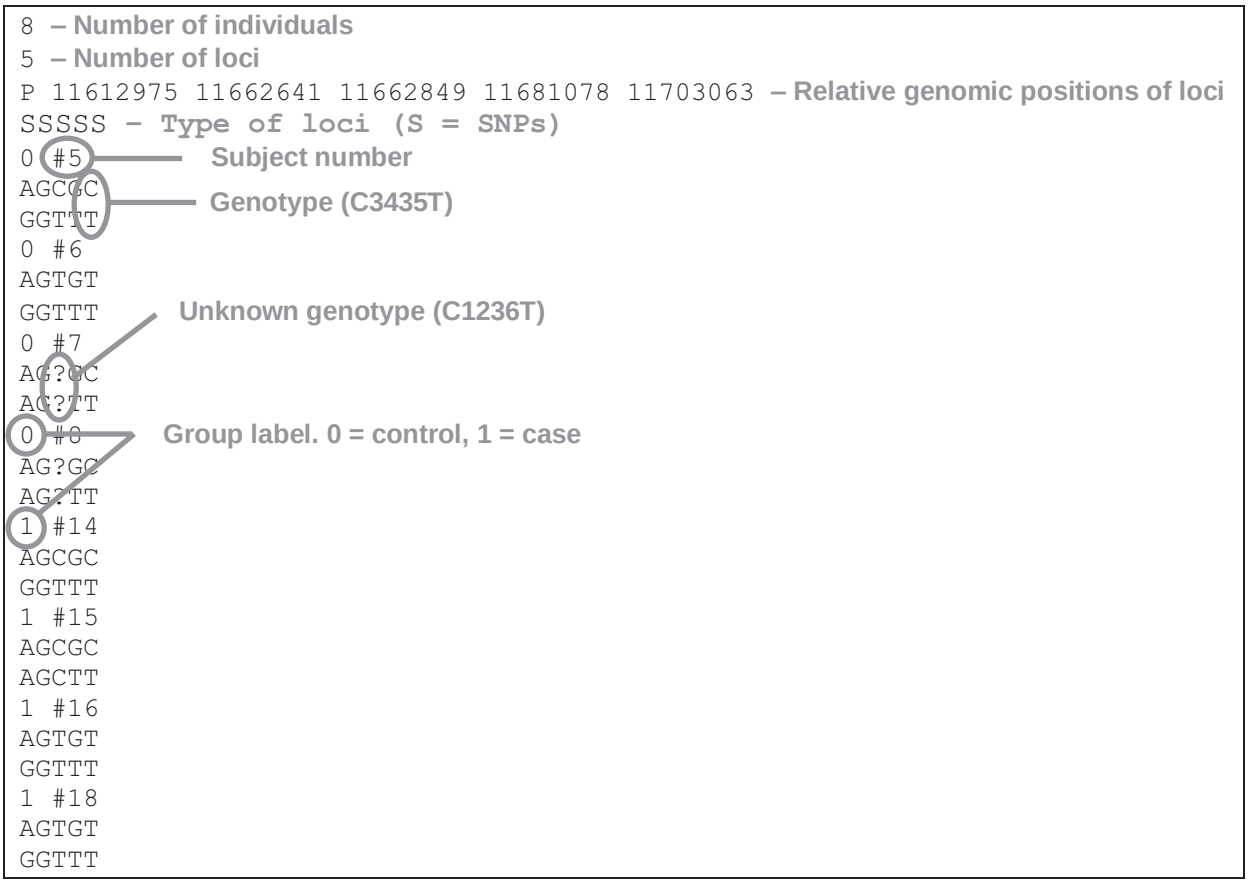

Figure 2-4. Example input file for PHASE version 2.1.

PHASE runs were executed in MS-DOS mode using the following command line;

./PHASE –c1000 filename.inp filename.out

The –c1000 flag indicates the presence of case-control designations and initiates a case-control permutation test of 1000 permutations. Filename.inp designates the input file, and filename.out designates the desired name of PHASE output files. The only alteration from PHASE default parameters was an increase from 100 to 1000 permutations for the case-control permutation analysis.

2.2.2.1.1. Validation of haplotype estimations

For validation of the PHASE haplotype estimation, haplotype predictions were performed using an initial data set of 60 non-opioid-dependent control, 60 MMT, and 32 BMT subjects

who had already been genotyped as part of the first retrospective study (see Chapter 3). Of these subjects, 14 had missing genotype data for the C1236T SNP. As per PHASE recommendations, the algorithm was applied 5 times using different seeds for the random number generator (using the –S flag), and the consistency of results checked by examining the haplotype designations for each subject, the population haplotype frequency estimates, and the goodness-of-fit measures for each run.

2.2.2.2. Linkage disequilibrium

Linkage disequilibrium was assessed using Arlequin version 3.11 software (Excoffier et al., 2005) freely available for download from http://cmpg.unibe.ch/software/arlequin3/. Briefly, a project file was formulated in Microsoft® Notepad according to Arlequin templates to allow for the input of haplotype data in the form of the absolute number of each haplotype observed in the population based on PHASE results. An example project file is shown in Figure 2-5.

```
[Profile]
     NbSamples=1 # - {Number of separate 'populations' to be tested}
     DataType=STANDARD
     GenotypicData=0
     GameticPhase=1
     LocusSeparator=NONE
     RecessiveData=0
     MissingData='?'
     Frequency=ABS
     FrequencyThreshold= 1.0e-5
     EpsilonValue= 1.0e-7

[Data]

[[Samples]]

     SampleName="Name of Population number 1"
     SampleSize=15
        SampleData={
        h1        5     AGCGC
        h2        6     AGTTT
        h3        3     AGCTT
        h4        1     AGCGT
     }
```

Number of times haplotype h1 (AGCGC) is observed in population (based on PHASE results)

Figure 2-5. Example input file for Arlequin version 3.11.

Whilst Arlequin is capable of performing its own haplotype predictions from unphased genotype data, this format allowed for the input of haplotype data (of known gametic phase) from the PHASE predictions already performed. This not only saved time, but also took advantage of the superior algorithm employed by PHASE for haplotype estimations. Furthermore, LD analyses by Arlequin are based simply on the relative frequencies of phased haplotypes, and do not use any information from raw unphased genotype data, or even the confidence of its own haplotype predictions. Therefore, no information relevant for LD was lost by omitting the phase prediction step in Arlequin.

The Arlequin program was able to compute the D, D' and r^2 coefficients of LD, as well as perform an 'Exact test of linkage disequilibrium' (Raymond & Rousset, 1995) for statistical significance, for each pairwise comparison of loci.

2.2.3. Results

2.2.3.1. Haplotype estimations

Using the validation set of 152 subjects, PHASE identified 13 haplotypes of *ABCB1* within the population. By far the most common haplotypes were the wild-type AGCGC (61A-1199G-1236C-2677G-3435C, 31%) and the AGTTT (31%) haplotypes. For 151 of the 152 individuals, their designated haplotypes did not change between replicate runs using different random number seeds. However, 4 out of the 5 replicate runs designated one subject (who had missing C1236T genotype data) as AGTTT/GGTGT (36-37% confidence), with one replicate designating the subject as AGTGT/GGTTT (34% confidence).

For the observed haplotypes, frequency estimates did not change significantly between replicate runs using different random number seeds (coefficients of variation (CVs) less than 10%). Variability between runs was inversely correlated with the overall frequency of the

haplotypes, such that haplotypes with a frequency estimate of greater than 5% had the least variability between runs (CVs = 0.5-2.3%).

PHASE was able to estimate ambiguous phase calls with an average confidence probability of 92% at the genotype level, and 79% for the diplotypes overall. The distributions of confidence probabilities for each loci and for the final diplotypes are shown in Figure 2-6 (those subjects with unambiguous genotypes, that is confidence probabilities of 1, are not shown). As would be expected, haplotypes of subjects with missing genotype data (open circles) were estimated with the least confidence.

Goodness-of-fit measures did not differ between replicate runs with different seeds (mean ± SD: -488 ± 2.0, -488 ± 1.8, -489 ± 2.4, -488 ± 2.0, and -488 ± 2.2).

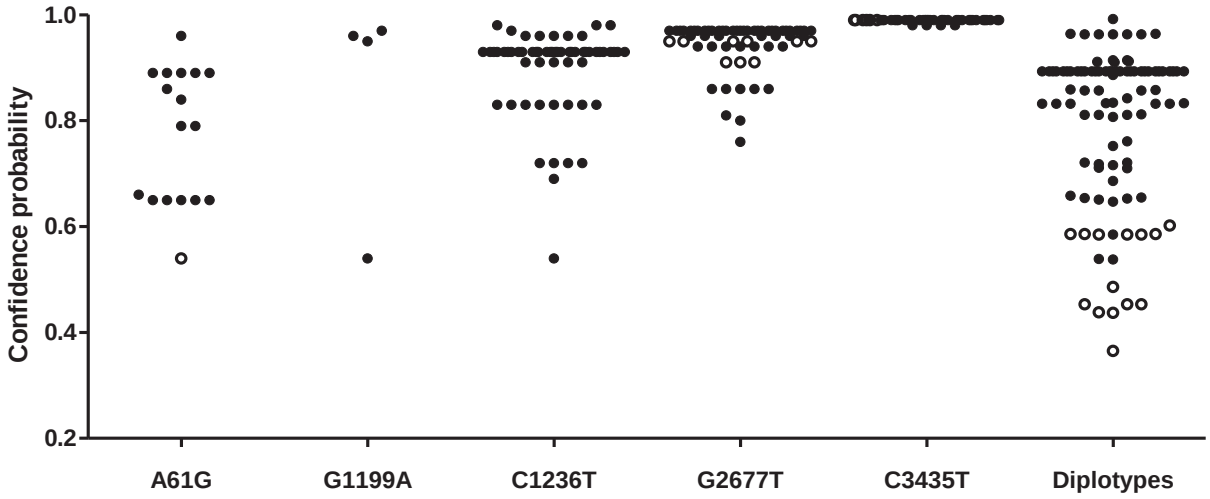

Figure 2-6. Confidence probabilities of ambiguous phase calls made by PHASE for each individual locus, and for the overall diplotype prediction.

Each point represents a subject with ambiguous gametic phase. Hollow circles represent subjects with missing genotype data at the C1236T SNP.

2.2.3.2. Linkage disequilibrium

Using the absolute haplotype frequencies of the validation set of samples from PHASE, Arlequin was able to calculate the pairwise D, D' and r^2, as well as perform an 'Exact test for linkage disequilibrium' for each pair of *ABCB1* loci. As expected from previous *ABCB1* haplotype studies (Kim et al., 2001; Kroetz et al., 2003), incomplete but statistically significant LD was reported between 1236T and 2677T (D' = 0.6, r^2 = 0.3), 2677T and 3435T (D' = 0.6, r^2 = 0.3), and 1236T and 3435T (D' = 0.8, r^2 = 0.4) SNPs ($P < 0.00001$ for all). Significant LD was also observed between 61G and 1236T, 1199G and 1236T, 61G and 3435T, and 1199G and 3435T alleles, however, the interpretation of the extent of LD between these loci is difficult due to the low frequency of A61G and G1199A variants (see section 2.2.2.2).

2.2.4. Discussion

Validation of PHASE inference of haplotypes from *ABCB1* genotype data was performed according to recommendations of the program creators. For subjects with complete genotype data, PHASE consistently predicted individual diplotypes between runs, with a median confidence of 89% (range: 54-99%) for haplotype calls. Alternatively, haplotypes of subjects with missing genotype data were generally called with lower confidence (36-60%). Furthermore, one individual was designated a different diplotype for one of the replicate runs. However, this ambiguity is likely due to a combination of the absence of C1236T genotype data, and the presence of a rare mutation of A61G in this subject.

Goodness-of-fit measures generated by PHASE did not differ between runs, indicating that the estimated haplotypes fitted well with the default recombination model employed and that the fit was robust. Further validation of the PHASE haplotype estimation can also be found in the high frequency of wild-type AGCGC and triple variant AGTTT haplotypes, implying a high degree of LD between the 1236, 2677 and 3435 variant alleles, in line with previous

investigations of *ABCB1* genetic variability (Kim et al., 2001; Kroetz et al., 2003). LD analysis with Arlequin confirmed the presence of significant (but incomplete) LD between the variants at these three loci.

2.2.5. Conclusion

PHASE was validated as an accurate and robust tool for the estimation of *ABCB1* haplotypes from complete genotype data. However, whilst PHASE was able to estimate haplotypes for individuals with missing genotype data, it did so with greater variability and lower confidence. Therefore, haplotype estimations for subjects with missing genotype data should be treated with caution. Finally, PHASE was able to perform case-control permutation analyses to test for significant inter-population differences in haplotype distribution, and haplotype data from PHASE was easily transferred to Arlequin for the calculation of pairwise LD parameters.

These methods were employed for the determination of *ABCB1* haplotypes (and LD) of subjects in the retrospective clinical studies described in Chapters 3 and 4. PHASE predictions were re-validated using the full data sets from these studies (see results sections of Chapters 3 and 4), and case-control permutation tests used to detect differences in haplotype distributions between opioid-dependent and control populations, as well as between treatment outcome groups. The PHASE protocols were also employed for the determination of *ABCB1* haplotypes in the prospective *ex vivo* study discussed in Chapter 5.

2.3. Summary

In addition to optimizing existing genotyping assays for the A61G, G1199A, G2677T and C3435T mutations of *ABCB1*, a PCR-RFLP method for identification of the C1236T SNP of *ABCB1* was developed and validated. Furthermore, statistical methods for the estimation of *ABCB1* haplotypes and LD were also developed and optimised. These methods were applied

for the genotype and haplotype analysis of subjects taking part in the clinical studies described in Chapters 3, 4 and 5.

Chapter 3. ABCB1 pharmacogenetics in standard dose opioid substitution treatment

3.1. Introduction

As discussed already, P-gp activity could potentially influence the CNS distribution of morphine following illicit heroin or morphine use. It may also play a role in the distribution of opioid peptides of the endogenous reward system. As such, P-gp may have the ability to modulate the rewarding/euphoric effects of illicit opioids, as well as the development and severity of opioid dependence. Therefore, it was hypothesised that *ABCB1* mutations, causing variability in P-gp activity, could provide a genetic basis for individual differences in risk and severity of opioid dependence.

In addition, it was hypothesised that an impact of *ABCB1* genetic variability on the pharmacokinetics of substitution opioids such as methadone and buprenorphine, by modulating their CNS distribution, could also directly (and predictably) influence patient responses to maintenance therapies for opioid dependence. Such a predictor of drug response, and hence daily dose requirements, could provide clinicians with a useful dose optimization tool for the successful treatment of opioid dependence. Alternatively, a clear understanding of the impact of *ABCB1* genetic variability on methadone's plasma PK/PD relationship may provide a significant aid for individualizing target plasma concentrations as part of potential future MMT therapeutic drug monitoring.

Finally, it was also hypothesised that *ABCB1* genotypes or haplotypes may also help in identifying those maintenance patients at higher risk of in-treatment withdrawal, adverse opioid side-effects, continued illicit opioid use and/or treatment drop-out. This in turn may provide vital additional decision support regarding the determination of optimal treatment approaches, the need for (and level of) in-treatment monitoring, and/or an increased provision of ancillary services.

3.2. Aims

To test these hypotheses, this retrospective study aimed firstly to compare *ABCB1* genetic variability between opioid-dependent individuals and non-opioid-dependent controls, in order to elucidate its general role in the development of opioid dependence. Secondly, it aimed to examine *ABCB1* genetic variability in opioid maintenance treatment patients to determine its impact on treatment parameters such as dose requirements and treatment response.

3.3. Materials and methods

3.3.1. Subjects

A total of 78 opioid-dependent subjects receiving MMT, 30 opioid-dependent subjects receiving BMT, and 98 non-opioid-dependent controls were investigated in this study, all of whom were Caucasian.

All opioid-dependent subjects had taken part in one of 6 clinical studies conducted by the Discipline of Pharmacology during the time period from January 2001 to June 2008. For these studies, opioid-dependent subjects had originally been recruited from clinics of the Drug and Alcohol Services South Australia, Yatala Labour Prison, Adelaide Pre-Release Centre, Adelaide Midnight Pharmacy, the Byrne Surgery (Redfern, NSW) or via South Australian private prescribers. All opioid-dependent subjects were receiving, or about to receive, substitution treatment with methadone or buprenorphine at the commencement of the original clinical studies.

All available opioid-dependent subjects were included in the analyses of pre-treatment data such as prior drug use and previous treatment episodes (see sections 3.3.4 and 3.3.5.1). However, only subjects in the stable maintenance phase of treatment (that is, in treatment for at least 1 month, and on a dose that had been individually optimized and had not changed for at least 2 weeks) for a period during the original clinical trials were included in analyses of in-

treatment parameters (such as opioid requirements and adverse events, see sections 3.3.4 and 3.3.5.2), with the exception of treatment outcome (see sections 3.3.4.2 and 3.3.5.2). Twenty-five of the opioid-dependent subjects had also taken part in a trial examining the safety of MMT and BMT in pregnancy, and as such, were pregnant during the original clinical study. Since this may have had a significant bearing on dose requirements, as well as treatment choice, motivation and hence response, these pregnant subjects were also excluded from all in-treatment analyses (including treatment response).

Non-opioid-dependent controls were healthy subjects free from disease and drug addiction who had also previously participated in clinical studies conducted by the Discipline of Pharmacology during the time period from January 2001 to June 2008.

All studies were approved by the Royal Adelaide Hospital Research Ethics Committee and the University of Adelaide Research Ethics Committee. All subjects provided written informed consent.

3.3.2. *ABCB1* genotyping

Genomic DNA was isolated from whole blood or tissue samples and genotyped for the A61G, G1199A, C1236T, G2677T and C3435T SNPs of *ABCB1* using procedures described in Chapter 2, section 2.1.

3.3.3. Haplotype prediction and linkage disequilibrium

Only subjects that had been genotyped for 4 or more SNPs were included in the haplotype estimation by PHASE. MMT (n = 78), BMT (n = 30) and control subjects' genotype data (n = 79) was entered into a single PHASE input file, with healthy controls flagged as 'controls', and opioid-dependent subjects (MMT and BMT subjects) flagged as 'cases'. Haplotypes were then estimated using the methods described in Chapter 2, section 2.2.2.1 The validity of PHASE haplotype predictions were checked again (using random seed replicates) as

described previously (Chapter 2, section 2.2.2.1.1), then a case-control permutation test comparing population haplotype frequencies between opioid-dependent (BMT and MMT subjects combined) and control subjects was performed (see Chapter 2, section 2.2.2.1).

In addition to recording the population frequency estimates for each haplotype from the PHASE output, 'observed' haplotype frequencies were calculated for the opioid-dependent (MMT and BMT subjects combined) and control subject groups based on each individual's predicted haplotypes (after excluding subjects with phase call probabilities less than 0.7).

The total (opioid-dependent and control combined) subject haplotype distribution from PHASE was then used for calculating linkage disequilibrium between loci in Arlequin (see Chapter 2, section 2.2.2.2).

3.3.4. Subject data

Subject demographics, drug use histories and maintenance treatment data were obtained from the original clinical study case notes. MMT and BMT subjects' age of first daily heroin use, and the number of any prior methadone or buprenorphine maintenance treatments were recorded, as were their self-reported heroin use for the month prior to entering treatment (recorded as the mean monetary amount in Australian dollars of heroin used per day), and any self-reported use of other drugs prior to treatment. For subjects who were commencing treatment at entry to the original studies, urine drug screen results were also used to identify pre-treatment drug use.

For MMT and BMT subjects receiving some form of intervention during the course of the original studies (i.e. additional drug treatment or any other deviation from standard substitution treatment protocol), daily dose requirements were recorded as the doses received at the time of study screening (n = 28 MMT and all 16 BMT subjects). Otherwise, the dose received at the final study session was used as the measure of maintenance dose requirement

(n = 34 MMT subjects). Trough (~24 hours post-dose) plasma concentrations of (R)- and (S)-methadone (C_{trough}, ng/mL) were known for 41 MMT subjects, and C_{trough} values for buprenorphine and norbuprenorphine were known for 13 BMT subjects. All subjects with C_{trough} values had matching dose data allowing for the calculation of dose-adjusted C_{trough} (C_{trough}/dose ($ng.mL^{-1}.mg^{-1}$) = C_{trough} (ng/mL) ÷ dose (mg/day)). For ease of reference, buprenorphine and norbuprenorphine C_{trough}/dose data are reported as $pg.mL^{-1}.mg^{-1}$.

Heroin and other drug use whilst in treatment was determined from subject self-report and urine drug screen results. Total self-reported heroin use (in Australian dollars) for the last month in treatment was used as the major measure of heroin use during treatment. However, where available, plasma morphine concentrations, determined by HPLC analysis (Doverty et al., 2001), were also used as indicators of heroin use during treatment.

3.3.4.1. Opioid withdrawal and adverse effects

Due to the use of different withdrawal or opioid effect scales and questionnaires between studies, specific symptoms listed as part of these questionnaires were chosen to determine whether subjects were experiencing withdrawal or adverse opioid effects during the course of their treatment. Following the groupings described by Dyer and White (1997), withdrawal was defined by the following symptoms: insomnia; muscle/bone/joint pains; nausea; craving; and reports of 'not holding'. Relevant pre-maintenance dose clinical opioid withdrawal scale, subjective opioid withdrawal scale, methadone symptoms checklist and visual analogue scale scores were converted into nominal (present / not present) values for each of these symptoms. These nominal scores were then used to categorise patients into those that had ever experienced withdrawal ('withdrawal-ever'), and whether they experienced withdrawal most (greater than 50%) of the time ('withdrawal-most'). The same procedure was then applied to determine whether subjects were experiencing direct opioid effects. This was defined by the following physiological symptoms: constipation; dry mouth; and itchy skin/nose (Dyer &

White, 1997). The relevant scores obtained following administration of subjects' maintenance doses were then used to categorise patients into those that ever experienced direct opioid effects ('opioid-ever'), and those that experienced direct opioid effects most (greater than 50%) of the time ('opioid-most').

3.3.4.2. Treatment outcome

Methadone and buprenorphine treatment outcomes were determined by considering subject data spanning the entire period for which they participated in the original clinical studies. Measures of treatment outcome were restricted to subject self-report of opioid use, plasma morphine concentrations, urine drug screen results, self-report of withdrawal symptoms, and treatment attendance. The specific criteria used for determining treatment outcomes are shown in Table 3-1. Where a subject had no data for any of these criteria, their treatment outcome was not classified. For each measure, individual study protocols and inclusion criteria were taken into account, as well as any concomitant medications. Treatment outcomes were determined blind to subjects' *ABCB1* genotype status.

Table 3-1. Criteria for treatment outcome classification.

	Treatment Outcome Classification	
	Successful	Poor[a]
Total self-reported illicit opioid use for last month in treatment	≤ $100	> $100
Plasma morphine concentration	≤ 2 ng/mL	> 2 ng/mL
Opiate urine screens	Negative	Positive
Self-reported withdrawal symptoms[b]	< 50% of the time	> 50% of the time ('withdrawal-most')

[a]Subjects meeting any of these criteria were classified as having poor treatment outcome. [b]See section 3.3.4.1 for definitions of withdrawal symptoms.

3.3.5. Statistical methods

Two separate groups of analyses were conducted in this study, the first examining the relationship between *ABCB1* genetic variability and opioid dependence, and the second examining the influence of *ABCB1* genetic variability on opioid substitution treatment.

3.3.5.1. *ABCB1* genetic variability and opioid dependence

For this part of the study, all MMT and BMT subjects (including those who were pregnant or not stable in treatment) were combined to form a single group of opioid-dependent subjects.

Individual SNP allele and genotype frequencies were compared between opioid-dependent subjects and healthy controls using Fisher's Exact Test (with Odds Ratio) and Chi-square Test, respectively. Where homozygous variant genotypes were too rare to conduct a Chi-square test, homozygous variant and heterozygous genotypes were combined and the data analysed by Fisher's Exact Test. If one or more of these tests gave a P-value less than 0.1, adjusted Odds Ratios were determined by combining genotype data from all 5 SNPs in a binary logistic regression model (SPSS for Windows, SPSS Inc., Chicago, IL, USA) (with sex as a covariate) to control for potential SNP interactions.

Genotype frequencies in opioid-dependent and control subjects were tested separately for Hardy-Weinberg Equilibrium by Chi-square test (or Fisher's Exact Test for SNPs with insufficient homozygous variant frequencies).

Haplotype distributions in opioid-dependent and control subjects were compared by case-control permutation test as described in section 3.3.3., whilst diplotype frequencies were compared using Fisher's Exact Test. Where multiple diplotypes displayed a P-value less than 0.1 (by Fisher's Exact Test), their adjusted Odds Ratios were determined by combining them in a binary logistic regression model (including sex as a covariate).

Age of first regular heroin use and prior heroin use data displayed log-normal distributions and therefore were log-transformed before comparing between genotype and haplotype groups using either two-tailed Mann-Whitney U Test (non-parametric t-test), or Kruskal-Wallis Test (non-parametric one-way ANOVA) with Dunn's Multiple Comparisons post-hoc test. The effect of sex on the relationships between genotypes/haplotypes and age of first regular heroin use and prior heroin use were determined using two-way ANOVA with Bonferroni post-hoc test.

3.3.5.2. *ABCB1* genetic variability and opioid substitution treatment

For the study of opioid substitution treatment parameters, all pregnant subjects and those not on a stabilised dose were excluded, and MMT and BMT subject groups analysed separately.

Continuous variables (dose, C_{trough}, C_{trough}/dose) were compared between genotype and haplotype groups using either two-tailed Mann-Whitney U Test, or Kruskal-Wallis Test with Dunn's Multiple Comparisons post-hoc test.

The effect of sex on the relationships between genotypes/haplotypes and continuous variables were determined using two-way ANOVA. Where two-way ANOVA detected a significant effect, a Bonferroni post-hoc test was used to test for differences between genotype/haplotype-matched males and females, whilst two-tailed Mann-Whitney U Test or Kruskal-Wallis Test (with Dunn's Multiple Comparisons post-hoc test) was used to test for sex-specific differences between genotypes/haplotypes.

Since subjects with poor treatment outcomes may not actually be receiving their optimal doses, it was important to ensure that their inclusion was not reducing the ability of the study to identify associations between *ABCB1* genetic variability and effective methadone requirements. As such, the effect of treatment outcome on the relationships between genotypes/haplotypes and continuous variables was examined in the same manner as sex.

To determine any other possible covariates, MMT doses and (R)-methadone C_{trough} were submitted to multiple linear regression analysis (SPSS) with stepwise inclusion (F probability < 0.05) of genotypes and haplotypes with frequencies greater than 5% (A61G, C1236T, G2677T, C3435T, AGCGC, AGCGT, AGCTT, AGTGC, AGTTT, GGTTT), sex, age, bodyweight, treatment outcome, time in treatment (log-transformed), in-treatment amphetamine use, in-treatment benzodiazepine use, in-treatment cannabis use, and in-treatment cocaine use. Similar multiple linear regression analyses were also performed for plasma (R)- and (S)-methadone C_{trough}/dose, but without treatment outcome as a covariate.

Since only 17 MMT subjects had prior heroin use data, this variable was not included in the linear regression analyses described above. However, to determine whether this might be an important covariate for future studies, the relationship between maintenance doses or plasma concentrations and prior heroin use (log-transformed) was examined using Pearson correlation tests (in both MMT and BMT subjects).

Individual SNP allele frequencies were compared between treatment outcome groups (successful versus poor, 'withdrawal-ever' versus no withdrawal, and 'opioid-most' versus not 'opioid-most') using Fisher's Exact Test (with Odds Ratio). Where one or more of these tests gave a P-value less than 0.1, adjusted Odds Ratios were determined by combining genotype data from all 5 SNPs in a binary logistic regression model (with sex and dose as covariates) to control for potential SNP interactions.

Haplotype frequencies were compared between treatment outcome groups using PHASE case-control permutation test. If a permutation test returned a significant result, post-hoc analysis of individual haplotype frequencies was performed using Fisher's Exact Test (with Odds Ratio).

3.4. Results

Whilst numerous pre- and in-treatment data were available for opioid-dependent subjects, due to the retrospective nature of the study, not all data were available for all participants. As such, actual n-values are given where data was missing for one or more subjects.

3.4.1. *ABCB1* genetic variability and opioid dependence

3.4.1.1. Subject demographics

The opioid-dependent group consisted of 108 subjects (78 MMT and 30 BMT), 60 males and 45 females (3 subjects had no sex information in case notes), with an average age of 33 years (n = 106; range = 19-56). Of the 98 control (non-opioid-dependent) subjects, 45 were males and 53 were females, with an average age of 52 years (n = 96; range = 18-80).

The pre-treatment tobacco, alcohol and illicit drug use demographics of the opioid-dependent subjects are shown in Table 3-2. As expected, the vast majority of opioid-dependent subjects were daily tobacco smokers, whilst the most commonly used illicit drug other than heroin was cannabis (67% of opioid-dependent subjects used daily). Around a third (34%) of opioid-dependent subjects had previously abused benzodiazepines regularly, whilst regular amphetamine, cocaine and excessive alcohol use was relatively rare (17, 2 and 3%, respectively). The age of first regular heroin used varied greatly, ranging from 13 to 36 years of age, as did the levels of self-reported heroin use prior to entering maintenance treatment ($10 to $2000 per day).

Table 3-2. Pre-treatment alcohol, tobacco and illicit drug use demographics of opioid-dependent subjects.

Drug	**(Users : Non-users)**
Alcohol[a]	2 : 69
Tobacco[b]	83 : 3
Amphetamines[c]	8 : 40
Benzodiazepines[c]	16 : 31
Cannabis[b]	31 : 15
Cocaine[c]	1 : 46
Age of first regular heroin use, n = 71 (median ± SD (range))	21 ± 6.6 (13-36)
Heroin use ($/day), n = 55 (median ± SD (range))	100 ± 298 (10-2000)

Non-prescription drug use in the month prior to entering maintenance. [a]At hazardous levels (greater than 40 g/day for males, 20 g/day for females (NHMRC, 2001)). [b]Daily use. [c]At least once a month. $: Australian dollars.

3.4.1.2. *ABCB1* genotypes

All 108 opioid-dependent subjects were genotyped for the A61G, G1199A, G2677T and C3435T SNPs, whilst only 103 were genotyped for the C1236T SNP (due to a shortage of blood samples for 5 subjects). In the control group, 95, 93, 78, 95 and 92 subjects were genotyped for the A61G, G1199A, C1236T, G2677T and C3435T SNPs, respectively, with 77 subjects genotyped for all 5 mutations. Genotype frequencies in both control and opioid-dependent subject groups did not deviate from Hardy-Weinberg Equilibrium ($P > 0.1$).

ABCB1 genotype and variant allele frequencies in opioid-dependent and control subjects are shown in Table 3-3. There were no significant differences in SNP allele or genotype frequencies between opioid-dependent and control subjects ($P > 0.17$).

Table 3-3. *ABCB1* SNP variant allele and genotype frequencies in control (C) and opioid-dependent (OD) subjects.

SNP	Subject group	Allele frequency n (%)				Genotype frequency n (%)				
		WT	V	OR (95% CI)	P	WT/WT	WT/V	V/V	$\chi 2$	P
A61G	C	168 (88.4)	22 (11.6)	0.61(0.31-1.20)	0.17	75 (78.9)	18 (18.9)	2 (2.1)	2.51	0.28
	OD	200 (92.6)	16 (7.4)			94 (87.0)	12 (11.1)	2 (1.9)		
G1199A	C	182 (97.8)	4 (2.2)	1.30(0.36-4.68)	0.76	90 (96.8)	2 (2.2)	1 (1.1)	1.77 (0.43-7.26)[a]	0.51
	OD	210 (97.2)	6 (2.8)			102 (94.4)	6 (5.6)	0 (0.0)		
C1236T	C	69 (44.2)	87 (55.8)	0.75(0.49-1.14)	0.20	14 (17.9)	41 (52.6)	23 (29.5)	1.96	0.37
	OD	106 (51.5)	100 (48.5)			26 (25.2)	54 (52.4)	23 (22.3)		
G2677T	C	100 (52.6)	90 (47.4)	0.89(0.60-1.32)	0.62	19 (20.0)	62 (65.3)	14 (14.7)	2.18	0.34
	OD	120 (55.6)	96 (44.4)			30 (27.8)	60 (55.6)	18 (16.7)		
C3435T	C	72 (39.1)	112 (60.9)	0.85(0.57-1.27)	0.48	13 (14.1)	46 (50.0)	33 (35.9)	0.71	0.70
	OD	93 (43.1)	123 (56.9)			18 (16.7)	57 (52.8)	33 (30.6)		

WT: Wild-type allele. V: Variant allele. OR (95% CI): Odds Ratio (95% confidence interval) of Fisher's Exact Test. χ^2: Chi-square.

[a]OR (95% CI) of Fisher's Exact Test after grouping WT/V and V/V genotypes for control subjects.

3.4.1.3. *ABCB1* haplotypes

3.4.1.3.1. Validation check

Haplotype predictions for each subject did not differ between random seed replicates. Similarly, frequency estimates for the observed haplotypes did not change significantly between replicates (coefficients of variation (CVs) less than 5%), and CVs were less than 2.4% for haplotypes with frequencies greater than 5%. PHASE was able to estimate ambiguous phase calls with an average confidence probability of 96% at the genotype level, and 86% for diplotypes overall. The distributions of confidence probabilities for each locus and for the final diplotypes are shown in Appendix B: Figure B-1. Finally, goodness-of-fit measures did not differ between replicate runs with different seeds (mean ± SD: -600 ± 1.9, -600 ± 2.1, -599 ± 1.6, -600± 1.9, and -600 ± 1.7) (see Chapter 2, section 2.2.2.1.1).

For 8 subjects (3 controls, 4 MMT and 1 BMT) with 61A/G, 1199G/G, 1236T/T, 2677G/T and 3435T/T genotypes, PHASE could not confidently differentiate between the AG**T**G**T**/**G**G**TTT** and AG**TTT**/**G**G**T**G**T** diplotypes (confidence probabilities around 0.5). Therefore, the MMT and BMT subjects with these genotypes were excluded from haplotype analyses (other than the PHASE case-control permutation test), as were any other subjects with PHASE call confidence probabilities of less than 0.7 (4 MMT, and 3 BMT subjects).

3.4.1.3.1.1. Linkage disequilibrium

Linkage disequilibrium values for pairs of *ABCB1* loci, as determined by Arlequin, are shown in Table 3-4. Significant linkage disequilibrium was reported for multiple pairs of loci, however, as expected, only the C1236T-G2677T, C1236T-C3435T and G2677T-C3435T pairs had moderate-to-high values for both D' and r^2 (see Chapter 2, section 2.2.1). No two loci were in complete linkage disequilibrium.

Table 3-4. D' (shaded) and r^2 (unshaded) measures of linkage disequilibrium between pairs of *ABCB1* SNP variant loci as determined by Arlequin (see Chapter 2, section 2.2.2.2).

	61G	**1199A**	**1236T**	**2677T**	**3435T**	
61G		-1.0	0.942***	0.378**	1.0***	
1199A	0.003		-1.0**	-0.332	-0.829**	
1236T	0.089***	0.028**		0.661***	0.746***	**D'**
2677T	0.018**	0.003	0.345***		0.828***	
3435T	0.073***	0.027**	0.407***	0.395***		
			r^2			

**P < 0.01, ***P < 0.001 by Arlequin Chi-square Test.

3.4.1.3.2. Haplotype frequencies

Thirteen different *ABCB1* haplotypes were observed among the subjects included for haplotype analysis. Of these, 11 were observed in both control and opioid-dependent subjects, whilst the A**A**CG**T** and **G**GCG**T** haplotypes were only observed in the opioid-dependent population (n = 1 in BMT and 1 in MMT, respectively), albeit at very low frequency (0.5% for both).

Frequencies of individual *ABCB1* haplotypes and common diplotypes in controls and opioid-dependent subjects are given in Table 3-5 and Table 3-6. A PHASE case-control permutation test found no significant difference in population haplotype frequency distributions between control and opioid-dependent subjects (P = 0.78). There were also no significant differences in diplotype frequencies between control and opioid-dependent subjects (P > 0.1).

Table 3-5. *ABCB1* haplotype frequencies in control and opioid-dependent subjects.

ABCB1 Haplotype[c]	Control		Opioid-dependent	
	Observed[a] (n = 74) n_h (%)	Estimated[b] (n = 79) %	Observed[a] (n = 97) n_h (%)	Estimated[b] (n = 108) %
AGCGC	48 (32.4)	29.2	63 (32.5)	29.8
AGCG**T**	11 (7.4)	7.6	16 (8.2)	8.3
AGC**T**C	2 (1.4)	1.8	7 (3.6)	3.8
AGC**TT**	4 (2.7)	3.6	12 (6.2)	6.6
AG**T**GC	7 (4.7)	5.3	13 (6.7)	7.0
AG**T**G**T**	10 (6.8)	8.2	8 (4.1)	5.9
AG**TTT**	46 (31.1)	29.5	59 (30.4)	28.3
AA**A**CGC	2 (1.4)	1.2	3 (1.5)	1.5
AA**A**CG**T**	0 (0.0)	0.0	1 (0.5)	0.6
AA**A**C**T**C	2 (1.4)	1.4	1 (0.5)	0.6
GGCG**T**	0 (0.0)	0.1	1 (0.5)	0.4
GG**T**G**T**	2 (1.4)	2.5	1 (0.5)	1.7
GG**TTT**	14 (9.5)	9.1	9 (4.6)	5.0

n = number of subjects included in analysis. Total number of haplotypes in population = 2n. [a]Absolute count of each haplotype (n_h) (% observed frequency = (n_h/2n) × 100) after excluding subjects with PHASE call probability less than 0.7. [b]Population haplotype frequency estimated by PHASE using entire group genotype data. [c]Haplotype locus order is 61, 1199, 1236, 2677, 3435. Variant loci are indicated in bold.

Table 3-6. *ABCB1* diplotype frequencies in control and opioid-dependent subjects.

Diplotype	Control (N = 74) n (%)	Opioid-dependent (N = 97) n (%)
AGCGC / AG**TTT**	20 (27.0)	24 (24.7)
AGCGC / AGCGC	8 (10.8)	8 (8.2)
AGCG**T** / AG**TTT**	4 (5.4)	6 (6.2)
AGCGC / **G**G**TTT**	5 (6.8)	4 (4.1)
AG**TTT** / AG**TTT**	3 (4.1)	6 (6.2)
AG**T**G**T** / AG**TTT**	4 (5.4)	4 (4.1)
AG**T**GC / AG**TTT**	4 (5.4)	3 (3.1)
AGCGC / AG**T**GC	1 (1.4)	6 (6.2)
AGCGC / AGCG**T**	1 (1.4)	5 (5.2)
AGCGC / AG**T**G**T**	3 (4.1)	2 (2.1)
AGCGC / AGC**TT**	1 (1.4)	4 (4.1)
AGC**T**C / AG**TTT**	1 (1.4)	4 (4.1)
AG**TTT** / **G**G**TTT**	3 (4.1)	1 (1.0)
AGC**TT** / AG**TTT**	2 (2.7)	2 (2.1)
AGCG**T** / AGCG**T**	2 (2.7)	1 (1.0)
AG**T**GC / **G**G**TTT**	2 (2.7)	1 (1.0)
AG**TTT** / AA**C**GC	1 (1.4)	2 (2.1)
GG**T**G**T** / **G**G**TTT**	2 (2.7)	0 (0.0)
AGCG**T** / AGC**TT**	0 (0.0)	2 (2.1)
AGC**TT** / AGC**TT**	0 (0.0)	2 (2.1)
Other	7 (9.5)	10 (10.3)

Only diplotypes observed more than once in either subject group are included. Haplotype locus order is 61, 1199, 1236, 2677, 3435. Variant loci are indicated in bold.

3.4.1.4. *ABCB1* genetic variability and pre-treatment heroin use

No significant differences between *ABCB1* genotypes (n = 72, P > 0.13) or haplotypes (n = 62, P > 0.12) were observed for opioid-dependent subjects' age of first regular heroin use. Similarly, there were no significant associations between opioid-dependent subjects' heroin use in the month prior to entering treatment ($AUD/day) and *ABCB1* genotypes (n = 55, P > 0.14) or haplotypes (n = 46, P > 0.17).

Two-way ANOVA examining sex as a co-factor revealed no significant sex or gene/sex-interaction effects for either age of regular heroin use or levels of prior heroin use ($P > 0.15$ and 0.06, respectively).

3.4.2. *ABCB1* genetic variability and opioid substitution treatment

3.4.2.1. Subject demographics

After excluding all pregnant subjects, 67 MMT and 16 BMT subjects remained. Their demographics, drug use and treatment parameters are shown in Table 3-7.

Treatment outcomes could be determined for 61 MMT and 16 BMT subjects based on the criteria set out in Table 3-1 (see section 3.3.4.2.). In addition, two MMT subjects dropped out of treatment during the original clinical studies, and as such were automatically classified as having poor treatment outcomes. This resulted in overall treatment success rates of around 56% for MMT and 63% for BMT subjects (Table 3-7).

Table 3-7. Demographics, drug use and treatment parameters of methadone (MMT) and buprenorphine (BMT) maintenance subjects included in the analysis of *ABCB1* genetic variability in opioid maintenance treatment.

	MMT (n = 67)	**BMT** (n = 16)
Male : Female	51 : 13	9 : 7
Age (years) (mean ± SD (range))	34 ± 8.5 (20-56) (n = 66)	35 ± 4.5 (22-42)
Weight (kg) (mean ± SD (range))	74 ± 15.2 (39-127) (n = 62)	80 ± 29.5 (54-165) (n = 12)
Age 1st regular heroin use (years)	22 ± 5.4 (13-36) (n = 31)	25 ± 5.1 (16-35)
Prior heroin use[a] ($/day)	110 ± 114.7 (40-400) (n = 17)	100 ± 252.8 (10-1000) (n = 14)

	MMT (n = 67)	**BMT** (n = 16)
Prior other drug use (users : non-users)		
Alcohol[b]	1 : 22	1 : 14
Tobacco[c]	46 : 2	15 : 0
Amphetamines[d]	1 : 23	1 : 1
Benzodiazepines[d]	10 : 13	0 : 2
Cannabis[c]	13 : 10	0 : 1
Cocaine[d]	1 : 22	0 : 2
Prior maintenance treatments (#)	1 ± 1.1 (0-4) (n = 51)	1 ± 1.3 (0-5)
Maintenance dose (mg/day)	70 ± 40.0 (15-180) (n = 62)	9 ± 6.0 (2-20)
Treatment duration (months)	7 ± 41.7 (1-208) (n = 62)	6 ± 6.6 (2-22)
In-treatment heroin use[e] ($/month)	50 ± 1073 (0-7000) (n = 46)	75 ± 73.0 (50-300)
In-treatment other drug use[f] (users : non-users)		
Alcohol		
Tobacco	46 : 2	15 : 0
Amphetamines	14 : 33	8 : 8
Benzodiazepines	12 : 35	5 : 11
Cannabis	23 : 24	13 : 3
Cocaine	3 : 44	3 : 13
Withdrawal (never : ever(most))[g]	9 : 11(8)	5 : 9(2)
Opioid adverse effects (never : ever(most))[g]	3 : 15(7)	-
Non-holders (never : ever(most))[g]	10 : 10(7)	4 : 7(2)
Treatment outcomes (successful : poor)	35 : 28	10 : 6

Data are median ± standard deviation (range) unless otherwise indicated. N-values are given for continuous variables where data was not available for all subjects. [a]Daily monetary amount of heroin used per day in the month leading up to treatment. $: Australian Dollars. [b]At hazardous levels (greater than 40 g/day for males, 20 g/day for females (NHMRC, 2001). [c]Daily use. [d]At least once a month. [e]Total monetary amount of heroin used in the last month of treatment. [f]Subjects were a 'user' if they used a specific drug at least once in the last month of treatment. [g]Number of 'ever' includes subjects designated 'most' (see section 3.3.4.1).

3.4.2.2. Methadone maintenance treatment

3.4.2.2.1. Dose requirements

None of the individual *ABCB1* genotypes significantly influenced daily methadone dose requirements (Table 3-8).

Table 3-8. Relationships between daily methadone maintenance dose requirements and *ABCB1* genotypes.

SNP	Genotype	n	Methadone dose (median ± SD, mg/day)	P-value[a]
A61G	A/A	54	65.0 ± 28.8	1.0
	A/G	6	60.0 ± 53.3	
	G/G	2	62.5 ± 3.5	
G1199A	G/G	57	65.0 ± 32.0	0.8
	G/A	5	60.0 ± 16.4	
C1236T	C/C	15	65.0 ± 41.4	0.9
	C/T	33	65.0 ± 24.5	
	T/T	13	60.0 ± 35.7	
G2677T	G/G	13	65.0 ± 40.0	0.9
	G/T	37	65.0 ± 26.9	
	T/T	12	60.0 ± 33.9	
C3435T	C/C	11	80.0 ± 38.9	0.3
	C/T	30	66.5 ± 26.7	
	T/T	21	65.0 ± 31.6	

[a]P-values are from Kruskal-Wallis test or Mann-Whitney U test where appropriate.

In terms of haplotypes, subjects homozygous for the wild-type AGCGC haplotype required significantly higher daily methadone doses (102.5 ± 41.7 mg/day) than both heterozygous AGCGC carriers (60.0 ± 27.0 mg/day) and homozygous non-carriers (65.0 ± 28.3 mg/day) (P = 0.03, Figure 3-1). Daily methadone dose requirements also differed significantly between AGC**TT** haplotype groups (Kruskal-Wallis test P = 0.006), with AGC**TT** carriers requiring significantly lower doses than non-carriers (Dunn's post test $P < 0.05$) (Figure 3-1).

No other haplotypes were associated with methadone dose requirements ($P \geq 0.07$, Table 3-9).

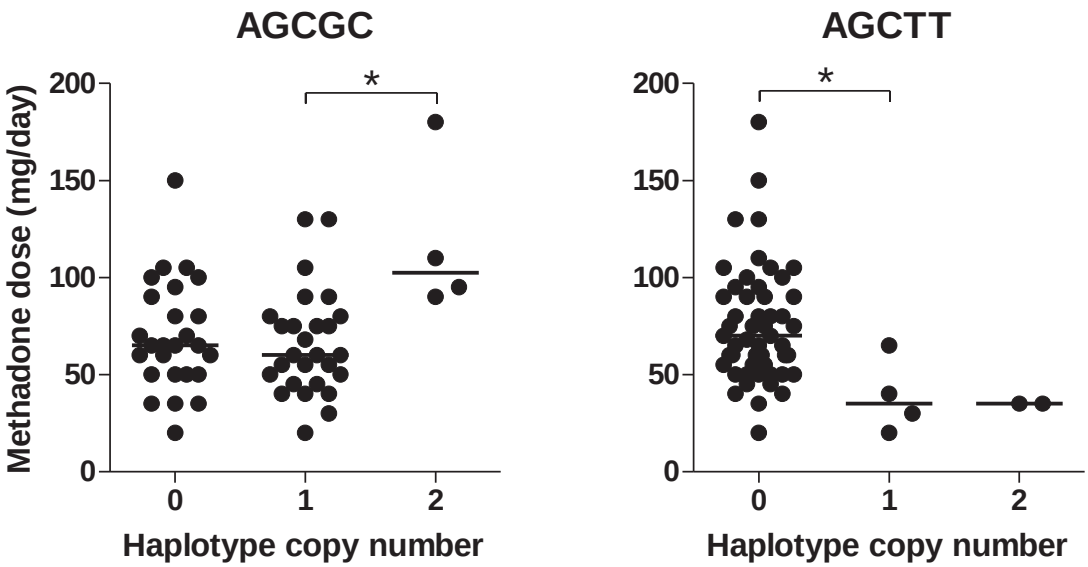

Figure 3-1. Associations of wild-type AGCGC and variant AGCTT haplotypes of *ABCB1* with daily methadone maintenance dose requirements.

*****P < 0.05 by Dunn's Multiple Comparison Test. Lines are medians. Haplotype copy number 0 = non-carriers; 1 = heterozygous carriers; 2 = homozygous carriers.

Table 3-9. Relationships between daily methadone maintenance dose requirements and *ABCB1* haplotypes not displayed in Figure 3-1.

Haplotype	Copy #	n	Methadone dose (median ± SD, mg/day)	P-value[a]
AGCG**T**	0	49	65.0 ± 32.3	0.8
	1	8	67.5 ± 22.8	
AGC**T**C	0	53	65.0 ± 31.7	0.3
	1	3	80.0 ± 17.6	
	2	1	100	
AG**T**GC	0	51	70.0 ± 31.9	0.07
	1	6	55.0 ± 11.7	
AG**T**G**T**	0	53	65.0 ± 40.0	0.8
	1	4	77.5 ± 37.2	
AG**TTT**	0	24	60.0 ± 37.0	0.3
	1	29	75.0 ± 26.4	
	2	4	55.0 ± 26.3	
A**A**CGC	0	54	65.0 ± 31.8	0.8
	1	3	80.0 ± 17.3	
GG**TTT**	0	52	65.0 ± 29.2	0.6
	1	4	97.5 ± 50.4	
	2	1	60	

[a]P-values are from Kruskal-Wallis test or Mann-Whitney U test where appropriate. Variant loci are indicated in bold. Copy # 0 = non-carriers; 1 = heterozygous carriers; 2 = homozygous carriers.

3.4.2.2.1.1. Covariates

No significant genotype-sex interactions were detected by two-way ANOVA (% of total variation < 11%, P > 0.05) (see Appendix A: Table A-5).

The influence of sex on the observed link between AGCGC homozygosity and increased methadone daily dose requirements could not be assessed due to the absence of homozygous wild-type female MMT subjects. However, two-way ANOVA comparing heterozygous AGCGC carriers and non-carriers revealed a significant haplotype-sex interaction (8.4% of total variation, P = 0.04), suggesting potential sex differences in the impact of AGCGC on methadone dose requirements. Male AGCGC homozygotes still required significantly higher methadone doses than AGCGC heterozygous carriers and non-carriers (P < 0.05 by Dunn's Multiple Comparison Test, Figure 3-2).

No significant haplotype-sex interactions were observed for any other *ABCB1* haplotypes (AGC**TT**, AG**T**GC, AG**TTT** and **G**G**TTT**) when analysed by two-way ANOVA (% of total variation < 4.5, P > 0.3) (see Appendix A: Table A-5).

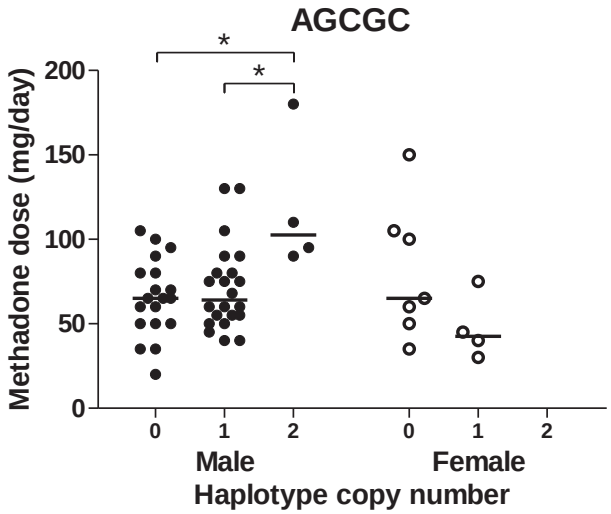

Figure 3-2. Sex differences in the relationship between the wild-type *ABCB1* haplotype (AGCGC) and MMT dose requirements.

*P < 0.05 by Dunn's Multiple Comparison Test. Lines are medians. Haplotype copy number 0 = non-carriers; 1 = heterozygous carriers; 2 = homozygous carriers.

Whilst two-way ANOVA indicated a significant gene effect for the **G**G**TTT** haplotype when taking into account treatment outcome (14.7% of total variation, P = 0.004. See Appendix A:Table A-6), post-hoc analysis within successful treatment outcome subjects revealed no significant differences in dose requirements between haplotype groups (P = 0.3). Treatment outcome had no influence on the relationship between other *ABCB1* genotypes/haplotypes and MMT dose requirements (% of total variation < 8.5, P > 0.08. See Appendix A:Table A-6).

Multiple linear regression analysis identified the AGC**TT** haplotype (P = 0.007) and treatment outcome (P = 0.036) as statistically significant predictors of MMT dose requirements, whilst time in treatment (P = 0.08) was also included in the final model (adjusted $r^2 = 0.24$).

Self-reported heroin use prior to entering treatment was significantly positively correlated with methadone dose ($r^2 = 0.32$, P = 0.03).

3.4.2.2.2. Trough plasma (R)-methadone concentrations

Trough plasma (R)-methadone concentrations were significantly higher in subjects who were heterozygous (C/T) or homozygous variant (T/T) for the C1236T SNP when compared to homozygous wild-type (C/C) subjects (Kruskal-Wallis P = 0.04, Dunn's post-hoc P < 0.05 for C/C versus C/T, Figure 3-3).

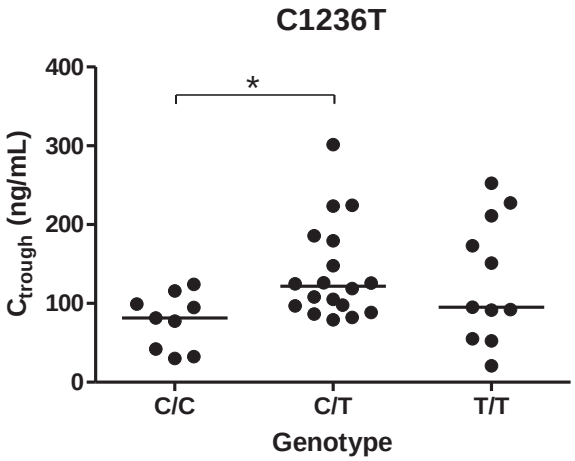

Figure 3-3. Association between *ABCB1* C1236T genotypes and trough plasma (R)-methadone concentrations (C_{trough}).

*P < 0.05 by Dunn's Multiple Comparison Test. Lines are medians.

No other genotypes were significantly associated with (R)-methadone trough concentrations (P > 0.2, see Table 3-10).

Table 3-10. Relationship between (R)-methadone C_{trough} requirements and *ABCB1* genotypes not displayed in Figure 3-3.

SNP	Genotype	n	(R)-methadone C_{trough} (median ± SD, ng/mL)	P-value[a]
A61G	A/A	32	112.1 ± 56.0	
	A/G	5	95.3 ± 119.5	0.6
	G/G	2	89.1 ± 3.6	
G1199A	G/G	36	112.1 ± 65.0	0.3
	G/A	3	97.8 ± 39.6	
G2677T	G/G	6	111.8 ± 18.9	
	G/T	26	106.7 ± 67.0	1.0
	T/T	7	92.0 ± 83.6	
C3435T	C/C	4	124.5 ± 47.5	
	C/T	17	97.8 ± 58.5	0.6
	T/T	18	121.0 ± 72.6	

[a]P-values are from Kruskal-Wallis test or Mann-Whitney U test where appropriate.

For haplotypes, AGC**TT** carriers had significantly lower C_{trough} values than other subjects (77.6 ± 33.4 versus 124.2 ± 64.5 ng/mL, P = 0.01, Figure 3-4). Alternatively, there was substantial variation in medians between homozygous AG**TTT** carriers (173.3 ± 80.3), heterozygous AG**TTT** carriers (126.1 ± 56.5), and AG**TTT** non-carriers (89.1 ± 66.2) (Kruskal-Wallis P = 0.04), but no significant difference between any group pair by Dunn's post-hoc test. As shown in Figure 3-4, a Mann-Whitney U test revealed a significantly higher median C_{trough} for AG**TTT** carriers (homozygous and heterozygous carriers combined), when compared to AG**TTT** non-carriers (137.0 ± 59.1 versus 89.1 ± 66.2, respectively, P = 0.01). No other haplotype was significantly associated with (R)-methadone C_{trough} among MMT subjects (P > 0.3, see Table 3-11).

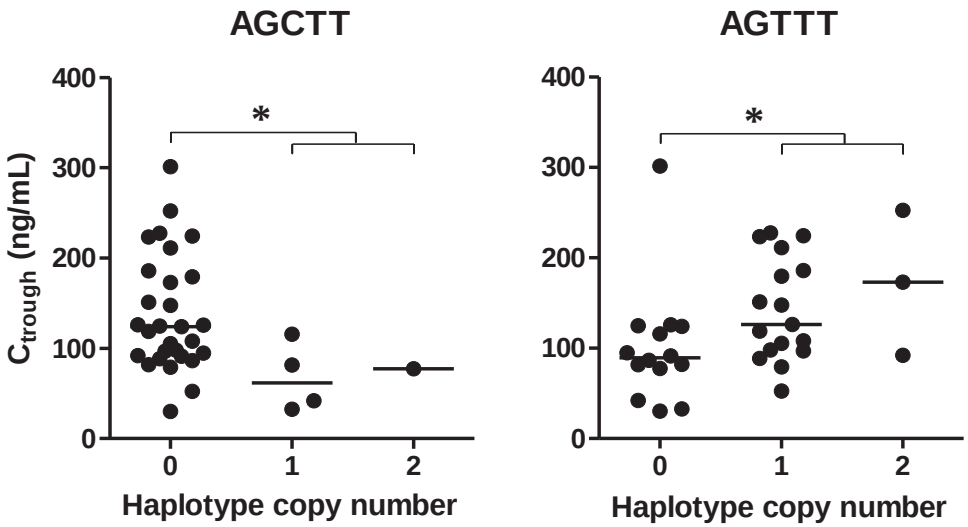

Figure 3-4. Association between *ABCB1* haplotypes and trough plasma (R)-methadone concentrations (C_{trough}).

*****P < 0.05 by Mann-Whitney U test comparing haplotype non-carriers to combined heterozygous and homozygous carriers. Lines are medians. Haplotype copy number 0 = non-carriers; 1 = heterozygous carriers; 2 = homozygous carriers.

Table 3-11. Relationship between (R)-methadone C_{trough} requirements and *ABCB1* haplotypes not displayed in Figure 3-4.

Haplotype	Copy #	n	(R)-methadone C_{trough} (median ± SD, ng/mL)	P-value[a]
AGCGC	0	18	121.0 ± 71.9	0.8
	1	15	105.1 ± 60.0	
	2	1	124.2	
AGCG**T**	0	27	105.1 ± 64.6	0.3
	1	7	126.1 ± 71.3	
AG**T**GC	0	31	108.3 ± 67.1	0.8
	1	3	124.7 ± 42.1	
AG**T**G**T**	0	31	108.3 ± 66.1	0.6
	1	3	151.1 ± 64.7	
GG**TTT**	0	30	112.1 ± 57.7	0.3
	1	3	227.6 ± 109.2	
	2	1	91.6	

[a]P-values are from Kruskal-Wallis test or Mann-Whitney U test where appropriate. Variant loci are indicated in bold. Copy # 0 = non-carriers; 1 = heterozygous carriers; 2 = homozygous carriers.

3.4.2.2.2.1. Covariates

A significant gene-sex interaction was detected (20.9% of total variation, P = 0.01) for the influence of the C1236T SNP on plasma (R)-methadone C_{trough} values, with median C_{trough} values significantly higher in female T/T subjects (227.6 ± 40.6) than male T/T subjects (92.0 ± 56.4, P < 0.05) (see Figure 3-5). In addition, the 3435 T/T variant genotype was associated with higher C_{trough} values in females, but not males, when compared to C/T genotype subjects (genotype effect = 16.7% of total variation, P = 0.02; genotype-sex interaction = 15.9% of total variation, P = 0.02). As such, 3435 T/T females had significantly higher median C_{trough} values (227.6 ± 40.6) than female C/T subjects (98.6 ± 30.0, P = 0.02) (see Figure 3-5).

A significant gene-sex interaction was also reported for G2677T genotype (28.2% of total variation, P = 0.005), with males and females seemingly displaying opposite genotype/haplotype-C_{trough} relationships (Figure 3-5). Indeed, female 2677 T/T subjects had a significantly greater median C_{trough} than male T/T subjects (227.6 ± 40.6 versus 84.6 ± 29.3, P < 0.01. Figure 3-5). However, no statistically significant association between G2677T genotype and C_{trough} was observed when each sex was analysed separately (P > 0.09).

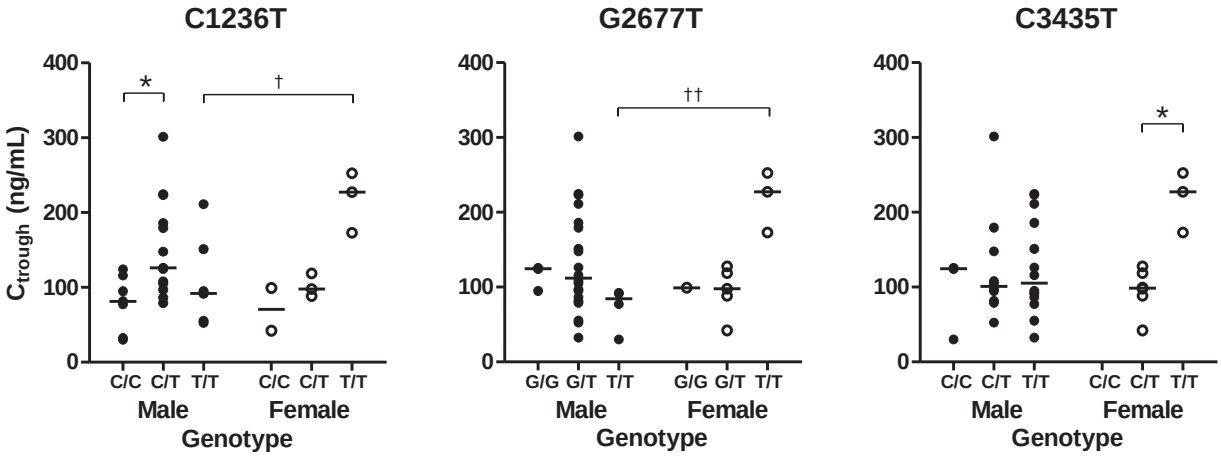

Figure 3-5. Sex differences in *ABCB1* genotype-C_{trough} relationships for (R)-methadone in MMT.

*****P < 0.05 by Dunn's Multiple Comparison Test. †P < 0.05, ††P < 0.01 by two-way ANOVA Bonferroni post-hoc test. Lines are medians.

Sex had no significant influence on the relationship between other *ABCB1* genotypes (A61G and G1199A) or any haplotype and (R)-methadone C_{trough} requirements (% of total variation < 13.0, P > 0.05. See Appendix A: Table A-7). Similarly, treatment outcome did not significantly influence genotype- or haplotype-C_{trough} relationships (% of total variation < 3.0, P > 0.4. See Appendix A: Table A-8).

Multiple linear regression analysis identified the AG**TTT** haplotype as the only significant predictor of plasma (R)-methadone C_{trough} (P = 0.03, final model adjusted $r^2 = 0.11$).

A positive correlation was observed between plasma (R)-methadone C_{trough} and prior heroin use ($r^2 = 0.36$, P = 0.02).

3.4.2.2.3. Methadone pharmacokinetics

No *ABCB1* genotype or haplotype was significantly associated with plasma (R)-methadone C_{trough}/dose ratios (P > 0.1) (Appendix A: Table A-9). Plasma (S)-methadone C_{trough}/dose ratios were significantly higher in C1236T C/T genotype subjects when compared to homozygous wild-types (1.9 ± 0.8 versus 1.4 ± 0.6, Dunn's Multiple Comparison test P < 0.05), but there was no difference between C/C and T/T (1.5 ± 0.9) subjects (Figure 3-6). AG**TTT** haplotype carriers also had significantly higher plasma (S)-methadone C_{trough}/dose ratios than non-carriers (1.9 ± 0.8 versus 1.5 ± 0.6, respectively. P = 0.03. Figure 3-6).

3.4.2.2.3.1. Covariates

In terms of sex differences, significant sex (13.2% of total variation, P = 0.03) and gene-sex interaction (11.0% of total variation, P = 0.04) effects were reported for the relationship between the G1199A SNP and (R)-methadone C_{trough}/dose, but with no significant genotype effect (7.5% of total variation, P = 0.09) (Figure 3-7). No other significant sex or gene-sex interaction effects were reported for (R)-methadone C_{trough}/dose (<5% of total variation (P > 0.2) and <9% of total variation (P > 0.2), respectively) (see Appendix A: Table A-10).

Fewer data were available for (S)-methadone, so sex-effect analysis was restricted to the G1199A, C1236T and G2677T genotypes, and AG**TTT** and AGC**TT** haplotypes. For these variants, there were no significant sex (<7% of total variation, P > 0.3) or gene-sex interaction (<3% of total variation. P > 0.5) effects for (S)-methadone C_{trough}/dose ratios.

Multiple linear regression analyses could not identify any significant predictors of plasma (R)- or (S)-methadone C_{trough}/dose.

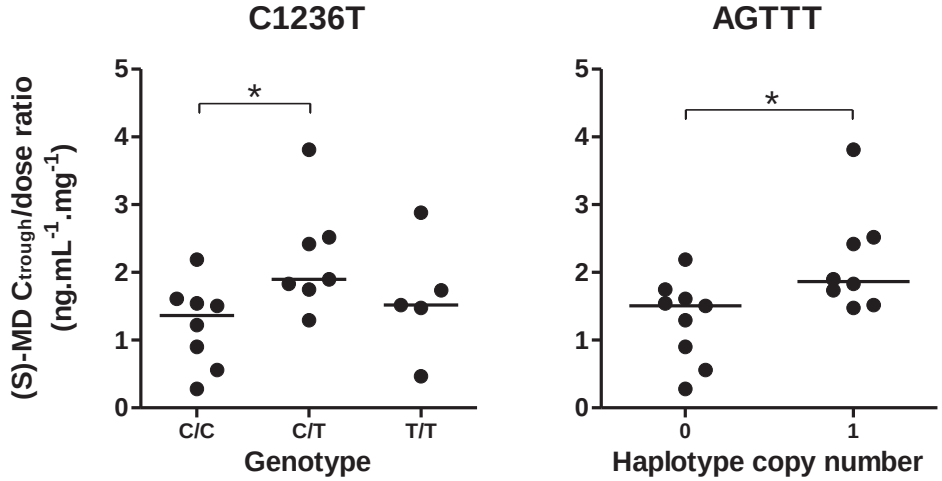

Figure 3-6. Association between the *ABCB1* C1236T SNP and AGTTT haplotype variants and (S)-methadone ((S)-MD) C_{trough}/dose ratios.

Lines are medians. Haplotype copy number 0 = non-carriers; 1 = heterozygous carriers; 2 = homozygous carriers.

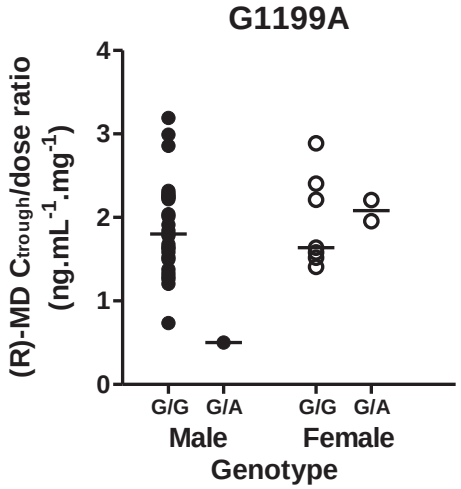

Figure 3-7. Potential genotype (*ABCB1* G1199A)-sex interaction influencing (R)-methadone dose-adjusted C_{trough}.

Lines are medians.

3.4.2.2.4. Methadone maintenance treatment response

3.4.2.2.4.1. Successful versus poor treatment outcome

A summary of the Fisher's Odds Ratios and P-values for associations between individual *ABCB1* genotypes and treatment success is given in Table 3-12. The C1236T variant frequency was significantly higher in poor treatment outcome subjects (60.7% in poor versus 36.8% in successful, P = 0.01), mostly due to a higher T/T genotype frequency in this group (C/C: 14.3 versus 35.3%, C/T: 50 versus 55.9%, T/T: 35.7 versus 8.8%, for poor and successful treatment outcome, respectively). This association was confirmed by binary logistic regression analysis with an adjusted Odds Ratio (95% CI) of 0.22 (0.06 to 0.72) (P = 0.01).

When analysed separately the A61G variant was associated with poor treatment outcome in males, however, the adjusted Odds Ratio was not significant in binary logistic regression analysis (P > 0.3).

Table 3-12. Summary table of results from Fisher's Exact Tests comparing the frequency of *ABCB1* variant alleles between successful and poor MMT outcome subjects.

	Fisher's Exact Test Odds Ratio (95% CI), P-value		
SNP	**All subjects**	**Males**	**Females**
A61G	0.21 (0.04 to 1.03), 0.08	**0.08 (0.009 to 0.71), 0.009****	6.60 (0.24 to 181.8), 0.3
G1199A	0.52 (0.08 to 3.22), 0.7	1.17 (0.10 to 13.34), 1.0	0.34 (0.01 to 7.99), 0.5
C1236T	**0.38 (0.18 to 0.78), 0.01***	**0.38 (0.16 to 0.87), 0.03***	0.39 (0.05 to 2.77), 0.6
G2677T	0.96 (0.47 to 1.94), 1.0	0.72 (0.32 to 1.65), 0.5	7.00 (0.69 to 70.78), 0.2
C3435T	0.64 (0.31 to 1.30), 0.3	0.64 (0.28 to 1.47), 0.3	1.00 (0.17 to 5.78), 1.0

High Odds Ratio indicates higher variant allele frequency in successful versus poor treatment outcome. CI: Confidence Interval. ***P < 0.05, **P < 0.01**.

A permutation test reported no significant difference in *ABCB1* haplotype distribution between successful and poor treatment outcome in MMT subjects overall (P = 0.2). However, permutation tests analysing sexes separately revealed a significant difference in haplotype frequencies between treatment outcome groups in males (P = 0.03) but not females (P = 0.3). Post-hoc analysis of individual haplotype frequencies in successful and poor treatment outcome male subjects revealed that all three **G**G**TTT** haplotype carriers (one of them homozygous) exhibited poor treatment outcomes, representing a statistically significant difference in haplotype frequency between the outcome groups (see Table 3-13).

Table 3-13. Comparison of *ABCB1* haplotype frequencies between male MMT subjects with successful or poor treatment outcome.

Haplotype	Fisher's Exact Test Odds Ratio (95% CI)	P-value
AGCGC	1.85 (0.74 to 4.65)	0.3
AGCG**T**	1.78 (0.34 to 9.34)	0.7
AGC**T**C	1.14 (0.10 to 13.04)	1.0
AGC**TT**	6.84 (0.37 to 127.6)	0.2
AG**T**GC	0.54 (0.10 to 2.86)	0.7
AG**T**G**T**	0.11 (0.005 to 2.31)	0.1
AG**TTT**	0.90 (0.36 to 2.22)	0.8
A**A**CGC	2.95 (0.14 to 63.28)	0.5
GG**TTT**	**0.06 (0.003 to 1.08)**	**0.02***

High Odds Ratio indicates higher haplotype frequency in successful versus poor treatment outcome. CI: Confidence Interval. ***P < 0.05.** Variant loci are bold.

3.4.2.2.4.2. In-treatment withdrawal and opioid side-effects

A summary of the Odds Ratios and P-values for associations between individual *ABCB1* genotypes and in-treatment withdrawal or opioid side effects is given in Table 3-14. The C1236T variant allele was significantly more frequent among subjects who reported experiencing withdrawal (63.6 versus 25.0% in non-withdrawal subjects), with an adjusted Odds Ratio of 5.33 (95% CI: 1.05 to 26.9, P = 0.04) after binary logistic regression analysis.

Table 3-14. Summary table of results from Fisher's Exact Tests comparing the frequency of *ABCB1* genotypes between subjects who did or did not experience withdrawal ('withdrawal-ever') or opioid side-effects ('opioid-most').

	Fisher's Exact Test Odds Ratio (95% CI), P-value	
SNP	**'Withdrawal-ever'[a]**	**'Opioid-most'[a]**
A61G	11.63 (0.60 to 226.4), 0.05	2.73 (0.39 to 18.88), 0.4
G1199A	2.58 (0.10 to 67.33), 1.0	0.49 (0.02 to 13.00), 1.0
C1236T	**5.25 (1.26 to 21.87), 0.03***	1.93 (0.50 to 7.49), 0.5
G2677T	1.04 (0.30 to 3.65), 1.0	1.44 (0.37 to 5.57), 0.7
C3435T	1.03 (0.25 to 4.14), 1.0	0.74 (0.16 to 3.40), 0.7

High Odds Ratio indicates higher variant allele frequency in subjects experiencing withdrawal or opioid side-effects. CI: Confidence interval. [a]See definitions in section 3.3.4.1 (pg 88). ***P < 0.05**.

There were no significant differences in *ABCB1* variant allele frequencies between subjects who did or did not experience opioid side-effects most of the time (Table 3-14), whilst permutation tests reported no significant differences in haplotype frequencies between withdrawal (P = 0.3) or opioid side-effect (P = 0.8) groups.

3.4.2.2.5. Summary

A summary of the major findings in MMT subjects is given in Table 3-15.

Table 3-15. Summary of major findings in MMT subjects.

	1236T M & F	**3435T** F	AGCGC M	AGC**TT** M & F	AG**TTT** M & F
Dose	-	-	⇑	⇓	-
C_{trough}	⇑	⇑	-	⇓	⇑
Outcome	**Poor**	-	-	-	-

Variants are bold. M = significant in male subjects only. F = significant in female subjects only. M & F = observed in both males and females. ⇑ = significantly higher in haplotype carriers or variant genotypes. ⇓ = significantly lower in haplotype carriers or variant genotypes. C_{trough} = (R)-methadone trough plasma concentration.

3.4.2.3. Buprenorphine maintenance treatment

3.4.2.3.1. Dose requirements

There were no significant differences in median buprenorphine dose requirements between *ABCB1* genotypes (Table 3-16) or haplotypes (Table 3-17) found in more than one subject. The single subject carrying the AGC**TT** haplotype had the equal lowest dose requirement (2 mg/day) of all BMT subjects.

Table 3-16. Associations between daily buprenorphine maintenance dose requirements and *ABCB1* genotypes.

SNP	Genotype	n	Buprenorphine dose (median ± SD, mg/day)	P-value[a]
A61G	A/A	13	10.0 ± 6.0	0.1
	A/G	3	2.8 ± 4.4	
C1236T	C/T	9	10.0 ± 7.2	0.8
	T/T	7	8.0 ± 4.4	
G2677T	G/G	2	7.0 ± 7.1	0.2
	G/T	11	10.0 ± 6.1	
	T/T	3	5.0 ± 3.0	
C3435T	C/C	1	12.0	0.2
	C/T	7	14.0 ± 7.1	
	T/T	8	6.0 ± 4.0	

[a]P-value from Kruskal-Wallis test or Mann-Whitney U test where appropriate.

Table 3-17. Associations between daily buprenorphine maintenance dose requirements and *ABCB1* variant haplotypes.

Haplotype	Copy #	n	Buprenorphine dose (median ± SD, mg/day)	P-value[a]
AGCGC	0	9	6.0 ± 4.6	0.05
	1	6	14.0 ± .3	
AG**T**GC	0	12	7.0 ± 6.6	1.0
	1	3	12 ± 6.0	
AG**T**G**T**	0	13	8.0 ± 6.5	-[b]
	1	2	10.0 ± 5.7	
AG**TTT**	0	3	2.8 ± 5.6	0.3
	1	10	12.0 ± 6.5	
	2	2	6.5 ± 2.1	

[a]P-value from Kruskal-Wallis test or Mann-Whitney U test where appropriate. [b]Too few heterozygous subjects to perform Mann-Whitney U test. Variant loci are indicated in bold. Copy # 0 = non-carriers; 1 = heterozygous carriers; 2 = homozygous carriers.

3.4.2.3.1.1. Covariates

Treatment outcome did not significantly influence the relationship between genotypes and buprenorphine dose requirements (% of total variation < 7, P > 0.2) (see Appendix A: Table A-11). Alternatively, two-way ANOVA indicated a significant AGCGC haplotype-treatment outcome interaction (23.5% of total variation, P = 0.03). Indeed, as shown in Figure 3-8, the association between AGCGC haplotype carriers and high buprenorphine dose requirements was just statistically significant when successful treatment outcome subjects were analysed separately (carriers = 20.0 ± 4.6; non-carriers = 5.0 ± 4.2; P = 0.04).

The influence of treatment outcome on the effects of other *ABCB1* haplotypes (AG**T**GC, AGC**TT**, AG**T**G**T**, AG**TTT**) on buprenorphine dose requirements could not be assessed due to insufficient subject numbers.

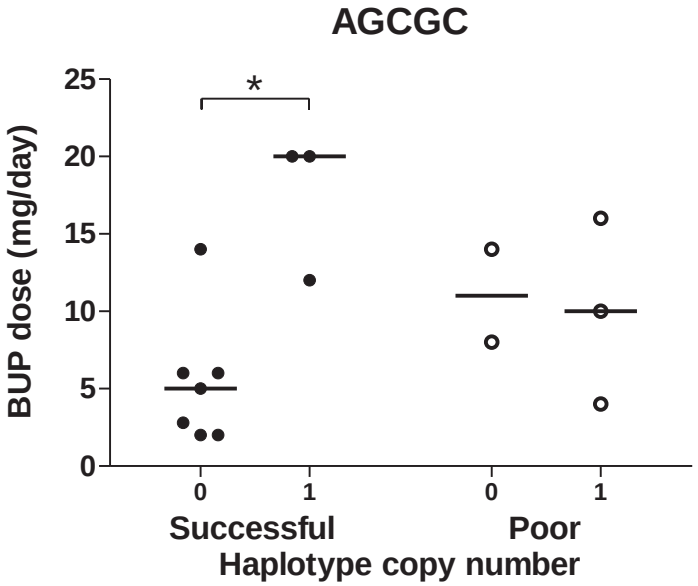

Figure 3-8. The influence of treatment outcome on *ABCB1* wild-type (AGCGC) haplotype-dose relationship in buprenorphine (BUP) maintenance treatment.

*P < 0.05 by Dunn's Multiple Comparison Test. Lines are medians. Haplotype copy number 0 = non-carriers; 1 = heterozygous carriers; 2 = homozygous carriers.

No clear sex differences in the relationship between the A61G, C1236T, G2677T or C3435T SNPs, or the AGCGC or AG**TTT** haplotypes, and buprenorphine dose requirements could be

detected (% of total variation < 19, P > 0.06) (see Appendix A: Table A-12). The influence of sex on the effects of other *ABCB1* genotypes (G1199A) and haplotypes (AG**T**GC, AGC**TT**, AG**T**G**T**) could not be assessed due to the insufficient subject numbers.

Self-reported prior heroin use was not significantly correlated with buprenorphine daily dose ($P = 0.6$, $r^2 = 0.02$).

3.4.2.3.2. Trough plasma concentrations

There were no significant differences in median C_{trough} for buprenorphine or norbuprenorphine between *ABCB1* genotypes or haplotypes found in more than one subject (P > 0.2) (see Appendix A: Table A-13 and Table A-14). Two-way ANOVA found no significant effects of treatment outcome or sex on the relationships between *ABCB1* genotypes/haplotypes and buprenorphine or norbuprenorphine C_{trough} (P > 0.1).

Self-reported prior heroin use was not significantly correlated with buprenorphine or norbuprenorphine C_{trough} ($P > 0.3$, $r^2 < 0.1$)

3.4.2.3.3. Buprenorphine pharmacokinetics

No *ABCB1* genotype or haplotype was significantly associated with changes in plasma buprenorphine or norbuprenorphine C_{trough}/dose (P > 0.07) (see Appendix A: Table A-15). However, consideration of sex effects by two-way ANOVA detected significant G2677T genotype effects for buprenorphine (77.6% of total variation, P = 0.0002) and norbuprenorphine (48.8% of total variation, P = 0.03), and a significant G2677T genotype-sex interaction effect for buprenorphine C_{trough}/dose (11.2% of total variation, P = 0.03) (see Table 3-18 and Table 3-19). As shown in Table 3-18, large C3435T genotype and AGCGC haplotype effects on buprenorphine C_{trough}/dose were also reported (20 and 25% of total variation, respectively), however, these effects did not reach statistical significance (P > 0.1).

Table 3-18. Sex differences in the relationships between dose-adjusted trough plasma buprenorphine (BUP) concentrations (C_{trough}/dose) and *ABCB1* genotypes/haplotypes.

		Males		Females		Two-way ANOVA factor effects (% of total variation (P-value))		
SNP	**Genotype**	**n**	**BUP C_{trough}/dose median ± SD (pg.mL^{-1}.mg^{-1})**	**n**	**BUP C_{trough}/dose median ± SD (pg.mL^{-1}.mg^{-1})**	Genotype	Sex	Interaction
A61G	A/A	6	63 ± 141	4	94 ± 83	0.6 (0.8)	2.3 (0.7)	1.9 (0.7)
	A/G	1	170	2	98 ± 74			
C1236T	C/T	5	70 ± 59	3	79 ± 101	7.7 (0.4)	4.4 (0.5)	11.9 (0.3)
	T/T	2	218 ± 252	3	108 ± 52			
G2677T	G/G	2	94 ± 107	0	-			
	G/T	4	63 ± 35	5	79 ± 46	**77.6 (2 x 10^{-4})*****[a]	8.2 (0.05)[a]	**11.2 (0.03)***[a]
	T/T	1	396	1	230			
C3435T	C/C	1	18	0	-			
	C/T	3	56 ± 43	3	79 ± 57	20.4 (0.2)[a]	2.8 (0.6)[a]	6.4 (0.4)[a]
	T/T	3	170 ± 167	3	108 ± 94			
Haplotype	**Copy #**							
AGCGC	0	4	120 ± 161	3	150 ± 62	24.9 (0.1)	0.1 (0.9)	0.0 (1.0)
	1	3	56 ± 52	2	58 ± 29			
AG**TTT**	0	2	94 ± 107	1	150			
	1	4	63 ± 35	4	94 ± 83	4.1 (0.6)[b]	11.4 (0.4)[b]	0.2 (0.9)[b]
	2	1	396	0	-			

[a]Male homozygous wild-type subjects excluded from two-way ANOVA analysis. [b]Male homozygous variant subjects excluded from two-way ANOVA analysis. ***P < 0.05**, ****P < 0.001**. Variant haplotype loci are indicated in bold. Copy # 0 = non-carriers; 1 = heterozygous carriers; 2 = homozygous carriers.

Table 3-19. Sex differences in the relationships between dose-adjusted trough plasma norbuprenorphine (NOR) concentrations (C_{trough}/dose) and *ABCB1* genotypes/haplotypes.

		Males		Females		Two-way ANOVA factor effects (% of total variation (P-value))		
SNP	**Genotype**	**n**	**NOR C_{trough}/dose median ± SD (pg.mL^{-1}.mg^{-1})**	**n**	**NOR C_{trough}/dose median ± SD (pg.mL^{-1}.mg^{-1})**	Genotype	Sex	Interaction
A61G	A/A	6	92 ± 98	4	173 ± 127	0.0 (1.0)	9.4 (0.4)	0.5 (0.8)
	A/G	1	110	2	211 ± 191			
C1236T	C/T	5	88 ± 47	3	227 ± 143	2.1 (0.6)	4.7 (0.5)	10.5 (0.3)
	T/T	2	205 ± 154	3	118 ± 146			
G2677T	G/G	2	79 ± 44	0	-	**48.8 (0.03)*[a]**	3.6 (0.5)[a]	0.1 (0.9)[a]
	G/T	4	92 ± 44	5	118 ± 117			
	T/T	1	314	1	360			
C3435T	C/C	1	48	0	-	0.4 (0.9)[a]	7.5 (0.4)[a]	4.3 (0.5)[a]
	C/T	3	96 ± 52	3	227 ± 136			
	T/T	3	110 ± 125	3	118 ± 153			
Haplotype	**Copy #**							
AGCGC	0	4	103 ± 108	3	346 ± 134	15.8 (0.2)	15.4 (0.2)	2.4 (0.6)
	1	3	73 ± 65	2	151 ± 107			
AG**TTT**	0	2	79 ± 44	1	346	6.4 (0.4)[b]	**52.6 (0.03)*[b]**	13.4 (0.2)[b]
	1	4	92 ± 44	4	173 ± 127			
	2	1	314	0	-			

[a]Male homozygous wild-type subjects excluded from two-way ANOVA analysis. [b]Male homozygous variant subjects excluded from two-way ANOVA analysis. ***P < 0.05**. Variant haplotype loci are indicated in bold. Copy # 0 = non-carriers; 1 = heterozygous carriers; 2 = homozygous carriers.

3.4.2.3.4. Buprenorphine maintenance treatment response

No *ABCB1* SNP was significantly associated with either treatment success or in-treatment withdrawal reports ($P > 0.7$, see Appendix A: Table A-16 and Table A-17). Similarly, permutation tests reported no significant difference in *ABCB1* haplotype distributions between treatment outcome ($P = 0.7$) or withdrawal ($P = 0.9$) groups. No data were available for in-treatment opioid side-effects in BMT subjects.

3.4.2.3.5. Summary

A summary of the major findings in BMT subjects is given in Table 3-20.

Table 3-20. Summary of major findings in MMT subjects.

	2677T	3435T	AGCGC
Dose	-	-	⇑[a]
BUP C_{trough}/dose	⇑	⇑	⇓
NOR C_{trough}/dose	⇑	-	-

⇑ = significantly higher, in haplotype carriers or variant genotypes. ⇑ and ⇓ = large but not significant genotype/haplotype effect by two-way ANOVA. BUP = buprenorphine. NOR = norbuprenorphine. C_{trough}/dose = dose-adjusted trough plasma concentration. [a]Only after excluding poor treatment outcome subjects.

3.5. Discussion

The main aims of this study were to retrospectively examine the roles of *ABCB1* genetic variability in opioid dependence and opioid maintenance treatment response. Importantly, the demographics of the opioid-dependent subjects of this study, such as age (mean: 33 years), sex (57% male), and age of first heroin use (mean: 21 years), as well as the use of multiple illicit drugs, were very similar to those reported among MMT patients surveyed as part of National Evaluation of Pharmacotherapies for Opioid Dependence (Mattick et al., 2001), and more recently the Australian Treatment Outcome Study (Ross et al., 2005) (29-33 years old, 57-59% male and first heroin use at 20 years). As such, the subjects included in this study are likely to represent a typical Australian treatment-seeking opioid-dependent population.

3.5.1. *ABCB1* genetic variability and opioid dependence

Twin and adoption studies have provided good evidence that there is a substantial genetic component to susceptibility to drug addiction (True et al., 1999a; True et al., 1999b; Ball & Collier, 2002; Hall et al., 2002). Based on existing evidence that the CNS distribution of the heroin metabolite, morphine, as well as opioid peptides of the endogenous reward system, might be influenced by P-gp activity, it was hypothesized that *ABCB1* genetic variability may be one such genetic component modulating an individual's risk and/or severity of opioid dependence. If this hypothesis were true, one would expect the frequencies of *ABCB1* variants to differ between opioid-dependent and control populations, and *ABCB1* genetic variants to be associated with certain aspects of the pathogenesis of heroin addiction.

In order to test this hypothesis, opioid-dependent and control subjects were genotyped for the A61G, G1199A, C1236T, G2677T and C3435T SNPs of *ABCB1*. These SNPs were chosen for investigation as they are five of the most common *ABCB1* variants observed in Caucasians, and have at least some prior *in vitro* evidence of an impact on substrate transport (see Chapter 1, section 1.6.4). However, this study revealed no significant difference in genotype frequencies between opioid-dependent and control subjects, with both populations displaying similar SNP frequencies to those reported previously in Caucasians (Hoffmeyer et al., 2000; Cascorbi et al., 2001; Kim et al., 2001). There was also no association between these genotypes and opioid-dependent subjects' heroin use demographics.

As discussed in Chapter 1 (section 1.6.4), *in vitro,* human *ex vivo* and human *in vivo* studies all indicate that haplotype analysis of *ABCB1* genetic variability is likely to prove more informative than the investigation of individual SNPs in isolation. As such, subject genotype data was used to predict and analyse *ABCB1* haplotypes for each individual.

3.5.1.1. Validation of haplotype predictions

As with the validation data set discussed in Chapter 2 (2.2), PHASE haplotype predictions using the complete data set were valid and consistent, and it was possible to determine *ABCB1* haplotypes with reasonable confidence for 94% of control and 90% of opioid-dependent subjects.

As expected, by far the most common haplotypes in both groups were the wild-type AGCGC and triple variant AG**TTT** haplotypes, with frequencies of 29-33% and 28-31%, respectively. Consequently, around a quarter of subjects were AGCGC / AG**TTT** heterozygotes. The frequencies of these common haplotypes were similar to those previously reported among Caucasians (15-36.5% for wild-type and 27-32% for 1236/2677/3435 variant (Kim et al., 2001; Kroetz et al., 2003), and strong linkage disequilibrium was confirmed between the 1236T, 2677T and 3435T variants (see Table 3-4) in support of previous studies (Hoffmeyer et al., 2000; Kim et al., 2001; Kroetz et al., 2003).

Interestingly, significant linkage disequilibrium was also reported between the 61G variant and each of the 1236T, 2677T and 3435T SNPs (D' = 0.9, 0.4 and 1.0, respectively), albeit with low r^2 values (< 0.08) due to the low frequency of the 61G allele. Alternatively, the 1199A variant displayed significant linkage disequilibrium with the 1236C and 3435C wild-type alleles (D' = 1.0 and 0.8, respectively), but again with a low r^2 (< 0.03) due to the low frequency of the 1199A variant (see Chapter 2, section 2.2.1 regarding interpretation of linkage disequilibrium measures). To my knowledge this is the first reported evidence of significant linkage disequilibrium between the 61G and 1199A variants and other SNPs of *ABCB1*, and may warrant further investigation. However, the low frequency of these alleles and their close genomic proximity to the other SNPs (particularly for the 1199 and 1236 loci) makes these findings difficult to interpret.

3.5.1.2. *ABCB1* haplotypes and opioid dependence

No significant differences in haplotype distributions were observed between opioid-dependent and control subject populations, nor did any haplotype appear to affect the age of onset of regular heroin use. As such, the first hypothesis of this thesis, that *ABCB1* genetic variability is associated with the risk of opioid dependence, was not supported by this study.

Whilst the identification of a genetic risk factor for opioid dependence is of scientific interest, beyond this, knowledge of such an association it is likely to be of little use regarding the prevention and treatment of illicit opioid abuse and dependence. However, if a genetic factor were able to identify illicit opioid users more likely to develop a severe form of dependence/addiction (in a similar manner to the *DRD2* A1 polymorphism and severe alcohol dependence (Connor et al., 2008)), this may have important implications for treatment choices and patient management (i.e. increased psychosocial intervention and support). As such, a potential association between *ABCB1* haplotypes and levels of prior heroin use was also investigated.

It should be noted that the acquisition of self-report data ultimately relies on the honesty of subjects, and can be confounded by flaws in recollection (particularly for subjects who have been in treatment for a long period of time (up to 17.5 years in this study)) as well as fluctuations in the price and purity of heroin over time. Furthermore, the amount of heroin an individual uses is not the only measure of the severity of opioid dependence/addiction. As such, self-report data on prior heroin use should be treated with caution. Nonetheless, this study provided no evidence for a role of *ABCB1* genetic variability in influencing the severity of opioid dependence as it relates to heroin use.

Therefore, *ABCB1* genetic variability does not appear to play a role in the risk or severity of opioid dependence. However, there may be one important caveat. The opioid-dependent subjects of this retrospective study represent only the treatment-seeking portion of heroin

addicts. Although previous Australian surveys have indicated that the demographics and drug use histories of individuals seeking maintenance treatment and those not seeking treatment are relatively similar (Mattick et al., 2001; Ross et al., 2005), it is still possible that those addicts who do not seek treatment could represent a distinct, but important, opioid abusing population. As such, a role for *ABCB1* genetic variability in influencing the aetiology and severity of opioid dependence within non-treatment-seeking individuals, or even the likelihood of seeking treatment itself, cannot be ruled out, and may provide an area for future investigation.

3.5.2. *ABCB1* genetic variability and opioid substitution treatment

Existing evidence suggests that variability in P-gp transport could influence the absorption, distribution and elimination of numerous opioids, including methadone. Therefore, based on the previous research discussed in Chapter 1, it was hypothesized that *ABCB1* genetic variants would be associated with decreased substitution opioid requirements in maintenance treatments for opioid dependence, and potentially less in-treatment withdrawal or greater adverse opioid side-effects. Thus the primary aim of this study was to determine whether *ABCB1* genetic variability could be used to predict substitution opioid dose requirements of maintenance treatment patients.

In addition to daily maintenance dose requirements, trough plasma (R)- and (S)-methadone or buprenorphine and norbuprenorphine concentrations (C_{trough}) were available for a number of MMT and BMT subjects, respectively. These data were analysed in two ways.

Firstly, raw C_{trough} values were employed as a direct measure of the effective plasma substitution opioid concentrations required to suppress withdrawal over the dosing period. It was hoped that this analysis would eliminate some of the potential confounding factors associated with comparisons of dose requirements, such as the significant inter-individual variability in absorption and metabolism (due to factors other than P-gp transport (see Chapter

1, section 1.4.2.1)), and therefore give an indication of the influence of *ABCB1* genetic variability on methadone and buprenorphine's PK/PD relationships. In addition, with the possibility of TDM becoming a part of standard opioid substitution treatment (at least for MMT) (Wolff et al., 2000), the prospect of being able to predict an individual's target C_{trough} is rather appealing.

Secondly, as in previous studies of methadone pharmacokinetics (Eap et al., 2000; Eap et al., 2002), dose-adjusted C_{trough} values were employed as a measure of methadone and buprenorphine bioavailability and/or systemic clearance.

Therefore, C_{trough} was used as an indicator of P-gp activity at the BBB, whilst dose-adjusted C_{trough} (C_{trough}/dose) was employed as a measure of P-gp activity in the liver, kidney and/or intestine.

Additional data from the original clinical studies also made it possible to examine the relationship between *ABCB1* genetic variability in basic measures of overall treatment response.

3.5.2.1. Methadone maintenance treatment

3.5.2.1.1. Methadone requirements and pharmacokinetics

The most significant findings of this study relate to one of the *ABCB1* variant haplotypes, AGC**TT**. Carriers (both homozygous and heterozygous) of this haplotype consisting of variants at the 2677 and 3435 loci, not only required 50% lower MMT doses than other subjects (confirmed by multiple linear regression analysis), but also had 38% lower (R)-methadone C_{trough} values. Importantly, these subjects had treatment success rates as good, if not better, than the MMT subject group as a whole (86 versus 56%, respectively). Therefore, subjects carrying the AGC**TT** variant haplotype can be said to require lower doses and lower plasma concentrations of methadone for the successful treatment of opioid dependence. In

terms of the mechanism behind this association, the lower C_{trough} requirements and the lack of an effect on C_{trough}/dose, indicate that the AGC**TT** haplotype is associated with a decreased P-gp activity at the BBB, resulting in an increased CNS exposure to methadone for a given dose or plasma concentration.

Conversely, subjects homozygous for the wild-type AGCGC haplotype required 1.7- and 1.6-fold higher MMT doses than heterozygous carriers and non-carriers, respectively. This supports the assumption that subjects with wild-type *ABCB1* haplotypes will have the highest levels of P-gp activity, and as such will require higher doses in order to achieve therapeutically effective CNS concentrations of methadone. Unfortunately, due to insufficient C_{trough} data for the homozygous wild-type (AGCGC) subjects, it was not possible to determine whether increased dose requirements were a result of decreased bioavailability, increased clearance, or decreased brain distribution. However, as discussed in Chapter 1 (see section 1.5.2), it is expected that, for high dose oral drugs such as methadone, P-gp activity at the BBB is likely to have the greatest impact on the eventual CNS drug distribution. The current findings for the AGC**TT** haplotype also tend to support this hypothesis. Therefore, it is likely that subjects who are homozygous for the wild-type (AGCGC) haplotype have higher P-gp activity at the BBB, such that their CNS exposure to methadone is decreased for a given dose, and consequently, higher doses are required to prevent withdrawal over the 24-hour dosing period.

Based on existing evidence for the functional effects of *ABCB1* SNPs on opioid response (Meineke et al., 2002; Skarke et al., 2003b; Campa et al., 2008), it was hypothesized that the common AG**TTT** haplotype, which is variant for the three linked 1236, 2677 and 3435 loci, would also be associated with decreased dose requirements. However, no significant differences in dose requirements were observed, even for homozygous AG**TTT** subjects. Furthermore, AG**TTT** haplotype carriers had significantly higher C_{trough} values than non-

carriers, an association confirmed by multiple linear regression analysis. Since no significant difference in C_{trough}/dose was observed between AG**TTT** carriers and non-carriers, these findings indicate that the increased C_{trough} associated with the AG**TTT** haplotype is due to a change in methadone PK/PD causing increased methadone plasma concentration requirements. This would indicate increased P-gp activity at the BBB among AG**TTT** variant subjects, which directly contradicts the hypothesis (based on existing studies) that *ABCB1* genetic variants are associated with decreased efflux activity. As such, the present findings for the AG**TTT** haplotype are unexpected.

Several possible explanations can be put forward as to the unexpected findings for the AG**TTT** haplotype, and why they differ from those for the AGC**TT** variant. Firstly, the results for either the AGC**TT** or AG**TTT** haplotypes, or both, may simply be chance (false positive) findings (see section 3.5.3) and not represent any functional impact on methadone transport. Alternatively, the two haplotypes differ in regards to the C1236T SNP, which unexpectedly displayed significant associations with both poor treatment response and higher C_{trough} values. As such, it is possible that the presence of the 1236T variant in AG**TTT** haplotype may be responsible for the high C_{trough} requirements, counteracting the effects of the 2677T and 3435T variants observed in AGC**TT** haplotype carriers. Finally, since the AGC**TT** haplotype represents a rare break in linkage disequilibrium between the 1236T, 2677T and 3435T variants, it is possible that this haplotype is linked to, and is acting as a marker for, a rare functional polymorphism of the *ABCB1* gene that is separate from the SNPs examined here. Indeed, as mentioned in Chapter 1, over 1200 polymorphisms have been reported within the *ABCB1* gene, and over 60 of these are found within the transcribed (exonic) sequence, with the functional consequences of the majority of these SNPs yet to be determined. Therefore, it is possible that the SNPs examined here have very little functional impact on methadone transport themselves, but the haplotype patterns they form may act as markers for rarer *ABCB1* mutations with true functional consequences.

Whatever the mechanism behind this apparent divergence in functional consequence for the AGC**TT** and AG**TTT** haplotypes, these findings reaffirm the importance of analysing *ABCB1* haplotypes rather than individual SNPs.

3.5.2.1.1.1. Covariates

One other interesting observation among MMT subjects was the potential sex difference in the effects of common *ABCB1* SNPs (C1236T, G2677T and C3435T), and the AGCGC haplotype, on methadone dose and C_{trough} requirements. For example, a significant association between MMT dose requirements and the AGCGC haplotype was observed in males, but not in females. In terms of C_{trough}, significant gene-sex interactions were detected by two-way ANOVA for the C1236T, G2677T and C3435T genotypes. A significant gene-sex interaction was also reported for the association between G1199A genotype and C_{trough}/dose, however, this was likely a spurious finding dependent solely on one male G/A genotype subject (see Figure 3-7).

Sex differences in the effects of *ABCB1* genetic variants are not entirely unexpected. Previous research has indicated significant sex differences in P-gp expression, with healthy males expressing 2.4-fold more hepatic P-gp than healthy females (Schuetz et al., 1995). This might explain specific observations of genotype/haplotype effects in one sex and not the other. Indeed, sex effects on the relationship between 2677T/3435T and artorvastatin treatment response have previously been reported, with an increased P-gp activity among 2677GG/3435CC homozygotes linked to decreased treatment efficacy in females but not males (Kajinami et al., 2004). Similarly, the variant 1236T-2677T-3435T haplotype has been associated with increased neuropsychiatric side effects of mefloquine in women but not men (Aarnoudse et al., 2006). However, simple sex differences in P-gp expression do not explain why, in the case of G2677T and C_{trough}, males and females display opposite effects, and why, contradictory to existing studies, some findings in females tend to indicate a decreased CNS

exposure in carriers of *ABCB1* variants. Possible explanations may be sex differences in percentage body fat (affecting methadone's V_d (Foster et al., 2004)), or perhaps a hormonal (progestin) interaction with P-gp (Garrigos et al., 1997; Shapiro et al., 1999; Frohlich et al., 2004), resulting in unexpected functional consequences for *ABCB1* variants among females. However, due to the limited data available in this retrospective study, it is difficult to draw any strong conclusions. Nonetheless, these results highlight sex as a potentially important co-factor for future studies of *ABCB1* pharmacogenetics, particularly in MMT.

Since subjects with poor treatment outcomes may not actually be receiving their optimal doses, it was important to ensure that their inclusion was not reducing the ability of the study to identify associations between *ABCB1* genetic variability and effective methadone requirements. As such, the effect of treatment outcome on the relationships between genotypes/haplotypes and continuous variables was examined. Multiple linear regression analysis did identify treatment outcome as a significant correlate (along with the AGC**TT** haplotype) of MMT dose requirements, which likely reflects previous observations that higher doses of methadone (60-100 mg) are associated with significantly better treatment outcomes when compared to lower doses (Ling et al., 1996; Faggiano et al., 2003). However, the relationships between *ABCB1* genetic variability and methadone requirements did not appear to differ between successful or poor treatment outcome subjects.

Finally, significant positive correlations were identified between prior heroin use and both MMT dose and C_{trough} requirements. Unfortunately, the small number of MMT subjects with prior heroin use data prohibited its inclusion in the multiple linear regression analyses of this study, but these findings indicate it could be an important cofactor worth considering in any future studies in MMT.

3.5.2.1.2. Methadone maintenance treatment response

In addition to associations between *ABCB1* genetic variants and methadone requirements, a number of interesting observations were also made regarding overall treatment outcome (separate from its analysis as a covariate for methadone requirements).

C1236T variant frequencies were higher among poor treatment outcome subjects and those subjects reporting in-treatment withdrawal. This was despite a lack of significant differences in maintenance doses, and significantly higher C_{trough} values in 1236T carriers, indicating that, contrary to previous *in vitro* functional studies (Salama et al., 2006; Kimchi-Sarfaty et al., 2007), the 1236T variant may be associated with increased P-gp activity at the BBB. However, whilst all 7 of the poor treatment outcome MMT subjects with complete adverse event data reported experiencing 'withdrawal-ever' (6 being 1236T carriers), 6 of these subjects (5 1236T carriers) also reported experiencing adverse opioid effects at least some of the time ('opioid-ever'), and 4 of these (all 1236T carriers) reported experiencing opioid side-effects most of the time ('opioid-most'). As such it appears that the association between the C1236T variant and poor treatment response is not due simply to withdrawal, but an overall unpleasant treatment experience encompassing both withdrawal and adverse opioid effects. It has previously been proposed that some patients may be more likely to report dissatisfaction with their treatment regardless of actual physical symptoms (Elkader et al., 2009a; Elkader et al., 2009b). Therefore, it is unclear whether the 1236T variant is influencing methadone distribution, or perhaps endogenous components of the stress, reward and/or addiction systems (such as β-endorphin).

When analysed individually, the 61G variant was also found to be significantly associated with poor treatment outcomes in males (but not females). However, binary logistic regression analysis indicated that this association was most likely due to linkage disequilibrium between

the 61G and 1236T variants (see section 3.5.1.1), which likely also explains the observed link between the **G**G**TTT** haplotype and poor treatment outcome in males.

3.5.2.1.3. Comparisons with other literature

Prior to commencing this research project, no study had investigated the potential link between *ABCB1* genetic variability and opioid dependence, or the response to opioid maintenance medications (either in patient populations or healthy controls). However, in early 2006, Lötsch and colleagues (2006) reported an investigation of the influence of *ABCB1* genetic variability on (R)-methadone response in healthy volunteers. Employing miosis as an endpoint for opioid CNS effect, they concluded that genetic variability at the 2677 and 3435 loci (both separately and as a haplotype) did not affect (R)-methadone response. In addition, they found no significant effect of these polymorphisms on the urinary recovery of (R)-methadone and its metabolites.

Despite the different subject populations investigated (healthy versus opioid-dependent), and the inclusion of SNP data from only 2 loci in Lötsch and colleagues (2006), their findings agree well with those of the present study. For example, neither investigation observed a significant effect of *ABCB1* genetic variability on methadone plasma pharmacokinetics, supporting the hypothesis that P-gp is more likely to affect methadone's CNS distribution, rather than absorption and clearance. Furthermore, no effects of the G2677T or C3435T SNPs on methadone response were detected when they were investigated separately. Finally, although the present observation of an association between the AGC**TT** haplotype and low methadone requirements may appear to contradict the findings of Lötsch and colleagues (2006), a post-hoc analysis of MMT subject data from this study reveals that, when considering only the 2677 and 3435 loci, there are no significant differences in methadone dose requirements (mg/day) between 2677T:3435T homozygous carriers (median ± SD = 55 ± 39.7), heterozygous carriers (68 ± 26.1) and homozygous non-carriers (70 ± 38.3) (P = 0.6).

Therefore, the lack of association between the G2677T and C3435T SNPs and methadone response described by Lötsch and colleagues (2006) simply aids in highlighting the importance of examining the full range of *ABCB1* genetic variability, in the form of haplotypes, as opposed to one or two popular SNPs. In particular, inclusion of the common, but rarely investigated, C1236T SNP, appears to be vital for the correct identification of rare but functionally significant *ABCB1* haplotypes such as AGC**TT**.

In late 2006, the initial findings of the current study, including the first 60 MMT and 60 control subjects, were published in Clinical Pharmacology and Therapeutics (Coller et al., 2006) (see Appendix D). In addition to the lack of association between *ABCB1* genetic variability and opioid dependence, it reported the significant associations between AGCGC homozygotes and high dose requirements, and the association between the AGC**TT** haplotype and low dose requirements. It is important to note that this published data included pregnant subjects and subjects with low phase call probabilities which were later excluded from the final analyses of methadone response presented here. Furthermore, an additional 18 MMT and 38 control subjects were genotyped following publication and were subsequently included in the final analyses described in this Chapter. Nonetheless, the major conclusions presented in this Chapter do not differ from those of the published data (Coller et al., 2006) (see Appendix D).

Published in the same journal issue, a study by Crettol and colleagues (2006) in 245 Swiss subjects receiving MMT (3-430 mg/day) investigated the A61G, G2677T and C3435T SNPs of *ABCB1*. They reported no association between these SNPs and dose requirements, which is in agreement with the present study. However, they did find that variant genotypes of the A61G and C3435T SNPs, and 61G-2677T-3435T variant haplotypes, were significantly associated with lower (R)- and (S)-methadone C_{trough}/dose. They concluded that this was due to a "wider distribution" of methadone as opposed to decreased absorption, although this

conclusion was not supported by their pharmacodynamic data. As discussed in section 3.5.2.1.1, the present study found no such relationship between the A61G or C3435T SNPs and dose-adjusted C_{trough}. However, the genotype effects observed by Crettol were relatively small (20-30% change), and as such the current study (with C_{trough} data available for only 38 subjects) may have had insufficient power to detect these differences.

Crettol and colleagues (2006) also reported that these variant genotypes and haplotype were associated with significantly higher plasma (R)- and (S)-methadone concentration peak-to-trough ratios, and concluded this was due to a decreased elimination half-life for *ABCB1* variant subjects. However, this conclusion contradicts not only the findings of the current study, but also previous clinical studies in morphine and loperamide (Meineke et al., 2002; Skarke et al., 2003b; Campa et al., 2008) that suggest, if an effect were to be observed, it should be in the form of a decrease in clearance due to decreased P-gp transport. Unfortunately, Crettol and colleagues (2006) offered no possible explanation for this unusual finding. However, it is possible that the altered peak-to-trough ratios merely reflected the significant changes in C_{trough}/dose (discussed above) due to altered methadone distribution, and thus may not be related to methadone elimination as they suggested. Alternatively, these results could bring into question whether dose-adjusted C_{trough} and dose-adjusted peak-to-trough concentration ratios are appropriate surrogates for methadone distribution and clearance when examining such a wide range of methadone doses (3-430 mg/day). To my knowledge this has yet to be investigated.

In a response to the Coller et al., (2006) publication, Crettol and colleagues subsequently genotyped 279 subjects for the G1199A and C1236T SNPs (in addition to the A61G, G2677T and C3435T SNPs) and conducted a full haplotype analysis. In a letter to the editor (Crettol et al., 2008b) they reported that, despite including all five SNPs (A61G, G1199A, C1236T, G2677T and C3435T), there were no significant associations between *ABCB1* haplotypes and

methadone dose requirements in their MMT population. Three possible explanations can be proposed regarding the discrepancies between this study and that of the Swiss group published in reply to Coller et al., (2006).

Firstly, in this study, all subjects received once-daily maintenance doses, whilst the Swiss MMT group included 46 subjects who split their daily dose into 2 or 3 intakes. Since splitting daily maintenance doses is likely to significantly influence both the total daily dose requirements, and the impact of P-gp activity on methadone CNS exposure, it is quite possible that split dosing subjects included in the Swiss study could have confounded any potential haplotype-dose relationships. This would be particularly true for rarer haplotypes such as AGC**TT** (n = 7 carriers in Crettol et al., 2008b) where analyses are particularly sensitive to just a few outliers within carrier groups. The 10 non-"white" subjects included in the Swiss study could similarly have confounded any haplotype-dose relationships, due to potential ethnic differences in the functional consequences of *ABCB1* genetic variants.

Secondly, the Australian MMT subjects of the present study, and the European subjects of Crettol and colleagues (2006, 2008a,b), may represent distinct opioid-dependent populations in terms of socioeconomic status, and pre- or in-treatment heroin and other drug use patterns. If so, they are likely to respond differently to MMT, and hence the influence of *ABCB1* genetics may vary.

Thirdly, and probably most importantly, individual clinic policies and treatment philosophies can play significant roles in determining what is an appropriate, safe or effective methadone maintenance dose, as well as how patients respond to treatment (see Chapter 1, section 1.3.4) (Bell et al., 1995; Magura et al., 1998; Magura et al., 1999). Therefore, the apparent discrepancies between these two studies may simply represent variability in the way dosing is optimized in different treatment settings, and how patients are managed. Indeed, the most obvious difference between this study and that of Crettol et al. (2008b) is the much larger

range of methadone doses employed in the Swiss MMT population (3-430 mg/day versus 15-180 mg/day in this study). In addition to the larger range of doses, the Swiss group also received higher doses on average (mean (95%CI) = 107 (99-116) mg/day) when compared to this MMT cohort (mean (95%CI) = 63 (62-71) mg/day). As such, the dose range investigated may also be an important determinant of whether *ABCB1* genetic variability significantly influences methadone response (see Chapter 4).

More recently, in subjects at an Israeli treatment clinic receiving 30-280 mg/day, Levran and colleagues (2008) also reported no association between any of 9 *ABCB1* SNPs (including C1236T, G2677T and C3435T) and MMT dose requirements. Unfortunately, Levran and colleagues did not investigate whether daily methadone maintenance dose requirements differed between *ABCB1* haplotypes. They did, however, compare the frequency of *ABCB1* haplotypes (formed by the C1236T, G2677T and C3435T SNPs) between MMT subjects designated as high dose (>150 mg/day) and low dose (<150 mg/day). Based on the findings of the present study, it would be expected that, because subjects who were homozygous for the AGCGC haplotype had higher methadone dose requirements, the frequency of the 1236CC/2677GG/3435CC haplotype would be significantly higher in MMT subjects receiving more than 150 mg/day. However, Levran and colleagues (2008) observed the opposite, with the homozygous 1236TT/2677TT/3435TT variant haplotype frequency significantly higher in high dose (>150 mg/day) compared to low dose (<150 mg/day) subjects (20.4% versus 4.5%, respectively, P = 0.026).

Therefore, there appears to be contradictory evidence as to the role of variant *ABCB1* haplotypes in determining MMT dose requirements, depending on the treatment setting (South Australia versus Switzerland versus Israel) and also the dose range of methadone investigated (15-180 versus 3-430 versus 30-280 mg/day).

Unfortunately, neither Crettol and colleagues (2006, 2008b) nor Levran and colleagues (2008) examined sex, treatment outcome, or prior heroin use as co-factors for the relationship between *ABCB1* genetic variability and methadone requirements or pharmacokinetics.

3.5.2.2. Buprenorphine maintenance treatment

3.5.2.2.1. Buprenorphine requirements and pharmacokinetics

Though not statistically significant, variant genotypes at the 61, 2677 and 3435 loci were associated with 50-72% lower buprenorphine dose requirements. These associations were enhanced to 62-73% reductions in dose requirements when successful treatment outcome subjects were analysed separately. Conversely, AGCGC haplotype carriers required 2.3-fold higher (P = 0.05) median buprenorphine doses than non-carriers, a difference which was enhanced and statistically significant when successful treatment outcome subjects were analysed separately (4-fold higher, P = 0.04).

With regards to the AGC**TT** haplotype, which was significantly associated with decreased dose requirements among MMT subjects, only one carrier was observed within the BMT group. However, this AGC**TT** carrier had the equal lowest dose of buprenorphine (2 mg/day) for all BMT subjects, and was successful in treatment, indicating that the AGC**TT** haplotype may also be related to buprenorphine requirements. However, this requires confirmation in a larger BMT subject population.

Taken together, these results support the hypothesis that *ABCB1* variants are associated with decreased BMT dose requirements.

With regards to the mechanism behind the influence of *ABCB1* genetic variability on buprenorphine dose requirements, no significant *ABCB1* genotype or haplotype differences in buprenorphine (or norbuprenorphine) C_{trough} were observed. As such, unlike methadone, it appears that *ABCB1* genetic variability was not influencing the PK/PD of buprenorphine or

norbuprenorphine, at least not to the extent of significantly altering plasma concentration requirements. Alternatively, C_{trough}/dose data suggest that *ABCB1* genetic variants may instead be linked with alterations in the plasma pharmacokinetics of buprenorphine and norbuprenorphine. See section 3.5.2.2.3 below for a more detailed discussion taking into account data from more recent studies.

3.5.2.2.2. Treatment outcome

Whilst no significant differences in *ABCB1* genotype or haplotype frequencies were observed between successful and poor treatment outcome BMT subjects, the small numbers in each group (n = 10 and 6, respectively) made it statistically difficult to detect an association. Therefore, whilst no evidence of a role for *ABCB1* genetic variability in determining BMT response was observed here, it cannot be ruled out.

3.5.2.2.3. Comparisons with other literature

Prior to commencing this project, buprenorphine had yet to be investigated as a P-gp substrate. However, as will be discussed in more detail in Chapter 6, attempts have since been made by others to evaluate its efflux by P-gp, with the balance of evidence so far indicating that buprenorphine is not a P-gp substrate.

It seems strange then that BMT dose requirements are affected by *ABCB1* genetic polymorphisms if buprenorphine is not a P-gp substrate. One possible explanation may be that, whilst buprenorphine is not a P-gp substrate, its opioid active metabolite, norbuprenorphine, is. Indeed, norbuprenorphine has demonstrated significant P-gp transport in human *ABCB1*-transfected HEK293 cell monolayers, which was over 5-fold that observed for methadone measured in the same study (Tournier et al., 2009). As such, a diminished norbuprenorphine biliary excretion, and subsequent inhibition of buprenorphine CYP3A4 metabolism (due to increased norbuprenorphine concentrations in hepatocytes) (Zhang et al.,

2003a), might explain the association between *ABCB1* variants and increased C_{trough}/dose observed in this study, but requires further confirmation.

Whatever the exact mechanism may be, to date this remains the only study to investigate and report an association between *ABCB1* genetic variability and BMT dose requirements.

3.5.3. Study limitations

In addition to the study limitations already discussed, the major limitation of this study was its retrospective approach. Drawing data from numerous different clinical studies, as well as missing data on original case report forms, meant that not all data were available for all subjects. This was a particular problem for covariate analyses where there was a mismatch in availability for different data. As such, in some cases subject numbers were prohibitively small, and consequently the statistical power to detect genotype/haplotype differences was significantly reduced, particularly for rarer *ABCB1* genetic variants.

Furthermore, the heterogeneity of the opioid-dependent populations (as a result of drawing subjects from multiple clinical studies, particularly for MMT subjects), is likely to have made it more difficult to detect subtle, or treatment setting- or duration-dependent, effects of *ABCB1* genetic variability. Indeed, the opioid-dependent subjects included in this study were recruited from various treatment settings, ranging from prison populations to privately-prescribed take-away dosing. Whilst this also represents a strength of this study, in that significant genetic factors determining methadone and buprenorphine response could still be detected despite such heterogeneous patient populations, future studies may benefit from concentrating on particular treatment settings. In addition, there was an indication from linear regression analyses that dose requirements may also be positively correlated with time in treatment, which suggests it may be beneficial to focus on one particular period of treatment. For example, examining the pharmacogenetics of opioid substitution treatments during the induction and early stabilisation period of treatment may be more likely to detect the impact

of *ABCB1* variants on methadone and buprenorphine response. Since this stage of treatment is when patients are at the greatest risk of adverse events, it may also prove more useful regarding eventual translation into clinical practice.

Considering the aforementioned limitations, the impact of rarer *ABCB1* genotypes (A61G and G1199A) and haplotypes on methadone or buprenorphine response cannot be ruled out, and may be revealed in a larger, more homogeneous patient population.

Finally, apart from those intrinsic to the statistical tests employed (e.g. case-control permutation, binary and linear regression, one- and two-way ANOVA, and chi-squared tests), no adjustments for multiple testing were made when determining statistical significance. As such, there is a risk that some observations represent type 1 (false positive) errors. However, the consistency in the effects of the AGCGC and AGC**TT** haplotypes between different parameters and between MMT and BMT subject groups, as well as their agreement with our *a priori* hypotheses, suggest that these are true positive findings. Nonetheless, it will be important to replicate these findings in different (preferably larger and prospective) cohorts of opioid substitution treatment subjects.

3.6. Conclusions

In conclusion, *ABCB1* genetic variability was not associated with the risk of opioid dependence, or heroin use demographics. Alternatively, significant associations were observed between *ABCB1* haplotypes and both MMT and BMT dose requirements.

For MMT, homozygosity for the wild-type haplotype AGCGC was linked to higher methadone dose requirements, whilst the AGC**TT** variant haplotype was associated with lower methadone dose and C_{trough} requirements. An association between the C1236T SNP and poor MMT treatment outcome was also observed. These effects of *ABCB1* genetic variability

appeared to be due to differences in P-gp activity at the BBB, regulating its CNS distribution, since no differences in plasma pharmacokinetics were detected.

The wild-type AGCGC haplotype was also associated with higher BMT dose requirements, significantly so among successful treatment outcome subjects. The mechanism behind differences in buprenorphine requirements remains unknown, but variability in clearance due to changes in norbuprenorphine transport may be one possibility.

Potentially significant covariates for the study of *ABCB1* pharmacogenetics in opioid substitution treatment were also identified. Specifically, sex appears to be a significant co-factor in MMT response, whilst treatment success, time in treatment, and/or prior heroin use may also be important considerations when examining the relationship between *ABCB1* genetic variability and substitution opioid requirements.

This study therefore provides the first evidence that determining *ABCB1* haplotypes of opioid-dependent patients may aid in individualizing opioid substitution treatments. However, subsequent investigations by others in other treatment populations have indicated that, at least for methadone, the impact of *ABCB1* genetic variability on dose requirements may be dependent on the treatment population, the dose range employed for opioid maintenance, and/or individual clinic policies. Therefore, large-scale multi-centre prospective trials are required to further elucidate whether *ABCB1* haplotyping might one day provide clinicians with a useful clinical tool for establishing individualized target doses and/or plasma concentrations required for efficacious opioid substitution treatment.

Chapter 4. ABCB1 pharmacogenetics in high dose methadone maintenance treatment

4.1. Introduction

The first retrospective study (Chapter 3) of *ABCB1* genetic variability in standard dose MMT subjects identified a significant association between the wild-type haplotype and high maintenance dose requirements, and between the AGC**TT** variant haplotype and low maintenance dose requirements. However, as discussed in Chapter 3, attempts by other research groups to replicate these findings have failed.

A study in Swiss MMT subjects receiving a much larger range of methadone doses (3-430 mg/day), has reported a lack of association between any *ABCB1* haplotype and dose requirements (Crettol et al., 2008b). Furthermore, a more recent study in an Israeli treatment centre (with doses ranging 30-280 mg/day), reported that the frequency of homozygous 1236**TT**-2677**TT**-3435**TT** haplotypes was significantly higher in subjects receiving high doses of methadone (>150 mg/day), when compared to those receiving less than 150 mg/day (20.4% versus 4.5%, respectively, P = 0.026) (Levran et al., 2008). These findings are in contrast to my results in Australian MMT subjects, and appear counterintuitive when considering our current understanding of *ABCB1* pharmacogenetics in relation to opioids (Meineke et al., 2002; Skarke et al., 2003b; Campa et al., 2008), and the hypothesised role of P-gp in methadone transport across the BBB. As discussed in Chapter 1, we would expect people carrying *ABCB1* genetic variants to have decreased P-gp efflux of opioids, and thus a greater exposure to methadone. Hence, *ABCB1* variant haplotypes should be associated with lower, not higher, doses. As such, there is conflicting evidence as to the role of variant *ABCB1* haplotypes in determining MMT dose requirements, depending on the treatment setting and also the dose range investigated (15-110 versus 3-430 versus 30-280 mg/day).

Therefore, the aim of this study was to investigate *ABCB1* genetic variability in an opioid-dependent population receiving a higher range of MMT doses more akin to those prescribed

in European treatment centres. By comparing variant frequencies between high dose MMT subjects, standard dose MMT subjects and non-opioid-dependent controls, as well as investigating the impact of *ABCB1* genetic variability on high dose methadone requirements and pharmacokinetics, this study hoped to establish whether methadone dose range is important in determining the impact of *ABCB1* pharmacogenetics in MMT.

4.2. Materials and methods

4.2.1. Subjects

Twenty-two high dose methadone maintenance (HD), 78 normal dose methadone maintenance (ND) and 98 control subjects were included in this retrospective study. HD subjects were part of a clinical study from the Specialist Medical Practice Clinic, Drug and Alcohol in Redfern, New South Wales, that was approved by the South East Sydney Area Health Service Ethics Committee. These subjects represented a small cohort of subjects who required higher than usual doses to reduce withdrawal symptoms and heroin use. ND subjects consisted of the same MMT patients described in Chapter 3. Healthy non-opioid-dependent controls were also the same as those studied in Chapter 3. Written informed consent for genotyping analysis was obtained for all subjects.

4.2.2. Demographics, methadone requirements and pharmacokinetic data

Demographic data of HD subjects were obtained from original study case notes, as were daily methadone dose requirements (mg/day) and time in treatment (months). In addition, plasma (R)- and (S)-methadone trough concentrations (C_{trough}, ng/mL) and (R)- and (S)-methadone apparent oral clearances (CL/F, L/h) of HD subjects had already been determined (as part of the original clinical study) by liquid chromatography with mass spectrometry and population pharmacokinetic models, respectively, using established methods (Foster et al., 2004).

As with the previous retrospective study, C_{trough} was used as an indicator of plasma methadone concentration requirements for suppressing withdrawal, whilst dose-adjusted C_{trough} (C_{trough}/dose) was employed as measure of P-gp activity influencing methadone bioavailability and/or systemic clearance (see Chapter 3, section 3.5.2).

4.2.3. *ABCB1* genotyping and haplotyping

ABCB1 genotypes and haplotypes of HD subjects were determined using the methods described in Chapter 2. In addition to recording the population estimates for each haplotype frequency from the PHASE output, 'observed' haplotype frequencies were calculated for the HD, ND and control subject groups based on each individual's predicted haplotypes (after excluding subjects with phase call probabilities less than 0.7).

In order to allow a direct comparison between this study and that of Levran and colleagues (2008), 3-SNP haplotypes formed by C1236T, G2677T and C3435T were also estimated using PHASE and analysed in the same manner as for the standard 5-SNP haplotypes.

4.2.4. Data analysis

Individual SNP allele and genotype frequencies were compared between HD and control, or HD and ND subject groups using Fisher's Exact Test (with Odds Ratio) (alleles) or Chi-square Test (genotypes). Where homozygous variant genotypes were too rare to conduct a Chi-square Test, homozygous variant and heterozygous genotypes were combined and the data analysed by Fisher's Exact Test. If one or more of these tests gave a P-value less than 0.1, adjusted Odds Ratios were determined by combining genotype data from all 5 SNPs in a binary logistic regression model to control for potential SNP interactions.

Genotype frequencies in opioid-dependent and control subjects were tested separately for Hardy-Weinberg Equilibrium by Chi-square test (or Fisher's Exact Test for SNPs with insufficient homozygous variant frequencies).

Case-control permutation tests were run to determine any differences in *ABCB1* haplotype distributions (for both the 5-SNP and 3-SNP haplotype models) between HD (case) and control (control) subject groups, and HD (case) and ND (control) subject groups as described in Chapter 2. Group differences in diplotype frequencies were analysed initially using Fisher's Exact Test. Where any diplotype displayed a P-value less than 0.1 (by Fisher's Exact Test), all diplotypes with a frequency greater than 10% (in any subject group) were combined a binary logistic regression model to determine their adjusted Odds Ratios.

Differences in HD subjects' daily dose, C_{trough}, dose-adjusted C_{trough} (C_{trough}/dose) or apparent oral clearance (CL/F) between *ABCB1* genotypes and haplotypes (with a frequency >5% in HD subjects) were investigated using Mann-Whitney U and Kruskal-Wallis tests (with Dunn's multiple comparisons post-hoc test) where appropriate.

Since the previous study identified time in treatment as a potential covariate related to dose requirements, the relationship between HD subjects' daily dose, C_{trough}, C_{trough}/dose or CL/F and time in treatment (log-transformed) was examined using Pearson correlation tests. Differences in time in treatment between *ABCB1* genotypes and haplotypes (with a frequency >5% in HD subjects) were investigated using Mann-Whitney U and Kruskal-Wallis tests (with Dunn's multiple comparisons post-hoc test) where appropriate.

For section 4.3.6, HD and ND subjects' dose and C_{trough} data were combined to give an indication of the apparent AGCGC and AGC**TT** haplotype effects when MMT subjects, over a wide range of doses, are treated as a single treatment population (as in Crettol et al. 2006). Differences between haplotype groups were analysed by Kruskal-Wallis tests (with Dunn's multiple comparisons post-hoc test).

$P < 0.05$ was considered statistically significant. All data are presented as mean (C_{trough}, CL/F) or median (dose, C_{trough}/dose) ± standard deviation.

4.3. Results

4.3.1. Subject demographics

Demographics of the HD subjects are shown in Table 4-1. The demographics of ND and control subjects are the same as those given in Chapter 3. One HD subject was excluded from the dose requirement- and pharmacokinetic-genotype/haplotype relationship analyses due to unclear dosing data, and another excluded due to a 400% higher clearance as result of concomitant ritonavir (a potent CYP3A inducer) treatment.

Table 4-1. Demographics of high dose methadone maintenance subjects.

	n = 22
Male : Female	19 : 3
Age (years) (mean (range))	39 (25-56)
Body weight (kg) (median ± SD (range))	82 ± 12 (50-103)
Methadone dose (mg/day) (median ± SD (range))	200 ± 43 (180-300)
Time in treatment (months) (median ± SD (range))	66 ± 74 (6-204)

4.3.2. *ABCB1* genetic variability and opioid dependence

Twenty-one HD subjects were genotyped for all 5 *ABCB1* SNPs, whilst one HD subject was genotyped for the A61G, C1236T and G2677T (but not the G1199A and C3435T) SNPs due to a shortage of blood sample (this was also the subject with unclear dosing data).

The frequencies of each *ABCB1* SNP, with regards to alleles and genotypes, in HD, ND and control subjects are shown in Table 4-2. There were no significant differences in allele or genotype frequencies between HD and control subjects when SNPs were analysed separately ($P \geq 0.06$), or together in a regression model ($P > 0.06$). There were also no significant differences in allele or genotype frequencies between or HD and ND subjects for any SNP ($P \geq 0.13$). All genotype frequencies were in Hardy-Weinberg equilibrium ($P \geq 0.4$).

Table 4-2. *ABCB1* SNP variant allele and genotype frequencies in high dose methadone maintenance (HD), standard dose methadone maintenance (ND) and non-opioid-dependent control (C) subjects.

SNP	Subject group	Allele frequency n (%)				Genotype frequency n (%)				
		WT	V	OR (95% CI)	P	WT/WT	WT/V	V/V	χ^2	P
A61G	HD	39 (88.6)	5 (11.4)			17 (77.3)	5 (22.7)	0 (0)		
	ND	144 (92.3)	12 (7.7)	0.65 (0.22-1.96)	0.54	68 (87.2)	8 (10.3)	2 (2.6)	0.44 (0.13-1.48)[a]	0.18[a]
	C	168 (88.4)	22 (11.6)	1.02 (0.36-2.87)	1.00	75 (78.9)	18 (18.9)	2 (2.1)	0.80 (0.26-2.47)[a]	0.77[a]
G1199A	HD	41 (97.6)	1 (2.4)			20 (95.2)	1 (4.8)	0 (0)		
	ND	151 (96.8)	5 (3.2)	1.36 (0.15-11.95)	1.00	73 (93.6)	5 (6.4)	0 (0)	1.37 (0.15-12.41)[a]	1.00[a]
	C	182 (97.8)	4 (2.2)	0.90 (0.10-8.28)	1.00	90 (96.8)	2 (2.2)	1 (1.1)	0.67 (0.07-6.75)[a]	0.56[a]
C1236T	HD	20 (45.5)	24 (54.5)			6 (27.3)	8 (36.4)	8 (36.4)		
	ND	79 (52.7)	71 (47.3)	0.75 (0.38-1.47)	0.49	20 (26.7)	39 (52.0)	16 (21.3)	2.41	0.30
	C	69 (44.2)	87 (55.8)	1.05 (0.54-2.06)	1.00	14 (17.9)	41 (52.6)	23 (29.5)	1.93	0.38
G2677T	HD	18 (40.9)	26 (59.1)			4 (18.2)	10 (45.5)	8 (36.4)		
	ND	85 (54.5)	71 (45.5)	0.58 (0.29-1.14)	0.13	20 (25.6)	45 (57.7)	13 (16.7)	4.04	0.13
	C	100 (52.6)	90 (47.4)	0.62 (0.32-1.21)	0.18	19 (20.0)	62 (65.3)	14 (14.7)	5.61	0.06
C3435T	HD	14 (33.3)	28 (66.7)			2 (9.5)	10 (47.6)	9 (42.9)		
	ND	69 (44.2)	87 (55.8)	0.63 (0.31-1.29)	0.22	14 (17.9)	41 (52.6)	23 (29.5)	1.72	0.42
	C	72 (39.1)	112 (60.9)	0.78 (0.38-1.58)	0.60	13 (14.1)	46 (50.0)	33 (35.9)	0.52	0.77

WT: Wild-type. V: Variant. OR (95% CI): Odds Ratio (95% Confidence Interval) of Fisher's Exact Test comparing HD and ND, or HD and C groups. χ^2: Chi-square comparing HD and ND, or HD and C groups. [a]OR (95% CI) and P-value of Fisher's Exact Test after grouping WT/V and V/V genotypes.

ABCB1 haplotypes could be determined for all 21 HD subjects with complete genotype data, with phase call probabilities greater than 0.84. Nine different haplotypes were observed in the HD group compared to 11 in ND and control subjects (Table 4-3). A case-control permutation test revealed no significant difference in overall haplotype frequencies between HD and control, or HD and ND subjects (P = 0.50 and 0.69, respectively).

Table 4-3. *ABCB1* haplotype frequencies in high dose methadone maintenance (HD), standard dose methadone maintenance (ND) and non-opioid-dependent control (C) subjects.

***ABCB1* Haplotype[c]**	**HD**		**ND**		**C**	
	Observed[a] (n = 21) **n_h (%)**	**Estimated[b]** (n = 21) **%**	**Observed[a]** (n = 70) **n_h (%)**	**Estimated[b]** (n = 78) **%**	**Observed[a]** (n = 74) **n_h (%)**	**Estimated[b]** (n = 79) **%**
AGCGC	10 (23.8)	22.7	45 (32.1)	29.2	48 (32.4)	29.2
AGCG**T**	3 (7.1)	7.0	12 (8.6)	8.4	11 (7.4)	7.6
AGC**T**C	0 (0.0)	0.7	6 (4.3)	4.5	2 (1.4)	1.8
AGC**TT**	5 (11.9)	11.7	9 (6.4)	6.8	4 (2.7)	3.6
AG**T**GC	2 (4.8)	5.1	10 (7.1)	7.4	7 (4.7)	5.3
AG**T**G**T**	1 (2.4)	3.3	4 (2.9)	4.9	10 (6.8)	8.2
AG**TT**C	1 (2.4)	2.4	0 (0.0)	0.2	0 (0.0)	0.2
AG**TTT**	15 (35.7)	35.1	42 (30.0)	27.8	46 (31.1)	29.5
A**A**CGC	1 (2.4)	2.4	3 (2.1)	2.1	2 (1.4)	1.2
A**A**C**T**C	0 (0.0)	0.0	1 (0.7)	0.8	2 (1.4)	1.4
GGCG**T**	0 (0.0)	0.0	1 (0.7)	0.5	0 (0.0)	0.1
GGTG**T**	0 (0.0)	0.0	0 (0.0)	1.6	2 (1.4)	2.5
GG**TTT**	4 (9.5)	8.8	7 (5.0)	5.4	14 (9.5)	9.1

n = number of subjects included in analysis. Total number of haplotypes in population = 2n. [a]Absolute count of each haplotype (n_h) (observed frequency (%) = (n_h/2n) × 100) after excluding subjects with PHASE call probability less than 0.7. [b]Population haplotype frequency estimated by PHASE using entire group genotype data. [c]Haplotype locus order is 61, 1199, 1236, 2677, 3435. Variant loci are indicated in bold.

Whilst the AGCGC / AGC**TT** diplotype was significantly more frequent in HD subjects (14.3%) when compared to non-opioid-dependent controls when analysed separately (1.4%, OR (95% CI): 12.2 (1.19 to 124.0), P = 0.03), the adjusted Odds Ratio was not significant when diplotypes (with frequencies greater than 10%) were combined in a binary logistic regression model (adjusted Odds Ratio (95% CI) = 6.60 (0.61 to 71.56). P = 0.12). There were no significant differences in diplotype frequencies between HD and ND subjects (P > 0.1).

Table 4-4. *ABCB1* diplotype frequencies in high dose methadone maintenance (HD), standard dose methadone maintenance (ND) and non-opioid-dependent control (C) subjects.

Diplotype	HD n (%)	ND n (%)	C n (%)
AGCGC / AG**TTT**	3 (14.3)	19 (27.1)	20 (27.0)
AGCGC / AGCGC	1 (4.8)	5 (7.1)	8 (10.8)
AGCG**T** / AG**TTT**	2 (9.5)	5 (7.1)	4 (5.4)
AGCGC / **G**G**TTT**	0 (0.0)	3 (4.3)	5 (6.8)
AG**TTT** / AG**TTT**	3 (14.3)	4 (5.7)	3 (4.1)
AG**T**G**T** / AG**TTT**	0 (0.0)	2 (2.9)	4 (5.4)
AG**T**GC / AG**TTT**	1 (4.8)	2 (2.9)	4 (5.4)
AGCGC / AG**T**GC	0 (0.0)	5 (7.1)	1 (1.4)
AGCGC / AGCG**T**	1 (4.8)	3 (4.3)	1 (1.4)
AGCGC / AG**T**G**T**	0 (0.0)	1 (1.4)	3 (4.1)
AGCGC / AGC**TT**	3 (14.3)	3 (4.3)	1 (1.4)*
AGC**T**C / AG**TTT**	0 (0.0)	3 (4.3)	1 (1.4)
AG**TTT** / **G**G**TTT**	2 (9.5)	1 (1.4)	3 (4.1)
AGC**TT** / AG**TTT**	0 (0.0)	0 (0.0)	2 (2.7)
AGCG**T** / AGCG**T**	0 (0.0)	1 (1.4)	2 (2.7)
AG**T**GC / **G**G**TTT**	0 (0.0)	0 (0.0)	2 (2.7)
AG**TTT** / A**A**CGC	0 (0.0)	2 (2.9)	1 (1.4)
GG**T**G**T** / **G**G**TTT**	0 (0.0)	0 (0.0)	2 (2.7)
AGCG**T** / AGC**TT**	0 (0.0)	2 (2.9)	0 (0.0)
AGC**TT** / AGC**TT**	0 (0.0)	2 (2.9)	0 (0.0)
AGC**TT** / **G**G**TTT**	2 (9.5)	0 (0.0)	1 (1.4)
Other	3 (14.3)	7 (10.0)	6 (8.1)

Only diplotypes observed more than once in any subject group are included. Haplotype locus order is 61, 1199, 1236, 2677, 3435. Variant loci are bold. *Fisher's Exact Test P < 0.05 for HD versus C.

ABCB1 3-SNP haplotypes could be determined, with phase calls probabilities greater than 0.8, for 21 HD, 75 ND, and 77 control subjects. All 8 possible haplotype combinations of C1236T, G2677T and C3435T SNPs were observed. Their frequencies in each subject group are shown in Table 4-5. There was no significant difference in 3-SNP haplotype frequencies between HD and control (P = 0.09), or HD and ND subjects (P = 0.27). Alternatively, the CGC / C**TT** diplotype was significantly more frequent in HD subjects (14.3%) when compared to controls (1.3%, OR (95% CI): 12.7 (1.24-129.1), P = 0.03). However, as with the AGCGC / AGC**TT** diplotype, the adjusted Odds Ratio was not significant when 3-SNP diplotypes (with frequencies greater than 10%) were combined in a binary logistic regression model (adjusted Odds Ratio (95% CI) = 6.86 (0.60 to 77.98). P = 0.12). There were no significant differences in 3-SNP diplotype frequencies between HD and ND subjects (P > 0.1).

Table 4-5. *ABCB1* 3-locus (C1236T, G2677T, C3435T) haplotype frequencies in high dose methadone maintenance (HD), normal dose methadone maintenance (ND) and non-opioid-dependent control (C) subjects.

	HD		ND		C	
***ABCB1* Haplotype[c]**	**Observed[a]** (n = 21) **n_h (%)**	**Estimated[b]** (n = 21) **%**	**Observed[a]** (n = 75) **n_h (%)**	**Estimated[b]** (n = 78) **%**	**Observed[a]** (n = 77) **n_h (%)**	**Estimated[b]** (n = 79) **%**
CGC	11 (26.2)	24.2	49 (32.7)	31.5	50 (32.5)	30.6
CG**T**	3 (7.1)	7.8	14 (9.3)	9.1	11 (7.1)	7.6
C**T**C	0 (0.0)	1.6	7 (4.7)	5.1	4 (2.6)	3.0
C**TT**	5 (11.9)	11.6	9 (6.0)	7.0	4 (2.6)	3.7
TGC	2 (4.8)	5.0	10 (6.7)	7.5	7 (4.5)	5.3
TG**T**	1 (2.4)	3.5	8 (5.3)	6.5	15 (9.7)	10.8
TTC	1 (2.4)	2.6	0 (0.0)	0.2	0 (0.0)	0.3
TTT	19 (45.2)	43.7	53 (35.3)	33.2	63 (40.9)	38.6

n = number of subjects included in analysis. Total number of haplotypes in population = 2n. [a]Absolute count of each haplotype (n_h) (observed frequency (%) = (n_h/2n) × 100) after excluding subjects with PHASE call probability less than 0.8. [b]Population haplotype frequency estimated by PHASE using entire group genotype data. [c]Haplotype locus order is 1236, 2677, 3435. Variant loci are bold.

Table 4-6. *ABCB1* 3-locus (C1236T, G2677T, C3435T) diplotype frequencies in high dose methadone maintenance (HD), normal dose methadone maintenance (ND) and non-opioid-dependent control (C) subjects.

Diplotype	HD n (%)	ND n (%)	C n (%)
CGC / **TTT**	3 (14.3)	24 (32.0)	25 (32.5)
TTT / **TTT**	5 (23.8)	6 (8.0)	6 (7.8)
CGC / CGC	2 (9.5)	6 (8.0)	8 (10.4)
TGT / **TTT**	0 (0.0)	6 (8.0)	9 (11.7)
CG**T** / **TTT**	2 (9.5)	6 (8.0)	5 (6.5)
TGC / **TTT**	1 (4.5)	2 (2.7)	6 (7.8)
CGC / C**TT**	3 (14.3)	3 (4.0)	1 (1.3)*
CGC / CG**T**	1 (4.8)	4 (5.3)	1 (1.3)
CGC / **T**GC	0 (0.0)	5 (6.7)	1 (1.3)
C**T**C / **TTT**	0 (0.0)	3 (4.0)	2 (2.6)
C**TT** / **TTT**	2 (9.5)	0 (0.0)	3 (3.9)
CGC / **T**G**T**	0 (0.0)	1 (1.3)	3 (3.9)
CG**T** / CG**T**	0 (0.0)	1 (1.3)	2 (2.6)
Other	2 (9.5)	8 (10.7)	5 (6.5)

Only diplotypes observed more than twice in total are included. Haplotype locus order is 1236, 2677, 3435. Variant loci are indicated in bold. *Fisher's Exact Test $P < 0.05$ for HD versus C.

4.3.3. *ABCB1* genetic variability and methadone requirements

HD subjects (n = 20) were receiving daily methadone doses ranging from 180 to 300 mg/day (median ± SD: 200 ± 43), whilst the mean ± SD C_{trough} of (R)-methadone and (S)-methadone for HD subjects were 332 ± 135 and 273 ± 133 ng/ml, respectively. Only one subject was variant at the G1199A SNP, as such, the impact of this SNP on methadone requirements and pharmacokinetics was not analysed. No other *ABCB1* genotype significantly influenced daily methadone dose ($P > 0.08$) or (R)-methadone C_{trough} ($P > 0.3$) requirements (Table 4-7). Similarly, there was no significant association between any *ABCB1* haplotype and daily methadone dose ($P > 0.06$) or (R)-methadone C_{trough} ($P > 0.1$) requirements (Table 4-8).

Table 4-7. Relationships between daily methadone maintenance dose or (R)-methadone C_{trough} requirements and *ABCB1* genotypes.

SNP	Genotype	n	Dose[a]	P-value[b]	C_{trough}[c]	P-value[b]
A61G	A/A	16	200 ± 34.8	0.08	330.4 ± 148.1	0.74
	A/G	4	280 ± 49.6		340.3 ± 80.1	
C1236T	C/C	5	200 ± 29.2	0.49	378.5 ± 63.6	0.34
	C/T	7	250 ± 49.6		300.2 ± 92.7	
	T/T	8	200 ± 37.8		331.7 ± 193.8	
G2677T	G/G	3	200 ± 0.0	0.96	327.6 ± 10.5	0.59
	G/T	9	200 ± 43.2		368.8 ± 152.0	
	T/T	8	200 ± 50.4		293.2 ± 141.0	
C3435T	C/C	1	200	0.57	339.4	0.59
	C/T	10	200 ± 37.8		362.9 ± 151.8	
	T/T	9	195 ± 51.4		297.8 ± 123.0	

[a]Dose = median ± SD methadone dose requirement (mg/day). [b]P-value of Mann-Whitney U test for A61G or Kruskal-Wallis test for C1236T, G2677T and C3435T. [c]C_{trough} = mean ± SD (R)-methadone trough plasma concentration (ng/mL).

Table 4-8. Relationships between daily methadone maintenance dose or (R)-methadone C_{trough} requirements and *ABCB1* haplotypes.

Haplotype	Copy #	n	Dose[a]	P-value[b]	C_{trough}[c]	P-value[b]
AGCGC	0	12	200 ± 45	0.47	317.1 ± 159.9	0.56
	1	7	250 ± 41		357.7 ± 100.0	
	2	1	200		339.4	
AGCG**T**	0	17	200 ± 43	0.06	344.3 ± 143.0	0.34
	1	3	180 ± 12		264.8 ± 51.4	
AGC**TT**	0	15	200 ± 40	0.24	315.9 ± 150.1	0.16
	1	5	260 ± 47		382.0 ± 64.3	
AG**TTT**	0	8	200 ± 42	0.26	361.6 ± 56.5	0.36
	1	9	200 ± 48		323.0 ± 167.8	
	2	3	190 ± 10		282.8 ± 207.5	
GG**TTT**	0	16	200 ± 35	0.08	330.4 ± 148.1	0.74
	1	4	280 ± 50		340.3 ± 80.1	

[a]Dose = median ± SD methadone dose requirement (mg/day). [b]P-value of Mann-Whitney U test for AGCG**T**, AGC**TT** and **G**G**TTT**, or Kruskal-Wallis test for AGCGC and AG**TTT**. [c]C_{trough} = mean ± SD (R)-methadone trough plasma concentration (ng/mL). Variant loci are indicated in bold. Copy # 0 = non-carriers; 1 = heterozygous carriers; 2 = homozygous carriers.

Subjects' time in treatment was significantly positively correlated with dose (r^2 = 0.62, P < 0.0001), but not plasma (R)-methadone C_{trough} (P = 0.2). Time in treatment was not related to any *ABCB1* genotype or haplotype (P > 0.1).

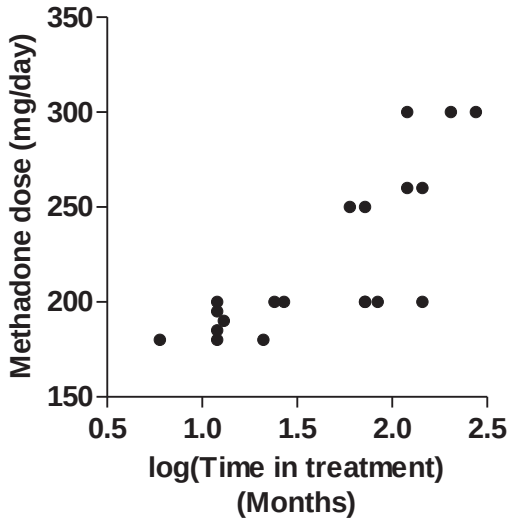

Figure 4-1. Correlation between HD subjects' time in treatment and MMT dose requirements.

Pearson r^2 = 0.62, P = 0.0001.

4.3.4. *ABCB1* genetic variability and methadone pharmacokinetics

The median ± SD plasma (R)- and (S)-methadone C_{trough}/dose and CL/F values for HD subjects were 1.44 ± 0.67 and 1.30 ± 0.67 $ng.ml^{-1}.mg^{-1}$, and 10.89 ± 4.27 and 11.85 ± 5.91 L/h, respectively. There was no significant association of either enantiomer's C_{trough}/dose or CL/F with any *ABCB1* genotype (Table 4-9) or haplotype (Table 4-10), or any correlation with time in treatment (P > 0.2).

Table 4-9. Relationship between plasma (R)- and (S)-methadone (MD) pharmacokinetics and *ABCB1* genotypes.

SNP			Genotype			P-value[c]
			WT/WT	WT/V	V/V	
A61G	C_{trough}/dose[a]	(R)-MD	1.58 ± 0.70	1.22 ± 0.60	-	0.60
		(S)-MD	1.44 ± 0.67	0.73 ± 0.71	-	0.64
	CL/F[b]	(R)-MD	11.56 ± 4.4	13.48 ± 3.70	-	0.37
		(S)-MD	12.8 ± 6.04	16.31 ± 5.07	-	0.24
C1236T	C_{trough}/dose	(R)-MD	1.86 ± 0.14	1.24 ± 0.23	1.25 ± 1.00	0.10
		(S)-MD	1.56 ± 0.19	0.73 ± 0.35	1.38 ± 0.93	0.24
	CL/F	(R)-MD	10.37 ± 0.65	12.56 ± 2.18	12.38 ± 6.53	0.55
		(S)-MD	10.90 ± 1.69	14.69 ± 3.56	14.06 ± 8.70	0.36
G2677T	C_{trough}/dose	(R)-MD	1.62 ± 0.05	1.56 ± 0.74	1.05 ± 0.71	0.33
		(S)-MD	1.69 ± 0.34	1.43 ± 0.64	0.69 ± 0.72	0.20
	CL/F	(R)-MD	8.77 ± 3.09	10.85 ± 2.92	14.35 ± 4.94	0.17
		(S)-MD	7.87 ± 3.79	12.12 ± 3.67	17.13 ± 6.65	0.08
C3435T	C_{trough}/dose	(R)-MD	1.70	1.61 ± 0.75	1.24 ± 0.62	0.62
		(S)-MD	1.44	1.52 ± 0.72	0.73 ± 0.65	0.64
	CL/F	(R)-MD	10.61	11.43 ± 5.13	12.66 ± 3.54	0.77
		(S)-MD	10.82	12.78 ± 7.38	14.57 ± 4.35	0.54

[a]C_{trough}/dose = median ± SD trough plasma concentration / daily dose ($ng.mL^{-1}.mg^{-1}$). [b]CL/F = mean ± SD oral clearance (L/hr). [c]P-value of Mann-Whitney U test for A61G, or Kruskal-Wallis test for C1236T, G2677T and C3435T.

Table 4-10. Relationship between plasma (R)- and (S)-methadone (MD) pharmacokinetics and *ABCB1* haplotypes.

Haplotype			Haplotype copy number			P-value[c]
			0	1	2	
AGCGC	C_{trough}/dose[a]	(R)-MD	1.27 ± 0.82	1.62 ± 0.44	1.70	0.68
		(S)-MD	0.91 ± 0.79	1.47 ± 0.53	1.44	0.93
	CL/F[b]	(R)-MD	12.30 ± 5.31	11.52 ± 2.27	10.61	0.99
		(S)-MD	14.24 ± 7.15	12.58 ± 3.71	10.82	0.89
AGCG**T**	C_{trough}/dose	(R)-MD	1.56 ± 0.72	1.32 ± 0.18	-	1.00
		(S)-MD	1.43 ± 0.72	1.17 ± 0.33	-	0.83
	CL/F	(R)-MD	12.14 ± 4.58	10.84 ± 1.72	-	0.60
		(S)-MD	13.93 ± 6.31	10.97 ± 1.62	-	0.53
AGC**TT**	C_{trough}/dose	(R)-MD	1.32 ± 0.75	1.86 ± 0.38	-	0.38
		(S)-MD	1.17 ± 0.73	1.43 ± 0.52	-	0.79
	CL/F	(R)-MD	12.10 ± 4.86	11.45 ± 1.78	-	1.00
		(S)-MD	13.37 ± 6.62	13.83 ± 3.50	-	0.66
AG**TTT**	C_{trough}/dose	(R)-MD	1.66 ± 0.29	1.29 ± 0.85	0.90 ± 1.00	0.38
		(S)-MD	1.50 ± 0.50	1.08 ± 0.76	0.66 ± 0.95	0.42
	CL/F	(R)-MD	10.45 ± 2.55	13.03 ± 4.75	12.67 ± 4.75	0.70
		(S)-MD	11.60 ± 4.54	14.97 ± 7.28	14.07 ± 4.81	0.64
GG**TTT**	C_{trough}/dose	(R)-MD	1.58 ± 0.70	1.21 ± 0.60	-	0.60
		(S)-MD	1.44 ± 0.67	0.73 ± 0.71	-	0.64
	CL/F	(R)-MD	11.56 ± 4.42	13.48 ± 3.69	-	0.37
		(S)-MD	12.78 ± 6.04	16.31 ± 5.07	-	0.24

[a]C_{trough}/dose = median ± SD trough plasma concentration / daily dose ($ng.mL^{-1}.mg^{-1}$). [b]CL/F = mean ± SD oral clearance (L/hr). [c]P-value of Mann-Whitney U test for AGCG**T**, AGC**TT** and **G**G**TTT** haplotypes, or Kruskal-Wallis test for AGCGC and AG**TTT** haplotypes. Variant loci are bold. Haplotype copy number 0 = non-carriers; 1 = heterozygous carriers; 2 = homozygous carriers.

4.3.5. Summary

In summary, the diplotype AGCGC / AGC**TT** (and consequently also the 3-SNP diplotype CGC / C**TT**) was more frequent in HD subjects when compared to controls. However, no significant *ABCB1* genotype or haplotype differences were observed between HD and ND subject groups, and there was no significant relationship between *ABCB1* genotypes or haplotypes and methadone requirements or pharmacokinetics in HD subjects.

4.3.6. *ABCB1* haplotype effects when ND and HD MMT subjects are combined

Figure 4-2 shows the relationships between the AGCGC and AGC**TT** haplotypes and methadone dose and C_{trough} requirements when considering the ND and HD subjects as a single treatment group. No significant haplotype differences are observed ($P > 0.08$).

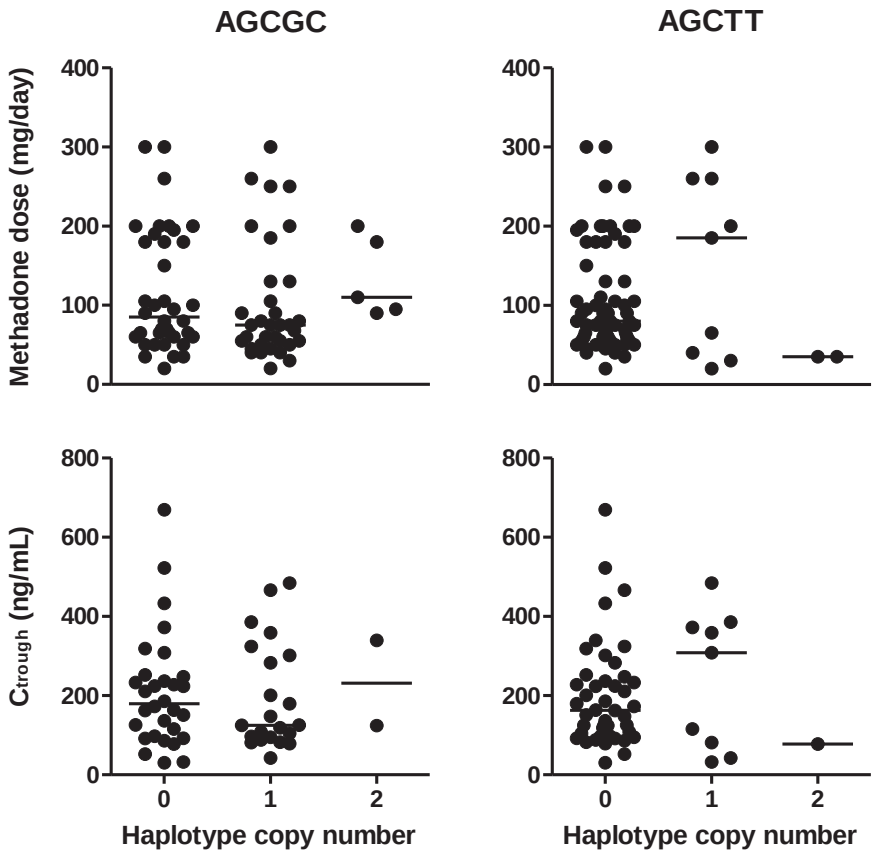

Figure 4-2. Relationship between the AGCGC and AGCTT haplotypes of *ABCB1* and methadone dose and trough plasma (R)-methadone concentrations (C_{trough}) of all MMT subjects (ND and HD subjects combined).

Haplotype copy number 0 = non-carriers; 1 = heterozygous carriers; 2 = homozygous carriers.

4.4. Discussion

The disparities in results between the study described in Chapter 3, and those studies of Crettol et al. (2006) and Levran et al. (2008), have suggested that the relative impact of *ABCB1* genetic variability on methadone requirements can differ between different clinical situations. More specifically, it appears that *ABCB1* haplotypes influence methadone dose requirements in patient populations receiving standard doses up to approximately 180 mg/day, but not when patients receive much higher ranges of doses (up to 430 mg/day). Therefore, this study aimed to investigate whether two distinct populations of standard and high dose MMT patients exist, which might explain the discrepancies between studies regarding the impact of *ABCB1* genetic variability on MMT response.

In this study, subjects receiving 15-180 mg/day (from Chapter 3) were designated as standard ('normal') dose (ND), whilst subjects receiving 180-300 mg/day were designated high dose (HD). However, MMT doses are typically highly individualized and highly (and continuously) variable. Thus in the absence of specific restrictive clinical guidelines or legislation regarding maintenance dosing, the specific designation of a cut-off for high and low dose MMT can seem rather arbitrary. As such, the concept of specific high and low dose MMT patient populations is a contentious one. Nonetheless, the idea of distinct high and low dose MMT populations is not new, with both Crettol et al. (2006) and Levran et al. (2008) previously designating similar high and low dose groups within their studies in MMT subjects, employing cut-offs of 120 and 150 mg/day, respectively. Furthermore, it has been shown that, for most patients, a dose of 100 to 150 mg/day is sufficient for both preventing withdrawal and blocking the euphoric effects of heroin (Donny et al., 2002; Donny et al., 2005). In addition, both Australian (Henry-Edwards et al., 2003) and European (Verster & Buning, 2003) MMT guidelines state that a dose between 60 and 100-120 mg/day is effective for the majority of patients. In South Australia, an upper limit of 150 mg/day has been

established for MMT (Hurley et al., 2004), whilst in Western Australia and New South Wales, state approval is required before dosing patients above 120 and 200 mg/day, respectively (NSW Department of Health, 2006; WA Drug and Alcohol Office, 2007). Therefore, at least in Australia, the combination of methadone's pharmacology, clinical experience and treatment guidelines identifies MMT patients requiring greater than ~120-200 mg/day as a distinct 'atypical' high dose treatment population.

In terms of *ABCB1* genetic variability, the previous study in Chapter 3 found that wild-type (AGCGC) and variant (AGC**TT**) haplotypes were associated with high and low methadone dose requirements, respectively. As such, it might be expected that the wild-type haplotype would be more frequent in the HD MMT subjects of this study, and variant haplotypes less frequent. However, the findings of this study indicate otherwise. For example, whilst not statistically significant, a high combined frequency of the AG**TTT** and **G**G**TTT** variant haplotypes (45%) was observed in HD subjects when compared to ND subjects (29%). In addition, 3-SNP haplotype analysis allowing direct comparison with Levran et al. (2008) revealed that 1236**TT**/2677**TT**/3435**TT** haplotypes were more frequent in HD (24%) versus ND (8%) subjects. Whilst this difference was not statistically significant (P = 0.06), it displays a similar pattern to Levran who reported a 20.4% and 4.5% frequency of this diplotype in subjects designated "high dose" (>150 mg/day) and "low dose" (<150 mg/day), respectively. Alternatively, there was a suggestion that AGCGC/AGC**TT** and CGC/C**TT** diplotypes may also be more frequent in HD subjects when compared to controls, with intermediate frequencies in ND subjects. Therefore, these findings and those of Levran seem to suggest an association between *ABCB1* variant haplotypes and high dose requirements. However, as discussed in Chapter 1, *ABCB1* genetic variants are expected to be associated with decreased P-gp efflux activity, and thus greater CNS exposure to P-gp substrates like methadone. Therefore, it would be expected that *ABCB1* variants would be associated with

lower and not higher dose requirements. As such, despite the apparent agreement between these two studies, this association is mechanistically unexpected.

It should be noted that HD subjects of this study had generally been in treatment much longer than ND subjects (median: 66 versus 7 months, respectively). Therefore, it is possible that the higher frequency of *ABCB1* variant haplotypes observed in HD subjects may actually be linked to an overall better treatment response, and hence longer treatment retention, for variant carriers. However, no relationship between any genotype or haplotype and time in treatment was observed in this study, and whether this also explains the findings of Levran and colleagues (2008) is unclear. Nonetheless, it raises the question as to whether *ABCB1* genetic variability may be affecting more general pathways of reward and treatment response, such as the endogenous opioid system (through β-endorphin), that may be distinct from, and potentially confounding, its modulation of methadone CNS exposure. As such, additional mechanistic studies with larger subject numbers are required to clarify why there appears (in this study and Levran et al. (2008)) to be a higher frequency of *ABCB1* variant haplotypes in high dose MMT populations.

In further disagreement with the findings described in Chapter 3, but in support of the hypothesis that *ABCB1* genetic variability no longer influences MMT at high doses, the present study found no significant association between any *ABCB1* haplotype and methadone dose in HD subjects. Unfortunately, the small group of HD subjects included in the present study represents only a very narrow range of high dose patients, and as such, the power to detect previously observed differences in methadone requirements was drastically reduced (for example, only 58% power to detect a 35 mg difference in dose between AGC**TT** carriers and non-carriers). In addition, there were too few HD subjects homozygous for the wild-type haplotype (n = 1) to allow for direct comparison with my previous study (Chapter 3). Nonetheless, there was clearly no association between the AGC**TT** haplotype (previously

associated with 50% reduction in methadone requirements) and dose. Furthermore, despite an almost 5-fold variability in (R)-methadone C_{trough} values among HD subjects, no significant association with *ABCB1* haplotypes was observed. Coupled with the absence of a high frequency of homozygous wild-type haplotype subjects in the HD group (which was expected based on previous results in ND subjects, Chapter 3), these findings suggest that, unlike in subjects receiving 15-180 mg/day, *ABCB1* haplotypes do not associate with methadone requirements in patients receiving high MMT doses (>120-200 mg/day). As such, when ND and HD subjects were combined and analysed as a single group receiving a large range of MMT doses (20-300 mg/day), the significant associations between AGCGC homozygotes or AGC**TT** carriers and methadone requirements previously observed in ND subjects were no longer apparent (Figure 4-2). Therefore, it seems that, when analysing MMT subjects receiving such a large range of doses, the absence of *ABCB1* haplotype effects on methadone requirements in HD subjects masks the significant effects observed in ND subjects, which provides a tangible explanation of why Crettol et al. (2008b) were unable to detect any haplotype effects in their subjects receiving an even larger range of doses (3-430 mg/day).

Despite the lack of significant differences between haplotype groups, no homozygous AGCGC subject required less than 90 mg/day, whilst no homozygous AGC**TT** subject required more than 35 mg/day, thus indicating that these haplotypes may still be useful as predictors of minimum or maximum dose requirements, respectively, for homozygous carriers. However, this needs to be validated by further prospective study, and the fact that these homozygous carriers combined represent no more than 10% of the MMT population is also likely to limit their clinical utility.

With respect to the relationship between genetic variability and methadone pharmacokinetics, it was found that *ABCB1* haplotypes did not influence either the dose-adjusted C_{trough}, or the CL/F of (R)- or (S)-methadone in HD subjects ($P > 0.24$). This is not surprising given that for

drugs such as methadone, P-gp is expected to have a relatively minor impact on intestinal absorption and elimination when compared to its influence on CNS distribution, especially at high doses (Lin & Yamazaki, 2003a; Lin & Yamazaki, 2003b).

In terms of potential covariates, whilst the previous study in Chapter 3 identified sex as important for the investigation of *ABCB1* genetic variability in MMT, exclusion of the three female HD subjects had no significant effect on the results (data not shown). Alternatively, a strong positive correlation was observed between HD subjects' dose requirements and their time in treatment. Whilst this may indicate the development of increased methadone tolerance over prolonged treatment, no correlation was observed between time in treatment and C_{trough} (representing pharmacodynamic tolerance) or CL/F (representing pharmacokinetic tolerance). Therefore, it is also possible that the correlation between time in treatment and dose may simply reflect an increase in treatment retention with higher doses, although, a correlation between time in treatment and C_{trough} may also be expected if this were the case.

Despite the lack of a correlation between time in treatment and CL/F, the (R)- and (S)-methadone CL/F of HD subjects were higher than those previously reported in an Australian MMT cohort receiving 7.5-160 mg/day (that is, similar to ND subjects) (mean ± SD: 11.9 ± 4.3 and 13.5 ± 5.9 versus 9.4 ± 3.9 and 9.5 ± 5.4 L/h, respectively (Foster et al., 2004)). It is unclear whether the increased CL/F observed in the HD population is a cause or a consequence of the high doses. For example, it is possible that pre-existing high CL/F may necessitate the use of higher doses to prevent withdrawal over the dosing interval in these patients. Alternatively, evidence exists for the auto-induction of methadone metabolism during the course of long-term (but not short-term, (Morton, 2007)) maintenance, which could result in increased clearance (Anggard et al., 1975; Verebely et al., 1975; Wolff et al., 2000). If the latter is true, and methadone clearance is induced at high doses, then it could foreseeably override the impact of *ABCB1* genetic variability, explaining the lack of

association between *ABCB1* mutations and methadone requirements in current HD subjects. However, such a conclusion cannot be made from this study alone.

Despite this increased clearance in HD subjects, their (R)-methadone C_{trough} values (332 ± 135 ng/mL) were still higher than those observed for ND subjects (see Chapter 3), as well as those previously reported for treatment responders in typical Australian treatment settings (223 ± 119 ng/mL, (Hallinan et al., 2006)). Therefore, this suggests there is additional variability in either CNS distribution or pharmacodynamics leading to increased methadone requirements. Whether this relates to pre-existing variability in CNS distribution and pharmacodynamics, or the development of CNS pharmacokinetic and pharmacodynamic tolerance related to time in treatment, is unclear.

In summary, contrary to the findings described in Chapter 3, no clear associations between *ABCB1* haplotypes and methadone dose or C_{trough} requirements were observed among HD subjects. This lends support to the hypothesis that two distinct MMT populations may exist with regards to *ABCB1* pharmacogenetics, the first being standard dose MMT (<150-200 mg/day) where *ABCB1* haplotypes influence methadone requirements, and the second being high dose MMT (>150-200 mg/day) where they do not. Unfortunately, the mechanistic basis behind this observation is unclear. One hypothesis could be that P-gp transport at the BBB is saturated at the concentrations observed in high dose MMT, thus removing any impact of P-gp transport, and hence *ABCB1* genetic variability, on methadone requirements. However, not enough is known about the kinetics of methadone P-gp transport at the human BBB to allow for such a conclusion at this stage. Alternatively, the potential influence of *ABCB1* genetic variability on overall treatment response, and possibly treatment retention, may be a confounding factor when investigating differences in *ABCB1* pharmacogenetics between high and normal dose MMT. Time in treatment itself may also be an important factor since, as mentioned previously, most HD subjects had been in treatment considerably longer than ND

subjects, and treatment duration was strongly correlated with increased dose requirements. As such, it is possible that an impact of *ABCB1* genetic variability on methadone requirements may only be observed in the earlier stages of maintenance treatment.

Another important consideration when interpreting differences between standard and high dose MMT populations, as well as discrepancies between previous studies, is the significant role individual clinic policies and philosophies may also play in determining both dose administered and patient response to treatment (Bell et al., 1995; Magura et al., 1998; Magura et al., 1999). For example, the majority of ND subjects (73 of 78) were recruited from South Australian treatment clinics, where an upper limit of 150 mg/day for MMT dosing applies. Alternatively, all HD subjects were recruited from a NSW clinic where dosing is allowed up to and above (subject to State approval) 200 mg/day. Therefore, different treatment settings, dosing strategies and legislative restrictions, may also have a significant bearing on the clinical impact of *ABCB1* pharmacogenetics in MMT. As such, any future studies should ideally compare high and standard dose MMT populations within the same treatment setting/clinic.

Finally, genetic factors influencing methadone's pharmacodynamics also need to be considered. For example, there is new evidence that a variant of the dopamine D_2 receptor gene (*DRD2*) may also contribute to interindividual variability in MMT response (Crettol et al., 2008a). Furthermore, a separate study in our laboratory has demonstrated that the frequency of the *OPRM1* A118G variant, associated with decreased mu-opioid receptor signalling efficacy, is significantly higher in HD subjects when compared to ND subjects. As such, in MMT patients requiring high methadone doses to control withdrawal and reduce illicit opioid intake, it is possible that P-gp-associated pharmacokinetic variability may be largely overshadowed by the impact of genetic variability influencing methadone pharmacodynamics.

However, in a similar manner to the previous observation by Campa and colleagues (2008) that genetic variants of *OPRM1* and *ABCB1* may interact to affect morphine pain relief, further studies in HD subjects by our research group have found a significant association of homozygous wild-type *OPRM1* A118G / homozygous variant *ABCB1* C3435T (AA / TT), and homozygous variant *OPRM1* A118G / heterozygous or homozygous wild-type *ABCB1* C3435T (GG / CC or CT) combined genotypes, with low and high methadone C_{trough} requirements, respectively. Importantly, this combined analysis of *OPRM1* A118G and *ABCB1* C3435T genotypes appeared to be a better predictor of the (R)-methadone C_{trough} than A118G alone, indicating that *ABCB1* genetic variability may still have some small influence on methadone CNS distribution at high doses, and that epistasis (multiple gene interaction) is a vital consideration when investigating methadone pharmacogenetics.

Based on the findings of Chapter 3, this study, and of other international research, the multiple factors influencing MMT can be summarised as shown in Figure 4-3.

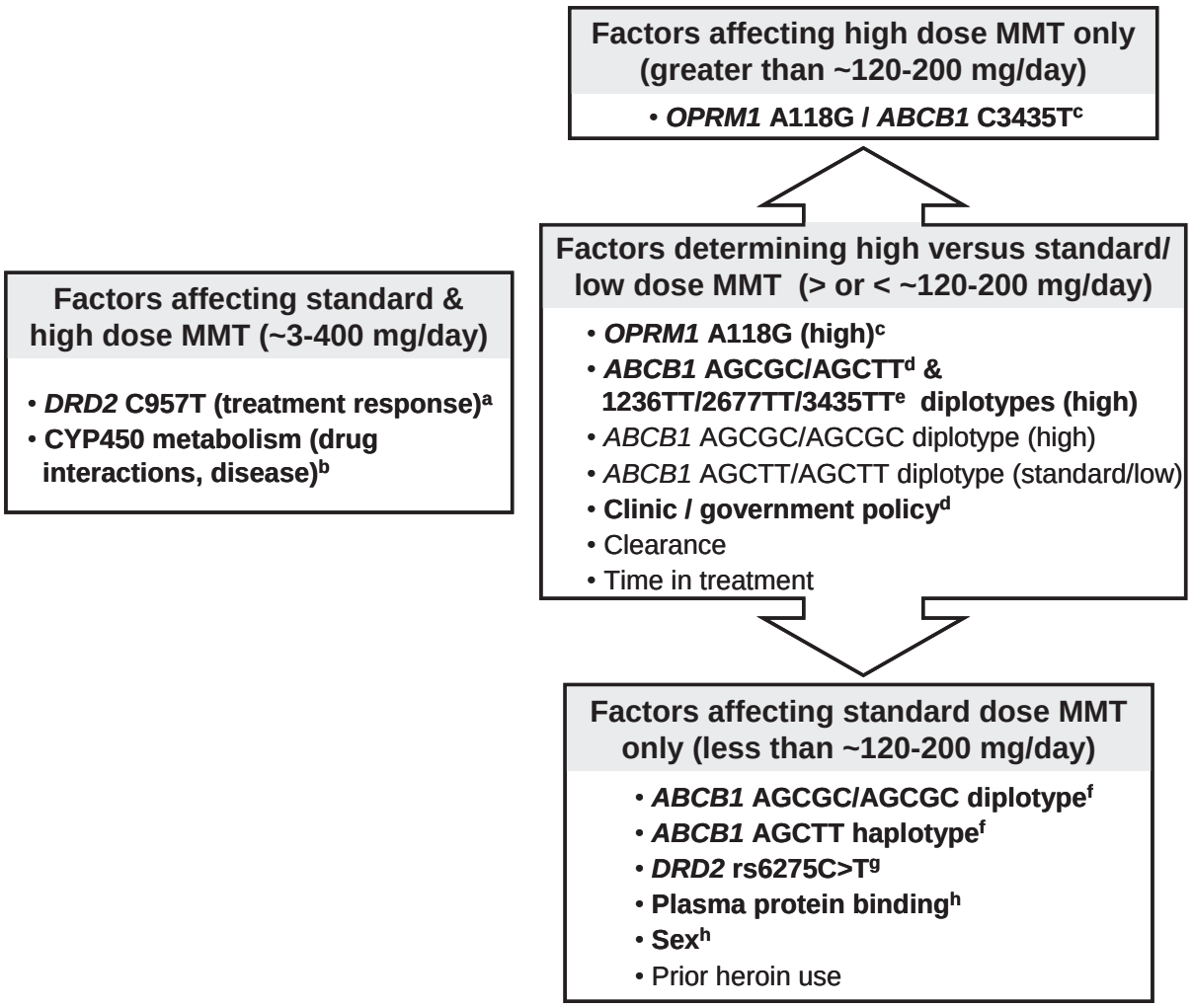

Figure 4-3. Summary of the multiple factors potentially influencing MMT dose requirements and response.

Factors in bold are significant associations identified in this thesis or by other researchers ([a]Crettol et al., (2008a); [b]see Chapter 1, section 1.4.2.1; [c]unpublished, Discipline of Pharmacology, University of Adelaide; [d]thesis Chapter 4; [e]Levran et al., (2008); [f]thesis Chapter 3; [g]Doehring et al., (2009); [h]Foster et al., (2000); Foster et al., (2004)). Factors not in bold are those for which there is no significant evidence, but the findings of Chapter 3 and 4 of this thesis suggest could also potentially be involved.

In conclusion, the impact of *ABCB1* genetic variability on methadone requirements and treatment response varies significantly between treatment populations. Whether this is due to the existence of distinct high and standard dose MMT populations, or simply related to patients' time in treatment, increased methadone clearance and/or clinic policies, is as yet unclear. Nonetheless, the observed complex relationships between dose range, clearance, treatment duration and genetic variability highlight the fact that variability in MMT response is complicated and multi-factorial. Therefore, a combined consideration of multiple genetic and environmental factors is required to provide a more complete picture of the factors governing the successful treatment of opioid dependence.

Chapter 5. Ex vivo expression and function of P-glycoprotein

5.1. Introduction

The findings of Chapter 3 indicate that *ABCB1* genetic variability may play some role in determining opioid response. However, the interpretation is made difficult by the lack of clear understanding of the functional consequences of *ABCB1* SNPs and haplotypes, and thus the mechanism by which they might influence methadone and buprenorphine pharmacokinetics.

As discussed in Chapter 1, numerous *in vitro* studies have tried to identify the functional consequences of *ABCB1* variants, but have failed to reach a consensus. In addition, whilst *ex vivo* analyses of P-gp expression and transport in isolated human tissues are believed to provide a more useful model for examining the functional consequences *ABCB1* genetic variability, they have been similarly inconclusive, and the current knowledge of the *ex vivo* impact of *ABCB1* haplotypes, as well as of the A61G, G1199A, C1236T SNPs, is restricted to the findings of only one or two studies each. Furthermore, whilst mRNA expression, P-gp protein expression and P-gp transport function have all been previously employed as measures of *ex vivo* P-gp variability, no single study has investigated all three elements at once. This may be important since the combined examination of mRNA, protein and transport variability is likely to provide the greatest insight into the exact mechanisms behind the functional consequences of *ABCB1* polymorphisms, and how they may interact in the form of haplotypes. Finally, and most importantly for this thesis, no *ex vivo* studies have been performed in opioid-dependent subjects, an important consideration since, as discussed in Chapter 1 (section 1.5.4.1), some opioids can induce P-gp expression. As such, exposure to illicit and/or substitution opioids may alter P-gp expression, potentially confounding the functional impacts (penetrance) of *ABCB1* polymorphisms.

Therefore the aims of this study were to:

(a) Develop methods for the simultaneous *ex vivo* analysis of *ABCB1* mRNA expression, P-gp protein expression and P-gp function in human lymphocytes.

(b) Apply these methods to a pilot clinical investigation of the complex interaction between *ABCB1* genetic variability, prior illicit opioid use, opioid substitution treatment, and P-gp expression and function.

5.2. Method development and validation

5.2.1. Introduction

As discussed in Chapter 1 (section 1.6.4.2), numerous tissues have been employed for the *ex vivo* quantification of P-gp expression and function, including duodenal, liver and renal tissue. However, by far the most commonly employed tissue for *ex vivo* analysis has been PBMCs. This is largely because PBMCs can be obtained relatively non-invasively from whole blood samples, and can be analysed using existing flow cytometric techniques to measure P-gp expression (using fluorescent P-gp antibodies) and function (using the fluorescent P-gp substrate Rhodamine 123) (Ford et al., 2003).

Unfortunately, where a flow cytometer is not available within the lab, as was the case in this study, one of the major drawbacks of using flow cytometry for evaluating P-gp expression and function is the cost. In addition, at the time of initiating the *ex vivo* study (early 2007) for which these methods were required, studies examining P-gp expression by flow cytometry could only quantify expression in terms of percentage of P-gp-positive cells (i.e. the proportion of total cells above a threshold fluorescence). As such, it was questionable whether these analytical methods possessed the quantitative sensitivity to resolve moderate individual variability in P-gp expression, within P-gp expressing cells, as a result of modulating factors such as genetic polymorphisms. Flow cytometric methods are also unable to determine the

mRNA expression of P-gp. With this in mind, an alternative method was sought for the quantification of P-gp expression (mRNA and protein) and function in PBMCs.

Whilst numerous studies have previously employed whole PBMCs for this form of analysis (see Appendix A: Table A-3), different lymphocyte subtypes have been shown to express different levels of P-gp, with relatively high P-gp expression observed in $CD56^+$ and $CD8^+$ lymphocytes ($CD56^+$ > $CD8^+$), and relatively low expression in $CD4^+$ lymphocytes (Chaudhary et al., 1992; Ford et al., 2003). As such, it may be more beneficial to examine P-gp expression and function in specific subsets of lymphocytes, rather than in PBMCs as a whole. Therefore, a new non-flow cytometric method for the isolation of specific lymphocyte subsets was also required.

As such, the assay development aims were:

(a) To develop and validate a new (non-flow cytometric) method for the simultaneous isolation of pure $CD4^+$, $CD56^+$ and $CD8^+$ lymphocyte fractions from human whole blood.

(b) To develop and validate a quantitative real-time PCR assay for the quantification of *ABCB1* mRNA expression in *ex vivo* human lymphocytes.

(c) To develop and validate a Western blot assay for the quantification of P-gp protein expression in *ex vivo* human lymphocytes.

(d) To develop and validate a fluorescent P-gp substrate accumulation and efflux assay for the evaluation of P-gp function in *ex vivo* human lymphocytes.

5.2.2. Materials

OptiPrep™ density gradient solution, bovine serum albumin (BSA), ammonium chloride, potassium bicarbonate, ethylenediaminetetraacetic acid (EDTA), dimethylsulfoxide (DMSO), isopropanol, paraformaldehyde, rhodamine 123, verapamil, RIPA buffer, Protease Inhibitor Cocktail, Tris-base, glycine, sodium dodecyl sulphate, bromophenol blue, β-mercaptoethanol,

and monoclonal mouse anti-human P-glycoprotein (clone F4) and monoclonal mouse anti-human calnexin (clone TO-5) antibodies, were purchased from Sigma-Aldrich (Castle Hill, Australia). Phosphate buffered saline (PBS), trypan blue and heat-inactivated fetal bovine serum (FCS) were purchased from the Central Services Unit of the School of Molecular and Biomedical Science, University of Adelaide (Adelaide, SA, Australia). Deoxyribonucleoside triphosphates (dNTPs) were manufactured by Finnzymes (Keilaranta, Finland, distributed by Genesearch, Arundel, Australia). ThermoPol Reaction Buffer and *Taq* DNA Polymerase were manufactured by New England Biolabs (Beverly, Massachusetts, USA, distributed by Genesearch). Oligonucleotides primers and pUC19/*Hpa*II DNA molecular weight marker were purchased from GeneWorks (Thebarton, Australia). MACS® CD4, CD56 and CD8 microbeads, monoclonal FITC-conjugated mouse anti-human CD4 and anti-human CD8 antibodies, and FITC- and PE-conjugated mouse IgG2a antibodies were purchased from Miltenyi Biotec Australia Pty Ltd (North Ryde, NSW, Australia). Monoclonal PE-conjugated mouse anti-human CD56 and mouse IgG2b antibodies were purchased from BD Biosciences (North Ryde, NSW, Australia). The RNeasy kit was purchased from QIAGEN Pty Ltd (Doncaster, Vic, Australia). The mRNA Catcher™ PLUS kit, RPMI 1640 medium and HEPES buffer were purchased from Invitrogen Australia Pty Ltd (Mulgrave, Vic, Australia). The High-Capacity cDNA Reverse Transcription Kit, TaqMan® Gene Expression Master Mix and TaqMan® Gene Expression Assay Kits (Hs00184491_m1 and Hs99999905_m1) were purchased from Applied Biosystems (Mulgrave, Vic, Australia). Baseline-ZERO™ DNase was manufactured by EPICENTRE Biotechnologies (Madison, WI, USA, distributed by Astral Scientific, Gymea, NSW, Australia). The BCA™ Protein Assay Kit was manufactured by Pierce (Rockford, IL, USA, distributed by Thermo Fisher Scientific, Scoresby, Vic, Australia). Precision Plus Protein Dual Colour standard, High Range Prestained SDS-PAGE standard and 30% 29:1 acrylamide:bis-acrylamide were purchased from Bio-rad Australia (Gladesville, NSW, Australia). High-range Rainbow Molecular Weight Marker, Hybond ECL

nitrocellulose (0.45 μm), ECL Advance Western Blotting Detection Kit (including ECL Advance blocking and detection reagents), and HRP-conjugated sheep anti-mouse IgG antibody were purchased from GE Healthcare Bio-Sciences Pty Ltd (Rydalmere, NSW, Australia). Methanol was purchased from Ajax Finechem Pty Ltd (Taren Point, NSW, Australia). Tween 20 detergent was manufactured by Amresco Inc (Solon, OH, USA, distributed by Astral Scientific). Glycerol was purchased from Merck Pty Ltd (Kilsyth, Vic, Australia). RNase-free pipette tips and tubes (Axygen, Union City, CA USA, distributed by Fisher Biotec Australia, Wembley, WA, Australia) were used for all RNA procedures.

5.2.3. Isolation of $CD4^+$, $CD56^+$ and $CD8^+$ lymphocytes

5.2.3.1. Methods

Where possible, all methods described in this section were performed using aseptic techniques in a laminar flow hood. Blood samples used for the development and validation of these samples were kindly donated by healthy volunteers.

5.2.3.1.1. Isolation of peripheral blood mononuclear cells

PBMCs were isolated from 6-18 mL of whole blood (taken in EDTA tubes) using OptiPrep™ according to the manufacturer's "Isolation of mononuclear cells from peripheral blood and from bone marrow by flotation through a density barrier" method (see product application sheet C5, http://www.axis-shield-density-gradient-media.com/CD2009/cells/C05.pdf). Following density gradient centrifugation, the PBMC layer was transferred to a new tube and washed three times with 10 mL of PBS (resuspending and pelleting at 350, 300 and 300 x g for 10 minutes each time). After the third wash, the PBMC pellet was resuspended in 1 mL of PBS before adding 10 mL of red blood cell lysis solution (155 mM NH_4Cl; 10 mM $KHCO_3$; 0.1 mM EDTA) and incubating at room temperature for 5 minutes. PBMCs were then washed a further two times in 10 mL PBS before being resuspended in 1 mL of cold (4°C) magnetic separation buffer (SB: PBS with 0.5% BSA, 2 mM EDTA). Ten microlitres of PBMC cell

suspension was diluted with 190 µL of trypan blue and cells quantified using a haemocytometer (Weber, England).

5.2.3.1.2. Magnetic positive selection

Positive selection for $CD4^+$, $CD56^+$ and $CD8^+$ lymphocytes was performed sequentially using MACS® CD4, CD56 and CD8 microbeads, respectively, on a MiniMACS™ Separation Unit with MS columns (Miltenyi Biotec Australia Pty Ltd, North Ryde, NSW, Australia). Magnetic cell separation was chosen as the method for isolating lymphocyte subsets from whole PBMCs, as it allows for the efficient and specific isolation of viable cells. Through the use of commercially available tiny (~50 nM in diameter) super-paramagnetic beads that bind to specific cell surface antigens, it is possible to isolate specific cell populations by magnetic separation. Importantly, the beads used in the methods described below are biodegradable and decompose in cell culture, and therefore cell function and viability can be preserved.

This technique was initially performed using the manufacturer's standard procedures ('Basic protocol'), however, results of flow cytometric validation experiments (see below, 5.2.3.2.2.1) prompted slight changes to the standard method resulting in an 'Optimised protocol'. The basic method and the optimized protocol changes are both described below.

5.2.3.1.2.1. Basic protocol

A diagram outlining the basic protocol following the manufacturer's standard procedure is shown in Figure 5-1.

Briefly, up to 2 x 10^7 lymphocytes were labelled with CD4 microbeads (so as not to exceed the column capacity of 1 x 10^7 labelled ($CD4^+$) cells), washed, and magnetically separated, with both the CD4-positive and negative cell fractions collected in separate tubes. The CD4-negative fraction was then combined with any remaining PBMCs not used in the CD4 selection, and the cells labelled with CD56 microbeads, washed, and magnetically separated,

with the CD56-positive and negative cell fractions both collected in separate tubes. The CD4/CD56-negative fraction was then labelled with CD8 microbeads, washed, and magnetically separated. The CD8-positive fraction was collected in a tube, whilst the CD4/CD56/CD8-negative fraction was discarded. In this manner, this procedure generated three separate fractions of $CD4^+$, $CD56^+$ and $CD8^+$ lymphocytes.

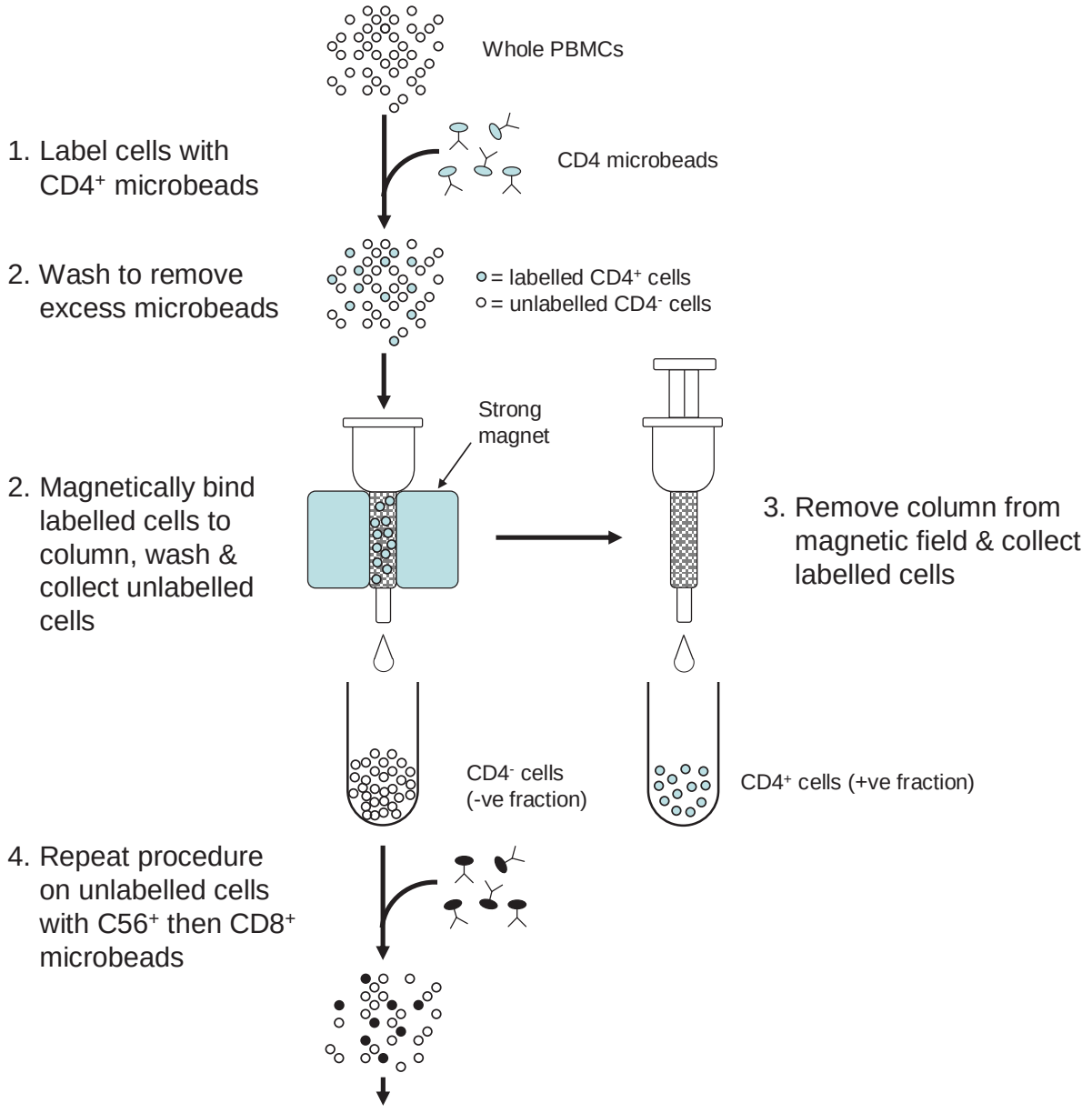

Figure 5-1. Basic protocol for magnetic bead positive selection and isolation of lymphocyte subsets.

–ve: negative. +ve: positive.

5.2.3.1.2.2. Validation of cell selection by flow cytometry

In order to validate the magnetic separation procedure for isolating pure fractions of $CD4^+$, $CD56^+$ and $CD8^+$ lymphocytes, each of the positive fractions, as well as whole PBMCs and a sample of a CD4/CD56/CD8-negative fraction (taken after the subset isolations), were analysed by dual colour flow cytometry.

Briefly, 5 x 10^5 cells were labelled with fluorescently tagged antibodies according to antibody manufacturers' instructions, washed, then fixed in 500 μL of 1% paraformaldehyde and stored at 4°C in the dark until analysis. A list of the different antibody combinations tested for each cell fraction is shown in Table 5-1. Flow cytometric samples were analysed at the Detmold Family Imaging Centre of the Institute of Medical and Veterinary Science (Adelaide, SA).

Table 5-1. List of antibodies (and their combinations) used for flow cytometry to test cell surface antigen expression in whole human PBMCs, magnetically isolated $CD4^+$, $CD56^+$ and $CD8^+$ lymphocytes, and the magnetic isolation negative fraction.

Whole PBMCs	$CD4^+$	$CD56^+$	$CD8^+$	-ve fraction
Isotype controls	Isotype controls	Isotype controls	Isotype controls	Isotype controls
CD4-FITC	CD4-FITC	CD4-FITC	CD4-FITC	CD4-FITC
CD8-FITC	CD56-PE	CD56-PE	CD56-PE	CD56-PE
CD56-PE	CD8-FITC	CD8-FITC	CD8-FITC	CD8-FITC
CD4-FITC/CD56-PE		CD4-FITC/CD56-PE		
CD8-FITC/CD56-PE		CD8-FITC/CD56-PE		

Isotype controls: Anti-mouse IgG2a-FITC and anti-mouse IgG2a-PE.

5.2.3.1.2.3. Optimised protocol

Based on the findings of the flow cytometric analysis, additional measures were added to the basic protocol to reduce the contamination of the $CD56^+$ fraction with $CD4^+$ cells (see section 5.2.3.2.2.1 and Table 5-3). Firstly, during the $CD4^+$ cell positive selection procedure, the first negative fraction to come off the magnetized column (prior to any washes) was run through the same magnetized column again to ensure all bead-labelled $CD4^+$ cells were captured and did not contaminate the negative fraction. Secondly, during the $CD56^+$ cell positive selection, $CD56^+$ cells were eluted off the demagnetized column as usual. However, in line with

recommendations from the manufacturer for the isolation of rare cell fractions, they were then applied back on to a second magnetized column. The washing procedure was then repeated in the $CD56^+$-enriched cell fraction to ensure the removal of any contaminating non-labelled $CD4^+$ (or other) cells. The purified $CD56^+$ fraction was then eluted off the (demagnetized) column and processed as usual. Only the negative fraction from the first column was used for the subsequent $CD8^+$ positive selection, whilst the negative fraction from the second column was discarded. A diagram outlining the optimized protocol process is shown in Figure 5-2.

5.2.3.1.2.4. Processing of positive fractions

For analysis of P-gp expression and function, as soon as possible after collection (using the optimised procedure), the $CD4^+$, $CD56^+$ or $CD8^+$ positive cell fractions were washed with 1 mL of PBS and quantified. For mRNA expression analysis, cells in 40 µL of PBS were snap-frozen using liquid nitrogen before being stored at -70°C. For protein expression, cells were pelleted, supernatant removed, and frozen at -20°C. For functional analysis, cells were pelleted and resuspended at 1 x 10^6 cells/mL in freezing medium (FCS with 10% DMSO), transferred to 2 mL Nunc™ cryovials (Rochester, NY, USA, distributed by In Vitro Technologies Pty Ltd, Noble Park, VIC, Australia) and frozen (placed in a Nalgene 'Mr Frosty' (In Vitro Technologies) isopropanol bath overnight at -70°C then transferred to liquid nitrogen). The actual number of cells required for each set of analyses was determined based on individual assay development results (see sections 5.2.4.4, 5.2.5.4 and 5.2.6.4).

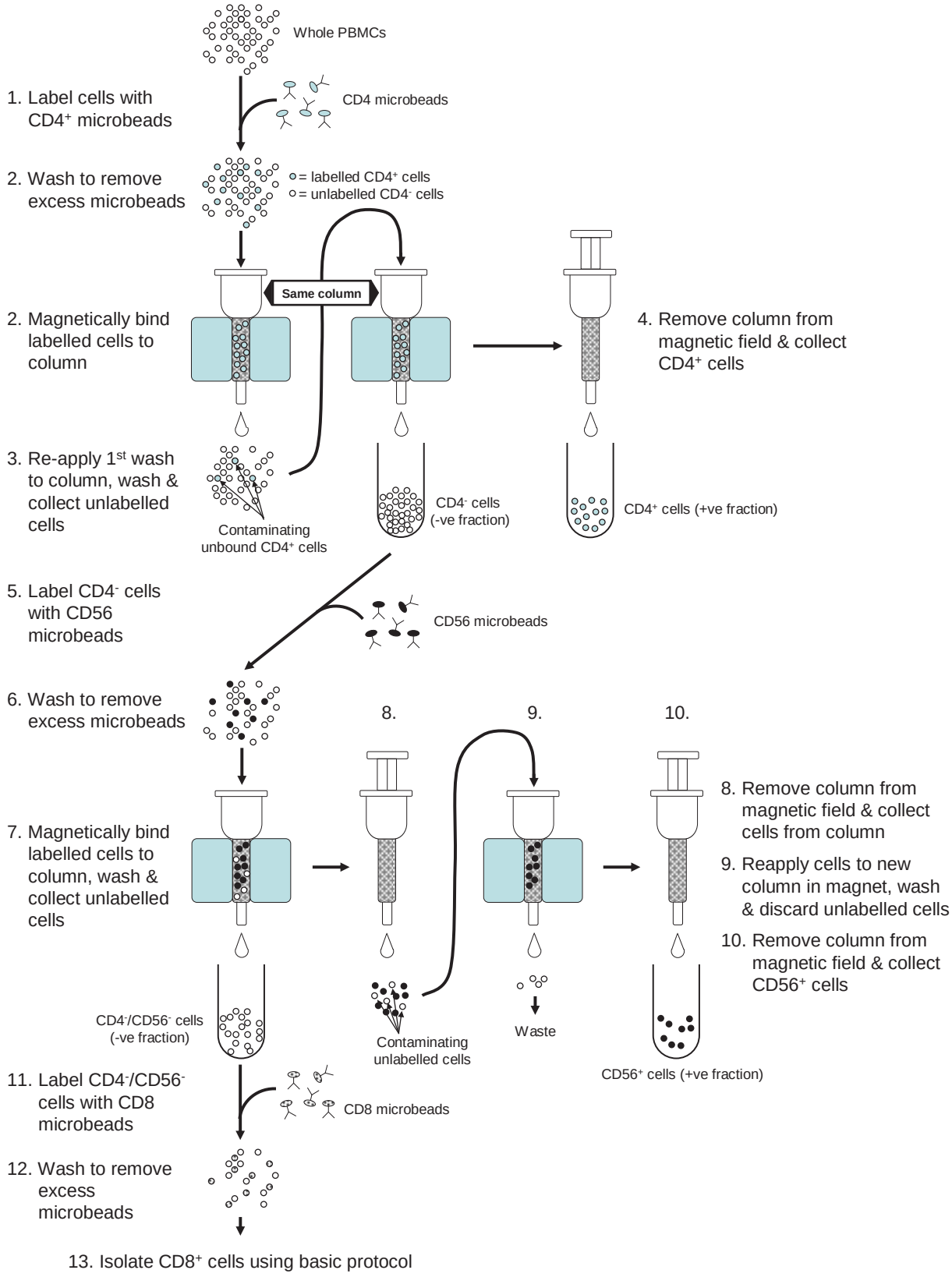

Figure 5-2. Optimised protocol for magnetic bead positive selection and isolation of lymphocyte subsets.

–ve: negative. +ve: positive.

5.2.3.1.3. Qualitative detection of CD4, CD56 and CD8 expression

In order to confirm the isolation of pure $CD4^+$, $CD56^+$ and $CD8^+$ lymphocyte fractions in subjects' samples, qualitative reverse transcription-PCR methods were developed for the detection of CD4, CD56 and CD8 mRNA. For all three assays, mRNA was isolated from control samples of $CD4^+$, $CD56^+$ or $CD8^+$ lymphocytes isolated using the optimised procedure. Five microlitres of the purified mRNA was then reverse transcribed to complementary DNA (cDNA) using the methods described in sections 5.2.4.1.1 and 5.2.4.1.2 below. These cDNAs were then used to develop CD4, CD56 and CD8 cDNA-specific PCR assays.

Primers used in the assays described below were all based on existing published methods, however, as a precaution, all primers were checked against the human genome and transcriptome using the online NCBI BLAST (http://blast.ncbi.nlm.nih.gov/Blast.cgi) program and GenBank sequences to ensure that they recognized the CD4, CD56 or CD8 mRNA sequence where appropriate, and that at least one primer was intron-spanning (and hence mRNA specific) (CD8) or, if they gave both mRNA and DNA products, that amplified cDNA and DNA bands were distinguishable from one another by size (CD4 and CD56). The primer sequences for each assay are shown in Appendix A: Table A-18.

In the publications on which these assays were based, very little information was given as to the specific PCR conditions. As such, in the absence of information other than primer sequences, *ABCB1* PCR conditions (specifically those used for A61G, G1199A and C1236T, see Chapter 2, Table 2-2) were used as a starting point. For all three assays, 15 μL of cDNA was used as a starting point for PCR, then based on these results, different cDNA amounts for each assay were tested to achieve optimal specific amplification. The PCR reaction conditions trialled for each of the three assays are shown in Table 5-2.

All PCR products were run on a 4% 2:1 gel and photographed using standard procedure (see Chapter 2, section 2.1.2.3.3).

Table 5-2. PCR conditions trialled for the qualitative detection of CD4, CD56 and CD8 cDNA.

Assay ►	CD4	CD56	CD8
Master mix (per reaction):			
[PCR reaction buffer]	1X	1X	1X
[dNTPs] (μM each)	50	50	50
[Primers] (μM each)	0.1	0.5	0.1 or 0.5
Taq DNA polymerase (Units)	2.5	2.5	1 or 2.5
cDNA (μL)	1, 5, 7.5, 10 or 15	5, 10 or 15	0.05, 0.1, 0.5, 1, 5, 10 or 15
Final reaction volume (μL)	30	30	30
Cycling conditions:			
Initial denaturation	93°C: 3 min	94°C: 5 min	94°C: 5 min
Denaturing	93°C: 1 min	94°C: 30 sec	94°C: 30 sec
Annealing	60°C: 1 min	63°C: 30 sec	60°C: 30 sec
Elongation	72°C: 2 min	72°C: 1.5 min	72°C: 1.5 min
► Number of cycles	35	35	35
Final elongation	72°C: 5 min	72°C: 5 min	72°C: 5 min
Storage	4°C	4°C	4°C

5.2.3.2. Results

5.2.3.2.1. Isolation of PBMCs

Using the method described in section 5.2.3.1.1, 7.6-8.6 mL of whole blood from healthy volunteers (n = 3) provided 1.4-2.35 x 10^7 PBMCs. Analysis by flow cytometry in one of these volunteers showed that, of these PBMCs, around 63% were $CD4^+$, 11% were $CD56^+$, and 27% were $CD8^+$, whilst around 7% were $CD56^+/CD8^+$ double-labelled (see Table 5-3). These values correspond well with the expected abundances of $CD4^+$, $CD56^+$, $CD8^+$ and $CD8^+/CD56^+$cells (34-67%, 5-15%, 10-42% and 2-5%, respectively) previously reported in healthy individuals (Whiteside & Herberman, 1989; Ohkawa et al., 2001; Gomella, 2002).

5.2.3.2.2. Magnetic positive selection

5.2.3.2.2.1. Basic protocol

Using the basic magnetic separation protocol, around 3-8 x 10^6 $CD4^+$, 0.9-1.5 x 10^6 $CD56^+$, and 1.5-1.9 x 10^6 $CD8^+$ cells were recovered from the PBMCs isolated above (n = 3), representing approximately 50%, 11% and 22% of the total PBMCs, respectively.

Results of flow cytometric analyses of each of the positive fractions in one volunteer (as well as the final CD4/CD56/CD8-negative fraction) are shown in Table 5-3. The purities of the $CD4^+$ and $CD8^+$ fractions were found to be very good (99% and 96.5%, respectively), whereas the $CD56^+$ fraction had less than 90% purity. As expected from the analysis of whole PBMCs, a large portion of the $CD56^+$ fraction was double-labelled for CD56 and CD8, accounting for all of the CD8 single-labelled cells in the CD56 fraction. As such, the majority of $CD56^+$ fraction contamination appears to come from the 10% of cells positive for CD4.

Analysis of the CD4/CD56/CD8-negative fraction revealed that the majority of $CD4^+$, $CD56^+$ and $CD8^+$ cells had been captured by the positive selection procedure.

Table 5-3. Flow cytometric analysis of human whole PBMCs and lymphocyte cell fractions isolated by the basic magnetic separation procedure.

Labelling	Whole PBMCs	$CD4^+$	$CD56^+$	$CD8^+$	-ve fraction
Isotype controls	2.0%	0.3%	1.3%	1.5%	9.1%
CD4-FITC	62.8%	**99.0%**	10.7%	4.7%	10.0%
CD56-PE	10.8%	0.3%	**89.3%**	3.8%	2.7%
CD8-FITC	26.6%	1.4%	24.1%	**96.5%**	14.6%
CD4-FITC / CD56-PE	0.4%	-	0.7%	-	-
CD8-FITC / CD56-PE	7.2%	-	25.4%	-	-

Values in bold highlight the desired high percentage of cells labelled with CD4, CD56 or CD8 fluorescent antibodies in the cell fractions positively selected with CD4, CD56 and CD8 microbeads, respectively.

5.2.3.2.2.2. Optimised protocol

The recovery of cell fractions from healthy volunteers (as percentages of total PBMC input) using the optimised protocol was 30-49% for $CD4^+$ (n = 3), 9% for $CD56^+$ (n = 2, incorrect concentration of CD56 microbeads used for the third subject) and 11-25% for $CD8^+$ (n = 3) cells, with total recoveries varying between individuals depending on the amount of total PBMCs extracted. See section 5.3.3.2 for the confirmation of fraction purities by qualitative reverse-transcription PCR.

5.2.3.2.3. Qualitative detection of CD4, CD56 and CD8 expression

CD4 PCR using 5, 7.5, 10 and 15 μL of $CD4^+$ cDNA all gave strong PCR products of 138 bp (the size expected from the mRNA sequence). One microlitre of cDNA also gave a clear 138 bp product, but was not as strong as the other volumes. As such, 2 μL was chosen as the volume of subject cDNA to be tested using the CD4 PCR conditions shown in Table 5-4.

CD56 PCR using 10 and 15 μL of $CD56^+$ cDNA gave clear PCR products at 279 bp (the size expected from the mRNA sequence), whereas 5 μL of cDNA gave no 279 bp product. As such, 10 μL was chosen as the volume of subject cDNA to be tested using the CD56 PCR conditions shown in Table 5-4.

CD8 PCR using 0.4 μM of each primer and/or 2.5 U of Taq DNA polymerase produced non-specific amplification of a similar size to the expected cDNA band (64 bp), even in negative (water instead of cDNA) controls. Alternatively, CD8 PCR using 0.1 μM of each primer and 1 U of Taq DNA polymerase had no non-specific amplification. Using these conditions, 1, 5, 10 and 15 μL of $CD8^+$ cDNA gave strong PCR products, 0.5 μL of cDNA gave a faint PCR product, and 0.1 and 0.05 μL of cDNA gave no PCR product. As such, 1 μL was chosen as the volume of subject cDNA to be tested using the CD8 PCR conditions shown in Table 5-4.

Table 5-4. Optimised CD4, CD56 and CD8 PCR conditions.

Assay ►	CD4	CD56	CD8
Master mix (per reaction):			
[PCR reaction buffer]	1X	1X	1X
[dNTPs] (μM each)	50	50	50
[Primers] (μM each)	0.1	0.5	0.1
Taq DNA polymerase (Units)	2.5	2.5	1
cDNA (μL)	2	10	1
Final reaction volume (μL)	30	30	30
Cycling conditions:			
Initial denaturation	93°C: 3 min	94°C: 5 min	94°C: 5 min
Denaturing	93°C: 1 min	94°C: 30 sec	94°C: 30 sec
Annealing	60°C: 1 min	63°C: 30 sec	60°C: 30 sec
Elongation	72°C: 2 min	72°C: 1.5 min	72°C: 1.5 min
Number of cycles	35	35	35
Final elongation	72°C: 5 min	72°C: 5 min	72°C: 5 min
Storage	4°C	4°C	4°C

5.2.3.3. Discussion

A new method for the sequential positive selection and isolation of $CD4^+$, $CD56^+$ and $CD8^+$ cell subsets was developed using magnetic microbeads. This method was found to be effective in isolating pure fractions of $CD4^+$ and $CD8^+$ cells from whole PBMCs. However, the $CD56^+$ cell fraction was found to be contaminated with $CD4^+$ cells (constituting around 10% of the fraction) when using the basic protocol. This is not entirely surprising given the high abundance of $CD4^+$ cells (~50-60% of cells) relative to $CD56^+$ cells (~11% of cells) in whole PBMC isolations. In addition, some aspects of the basic protocol provide potential opportunities for contamination. For example, the initial labelling and isolation of $CD4^+$ cells was limited to the use of a maximum of 2×10^7 total PBMCs, so as not to exceed the column capacity for 1×10^7 labelled cells. Therefore, if the abundance of $CD4^+$ cells greatly exceeds 50% for an individual, a small percentage of bead-labelled $CD4^+$ cells may escape positive selection, contaminate the negative fraction, and be extracted with bead-labelled $CD56^+$ in the following stage of the procedure. In addition, most often the CD4-negative fraction was

combined with any PBMCs not used in the $CD4^+$ isolation procedure in order to increase the yield of less abundant $CD56^+$ and $CD8^+$ lymphocytes. Therefore, there was likely a significant proportion of $CD4^+$ cells from the non-depleted fraction remaining in the cells used for $CD56^+$ selection. As such, if these cells aren't efficiently removed by washing, they can contaminate the $CD56^+$ fraction and, as seen in Table 5-3, can form a significant portion of the fraction due the overall low abundance of $CD56^+$ cells.

To combat these issues, an additional $CD4^+$ positive selection step was incorporated into the protocol to ensure the capture of all bead-labelled $CD4^+$ cells, and an extra positive selection and washing step in the $CD56^+$ procedure to was included to ensure that all non-labelled contaminating cells were removed from the $CD56^+$ positive fraction. Using this optimised protocol, the abundance of each fraction matched well with the abundances observed in the flow cytometric analysis of whole PBMCs, and those reported previously in healthy individuals (Whiteside & Herberman, 1989; Ohkawa et al., 2001; Gomella, 2002). Unfortunately, due to a shortage of antibodies, it was not possible to confirm by flow cytometry the purity of the fractions obtained using the optimised protocol. However, as discussed in section 5.2.3.1.3, methods were developed to allow qualitative detection of CD4, CD56 and CD8 mRNA by reverse transcription-PCR, which were used to confirm the absence of detectable CD4 contamination of $CD56^+$ lymphocyte isolations in subject samples (see section 5.3.3.2).

5.2.3.4. Conclusion

In conclusion, a new and optimized protocol was successfully developed for the isolation and purification of $CD4^+$, $CD56^+$ and $CD8^+$ lymphocyte subsets from as little as 8 mL of whole blood. The isolated cells were viable, and could be stored for later analysis of gene/protein expression and function.

5.2.4. *ABCB1* mRNA expression by qRT-PCR

5.2.4.1. Methods

Quantitative real-time PCR (qRT-PCR) determines the expression of a gene by measuring the exact or relative number of copies of mRNA gene transcript. As the first step, RNA is isolated from the tissue of interest and reverse transcribed to cDNA, which has the same sequence as the exonic sequence of the gene (i.e. the gene sequence minus untranscribed introns), but is more stable than mRNA. This cDNA is then used as a template for gene-specific PCR employing probes that generate fluorescence when incorporated into a PCR product. Real-time PCR machines (such as the Rotor-Gene used in these methods) are able to detect the fluorescence generated, which is proportional to the number of copies of amplified fragment that increases with each cycle of the PCR. Therefore, the more mRNA expression, the more cDNA is produced by reverse transcription, and the more amplified fragments (and hence fluorescence) is observed for a given number of PCR cycles. In this manner, the gene expression of two samples can be compared by measuring how many cycles it takes to reach a certain level of fluorescence. The number of cycles required to reach this fluorescence threshold is termed C_T, with a lower C_T indicating higher gene expression.

A relative quantification approach was chosen for this study as the absolute copy number of gene transcripts was of no particular interest. This method involves the normalisation of target gene expression to an endogenous control gene within the same sample, resulting in a ΔC_T value ($C_{Ttarget}$ - $C_{Tcontrol}$). The endogenous control gene acts as a form of 'loading control', allowing for the comparison of ΔC_T values (and thus gene expression) between different samples. More detail on C_T data analysis is given in section 5.2.4.1.3.2 below.

5.2.4.1.1. mRNA isolation

Due to the finite number of cells available for analysis of subject samples, it was important to minimize, where possible, the number of cells used for each analysis. Initially, total RNA isolations were performed using a QIAGEN RNeasy kit according to the manufacturer's instructions. Using this method, only approximately 900 ng of RNA (quantified by absorbance at 260 nm) was recovered from 5 x 10^5 $CD4^+$ cells, which was deemed insufficient based on a previous study by (Vaclavikova et al., 2008) that employed a similar protocol and instrument to the methods described below. As such, an alternative RNA isolation method was sought that would allow fewer cells to be used.

To this end, an mRNA Catcher^{TM} PLUS kit, which could specifically isolate polyA-tailed mRNA (the small fraction of RNA relevant for gene expression analysis), was trialled. Using the manufacturer's recommended procedure, 80 μL of purified mRNA was isolated from 1 x 10^5 lymphocytes, 1 μL of RNase inhibitor was then added, and the sample frozen at -70°C until required for reverse transcription. Unfortunately, due to the small number of cells from which the mRNA was isolated, combined with mRNA forming only a small fraction of total RNA usually isolated from cells, the mRNA concentrations in samples were too low to be detected by a spectrophotometer. However, with the advantage of reverse transcribing mRNA only (and not whole RNA), the mRNA acquired from 1 x 10^5 lymphocytes was estimated to produce sufficient cDNA for qRT-PCR analysis of *ABCB1* expression.

5.2.4.1.2. cDNA synthesis

5.2.4.1.2.1. Protocol development

Reverse transcription of mRNA to cDNA was performed using a High-Capacity cDNA Reverse Transcription Kit according to the manufacturer's instructions. Using this procedure, up to 14.2 μL of mRNA could be used for cDNA synthesis, with a final volume of 20 μL. For

each mRNA sample, reverse transcription reactions were run in duplicate, and the cDNA products combined after synthesis to give a total of 40 μL of cDNA.

Reverse transcription reactions were initially trialled using 10 μL of mRNA from 1 x 10^5 $CD4^+$, $CD56^+$ and $CD8^+$ cells from healthy volunteers. The effectiveness of cDNA synthesis was then tested by performing C1236T PCR (see Chapter 2, Table 2-2) using 13 μL of each cDNA (instead of DNA), as well as a PCR positive control (100 ng of DNA) and negative control (no DNA or cDNA). The C1236T primers are located in separate exonic regions, and amplify both DNA and cDNA template, but with different sized products due to the absence of the intronic sequence in cDNA (DNA = 527 bp, cDNA = 244 bp). As shown in Figure 5-3, *ABCB1* cDNA was clearly detected in CD56 and CD8 lymphocyte samples (CD56 > CD8, as expected). Though not visible in Figure 5-3, a faint CD4 cDNA band was also detectable in the original image. However, for all cDNA samples there was significant DNA contamination (Figure 5-3). As such, it was decided to treat mRNA with DNase enzymes prior to performing reverse transcription to ensure removal of any DNA contamination.

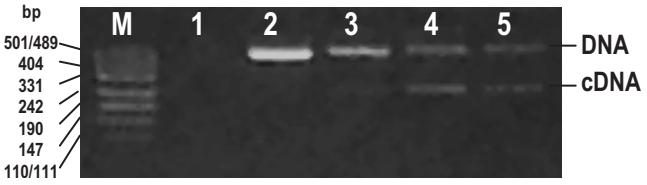

Figure 5-3. Detection of both cDNA and DNA in $CD4^+$, $CD56^+$ and $CD8^+$ lymphocyte reverse transcription products by C1236T PCR amplification.

bp: size of marker bands in base pairs; **M:** pUC19/*Hpa*II DNA molecular weight marker; **1:** water PCR negative control; **2:** 100 ng DNA PCR positive control; **3:** $CD4^+$ reverse transcription PCR product; **4:** $CD56^+$ reverse transcription PCR product; **5:** $CD8^+$ reverse transcription PCR product.

5.2.4.1.2.2. DNase treatment and cDNA purification

In order to test the effectiveness of DNase treatment, 80 μL of mRNA sample was treated with 1 U of Baseline-ZERO™ DNase according to the manufacturer's instructions, cDNA was then synthesized from the DNased mRNA, and amplified by C1236T PCR as before.

Surprisingly, whilst the Baseline-ZERO™ DNase treatment protocol included an enzyme inactivation step, no PCR products (DNA or cDNA) could be detected for cDNA samples produced from DNase-treated mRNA. Therefore, in order to determine whether DNase treatment was degrading the mRNA, cDNA or PCR products, or possibly inhibiting the cDNA synthesis or PCR, samples of DNase-treated and untreated mRNA were purified using the RNA clean-up protocol of an RNeasy Mini Kit, and eluted in 30 μL of RNase-free water each. Reverse transcription reactions were then performed using 13.2 μL of each purified mRNA sample. The cDNA products were amplified by C1236T PCR as before, along with a negative (water) control, a DNA positive control, and a DNA positive control containing inactivated DNase treatment components (to test for PCR inhibition).

As shown in Figure 5-4, incorporation of the 'inactivated' DNase treatment components into the DNA positive control PCR completely eliminated any PCR product, indicating that the DNase treatment components were either inhibiting the PCR, or degrading the PCR products. More importantly, by purifying the DNase-treated mRNA, a clear C1236T PCR amplified cDNA band could be detected, and the DNase-treated sample displayed little or no DNA contamination when compared to the DNase-untreated product. Therefore, DNase-treatment was effective in removing contaminating DNA, and purification of the DNased mRNA removed any PCR-inhibitory components of the DNase treatment.

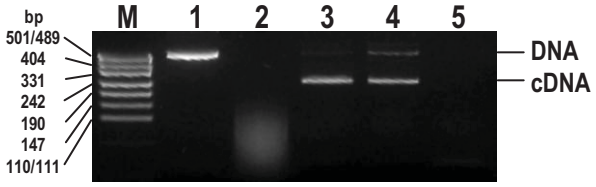

Figure 5-4. DNase treatment components inhibit PCR amplification (lanes 1 versus 2), but purification of DNase-treated mRNA is effective in removing these PCR-inhibitory DNase components (lanes 2 versus 3), revealing that DNase treatment is effective in removing DNA contamination in mRNA (lanes 3 versus 4).

Lane 1: C1236T PCR amplification of 100 ng genomic DNA. **2:** C1236T PCR amplification of 100 ng genomic DNA in the presence of DNase treatment components. **3:** C1236T PCR amplification of cDNA generated from DNase-treated and purified mRNA. **4:** C1236T PCR amplification of cDNA generated from DNase-untreated mRNA. **5:** C1236T PCR amplification of water negative control. **bp:** size of marker bands in base pairs. **M:** pUC19/*Hpa*II DNA molecular weight marker.

5.2.4.1.2.3. Optimised protocol for cDNA synthesis

Based on the above experiments, the reverse transcription protocol was optimized to include a DNase-treatment of mRNA (using 4.5 U of Baseline-ZERO^{TM} DNase to ensure complete removal of DNA), and an extra mRNA purification step (to remove DNase treatment components) prior to performing reverse transcription. The optimal volumes of purified mRNA to be used in cDNA synthesis were determined as part of the development and optimization of the qRT-PCR procedure described below.

5.2.4.1.3. Quantitative real-time PCR

The qRT-PCR reactions described here consist of three major components, the cDNA template, a master mix containing enzymes and buffers required for amplification, and a primer/probe mix consisting of mRNA-specific primers (specific to the gene of interest) as well as fluorophore-labelled probe oligonucleotides. As discussed above, these reactions are run in a similar manner to PCR to amplify gene-specific fragments of cDNA, and the fluorescence emitted by the reaction (due to incorporation of probe oligonucleotides into PCR

product) is measured after each cycle of amplification to quantify the number of gene copies produced. Since a relative quantification approach was chosen, in addition to determining *ABCB1* expression, *GAPDH* expression was also measured as the endogenous control gene to which *ABCB1* expression could be normalized.

5.2.4.1.3.1. General protocol

Real-time PCR reactions were performed using TaqMan® Gene Expression Master Mix and gene-specific primer/probe kits, according to manufacturer's instructions. Briefly, each reaction consisted of 1X TaqMan® Gene Expression Master Mix, 1X primer/probe mix, and up to 9 μL of purified cDNA in a total volume of 20 μL. For *ABCB1* gene expression, the primer/probe mix was TaqMan® Gene Expression Assay Kit Hs00184491_m1. For *GAPDH* gene expression, the primer/probe mix was TaqMan® Gene Expression Assay Kit Hs99999905_m1. For both *ABCB1* and *GAPDH*, the TaqMan® MGB probes used a FAM™ reporter dye, as such, *ABCB1* and *GAPDH* reactions were run in separate tubes.

Within a designated PCR set-up area, separate master mixes (consisting of the TaqMan® Gene Expression Master Mix and appropriate primer/probe mix) were prepared for *ABCB1* and *GAPDH* reactions on ice, and the appropriate volume of master mix aliquoted into 0.1 mL PCR tubes (Corbett Life Science, distributed by Adelab Scientific, Thebarton, SA, Australia) specially designed for the Rotor-Gene instrument. Purified cDNA was then added to each tube and mixed by pipetting outside of the designated PCR set-up area. Where possible, each sample had triplicate reactions for both *ABCB1* and *GAPDH*.

The qRT-PCR reactions were run on a Rotor-Gene 6000 real-time cycler (Corbett Life Science) using the following conditions: 50°C for 2 minutes; 95°C for 10 minutes; up to 75 cycles of 95°C for 15 seconds then 58°C for 60 seconds. The auto-gain optimization provided by the software (Rotor-Gene 6000 Series Software 1.7 (Build 87)) was set to optimize gain prior to the first data acquisition using the 1st tube in the rotor, as such, the sample expected to

have the highest expression was always placed as the first sample. Fluorescence was then acquired for every tube on the 'Green' channel (source = 470 nm, detector = 510 nm) at the end of each 58°C step of the 75 cycles.

As controls for non-specific background amplification, each run of samples included a water control (no reverse transcription product, i.e. just water and gene expression master mix), as well as a negative cDNA control (i.e. the product of a reverse transcription reaction performed with no mRNA), for each gene (*ABCB1* and *GAPDH*).

5.2.4.1.3.2. Data analysis

The Rotor-Gene 6000 software automatically generates a graph of raw fluorescence versus cycle number for all samples (see Figure 5-5A). Whilst this graph can be used to designate a threshold fluorescence value and thus calculate C_T values, the software also offers automatic 'dynamic tube normalization' and 'noise slope correction' functions for taking into account background fluorescence changes that occur between cycles. By applying these background normalization functions, the replicates of samples were found to be significantly improved over the raw data (see Figure 5-5B). As such, all fluorescence thresholds were set using graphs of normalized fluorescence, and were manually selected in the area above background noise and below the onset of signal plateau. As can be seen in Figure 5-5, *ABCB1* and *GAPDH* fluorescence curves were quite distinct from one another. Therefore it was decided that, for all runs, separate fluorescence thresholds would be set for *ABCB1* and *GAPDH* data to ensure the best threshold fits. Variability in the designated threshold for a gene between assay runs was not important for validation experiments, as ΔC_T values were only ever compared within an assay run. Furthermore, each assay run was to include a standard control sample to which all subject samples would be normalized (see below), as such, expression values from different runs could still to be compared, regardless of differences in fluorescence thresholds between runs.

Having designated a fluorescence threshold, the Rotor-Gene software automatically calculated the C_T value for each tube, generating three replicate C_T values for each gene per sample. For analysis of variability within these triplicate measurements, C_T values were converted to the linear form, 2^{-C_T} (as recommended by Livak and Schmittgen (2001)), and coefficients of variation (CV) of these values calculated using GraphPad Prism 5. Where the CV of triplicate values was greater than 10%, significant outliers were detected using Grubbs' test (Z = (triplicate mean – suspected outlier value)/triplicate standard deviation) and C_T values with a Z-score greater than 1.15 were excluded from further analysis.

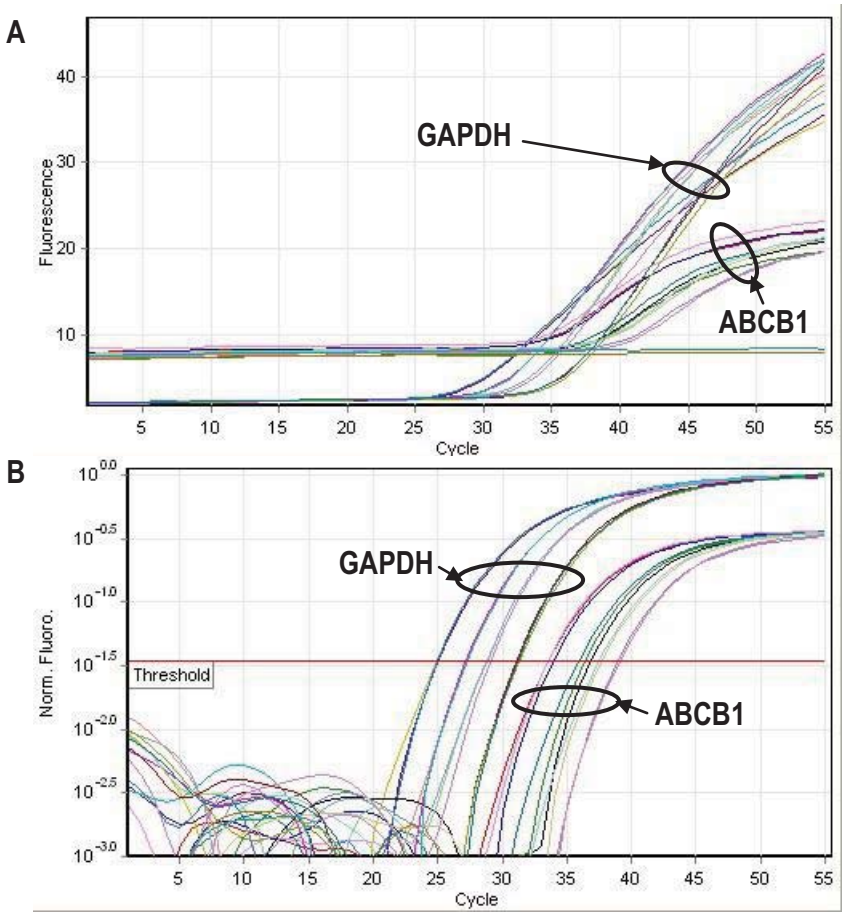

Figure 5-5. Examples of *ABCB1* and *GAPDH* real-time PCR data graphs generated by the Rotor-Gene 6000 software and the designation of a fluorescence threshold.

A: Raw fluorescence data. **B:** Fluorescence data normalized for background fluorescence using the 'dynamic tube normalisation' and 'noise slope correction' functions. Horizontal line in B is the manually designated fluorescence threshold.

The next step in analysis involved determining the ΔC_T for each sample, which was calculated as the triplicate mean *ABCB1* C_T minus the triplicate mean *GAPDH* C_T. Subjects' ΔC_T values were then normalized to the ΔC_T of a control sample (included in all runs with subject samples) using the $2^{-\Delta\Delta C_T}$ method described by Livak and Schmittgen (2001). Briefly, $2^{-\Delta\Delta C_T}$ is calculated as $2^{-(\Delta CT sample - \Delta CT control)}$, and gives the fold difference in *ABCB1* expression between the subject and control samples (hence the $2^{-\Delta\Delta C_T}$ value for the control sample will always be equal to 1). For example, a $2^{-\Delta\Delta C_T}$ value of 0.5 indicates that the subject sample gene expression is half that of the control sample, whilst a $2^{-\Delta\Delta C_T}$ value of 2 indicates that the subject gene expression is twice that of control.

All $2^{-\Delta\Delta C_T}$ data are expressed as mean ± range, where range is the minimum and maximum values derived from all possible combinations of individual *ABCB1* and *GAPDH* C_T values.

5.2.4.1.4. Validation experiments

One important aspect of relative quantification is that, in order for comparisons of ΔC_T values between samples, and hence the $2^{-\Delta\Delta C_T}$ method, to be valid, the gene of interest and the endogenous control gene need to have approximately equal amplification efficiencies. That is, the ΔC_T ($C_{TABCB1} - C_{TGAPDH}$) of a sample should remain the same, independent of the total amount of mRNA or cDNA used in the process. This can be tested by determining the stability of a sample's ΔC_T over a range of dilutions of mRNA or cDNA. If the ΔC_T changes over the dilution range, then the reaction efficiencies are not equal, and thus use of the ΔC_T values for comparisons between samples is not valid.

Therefore, four validation experiments were performed to test the amplification efficiencies of the *ABCB1* and *GAPDH* real-time PCR. As the actual concentration of mRNA could not be measured in samples, an arbitrary unit for representing mRNA concentrations was required.

The quantities of mRNA tested in these experiments are reported as mRNA units, where one unit is equivalent to 1 μL of the 30 μL of mRNA isolated from 1 x10^5 cells.

Experiments 1, 2 and 3 - mRNA dilutions:

(1) mRNA was isolated from $CD4^+$ cells, as these were expected to have the lowest *ABCB1* expression of the three lymphocyte subtypes to be tested. mRNA from 8 x 10^5 $CD4^+$ cells was DNase treated, purified and eluted in a total of 120 μL of RNase-free water, producing a 2-fold concentrated mRNA solution (relative to standard isolation of 1 x 10^5 cells eluted in 30 μL). Reverse transcription reactions were then performed using 1, 4, 7, 10 and 14 μL of the 2X mRNA, and triplicate real-time PCR reactions prepared for each of these cDNA concentrations, using 5 μL of cDNA for *ABCB1*, and 1 μL of cDNA for *GAPDH* reactions. As such, this experiment tested a range of $CD4^+$ mRNA dilutions equivalent to 2, 8, 14, 20 and 28 units of mRNA.

(2) Essentially a repeat of the first experiment, this examined a greater range of mRNA concentrations. As such, $CD4^+$ mRNA was isolated and purified to 4-fold the standard concentration. A range of mRNA dilutions, equivalent to 1, 7, 14, 28 and 56 units of mRNA, were then reversed transcribed to cDNA and real-time PCR performed using the same cDNA volumes as previously.

(3) The third validation experiment examined a range of dilutions of mRNA isolated from $CD56^+$ cells, which were expected to express the most *ABCB1* of the lymphocyte subtypes to be tested. Reverse transcription reactions were performed using the equivalent of 1.4, 7, 14, 35 and 70 units of mRNA, and real-time PCR performed using standard cDNA volumes.

Experiment 4 - cDNA dilutions: $CD4^+$ cDNA was diluted to a range of cDNA solutions equivalent to 0.08, 0.6, 1.6 and 7.2 units of mRNA, and real-time PCR performed as before.

For these experiments, the stability of the *ABCB1* and *GAPDH* real-time PCR amplification efficiencies over the range of template concentrations tested was examined by linearising the C_T values to 2^{-C_T} and then plotting them against template concentration (equivalent units of mRNA). A linear relationship between 2^{-C_T} and template concentration indicates that the real-time PCR efficiency is stable over the concentration range tested. In addition, to determine whether the amplification efficiencies of *ABCB1* and *GAPDH* real-time PCRs were equivalent, ΔC_T values were plotted against template concentrations (equivalent units of mRNA) for each validation experiment. Data obtained from the first three experiments were also combined by first normalizing ΔC_T values to the ΔC_T value or 14 mRNA units within each experiment, then plotting the normalized values from all experiments together.

5.2.4.2. Results

Real-time PCR analysis was able to detect *ABCB1* mRNA expression from as little as 0.6 μL (but not 0.08 μL) of $CD4^+$ mRNA solution (purified from 1 x 10^5 cells into 30 μL). Assessment of *GAPDH* real-time PCR amplification efficiency revealed that it was relatively stable over the more than 100-fold range of mRNA dilutions tested. As shown in Figure 5-6B, the relationship between *GAPDH* 2^{-C_T} and mRNA concentration was linear in the range of 0.6 to 28 mRNA units in all validation experiments. Furthermore, plots of *GAPDH* C_T values versus $\log_2$(mRNA concentration) over this range for each validation experiment were also all linear and had very similar slope functions, even for the cDNA dilution experiment (slope ± standard error: -1.18 ± 0.03, -1.10 ± 0.03, -1.01 ± 0.04 and -1.07 ± 0.02) (see Figure B-2). As such, in the absence of direct quantification of mRNA for subjects samples, if initial qRT-PCR results indicated a large variability in mRNA starting concentrations (i.e. subject

samples had highly variable *GAPDH* C_T values), it was possible to adjust and equalize the mRNA concentrations of samples based on their *GAPDH* C_T values as follows;

$$\textbf{Adjusted volume} = V \div \left(2^{\wedge}\left(\frac{C_{TGAPDH} - C_{Tcontrol}}{slope}\right)\right)$$

where V is the volume of mRNA or cDNA used initially, C_{TGAPDH} is the mean initial *GAPDH* C_T value of the subject sample to be adjusted, $C_{Tcontrol}$ is the mean *GAPDH* C_T value of a control sample measured in the same assay (to which all samples are normalized), and slope is the mean slope function (-1.09) derived from the linear *GAPDH* C_T versus $\log_2$(mRNA concentration) relationships determined in the validation experiments described above.

Unfortunately, as shown in Figure 5-6A, the relationship between *ABCB1* 2^{-C_T} and mRNA concentration was not linear over all mRNA dilution ranges tested. Validation experiments 2 and 3 indicated that at concentrations above 14 and 35 mRNA units, respectively, the *ABCB1* real-time reaction efficiency began to decrease (see Figure 5-6, A2 and A3). This resulted in a divergence in reaction efficiencies between *ABCB1* and *GAPDH* at higher mRNA concentrations, which was observed as a concentration-dependent increase in the ΔC_T values for concentrations above 14 mRNA units (Figure 5-7). However, combining the mRNA dilution results of validation experiments 1, 2 and 3 using normalized ΔC_T values (see section 5.2.4.1.4) revealed that the ΔC_T values remained relatively stable in the dilution range from 2 to 20 mRNA units (indicated by the vertical dotted lines in Figure 5-7).

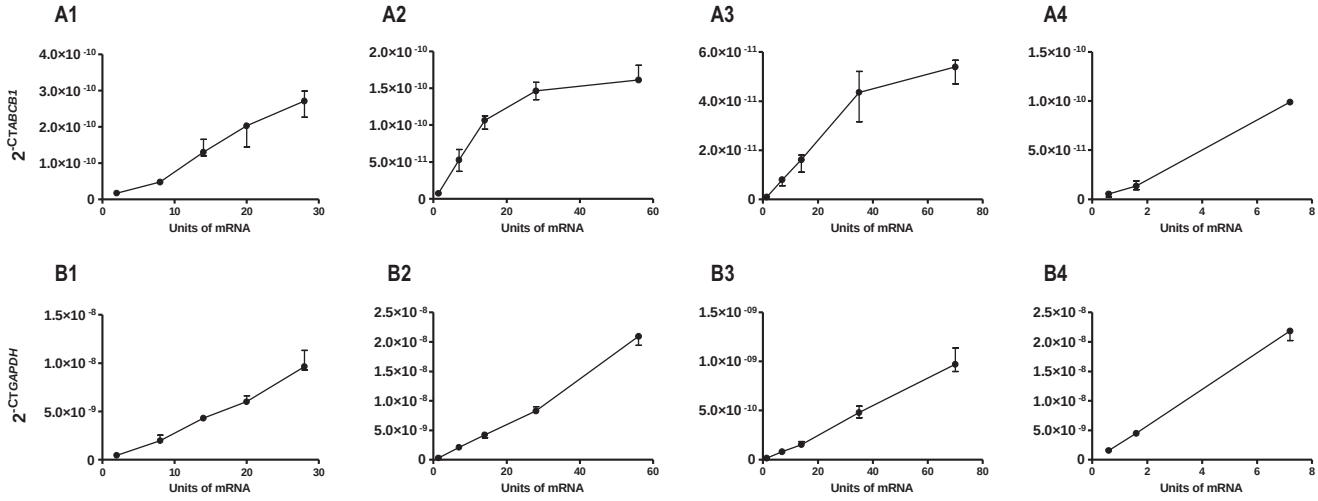

Figure 5-6. Association between template concentrations and linearised C_T values from validation experiments.

A: Relationship between equivalent mRNA concentrations and 2^{-CT} values for real-time *ABCB1* PCR performed in the first (A1), second (A2), third (A3), and fourth (A4) validation experiments, indicating a non-linear relationship at mRNA concentrations greater than 14 (A2) to 35 (A3) units. **B:** Linear relationship between equivalent mRNA concentrations and 2^{-CT} values for real-time *GAPDH* PCR performed in the first (B1), second (B2), third (B3), and fourth (B4) validation experiments.

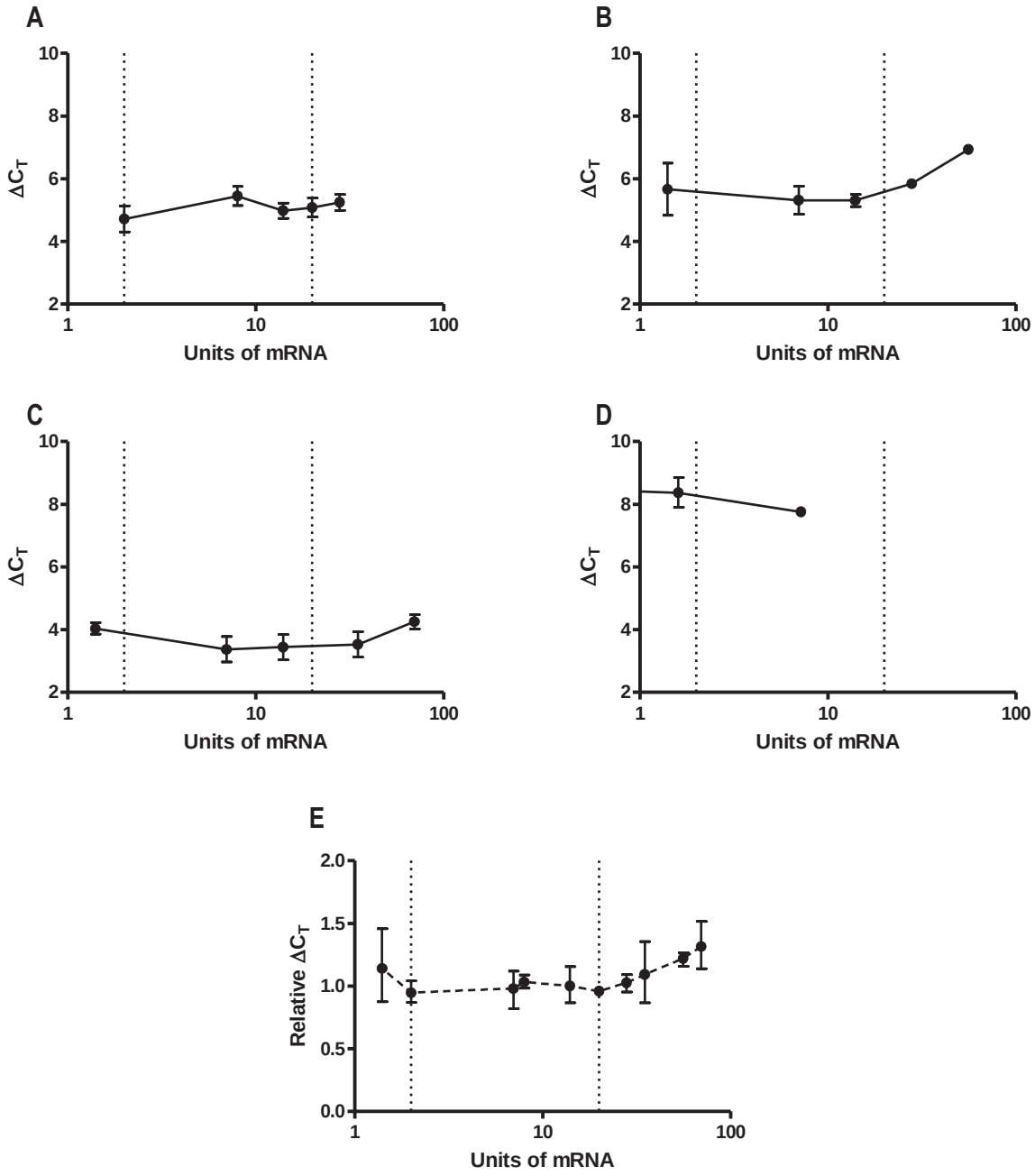

Figure 5-7. Association between total template concentration and ΔC_T for quantification of *ABCB1* in lymphocytes.

A & B: varying $CD4^+$ cell mRNA dilutions examined in the first and second validation experiments, respectively. **C:** varying $CD56^+$ cell mRNA dilutions examined in the third validation experiment. **D:** varying $CD4^+$ cell cDNA dilutions examined in the fourth validation experiment. **E:** Combined relative ΔC_T values (see section 5.2.4.1.4) of all mRNA dilution validation experiments. Vertical dotted lines indicate x = 5 and 20 units of mRNA. ΔC_T values (A-D) are mean ± SD, where SD was calculated as $\sqrt{[(\text{SD of } \textit{ABCB1} \text{ triplicate } C_T \text{ values})^2 - (\text{SD of } \textit{GAPDH} \text{ triplicate } C_T \text{ values})^2]}$. Relative ΔC_T values (E) are mean ± range.

5.2.4.3. Discussion

5.2.4.3.1. mRNA isolation and cDNA synthesis

A protocol was successfully developed for the isolation of mRNA from human lymphocyte samples using the mRNA Catcher^{TM} PLUS kit. In addition to the basic manufacturer's protocol, a DNase treatment of mRNA prior to cDNA synthesis was required (to eliminate DNA contamination), as was a subsequent purification of the DNase-treated mRNA (to remove PCR-inhibiting components of the DNase treatment). Using these optimized methods, mRNA isolated from as little as 1 x 10^5 lymphocytes could be reverse transcribed and *ABCB1* cDNA detected by standard *ABCB1* C1236T PCR (with no DNA contamination).

5.2.4.3.2. Quantitative real-time PCR

A protocol for the determination of *ABCB1* mRNA expression in lymphocyte cDNA by quantitative real-time PCR was also successfully developed and validated. A relative quantification approach was chosen using *GAPDH* expression as an endogenous control. As such, the real-time PCR amplification efficiencies of *ABCB1* and *GAPDH* were assessed over a large range of mRNA concentrations. From these validation experiments, it was found that the amplification efficiencies of *ABCB1* and *GAPDH* real-time PCR were equal, and thus the relative quantification approach valid, in the range of 2 to 20 mRNA units (for definition of mRNA units see section 5.2.4.1.4). Therefore, it was decided that 5 μL of mRNA (isolated from 1 x 10^5 cells and eluted in 30 μL) would be optimal as a starting point for cDNA synthesis of subject samples, with 5 and 1 μL of cDNA in *ABCB1* and *GAPDH* real-time PCR, respectively (equivalent to 5 mRNA units per reaction).

A consistent and linear relationship between $\log_2$(mRNA concentration) and *GAPDH* C_T was observed in validation experiments. As such, a formula was derived by which the volume of subjects' mRNA (or cDNA) used in the qRT-PCR could be subsequently adjusted (based on initial qRT-PCR results) such that all samples would have approximately equal *GAPDH* C_T

values (and hence approximately equal mRNA concentrations). Using this approach with subject samples, it was hoped that assay variability could be reduced, and that it would circumvent any remaining potential issues regarding variable reaction efficiencies.

GAPDH was chosen as the sole endogenous control gene for these experiments based on previous publications examining *ABCB1* gene expression in lymphocytes (Vaclavikova et al., 2008; Chandler et al., 2007; Owen et al., 2004a,b; Hirano et al., 2004; Zanker et al., 1997). However it is worth noting that the stability of *GAPDH* expression in lymphocytes has been questioned (Vandesompele et al., 2002; Sudchada et al. 2010), and currently the best practice for gene expression studies is to include multiple endogenous controls. Therefore, the inclusion of additional genes (such as *actin-β* and/or *β-2M*), preferably validated for their stability in lymphocytes, may be recommended for any future studies.

5.2.4.4. Conclusion

In conclusion, a qRT-PCR method for the quantitative analysis of *ABCB1* gene expression from only 1 x 10^5 *ex vivo* human lymphocytes was successfully developed and validated. This qRT-PCR method was subsequently used in the *ex vivo* pilot study described below.

5.2.5. P-gp protein expression by Western blot

Western blots have been used extensively in the past for the detection and quantification of P-gp in overexpressing *ABCB1*-transfected cell lines. Briefly, the Western blot technique involves firstly separating cell proteins (based on size) by sodium dodecyl sulphate – polyacrylamide gel electrophoresis (SDS-PAGE). Next, the proteins in the gel are electrophoretically transferred to a membrane which can then be probed with protein-specific primary antibodies, which themselves are then probed with fluorescently-tagged secondary antibodies. Using this method, proteins of interest can be quantified by measuring the chemiluminescence of specific protein bands.

For P-gp, most studies report the detection of a single broad band of between 150-190 kDa, however, optimised Western blot analysis should be able to detect two distinct P-gp bands, one at 170 kDa representing the mature fully N-glycosylated protein, and the other at 150 kDa representing the immature core-glycosylated protein (Hung et al., 2008). Unfortunately, few studies have employed Western blotting for the detection of basal expression of P-gp in normal human tissues, a process that has proven to be more difficult than quantitative detection in overexpressing cell lines. Indeed, examination of previous published studies has revealed a number of pitfalls in the use and interpretation of Western blotting for quantitative analysis of P-gp expression. Firstly, the size and SDS-PAGE migration of P-gp in previous studies has been inconsistent, with bands detected by P-gp antibodies reported anywhere in the range between 150 to 200 kDa (Drewe et al., 1999; Greiner et al., 1999; Canaparo et al., 2007). Secondly, the majority of antibodies previously employed for Western blotting cross-react with at least one other protein and, depending on the clone, these cross-reactive proteins often exist within or near the 150-200 kDa range in which P-gp has been detected. A prime example of this is the most commonly used P-gp antibody clone, C219, which is known to cross-react with the *MDR3* gene product (which is the same size as P-gp) (Schinkel et al., 1991), as well as HER-2 at 185 kDa (Chan & Ling, 1997; Liu et al., 1997) and a muscle-related protein at approximately 200 kDa (Thiebaut et al., 1989). Finally, many previous studies have failed to include the appropriate loading controls and/or P-gp positive controls necessary for the valid quantification of P-gp protein expression.

Prior to developing this assay, an attempt was made to identify existing methods for the Western blot detection of P-gp in normal human tissues. To this end, 7 previous studies employing Western blot analysis to quantify *ABCB1* genotype effects on P-gp protein expression in normal human tissue were found (Hoffmeyer et al., 2000; Tanabe et al., 2001; Hitzl et al., 2004; Meissner et al., 2004; Owen et al., 2005; Meier et al., 2006; Rahi et al., 2008). Of these 7 studies, 2 lacked a P-gp positive control (and as such it can not be

confirmed that the detected bands were actually P-gp) (Owen et al., 2005; Meier et al., 2006), 4 studies lacked an appropriate loading control (and thus were not valid for quantitative analysis) (Hoffmeyer et al., 2000; Meissner et al., 2004; Meier et al., 2006; Rahi et al., 2008), and 3 studies had employed the cross-reactive C219 clone (Hoffmeyer et al., 2000; Meissner et al., 2004; Owen et al., 2005). Furthermore, none of these studies clearly distinguished the separate 170 kDa and 150 kDa bands described above, and as such, could not differentiate between mature N-glycosylated P-gp and immature core-glycosylated P-gp. Since *ABCB1* polymorphisms may affect P-gp glycosylation, identification of P-gp in its separate glycosylated states may be important for the pharmacogenetic analysis of P-gp protein expression. Therefore, the aim was to develop a new Western blot assay capable of specifically and quantitatively detecting P-gp protein expression in normal human tissue (in this case lymphocytes), that was also able to differentiate between N-glycosylated 170 kDa P-gp and core-glycosylated 150 kDa P-gp.

5.2.5.1. Methods

5.2.5.1.1. Protein isolation and quantification

Frozen lymphocyte pellets for Western blot analysis were lysed with cold (4°C) RIPA buffer containing 0.5% (v/v) Protease Inhibitor Cocktail (RIPA-PI) by vortexing for 1 minute, incubating on ice for 5 minutes, then vortexing for 1 minute again. Lysates were then clarified (to remove viscous DNA) by centrifugation at 8000 x g at 4°C for 10 minutes, and clarified lysate transferred to a new tube on ice. Clarified lysates were stored at -20°C until required.

A commercial bicinchoninic acid (BCA) colorimetric assay was employed for the quantification of protein in lymphocyte lysis samples. Briefly, a protein standard curve was prepared using 25, 50, 100, 250, 500, 1000, 1500 and 2000 μg/mL of BSA with RIPA-PI as the diluent. Triplicates of 10 μL of each standard, blank RIPA-PI, or unknown samples were loaded onto a 96-well clear microplate (Nunc^{TM}) and treated with BCA reagents as per the 10

μL microplate procedure described by the manufacturers. Absorbance at 560 nm was then measured on a BMG Polarstar microplate reader (BMG Lab Technologies, Offenburg, Germany) using a 560-10 nm excitation filter. Mean absorbance of blank samples were subtracted from the absorbance values of standard samples, and blank-adjusted absorbances plotted against BSA concentration to produce a BSA standard curve. Using their blank-adjusted absorbance values, unknown sample concentrations were then interpolated from the standard curve using non-linear (quadratic) regression as recommended by the manufacturer. A representative BSA standard curve is shown in Figure 5-8.

To determine the protein content of lymphocytes, separate lots of 5 x 10^5 and 1 x 10^6 whole PBMCs were lysed with 100 μL of RIPA-PI each and clarified by centrifugation. Quantification by BCA assay indicated that 5 x 10^5 and 1 x 10^6 lymphocytes yielded 15 and 35 μg of protein, respectively. Troost and colleagues (2004), in one of the few studies to measure lymphocyte P-gp by Western blot, were able to detect P-gp from 20 μg of whole cell protein. Therefore, it was decided that, by employing enhanced detection reagents (see below), 5 x 10^5 lymphocytes (15 μg) would be an appropriate sample size for trialling the Western blot protocol.

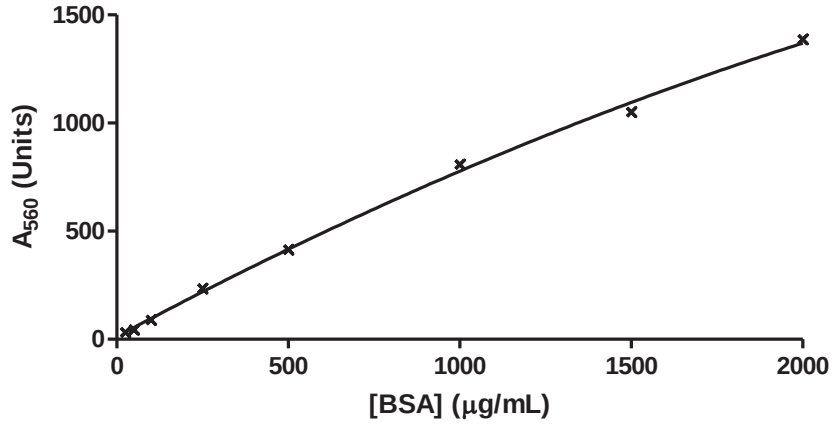

Figure 5-8. Example of a BSA standard curve produced using the 10 μL microplate BCA protocol.

Standards are 25, 50, 100, 250, 500, 1000, 1500 and 2000 μg/mL BSA in RIPA buffer + 0.5% (v/v) protease inhibitor cocktail. Line is non-linear (quadratic) regression best-fit curve (r^2 = 0.998).

5.2.5.1.2. SDS-PAGE

5.2.5.1.2.1. Gel preparation

Using a Mini-PROTEAN® 3 Cell setup (Bio-rad), discontinuous SDS-PAGE gels, consisting of a 4% polyacrylamide (29:1 acrylamide:bis-acrylamide) stacking gel over a 6% polyacrylamide resolving gel, were prepared by hand according to the manufacturers instructions. Each gel was 8 cm wide x 7.3 cm high x 1 mm thick and contained 10 wells able to accomodate up to 44 μL of sample each.

Following polymerization, gels were transferred to an electrode assembly of the Mini-PROTEAN® 3 Cell setup according to the instruction manual. The inner chamber of the assembly was filled with fresh running buffer (0.3% Tris base, 1.4% glycine, 0.1% SDS, pH 8.3) before removing the well comb and rinsing the wells with running buffer. After adding ~300-400 mL of running buffer to the outer chamber, the gel was ready for electrophoresis.

5.2.5.1.2.2. Sample preparation

Up to 20 μL of clarified lysate (or protein ladder) was combined with an equal volume of 2X sample loading buffer (85 mM Tris-HCl pH 6.8, 35% glycerol, 3% SDS, 0.01% bromophenol blue, 0.05% β-mercaptoethanol). In initial experiments, the samples were then denatured at 95°C for 5 minutes.

5.2.5.1.2.3. Gel electrophoresis

Up to 40 μL of prepared sample or protein marker ladder (GE High-Range Rainbow Molecular Weight Marker, Bio-rad Precision Plus Dual Colour Marker, or Bio-rad High Range Prestained SDS-PAGE Standard) was loaded into each well. Thirty microlitres of 1X sample loading buffer was then added to any empty wells to ensure even running of the gel. Gel electrophoresis was subsequently performed at 50 V until the bands reached the stacking-

resolving gel interface, then increased to 100 V for the remainder of the run. Electrophoresis was stopped before the bromophenol blue band reached the bottom of the gel.

5.2.5.1.3. Gel transfer

Following electrophoresis, the gel was carefully removed from the electrode assembly and gel cassette, the stacking gel cut away, and the resolving gel equilibrated in fresh transfer buffer (0.6% Tris base, 0.3% glycine, 0.05% SDS, 10% methanol) for 30 minutes (with mixing). Simultaneously, a piece of Hybond ECL nitrocellulose membrane (0.45 μm) was cut to size, pre-wet in distilled water, then soaked in transfer buffer for 30 minutes (with mixing).

Semi-dry electrophoretic transfer was then performed using a Trans-Blot® SD Semi-Dry Electrophoretic Transfer Cell (Bio-rad). Briefly, the gel transfer stack (consisting of the membrane and gel sandwiched between pre-wet filter paper), was prepared according to the manufacturer's instructions. The gel was transferred for 3 hours at 10-20 V.

5.2.5.1.4. Western blot

Two different primary antibodies were used in these experiments. For detection of P-gp, a mouse monoclonal anti-P-glycoprotein (clone F4) was employed. This F4 clone was chosen as it does not recognise the non-functional *MDR3* gene product (Chu et al., 1994).

Calnexin (an integral endoplasmic reticulum protein) was chosen as the protein loading control for this assay, and was detected using mouse monoclonal anti-calnexin. As a large protein (~90 kDa), calnexin can be detected using the lower percentage SDS-PAGE gels and longer electrophoresis times required to separate the 150 and 170 kDa bands of P-gp, whereas other smaller proteins typically employed as loading controls (e.g. β-actin ~43 kDa, α-tubulin ~50 kDa), would be poorly separated or lost.

The secondary antibody used to detect both anti-P-gp and anti-calnexin was an ECL anti-mouse IgG, Horseradish Peroxidase-Linked Species-Specific Whole Antibody from sheep.

5.2.5.1.4.1. Membrane treatment

Following the transfer of SDS-PAGE-separated proteins to the nitrocellulose membrane, the membrane was placed in PBS containing 0.1% Tween 20 (PBST) and cut along the width of the membrane in three places, at ~220-250 kDa, at ~120 kDa, and at ~60 kDa (based on pre-stained protein marker bands). The 120-250 kDa strip was then used for P-gp detection, and the 60-120 kDa strip used for calnexin detection. The two membrane sections were then blocked in 2% blocking solution (2% ECL Advance Blocking Agent, 0.1% Tween20 in PBS) at 4°C overnight (with mixing).

Membranes were rinsed twice with PBST before incubating the P-gp and calnexin sections in 2% blocking solution containing anti-P-gp or anti-calnexin antibodies, respectively (for optimized antibody dilutions see section 5.2.5.2.1). Primary antibody incubations were performed at room temperature for 2 hours, with mixing.

Following the primary antibody incubations, membranes were rinsed twice with PBST, then incubated for 15 minutes followed by 3 lots of 5 minutes in PBST (fresh PBST each wash) with mixing. The P-gp and calnexin sections were then incubated separately in 2% blocking solution containing secondary antibody for 1 hour at room temperature, with mixing (for optimized secondary antibody dilutions see sections 5.2.5.2.1 and 5.2.5.2.2). Membranes were then rinsed twice with PBST, then incubated for 15 minutes followed by 2 lots of 5 minutes in PBST (fresh PBST each wash) with mixing, and a final wash for 5 minutes in PBS.

Finally, the membranes were treated with ECL Advance Detection Reagents according to the product protocol, and chemiluminescence detected immediately.

5.2.5.1.4.2. Chemiluminescence imaging and data analysis

Chemiluminescence was detected by CCD camera on an ECL ImageQuant Imager apparatus (GE Healthcare Bio-Sciences). Optimal exposure times were determined using the inbuilt auto-exposure function of the imager software, which ensured there was no image saturation. Band intensities were then determined using ImageQuant TL software (GE Healthcare Bio-Sciences), which calculated (among other parameters) band peak height and band peak volume, with or without subtraction of a user-designated background chemiluminescence.

5.2.5.1.5. Dot blot optimization of antibody dilutions

Dot blots were employed as a quick and effective method for optimising the primary and secondary antibody dilutions required for quantitative detection of P-gp and calnexin.

5.2.5.1.5.1. P-glycoprotein dot blot

Six lots of 2 μg (in 8 μL) of $CD4^+$ cell lysate were spotted onto a section of nitrocellulose membrane and dried for 5 minutes at room temperature. The membrane was then washed 4 times in 2% blocking solution before being blocked for 1 hour at room temperature in fresh 2% blocking solution (with mixing).

The membrane was then washed twice in PBST, cut into 3 lots of 2 spots, and each segment placed in 2% blocking solution containing either a 1:1,000, 1:2,000 or 1:5,000 final dilution of anti-P-gp primary antibody. Membranes were then incubated in the primary antibody overnight at 4°C (with mixing).

Membrane sections were washed twice in PBST, incubated for 15 min at room temperature in PBST, and then for a further 3 lots of 5 minutes, using fresh PBST each time. Each membrane section was then cut in half, leaving one spot on each fragment, and one half placed in 2% blocking solution containing a 1:5,000 final dilution of secondary antibody, whilst the other

was placed in 2% blocking solution containing a 1:10,000 final dilution of secondary antibody. These were then incubated at room temperature for 1 hour (with mixing).

All membrane sections were washed with PBST as before, however, the final 5 minute wash was performed in PBS only. Each membrane section was then treated with ECL Advance Detection Reagents as per the manufacturer's instructions and the chemiluminescence of each membrane section detected as described above (section 5.2.5.1.4.2).

5.2.5.1.5.2. Calnexin dot blot

Dot blot optimization of calnexin detection was performed using the same method as for P-gp. The primary antibody (anti-calnexin) dilutions tested were 1:1,000, 1:5,000 and 1:10,000, whilst secondary antibody dilutions were 1:10,000 and 1:20,000.

5.2.5.1.6. Additional Western blot trial experiments

Having performed the dot blot optimization of antibody dilutions, three trial Western blots were performed to further test and validate the assay.

Experiment 1: Due to the results of the calnexin dot blot experiment (see below, section 5.2.5.2.1), an additional 1:50,000 dilution of secondary antibody was tested against the 1:10,000 dilution (using 1:10,000 of primary anti-calnexin antibody for both) to see if background chemiluminescence could be reduced further. In addition, to validate calnexin as an appropriate loading control, different quantities of whole PBMC lysate were trialled to ensure quantitative detection of calnexin. As such, two lots of 1, 5 and 10 μg of whole PBMC protein were subjected to SDS-PAGE and transferred to nitrocellulose as usual. The membrane was then split, and one section probed using 1:10,000 anti-calnexin and 1:10,000 secondary antibody, whilst the other was probed using 1:10,000 anti-calnexin and 1:50,000 secondary antibody, using standard Western blot procedures. Each section contained 1, 5 and 10 μg samples as well as a protein ladder. The relative backgrounds and band intensities were

compared between the two membranes to determine which secondary antibody dilution gave the clearest calnexin bands, whilst the band intensities of different protein concentrations were compared within treatments to see if calnexin was quantitatively detected.

Experiment 2: This aimed to test the Western blot procedure using different lymphocyte populations. As such, SDS-PAGE Western blot was performed for 8 μg of $CD4^+$, 4 μg of $CD8^+$, and 10 μg of whole PBMC protein, using the standard procedure and optimised antibody dilutions (see section 5.2.5.3).

Experiment 3: This aimed to investigate whether clarification of the lysate at all, or clarification from large or small volumes, was affecting the detection and banding pattern of lymphocyte samples. In addition, some literature had suggested that P-gp can aggregate at high temperatures (Germann, 1997), therefore, another aim was to trial an alternative incubation at 37°C for 10 min (instead of 95°C for 5 min) prior to gel loading. As such, 6 different protein samples for electrophoresis were prepared for this experiment;

(1) 5 x 10^5 $CD4^+$ cells were lysed in 23 μL of RIPA-PI, and the lysate clarified using standard procedure. Ten microlitres of sample was then combined with sample loading buffer and heated at 37°C for 10 minutes prior to loading.
(2) Same as (1) except heated at 95°C for 5 minutes (instead of 37°C for 10 minutes) prior to loading.
(3) 2 x 10^6 $CD4^+$ cells lysed in 82 μL of RIPA-PI. Without clarifying the lysate, a 13 μL sample was taken, 10 μL was then combined with sample loading buffer and heated at 37°C for 10 minutes prior to loading.
(4) From the same sample of unclarified lysate as sample (3), 13 μL was taken, 10 μL was then combined with sample loading buffer and heated at 95°C for 5 minutes prior to loading.

(5) The remaining lysate from (3) was clarified using standard procedure, 13 μL was taken, 10 μL was then combined with sample loading buffer and heated at 37°C for 10 minutes prior to loading.

(6) Same as (5) except heated at 95°C for 5 minutes prior to loading.

SDS-PAGE and Western blot was then performed as usual using optimal antibody dilutions (see section 5.2.5.3). The protein content of 3 μL of each sample was also quantified using the BCA assay. For each sample, the volumes and peak heights of calnexin bands were compared to the BCA protein quantification values, as well as the volumes and peak heights for P-gp.

Experiment 4: To confirm that the detected bands were in fact P-gp, a sample of *MDR1*-transfected LLC-PK1 cells, kindly donated by Dr Janet Coller (Discipline of Pharmacology, University of Adelaide), was lysed and 2 and 15 μg of the LLC-PK1-*MDR1* total protein subjected to SDS-PAGE and Western blot alongside a 5 μg sample of $CD4^+$ cell lysate.

5.2.5.2. Results

5.2.5.2.1. Dot blot optimization

As shown in Figure 5-9, a primary antibody (anti-P-gp) dilution of 1:5,000 and secondary antibody dilution of 1:10,000 (Figure 5-9F) gave adequate staining of the protein dot, with little or no background staining of the membrane.

Figure 5-10 shows that, of the dilutions tested in this experiment, the primary antibody (anti-calnexin) dilution of 1:10,000 and secondary antibody dilution of 1:20,000 (Figure 5-10F) stained for calnexin and gave the least background staining of the membrane. However, significant background chemiluminescence was still observed at these dilutions.

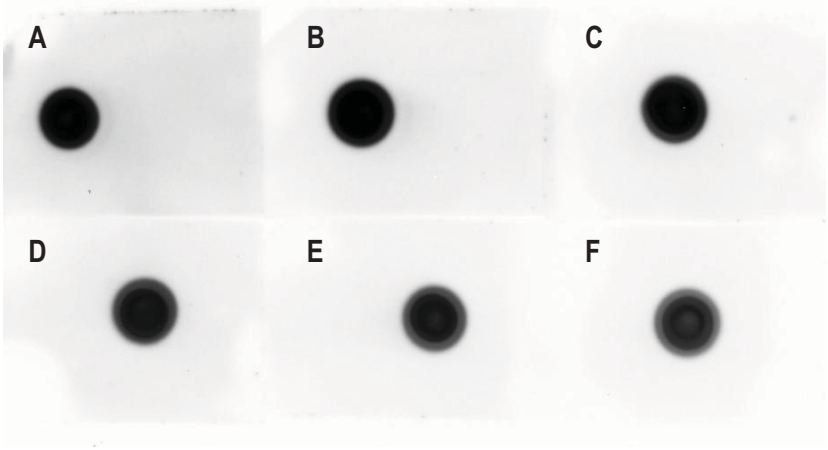

Figure 5-9. Dot blot experiment identifying 1:5,000 and 1:10,000 as optimal primary and secondary antibody dilutions, respectively, for detecting P-gp (black dots) with minimal or no background membrane staining.

Primary antibody (mouse anti-human P-gp (clone F4)) / secondary antibody (sheep anti-mouse-HRP) dilutions were **(A)** 1:1,000/1:5,000, **(B)** 1:2,000/1:5,000, **(C)** 1:5,000/1:5,000, **(D)** 1:1,000/1:10,000, **(E)** 1:2,000/1:10,000, and **(F)** 1:5,000/1:10,000.

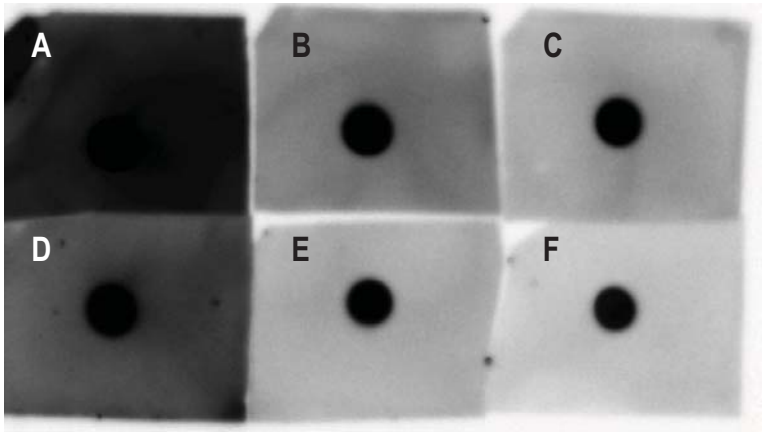

Figure 5-10. Dot blot experiment identifying significant background staining for all primary and secondary antibody dilutions tested for detection of calnexin.

Primary antibody (mouse anti-human calnexin) / secondary antibody (sheep anti-mouse-HRP) dilutions were **(A)** 1:1,000/1:10,000, **(B)** 1:5,000/1:10,000, **(C)** 1:10,000/1:10,000, **(D)** 1:1,000/1:20,000, **(E)** 1:5,000/1:20,000, and **(F)** 1:10,000/1:20,000.

5.2.5.2.2. Trial experiment 1: Further optimisation of calnexin detection

As shown in Figure 5-11, further dilution of the secondary antibody to 1:50,000 for the detection of calnexin was found to significantly reduce the background staining of the membrane. Using this dilution, calnexin could be detected in 10 and 5 µg, but not 1 µg, of

whole PBMC total protein. However, analysis of band intensity (peak volume) showed a better quantitative relationship between chemiluminescence and calnexin content for the 1:50,000 secondary antibody dilution (ratio of 10 to 5 μg peak volume = 1.93:1), compared to the 1:10,000 dilution (ratio of 10 to 5 μg peak volume = 1.25:1, ratio of 5 to 1 μg peak volume = 4.11:1). Therefore, 1:50,000 was chosen as the optimal secondary antibody dilution for detection of calnexin.

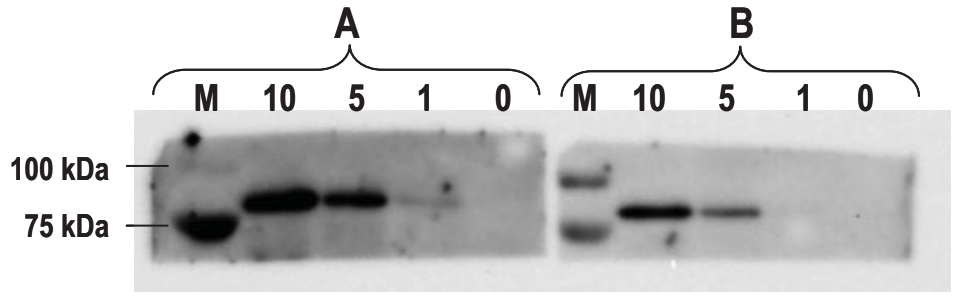

Figure 5-11. Additional dilution of secondary antibody from 1:10,000 to 1:50,000 produces reduction in background membrane staining, whilst maintaining adequate quantitative detection of calnexin by Western blot.

(A) 1:10,000 dilution of secondary antibody. **(B)** 1:50,000 dilution of secondary antibody. Both **(A)** and **(B)** employed 1:10,000 dilution of primary anti-calnexin antibody. **M:** 100 kDa and 75 kDa protein bands of Precision Plus Dual Colour Marker. **10:** 10 μg of whole PBMC protein used in SDS-PAGE. **5:** 5 μg of whole PBMC protein used in SDS-PAGE. **1:** 1 μg of whole PBMC protein used in SDS-PAGE. **0:** No protein loaded.

5.2.5.2.3. Trial experiment 2: Differences between lymphocyte populations

As shown in Figure 5-12, two P-gp bands at 170 and 150 kDa could be detected in $CD4^+$ and $CD8^+$ lymphocytes, but not in whole PBMCs, whilst calnexin (loading control) was detected in all three samples. The $CD8^+$ cells showed a higher P-gp expression than $CD4^+$ cells, with a 3-fold greater calnexin-adjusted total P-gp content (1.2 versus 0.4).

The whole PBMC lysate sample displayed a different calnexin banding pattern to the $CD4^+$ and $CD8^+$ cell samples (Figure 5-12 bottom panel), and the calnexin band was less intense than expected from the relatively high protein content (10 μg versus 8 and 4 μg, respectively).

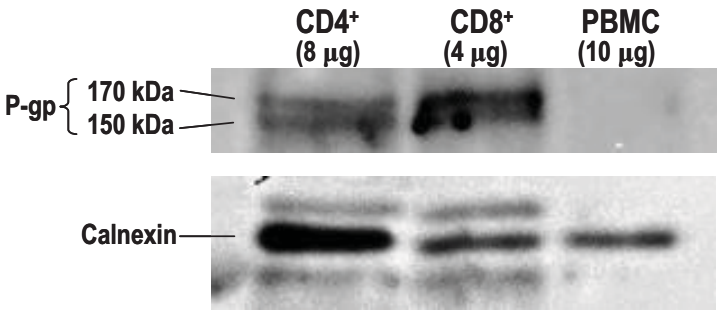

Figure 5-12. Western blot detection of P-gp in $CD4^+$ and $CD8^+$ lymphocytes but not whole PBMC cell lysate.

Core-glycosylated (150 kDa) and N-glycosylated (170 kDa) P-glycoprotein (top panel) was detected in 8 µg of $CD4^+$ and 4 µg of $CD8^+$ lymphocyte lysate, but could not be detected in 10 µg of whole PBMC lysate. Calnexin loading control (bottom panel) was detected in all three sample types.

5.2.5.2.4. Trial experiment 3: Effects of lysate preparation

The total amounts of protein loaded for samples 1-6, as determined by BCA assay, were 4.5, 3.8, 2.9, 1.7, 3.5 and 2.5 µg, respectively. All 6 samples displayed similar banding patterns for both P-gp and calnexin, and, importantly, all samples displayed two distinct P-gp bands at 150 and 170 kDa (Figure 5-13). In terms of band intensity, samples 1 and 2 (smaller lysis volume) had a greater 170 kDa P-gp peak volumes (96,099 and 134,138) than samples 3-6 (77,969, 81,544, 67,196 and 58,860, respectively). This was also observed for the calnexin bands (142,732 and 166,942, versus 126,913, 116,013, 95,459 and 84,150). A similar pattern was seen when measuring band peak heights.

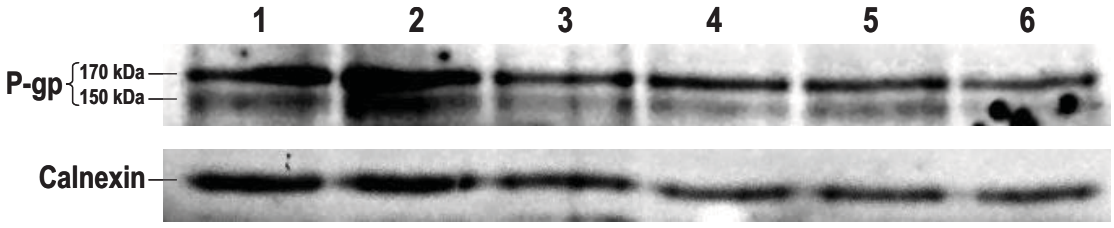

Figure 5-13. Influence of protein sample preparation on detection of P-gp and calnexin in $CD4^+$ lymphocytes.

(1) Small volume lysis (23 µL), clarified lysate, non-denatured. **(2)** Small volume lysis, clarified lysate, denatured. **(3)** Large volume lysis (82 µL), non-clarified lysate, non-denatured. **(4)** Large volume lysis, non-clarified lysate, denatured. **(5)** Large volume lysis, clarified lysate, non-denatured. **(6)** Large volume lysis, clarified lysate, denatured.

Calnexin band intensities (both band volume and peak height) correlated poorly with the protein content quantified by BCA assay (Figure 5-14 A and B). However, P-gp and calnexin band intensities correlated well for both band volume and band peak height measures, particularly for clarified lysate samples (Figure 5-14 C and D). As such, calnexin-adjusted P-gp quantities varied very little between samples for both peak volume (samples 1-6 = 0.67, 0.80, 0.61, 0.70, 0.70 and 0.70, respectively. CV = 8.7%) and peak height (samples 1-6 = 0.70, 0.74, 0.63, 0.66, 0.71 and 0.71, respectively. CV = 5.8%) measurements.

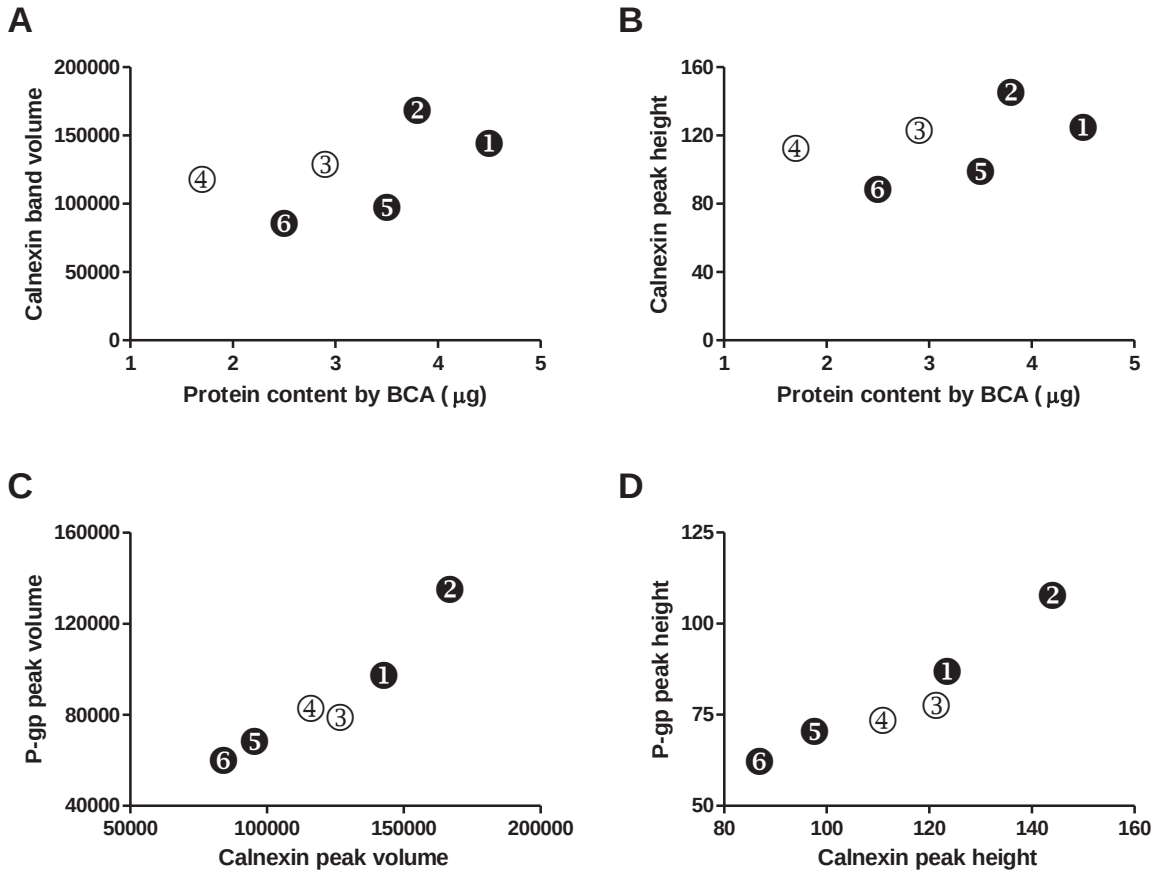

Figure 5-14. Influence of protein sample preparation on correlations between BCA protein quantification and loading control (calnexin) band volume (A) and peak height (B), and between loading control and P-gp band volumes (C) and peak heights (D).

Even numbered samples (2, 4 and 6) were heat denatured (95°C). Dark circles (1, 2, 5 and 6) were clarified lysates, white circles (3 and 4) were non-clarified lysates.

5.2.5.2.5. Trial experiment 4: Positive control for P-gp detection

As shown in Figure 5-15, the P-gp overexpressing LLC-PK1-*MDR1* cell lysates produced large and diffuse P-gp bands spanning approximately 130-180 kDa. More importantly, the P-gp bands observed for the $CD4^+$ protein sample lay within the LLC-PK1-*MDR1* P-gp detection range, confirming that the double bands detected in lymphocyte sample are P-gp.

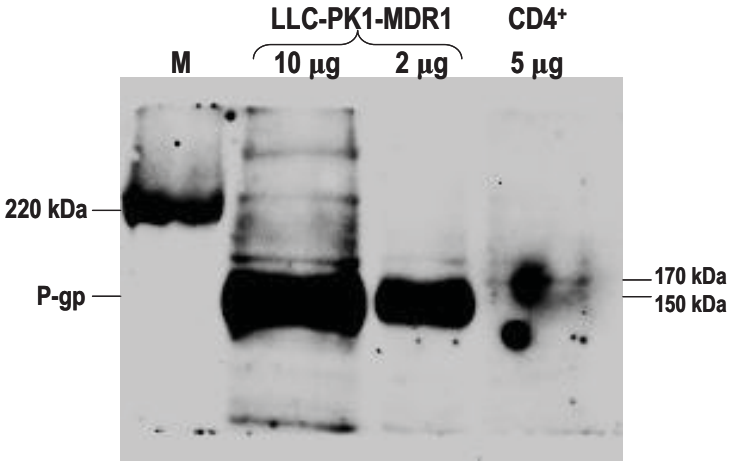

Figure 5-15. Confirmation of P-gp detection in $CD4^+$ lymphocytes using overexpressing *MDR1*-transfected LLC-PK1 cells as a positive control.
M: 220 kDa band of Precision Plus Dual Colour Marker.

5.2.5.3. Discussion

Discontinuous SDS-PAGE employing a 4% stacking and 6% resolving gel was able to separate the 150 and 170 kDa bands of core-glycosylated and N-glycosylated P-gp, respectively, from lymphocyte whole protein lysates. Furthermore, the separation of P-gp and calnexin bands was sufficient for the safe dissection of transferred membranes into specific P-gp and calnexin segments, which allowed for the separate, but simultaneous, probing of P-gp and calnexin. As such, this method had the added benefit of eliminating the need for stripping and reprobing the membrane.

Through the use of dot blot and SDS-PAGE Western blot experiments, the optimal antibody dilutions for the detection of P-gp and calnexin proteins in human lymphocytes were determined as 1° 1:5,000 / 2° 1:10,000 and 1° 1:10,000 / 2° 1:50,000, respectively.

5.2.5.3.1. Sensitivity and specificity

Using these optimized dilutions, P-gp could be detected in as little as 2 μg of $CD4^+$ and 4 μg of $CD8^+$ lymphocyte protein, but not in 10 μg of whole PBMC protein. Since calnexin was detected at similar levels in the $CD8^+$ and PBMC samples tested, it appears that P-gp expression in whole PBMCs is significantly lower than in specific lymphocyte subsets (such as $CD4^+$ and $CD8^+$ cells). Interestingly, $CD4^+$ and $CD8^+$ samples also displayed different calnexin banding patterns to the whole PBMC sample, raising the possibility that variations in the effectiveness of lysate clarification between large (200 μL for the PBMC sample) and small (13 μL for $CD4^+$ and $CD8^+$ samples) lysis volumes, was affecting the complement of proteins within a sample, and hence the detection of P-gp. However, trial experiment 4 was able to show that lysate clarification (and the volumes in which this was performed), had little or no effect on the detection of P-gp or calnexin. These findings also indicated that a control sample of clarified $CD4^+$ lysate (~5 μg), rather than whole PBMCs, would therefore be the most appropriate positive control for subsequent analyses of subject samples.

Trial experiments also showed that denaturing the protein sample at 95°C (or not) prior to performing SDS-PAGE had little effect on the detection of either P-gp or calnexin. As such, it was concluded that 2 μg of whole protein in clarified, non-denatured $CD4^+$, $CD8^+$ or $CD56^+$ lysate would be sufficient for detection of P-gp and calnexin. (Whilst $CD56^+$ cell lysates were not tested in these trial experiments, they express higher levels of P-gp than $CD4^+$ and $CD8^+$ cells, and as such it was reasonably expected that P-gp could also be detected in these cells.)

Finally, *MDR1*-transfected LLC-PK1 cells were successfully used to confirm that the protein bands detected by the anti-P-gp antibody were indeed P-gp.

5.2.5.3.2. Quantitative validity

Trial experiments showed that calnexin could be detected in a quantitative manner from different protein loading amounts (experiments 1 and 3), and whilst calnexin band intensities correlated poorly with the lysate total protein contents determined by the BCA assay, they displayed a good correlation with P-gp band intensities. Furthermore, normalization of P-gp band intensities to their corresponding calnexin values was able to significantly decrease inter-sample variability. For example, in trial experiment 4, the coefficients of variation for P-gp band peak volumes and peak heights were 31.2% and 20.2%, respectively, prior to normalization, and 8.7% and 5.8%, respectively, following normalization to calnexin band intensities. Therefore, it was concluded that calnexin was an appropriate loading control for the quantification of P-gp protein expression on human lymphocytes.

Using this method, P-gp protein expression was found to be higher in $CD8^+$ than $CD4^+$ cells, which was expected from previous studies, further confirming the validity of this assay as a quantitative measure of P-gp protein expression.

It is unclear why there is a lack of a clear correlation between BCA and calnexin values. Whilst it could be due to variability in the loading of samples onto the SDS-PAGE gel, it may also be a result of a deficit in the BCA assay to accurately measure protein content in these samples. As such, care should be taken regarding adjusting sample lysate loading amounts based on BCA protein quantification results.

5.2.5.4. Conclusion

To my knowledge, this is the first Western blot protocol adequately validated (with appropriate positive and loading controls, and the use of a non-cross-reactive P-gp antibody) to quantitatively detect and distinguish the mature N-glycosylated and immature core-glycosylated forms of P-glycoprotein in human lymphocytes. As mentioned previously,

ABCB1 polymorphisms may affect P-gp glycosylation, thus identification of P-gp in its separate glycosylated states may be important for the pharmacogenetic analysis of P-gp protein expression. As such, this protocol has a distinct advantage over Western blot methods previously employed for *ABCB1* pharmacogenetic studies that could not distinguish between the mature and immature forms of the protein. Furthermore, quantitative detection of 170 and 150 kDa human P-gp was possible from as little as 2 μg of total protein from $CD4^+$, $CD8^+$ or $CD56^+$ human lymphocytes, thus limiting the number of lymphocytes (< 1 x 10^5 cells), and hence the volume of blood (< 1 mL), required for analysis. This is important when considering the intended opioid-dependent study population who typically experience peripheral immunosuppression (and thus lower PBMC counts) (Nair et al., 1986; Vallejo et al., 2004), and may also have poor venous access.

Based on the results from Western blot development and validation experiments, 5 x 10^5 cells (~15 μg total protein) was chosen as the sample size required for the Western blot analysis to be employed for quantification of lymphocyte P-gp protein expression in the *ex vivo* pilot study described below.

5.2.6. P-gp function by rhodamine efflux assay

5.2.6.1. Methods

This assay, developed for the evaluation P-gp transport in lymphocytes, was based loosely on the flow cytometric assay protocol of Klimecki and colleagues (1994). Employing rhodamine-123 (hereafter referred to as rhodamine) as the fluorescent P-gp substrate, and verapamil as the P-gp inhibitor, a basic plan for the functional assay procedure is shown in Figure 5-16. Briefly, lymphocytes are incubated in a medium containing fluorescent rhodamine, with or without the P-gp inhibitor verapamil, for a set period of time. The difference in rhodamine accumulation between verapamil treated and untreated cells provides an indication of P-gp activity influencing drug accumulation. Cells can then be transferred to substrate-free

medium, allowing the cells to efflux the substrate for a period of time, and the amount/rate of efflux (with and without verapamil) can be determined. Whilst Klimecki and colleagues (1994) employed flow cytometry for measuring intracellular rhodamine fluorescence, this assay was adapted for fluorescence measurement using a microplate reader where it is not only possible to measure the intracellular concentration of a substrate (as in flow cytometry), but also the amount of substrate in the extracellular media (not possible with flow cytometry).

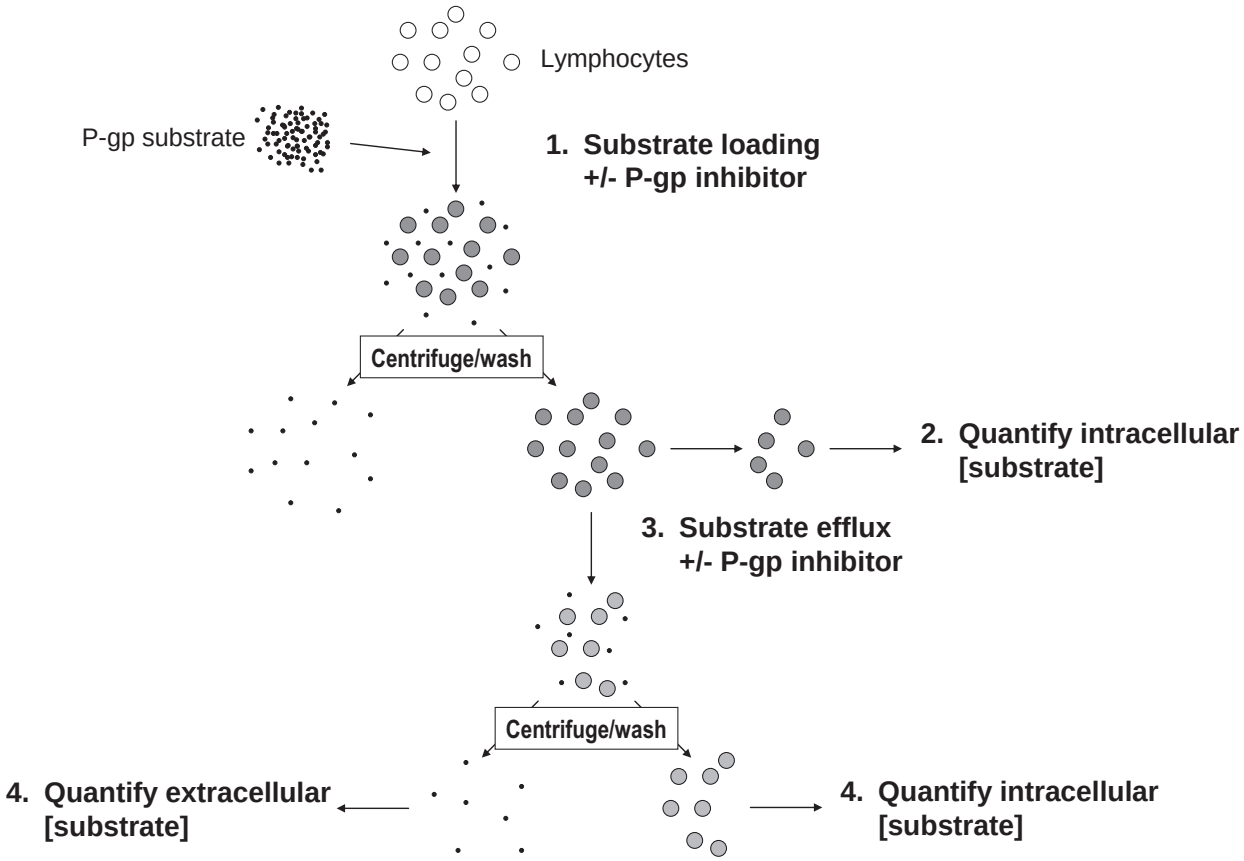

Figure 5-16. Outline of proposed functional assay procedure.

5.2.6.1.1. Lymphocyte preparation

Prior to performing this functional assay, frozen lymphocytes were defrosted rapidly in a 37°C waterbath, washed with PBS, then resuspended in 1.4 mL of assay medium (RPMI1640 + 10mM HEPES + 10% FCS). The cells were incubated at 37°C for 1 hour to allow for rehydration then quantified and checked for viability using a haemocytometer. A sample of

lymphocytes (1.2-1.8 x 10^5 cells) was taken at this point and later used to determine the background fluorescence of cell lysate.

5.2.6.1.2. Step 1: Substrate loading

Two different general substrate loading protocols were trialled. Because the original aim of this assay was to measure variability in cellular accumulation of rhodamine (in addition to efflux), the first protocol divided cells into four separate sample loading groups that could assess rhodamine accumulation in the presence and absence of P-gp activity. Using this method, two lots of cells were suspended in assay medium containing 150 ng/mL rhodamine, one lot was suspended in assay medium containing 150 ng/mL rhodamine plus 50 μM verapamil, and one lot was suspended in assay medium containing 150 ng/mL rhodamine plus 100 μM verapamil. One lot of rhodamine-only cells was then incubated at 4°C (to inhibit all active transporters) for 15 or 30 minutes with shaking, whilst the other 3 lots of cells were incubated at 37°C for 15 or 30 minutes (with shaking).

The second protocol employed a simpler method whereby all hydrated cells were loaded together for 30 minutes at 37°C using 150 ng/mL rhodamine in assay medium (with no verapamil). Whilst this method provides less data regarding P-gp activity influencing substrate accumulation, it significantly reduces the within-sample variability prior to the efflux section of the experiment.

The loading concentration of rhodamine (150 ng/mL) was the same as that used by Klimecki and colleagues (1994), and was also close to the maximum concentration that could be measured on the microplate reader without saturating the detector (see section 5.2.6.1.6.1). Verapamil concentrations of 50 and 100 μM were chosen based on experience using verapamil in the transport experiments described in Chapter 6.

All substrate loading procedures were performed at a cell density of 1 x 10^6 cells/mL, with rocking during incubations to ensure the maintenance of a cell suspension.

5.2.6.1.3. Step 2: Quantifying substrate accumulation

There were also two possible measures of substrate accumulation. The first and most useful measure was the intracellular concentration of rhodamine at the end of the loading period. The second possible measure was the extent of reduction of extracellular rhodamine concentrations as the substrate was taken into the cells. However, whilst extracellular concentrations after the loading period were determined for early experiments, its utility as a measure of cellular uptake of rhodamine was limited. This was because the intracellular distribution volume of the lymphocytes was negligible when compared to that of the supernatant, and as such, the uptake of rhodamine into the cells had no significant effect on the rhodamine concentration in the extracellular loading medium. Therefore, intracellular rhodamine concentrations were chosen as the primary measure of substrate accumulation during the loading period.

To determine the intracellular rhodamine accumulation following substrate loading, loaded lymphocytes were pelleted by centrifugation at 4°C. The supernatants were then removed and, if desired, the extracellular rhodamine concentration determined (see section 5.2.6.1.6.1).

For samples loaded using the first loading protocol, rhodamine-only cells were washed twice with cold PBS or assay medium, whilst rhodamine + verapamil (50 or 100 μM) treated cells were washed twice with cold (4°C) PBS or assay medium containing corresponding concentrations of verapamil (50 or 100 μM). Half of each group of cells was then taken, pelleted, supernatant removed, and the cell pellet frozen at -20°C until ready for quantification of intracellular rhodamine (see section 5.2.6.1.6.2).

For samples loaded using the second loading protocol, cells were washed once with cold PBS or assay medium before being split into two. One half of the cells was then washed again in cold PBS or assay medium before being resuspended to 1.5 x 10^6 cells/mL in cold assay medium. The other half of the cells were washed in cold PBS or assay medium containing 100 μM verapamil, before being resuspended to 1.5 x 10^6 cells/mL in cold assay medium containing 100 μM verapamil. Cell samples from each lot were then taken, pelleted, supernatants removed, and the cell pellets frozen at -20°C until ready for quantification of intracellular rhodamine (see section 5.2.6.1.6.2).

5.2.6.1.4. Step 3: Substrate efflux

Substrate-loaded cells were suspended at 1.5 x 10^6 cells/mL in assay medium (no rhodamine), with or without 100 μM verapamil, and cells were either kept together, or split into 2 or 3 tubes each to act as replicates. The cells were then allowed to efflux at 37°C (with rocking) for 30, 60 or 120 minutes.

5.2.6.1.5. Step 4: Quantifying substrate efflux

As with substrate accumulation, there were two possible measures of substrate efflux. Firstly the reduction in intracellular rhodamine concentrations, and secondly the increase in extracellular rhodamine concentrations, following the efflux period. These values were determined by pelleting each cell sample by centrifugation at 4°C and taking a sample of the supernatant for extracellular rhodamine quantification. The cells were then washed twice with PBS or assay medium, pelleted, the supernatants removed, and the cell pellets frozen at -20°C until ready for quantification of intracellular rhodamine (see section 5.2.6.1.6.2).

5.2.6.1.6. Rhodamine quantification

The only major difference between this assay, and that of Klimecki and colleagues (1994), was that detection of rhodamine fluorescence was performed using a microplate reader,

instead of a flow cytometer. As such, the sensitivity of the microplate reader to detect rhodamine fluorescence in extracellular fluid, as well as in cell lysates, needed to be tested.

5.2.6.1.6.1. Extracellular rhodamine quantification

Firstly, a standard curve of 0.005, 0.01, 0.05, 0.1, 0.5, 1, 10, 100, 1,000 and 20,000 ng/mL of rhodamine in RPMI assay medium was prepared. Quadruplicate 100 μL samples of each standard concentration, and an RPMI assay medium blank, were loaded onto a white 96-well microplate (Nunc^{TM}) and fluorescence measured on a microplate reader using 485 nm excitation and 520 nm emission filters. Using this method, the 20,000 and 1,000 ng/mL standards saturated the microplate detector, whilst the 0.005, 0.01 and 0.05 ng/mL standards gave poor accuracy and precision. As such, 0.1 ng/mL was concluded to be the lower limit for rhodamine quantification by this microplate procedure.

Secondly, in order to more accurately define the minimum and maximum possible rhodamine concentration for microplate detection, two separate standard curves were prepared. The first consisted of 0.1, 0.5, 1, 5, 10, 25, 50, 100, 200, 400, 600 and 800 ng/mL of rhodamine in RPMI assay medium, whilst the other consisted of 0.1, 0.2, 0.3, 0.4, 0.5, 0.6, 0.7, 0.8, 0.9, 1, 2 and 3 ng/mL. Quadruplicates of each standard and blank were analysed as before. The detector was saturated at rhodamine concentrations greater than 400 ng/mL, and close to saturation at 200 ng/mL, whilst the second standard curve was linear down to 0.2 ng/mL.

Therefore, extracellular (supernatant) rhodamine was quantifiable in the range of 0.2 to a maximum of between 100 and 200 ng/mL. Standard curves over the range of 0.2 to 150 ng/mL were best fitted using 3rd-order polynomial non-linear regression with $1/Y^2$ weighting, however, standards below 0.5 ng/mL displayed poor accuracy (error > 20%) and precision (error > 13%) when compared to standards of 0.5 ng/mL and greater (accuracy error < 12% and precision error < 7%).

Thirdly, since some of the samples were to contain verapamil, the influence of verapamil on rhodamine quantification needed to be tested. As such, two standard curves consisting of 0.25, 0.5, 0.75, 1, 2.5, 5, 10, 25, 50, 75, 100 and 150 ng/mL rhodamine were prepared, one in blank RPMI assay medium, and the other in RPMI assay medium containing 100 μM verapamil. Triplicate 100 μL samples of each standard and blank (± verapamil) were then measured on the microplate reader as before. Blank fluorescence values did not differ in the presence or absence of verapamil and, as shown in Figure 5-17, the two standard curves were almost identical. Indeed, when input into the best-fit curve defined by the non-verapamil standards, rhodamine + verapamil fluorescence values interpolated standard concentrations with an error of less than 12%. Therefore, there was no need to perform separate rhodamine standard curves for extracellular samples containing verapamil.

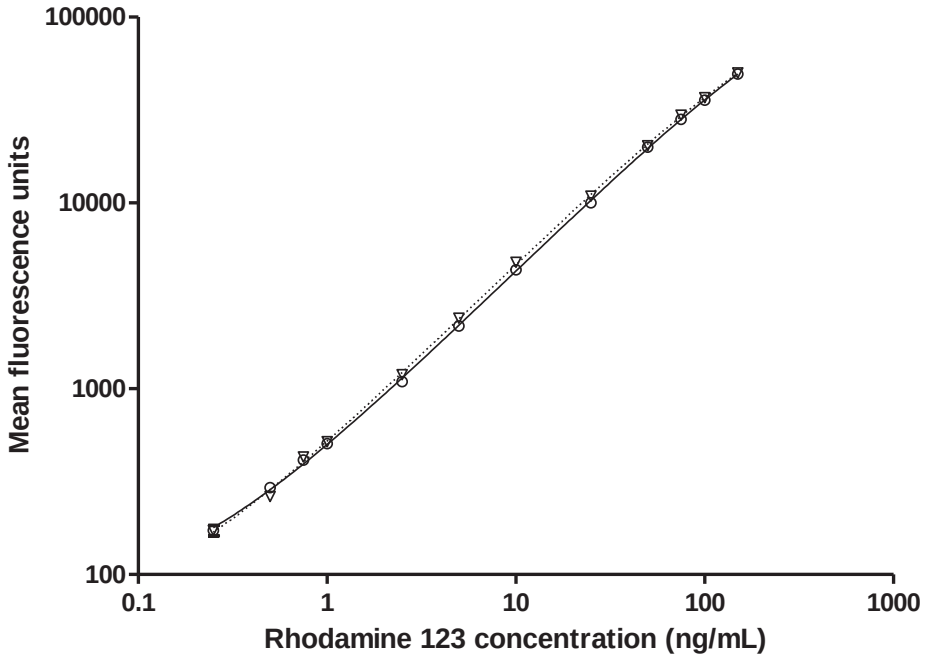

Figure 5-17. Rhodamine fluorescence standard curves in the presence (--△--) and absence (—○—) of 100 μM verapamil.

Lines are 3rd-order polynomial non-linear regression (with $1/Y^2$ weighting) curve fits (r^2 = 1.00 for both curves). For the 3rd-order equation ($y = ax^3 + bx^2 + cx + d$) coefficient best-fit values (95% CI) in the presence and absence of verapamil were: a = 9.7×10^{-4} (-3.4×10^{-3} to 5.4×10^{-3}) and 2.5×10^{-3} (-3.7×10^{-3} to 8.6×10^{-3}); b = -0.82 (-1.5 to -0.14) and -1.3 (-2.2 to -0.33); c = 430 (411 to 450) and 471 (444 to 499); d = 72 (58 to 85) and 51 (33 to 69).

Finally, experiments measuring 50, 100, 150 and 200 μL of blank RPMI assay medium in each well revealed that background fluorescence was volume-dependent, therefore sample and standard volumes also needed to be kept constant.

5.2.6.1.6.2. Intracellular rhodamine quantification

In order to quantify the intracellular rhodamine concentrations, cell samples were lysed in SDS lymphocyte lysis buffer (1% SDS, 20 mM Tris-HCl, pH 7.2) for 10 minutes at room temperature. The lysates were then clarified by centrifugation (14,000 x g for 10 minutes) before measuring rhodamine fluorescence.

In order to determine the appropriate diluent for intracellular rhodamine standard curves, two separate standard curves consisting of 0.2, 0.4, 0.8, 2.5, 10, 50, 100 and 150 ng/mL rhodamine were prepared using blank lymphocytes lysis buffer, or clarified cell lysate (5 x 10^5 cell/mL), as the diluent. Triplicate 100 μL samples of each standard and blank were then measured on the microplate reader as before. As shown in Figure 5-18A, the standard curves using blank lysis buffer and cell lysate were sufficiently different to necessitate using blank cell lysate as the diluent for intracellular rhodamine standard curves. As such, a stock of clarified PBMC cell lysate (1 x 10^6 cells/mL) was prepared and used for preparation of subsequent intracellular rhodamine standard curves. An example of an intracellular standard curve used in trial assays is given in Figure 5-18B. Using a 3rd-order polynomial non-linear regression with $1/Y^2$ weighting as before, standard concentrations were interpolated with a mean relative accuracy error of less than 12%.

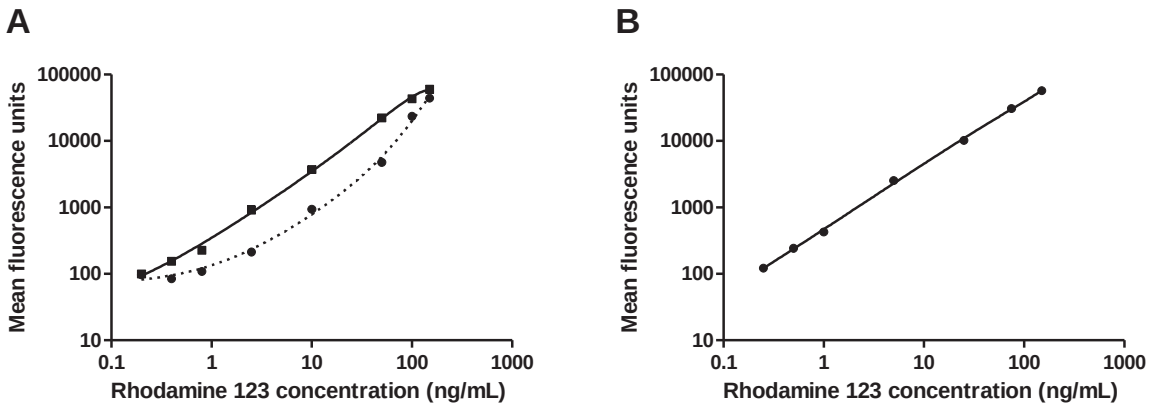

Figure 5-18. Standard curves for quantification of intracellular rhodamine concentrations.

A: Comparison of rhodamine standard curves in blank lymphocyte lysis buffer (--●--) and clarified cell lysate (—■—). **B:** Example of a cell lysate rhodamine standard curve used for quantification of intracellular rhodamine concentrations. Lines are 3rd-order polynomial non-linear regression (with $1/Y^2$ weighting) curve fits ($r^2 = 0.99$ for both curves in graph A, $r^2 = 1.00$ for graph B).

5.2.6.1.6.2.1. Normalisation to protein content

To account for any variations in the number of cells used for each quantification, lysate rhodamine concentrations were to be normalised to lysate protein content. As such, a BCA assay employing a BSA standard curve was established as described previously (see section 5.2.5.1.1) using lymphocyte lysis buffer as the diluent. The influence of rhodamine in the lysate on BCA protein quantification was also tested by spiking lysates of different protein concentrations with up to 150 ng/mL of rhodamine. It was found that rhodamine increased the background absorbance of lymphocyte lysis buffer up to 3-fold. However, since the background absorbance was negligible when compared to absorbance values of the protein standards, the effects on protein quantification were minimal. For example, protein quantification in a sample of cell lysate without rhodamine, or spiked with rhodamine to a final concentration of 1, 50 or 100 ng/mL, resulted in similar calculated protein concentrations (67.3, 65.0, 61.4 and 65.9 μg/mL, respectively). Therefore, the rhodamine content of cell lysates was deemed to have no significant influence on protein quantification by the BCA assay.

5.2.6.1.7. Quantifying cell loss

In order to determine whether PBS or assay medium was the best solution for washing cells, complete assay protocols were performed using the second, simple loading procedure, and efflux periods of 30, 90 or 150 minutes. During these procedures, instead of taking samples for rhodamine quantification, cell concentrations were quantified in the samples before and after every wash step, and at the beginning and end of each incubation step, in order to quantify any cell loss.

In order to check the viability of cells over the intended assay period, a separate experiment was performed where lymphocytes were incubated for 3 hours at 37°C in either blank assay medium or assay medium containing both 300 ng/mL rhodamine and 100 μM verapamil. Viable cells were quantified before and after the incubation period to determine if there was any lymphocyte loss.

5.2.6.1.8. Data analysis

Rhodamine accumulation was calculated by normalizing the cell lysate rhodamine concentration (after substrate loading) to the protein concentration of the lysate sample. Efflux for any time-point after loading was calculated as $(C_{SN.t} \times C_{protein.t}) / (C_{IC.t} \times N_t)$, where C_{SN} was the supernatant rhodamine concentration (ng/mL), $C_{protein}$ was the lysate sample protein concentration (μg/mL), C_{IC} was the lysate rhodamine concentration (ng/mL), and N was the cell concentration in the sample prior to pelleting and taking supernatant for quantification (cells/mL), all at time *t* after initiation of efflux.

5.2.6.2. Results

5.2.6.2.1. Substrate loading

Using the first protocol for substrate loading, trial experiments displayed large variability between samples in terms of substrate accumulation. Furthermore, this loading method failed

to demonstrate a consistent increase in rhodamine accumulation in cells loaded on ice or in the presence of verapamil. Loading the cells for 15 or 30 minutes had no effect on the variability observed using this protocol.

The second, simpler loading method produced consistent intracellular rhodamine concentrations both within and between the three trial experiments. Lysate rhodamine concentrations after the loading period ranged from 0.42 to 0.48 ng/mL, which equated to 4.4-4.9 ng of rhodamine per 100 µg of protein.

5.2.6.2.2. Substrate efflux

As shown in Figure 5-19, the difference in efflux between verapamil treated and untreated samples was greatest after 120 minutes (4.9-fold), when compared to 30 (3.5-fold) and 60 (2-fold) minutes of efflux. Where loaded samples were split into 2 or 3 replicates for efflux, they displayed an average 3.1- to 4.6-fold decrease in efflux in the presence of verapamil (after 120 minutes). However, whilst values in the presence and absence of verapamil did not overlap, there was 3- to 12-fold variability in efflux within the replicate samples for each treatment group. In addition, in some trial experiments, the intracellular rhodamine concentrations after efflux were below the lower limit of quantification.

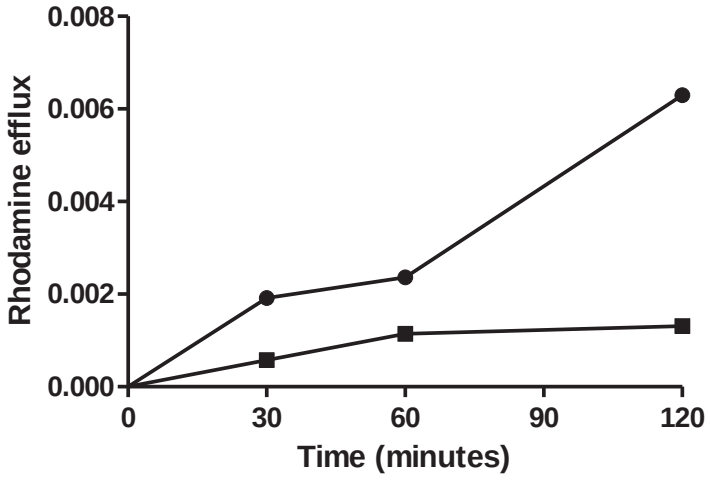

Figure 5-19. Time-course of rhodamine efflux in the presence (■) and absence (●) of 100 µM verapamil.

5.2.6.2.3. Cell loss

Up to 80% of cells were lost by the end of the assay procedure when using PBS for washing cells. Alternatively, when cells were washed with assay medium instead, no cell loss could be detected. After 150 minutes, no cell loss was observed when incubating in blank assay medium, whilst 14% of cells were lost when incubating in assay medium containing rhodamine (300 ng/mL) and verapamil (100 μM).

5.2.6.3. Discussion

The original aim of this assay was to measure variability in cellular accumulation of rhodamine as well as efflux. However, the split loading method was unable to consistently distinguish accumulation between verapamil treated and untreated cell samples. Therefore, a simpler substrate loading protocol was chosen as the preferred method for measuring rhodamine accumulation. The reduction in both the manipulation of cells (that is, pipetting, pelleting, resuspending etc.), and the elimination of sample variability prior to efflux, were also important considerations when choosing the simpler rhodamine loading protocol.

Based on trial experiments, 120 minutes was chosen as the optimal efflux time for differentiating verapamil treated and untreated cells, however, there was significant variability within the replicates of each treatment group. Furthermore, the observed intracellular rhodamine concentrations after 120 minutes of efflux were very near or, in some trial experiments, below the limit of quantification (0.2 ng/mL). As such, even after improving cell recovery by washing cells with assay medium instead of PBS, the functional assay was far from optimal.

Unfortunately, at this stage of development, problems encountered with the pilot *ex vivo* lymphocyte study (described below in section 5.3.2.2) meant that subject samples originally set aside for the functional assay were no longer available. Therefore, the further development

and optimisation of this assay was abandoned. However, a number of suggestions can be made regarding possible improvements to the assay.

Firstly, a greater intracellular rhodamine concentration after loading is required such that intracellular concentrations post-efflux are always within the quantitative range of the microplate reader. This could be achieved by loading the cells at 4°C (instead of 37°C), a method previously used by others (Chaudhary et al., 1992; Park et al., 2003) to inhibit any active drug transporters limiting the entry and accumulation of rhodamine into the cells. Increasing the loading medium concentrations of rhodamine, and increasing the loading time, may also help to increase the starting intracellular rhodamine concentrations.

Secondly, rather than splitting loaded cells into duplicate or triplicate samples for each treatment, a single sample for each treatment (that is, one tube for rhodamine only, and one tube for rhodamine + verapamil) could be used. This would increase the number of cells in each sample and hence allow an increase in the final lysate rhodamine concentrations (by lysing at greater than 1 x 10^6 cells/mL), or allow for more replicate measurements of lysate concentrations due to a greater lysis volume (by still lysing at 1 x 10^6 cells/mL). Similarly, with the larger efflux medium volume (due to the larger number of cells), more replicates of the supernatant could be used for measuring extracellular rhodamine concentrations. Furthermore, at only two tubes per subject, this would allow the assay to be performed for multiple subjects at once. Therefore, assay variability, both within and between subjects, could be greatly reduced by not splitting the treatment groups into replicates.

Finally, this assay was developed using whole human PBMCs, however, as was shown during the development of the Western blot assay, whole PBMCs express negligible amounts of P-gp when compared to specific lymphocyte subsets such as $CD4^+$, $CD56^+$ or $CD8^+$ cells (see section 5.2.5.2.3). Therefore, a trial of this assay in one of these lymphocyte subsets would be

more prudent, as the efflux due to P-gp (and thus the difference between verapamil treated and untreated samples) would be expected to be more pronounced in these cells.

5.2.6.4. Conclusion

In conclusion, the method described here provides the basis for an assay to determine the functional effect of P-gp on substrate efflux in human lymphocytes. Based on the initial assay development results, 0.75-1.6 x 10^6 cells was chosen as the appropriate number of lymphocytes to be set aside for functional analysis. However, further optimization and validation in specific lymphocyte subsets is recommended before applying this assay, as it stands, in a clinical study setting.

5.2.7. Summary

For the *ex vivo* lymphocyte pilot study described below, a new magnetic separation method for the isolation of separate $CD4^+$, $CD56^+$ and $CD8^+$ cell subsets from human whole PBMCs was developed and validated. Quantitative real-time PCR and Western blot assays were then successfully developed and validated for the quantification of *ABCB1* mRNA and P-gp protein expression, respectively, in these lymphocyte subsets. Finally, an attempt was also made to develop a new non-flow-cytometric assay for the quantification of P-gp function in *ex vivo* human lymphocytes. However, further optimization of this functional assay was abandoned due to time constraints and the loss of subject samples originally designated for this assay (see below section 5.3.2.2).

5.3. Pilot study

5.3.1. Introduction

As discussed in section 5.1, an interpretation of the findings of Chapters 3 and 4 is difficult without a clear understanding of the functional consequences of *ABCB1* genotypes and haplotypes. Unfortunately, limited *ex vivo* data are available regarding the effects of *ABCB1*

genetic variants on tissue expression and function of P-gp in humans. Furthermore, since some opioids have previously been shown to induce P-gp expression, it can be hypothesised that long-term illicit (heroin) and/or maintenance (methadone or buprenorphine) opioid administration may cause changes in P-gp expression and/or function, resulting in different levels of P-gp activity in the opioid-dependent population compared to healthy individuals. Therefore, due to the confounding influence of P-gp induction, it is possible that the functional consequences of *ABCB1* genetic variability may differ between opioid-dependent and healthy individuals. As such, the aims of this pilot study were to:

(a) identify any differences in P-gp expression and function between opioid-dependent individuals and healthy non-drug-dependent controls;

(b) investigate the effect of chronic exposure to methadone and buprenorphine on P-gp expression and function;

(c) determine whether P-gp expression and function were related to *ABCB1* genetic variability and maintenance opioid requirements.

5.3.2. Methods

Originally, this study planned to assess P-gp expression and function in opioid-dependent subjects seeking entry into opioid substitution treatment, as well as healthy non-opioid-dependent controls, with opioid-dependent subjects assessed both prior to entering treatment, and again once stabilised on either methadone or buprenorphine. In this manner, the influence of illicit opioid use on P-gp expression and function could be determined by comparing healthy controls and pre-treatment opioid-dependent subjects. Alternatively, the influence of opioid substitution treatments on P-gp expression and function, as well as the relationship between P-gp expression and function and substitution opioid response, could be determined by comparing pre-treatment and in-treatment opioid-dependent subjects. Finally, all subjects

were to be genotyped for *ABCB1* genetic polymorphisms, allowing for the assessment of their functional consequences in both healthy and opioid-dependent subjects.

Unfortunately, due to time constraints, this pilot study was eventually restricted to the investigation of a small group of stabilized MMT subjects only.

With permission from the Royal Adelaide Hospital Research Ethics Committee, existing MMT patients already taking part in the control arm of a larger clinical trial conducted by the Discipline of Pharmacology were asked to donate extra whole blood for *ex vivo* analysis. Those who volunteered (n = 6) had a single extra blood sample taken (20 mL in an EDTA tube) as part of a normal study session of the clinical trial. All subjects were in the stabilization phase of treatment, and all blood samples were taken at trough methadone plasma concentration time points, that is, approximately 24-hours post-dose and prior to receiving their next daily methadone dose.

Blood samples were kept at room temperature and processed within 2 hours of sampling. Twelve to sixteen millilitres of blood was used for isolating $CD4^+$, $CD56^+$ and $CD8^+$ lymphocytes using the optimized methods described in section 5.2.3. Based on assay development results, at least 1 x 10^5 cells for mRNA expression (see section 5.2.4.4), 5 x 10^5 cells for P-gp protein expression (see section 5.2.5.4) and 7.5 x 10^5 cells for functional analysis (see section 5.2.6.4) were processed as described in section 5.2.3.1.2.4. One millilitre of blood was also frozen at -20°C until ready for DNA isolation and *ABCB1* genotyping/haplotyping using the methods described in Chapter 2.

Subjects' demographics, methadone dose and (R)-methadone C_{trough} data (specific to the study days on which the blood samples were taken), were obtained from clinical study case notes.

For the qRT-PCR and Western blot experiments described below, $CD4^+$ lymphocytes of a healthy non-opioid-dependent volunteer (*ABCB1* haplotype: AGCG**T** / AG**TTT**) were used as control samples.

5.3.2.1. qRT-PCR

ABCB1 mRNA expression in $CD4^+$, $CD56^+$ and $CD8^+$ lymphocytes was quantified using the protocol described in section 5.2.4. $CD4^+$, $CD56^+$ and $CD8^+$ lymphocytes were analysed separately, however, within each subset of lymphocytes, all subjects were analysed at the same time. For each lymphocyte subset, *ABCB1* expression was initially determined using the standard optimised mRNA and cDNA volumes. Based on these results, samples were reanalysed using volumes of mRNA and/or cDNA adjusted to produce identical *GAPDH* C_T values (using the method described in section 5.2.4.2.). Subjects' ΔC_T values were then normalised to the ΔC_T of the control sample that was analysed within each batch of samples (using the $2^{-\Delta\Delta C_T}$ method described in section 5.2.4.1.3.2).

In order to confirm the purity of lymphocyte subsets, remaining mRNA and/or cDNA samples were used for the qualitative detection of $CD4^+$, $CD56^+$ and $CD8^+$ mRNA, using the protocol described in section 5.2.3.1.3.

5.3.2.2. Western blot

P-gp Western blot analysis was performed for $CD4^+$, $CD56^+$ and $CD8^+$ lymphocyte samples using the protocol described in section 5.2.5. However, using this method, P-gp could not be detected in the patient samples (5×10^5 cells) designated for Western blot analysis. As such, lymphocyte samples designated for the functional assay ($0.9\text{-}1.6 \times 10^6$ cells) were used. Since these samples had been stored in freezing medium (see section 5.2.3.1.2.4), they were washed three times in PBS before being pelleted and lysed as usual. In addition, since detection of P-

gp in the control sample was also inconsistent, for these assays, control lysate spiked with 1 μg of LLC-PK1-*MDR1* lysate was used as the positive control.

Due to the significant background and multiple band staining of subject samples (see Figure 5-24), peak heights, and not peak volumes, of 170 kDa bands were used to quantify P-gp protein expression (see section 5.2.5.1.4.2).

5.3.2.3. Functional assay

As mentioned above, lymphocytes (single or duplicate samples of 0.9-1.6 x 10^6 cells) were originally set aside for functional analysis. However, due to their use in the Western blot experiments, the functional assay could not be performed.

5.3.2.4. Data analysis

Due to the small number of subjects, no statistical analyses were performed regarding differences in P-gp expression (mRNA or protein) between *ABCB1* genotypes or haplotypes. Associations between P-gp expression and daily methadone maintenance dose or (R)-methadone C_{trough}, and between mRNA and protein expression, were analysed by Spearman rank correlation.

5.3.3. Results

5.3.3.1. Subject demographics & genetic variability

The demographics, treatment parameters, recent drug use history and *ABCB1* genetic variability of the *ex vivo* MMT subjects are shown in Table 5-5. Two subjects, S1 and S6, did not have (R)-methadone C_{trough} data available.

Table 5-5. Subject demographics, treatment history and *ABCB1* genetic variability.

	S1	S2	S3	S4	S5	S6
Sex	F	M	F	F	M	M
Age (years)	34	29	26	32	36	30
Weight (kg)	74	68	55	54	60	92
Smoker	Y	Y	Y	Y	Y	Y
Dose (mg/day)	65	75	100	35	130	75
C_{trough} (ng/mL)	-	103.3	216.4	63.0	408.0	-
Time in treatment (months)	9	8	8	7	8	6
Prior treatments	0	1	0	2	1	0
In-treatment drug use						
Heroin ($/month)	1000	50	50	50	30	0
Amphetamines	Y	N	N	Y	N	N
Benzodiazepines	Y	N	Y	N	N	N
Cannabis	N	Y	Y	Y	N	Y
***ABCB1* genotype**						
A61G	A/A	A/A	A/A	A/A	A/A	A/A
G1199A	G/G	G/G	G/G	G/G	G/G	G/G
C1236T	T/T	C/T	C/C	C/C	C/T	C/T
G2677T	G/G	G/T	T/T	T/T	G/T	G/T
C3435T	C/T	C/T	C/C	T/T	C/T	C/T
***ABCB1* haplotype**	AG**T**GC AG**T**G**T**	AGCGC AG**TTT**	AGC**T**C AGC**T**C	AGC**TT** AGC**TT**	AGCGC AG**TTT**	AGCGC AG**TTT**

Variant loci in haplotypes are bold.

5.3.3.2. Lymphocyte isolation

Subject blood samples yielded a total of 1.1-3.3 x 10^7 PBMCs (0.8-1.9 x 10^6 cells per mL of blood), with 4.5-7.4 x 10^6 $CD4^+$, 0.5-2.7 x 10^6 $CD56^+$, and 1.5-5.7 x 10^6 $CD8^+$ lymphocytes recovered for analysis. As such, for the majority of subjects, there were enough lymphocytes to provide samples for all three assays based on assay development results. However, for subject S3, the $CD8^+$ mRNA pellet was lost during the snap freezing process, whilst for subject S4, there were sufficient $CD56^+$ lymphocytes for protein analysis only.

Qualitative reverse transcription PCR confirmed the presence of CD4 mRNA in $CD4^+$ lymphocyte samples of all 6 subjects. A slight CD4 PCR band was also detected in the $CD56^+$ sample of subject S2, as such, this sample was excluded from expression analyses. All other $CD56^+$ samples and all $CD8^+$ samples were negative for CD4 expression.

$CD56^+$ samples for S1, S2, S3 and S6 were all positive for CD56 expression (no mRNA sample for S4, see above). No CD56 mRNA was detected in the $CD56^+$ sample of S5, however, since *ABCB1* and *GAPDH* expression was also undetectable in this sample (see below), it is likely that this sample had no quantifiable mRNA. All $CD4^+$ and $CD8^+$ samples were negative for CD56 expression.

All $CD8^+$ cell samples were positive for CD8 expression, whilst all $CD4^+$ cells were negative for CD8. For $CD56^+$ cells, very slight CD8 PCR bands were detected in some samples.

No sample displayed CD4 or CD56 PCR products of the size generated from genomic DNA.

5.3.3.3. *ABCB1* mRNA expression

Initial qRT-PCR analyses (using equal mRNA and cDNA volumes for all samples) displayed large variability in *GAPDH* 2^{-C_T} between subjects (CV = 39% for $CD4^+$, 96% for $CD56^+$ and 29% for $CD8^+$). However, adjusting the mRNA and/or cDNA volumes used for each sample (see method described in section 5.2.4.2) was successful in drastically reducing variability in endogenous control values (CV = 8% for $CD4^+$, 22% for $CD56^+$ and 9% for $CD8^+$).

ABCB1 mRNA expression in $CD4^+$, $CD56^+$ and $CD8^+$ lymphocytes of MMT subjects relative to $CD4^+$ lymphocytes of a non-opioid-dependent healthy control are shown in Table 5-6.

There were no statistically significant rank correlations between $CD4^+$ and $CD56^+$, or $CD4^+$ and $CD8^+$ *ABCB1* mRNA expression, whilst only two subjects had data for both $CD8^+$ and $CD56^+$ expression (thus not allowing statistical analysis) (Figure 5-20).

Table 5-6. *ABCB1* mRNA expression[a] in $CD4^+$, $CD56^+$ and $CD8^+$ lymphocytes of each MMT subject relative to $CD4^+$ lymphocytes of a non-opioid-dependent healthy control.

	$CD4^+$	$CD56^+$	$CD8^+$
S1	0.63 (0.58-0.68)	1.47 (1.32-1.67)	1.37 (1.32-1.42)
S2	0.47 (0.45-0.51)	-	1.21 (1.12-1.30)
S3	0.54 (0.49-0.61)	3.60 (2.73-4.58)	-
S4	0.29 (0.21-0.36)	-	1.68 (1.59-1.82)
S5	0.98 (0.88-1.07)	-	2.54 (2.09-3.09)
S6	0.87 (0.79-0.94)	1.70 (1.57-1.80)	3.04 (2.74-3.57)

[a]*ABCB1* mRNA expression (normalised to *GAPDH*) relative to $CD4^+$ lymphocytes of a healthy non-opioid-dependent control. Values are triplicate means (range of possible values).

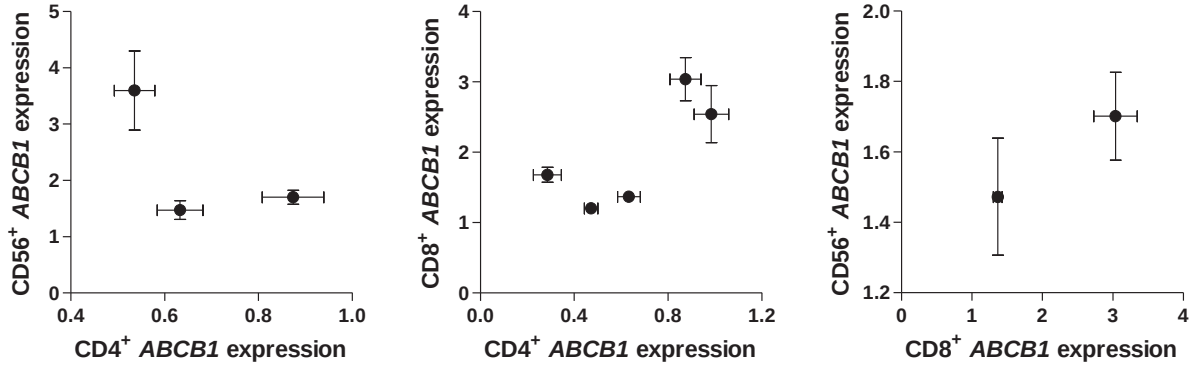

Figure 5-20. Lack of significant correlations between $CD4^+$ and $CD56^+$ (Spearman r (r_s) = -0.50, P = 1.0), $CD4^+$ and $CD8^+$ (r_s = 0.6, P = 0.4) or $CD56^+$ and $CD8^+$ lymphocyte *ABCB1* expression[a] in MMT subjects.

[a]*ABCB1* mRNA expression (normalised to *GAPDH*) relative to $CD4^+$ lymphocytes of a healthy non-opioid-dependent control. Values are mean ± range.

Haplotype differences in *ex vivo* $CD4^+$, $CD56^+$ and $CD8^+$ lymphocyte *ABCB1* mRNA expression are shown in Figure 5-21. $CD4^+$ lymphocyte *ABCB1* mRNA expression was lowest in the subject homozygous for AGC**TT**.

The relationships between dose requirements and *ABCB1* mRNA expression in $CD4^+$, $CD56^+$ and $CD8^+$ lymphocytes are shown in Figure 5-22. The relationships between plasma (R)-methadone C_{trough} and *ABCB1* mRNA expression in $CD4^+$ and $CD8^+$ lymphocytes are shown in Figure 5-23. Only one subject had both $CD56^+$ *ABCB1* mRNA expression and C_{trough} data.

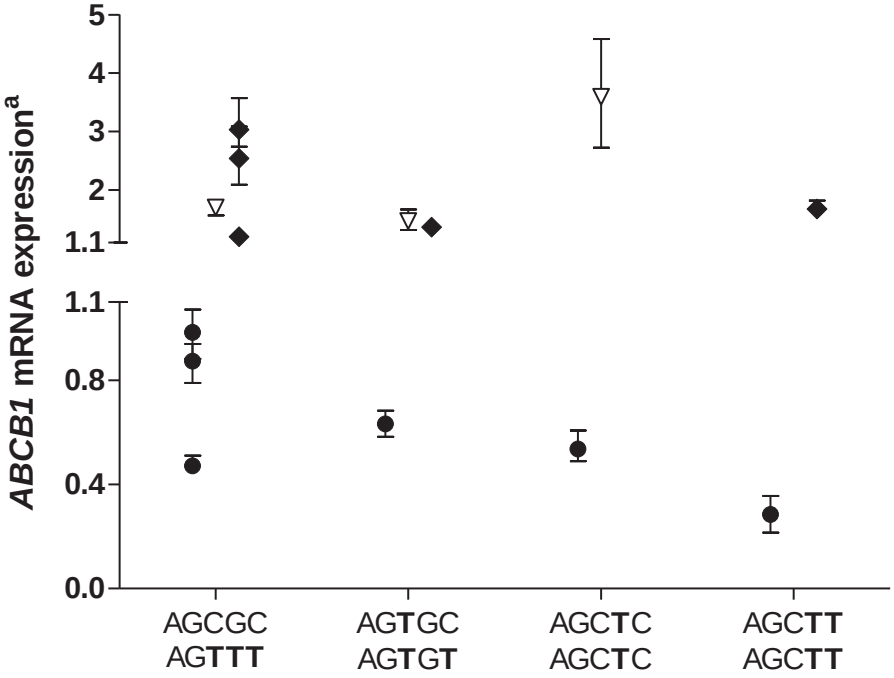

Figure 5-21. Relationship between *ABCB1* diplotypes and *ex vivo* CD4$^+$ (●), CD56$^+$ (▽) and CD8$^+$ (◆) lymphocyte *ABCB1* mRNA expression in MMT subjects.

[a]*ABCB1* mRNA expression (normalised to *GAPDH*) relative to CD4$^+$ lymphocytes of a healthy non-opioid-dependent control. Data are mean ± range for each individual.

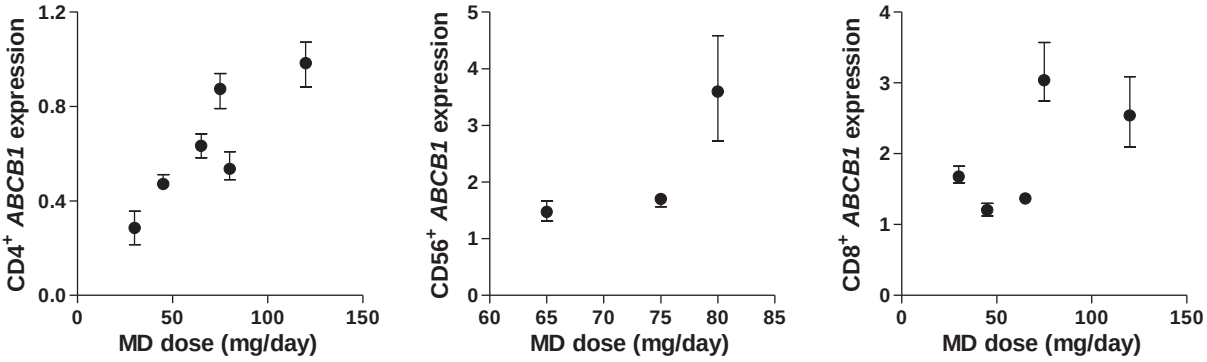

Figure 5-22. Relationship between MMT dose requirements and relative *ABCB1* mRNA expression[a] in CD4$^+$ (r_s = 0.83, P = 0.06), CD56$^+$ (r_s = 1.00, P = 0.3) and CD8$^+$ (r_s = 0.6, P = 0.4) lymphocytes of MMT subjects.

[a]*ABCB1* mRNA expression (normalised to *GAPDH*) relative to CD4$^+$ lymphocytes of a healthy non-opioid-dependent control. Data points are mean ± range for each individual.

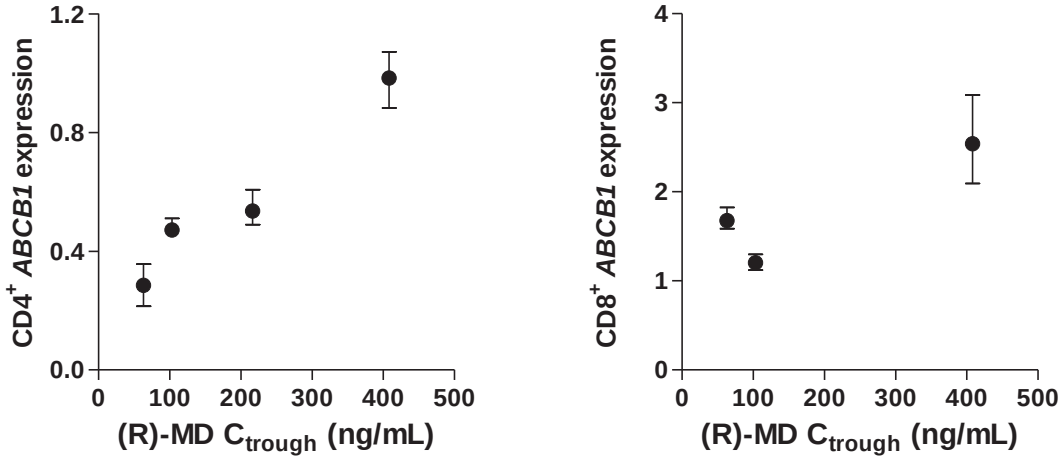

Figure 5-23. Relationship between (R)-methadone (MD) C_{trough} and relative *ABCB1* mRNA expression[a] in $CD4^+$ (r_s = 1.00, P = 0.08) and $CD8^+$ (r_s = 0.50, P = 1.0) lymphocytes of MMT subjects.

[a]*ABCB1* mRNA expression (normalised to *GAPDH*) relative to $CD4^+$ lymphocytes of a healthy non-opioid-dependent control. Data points are mean ± range for each individual.

5.3.3.4. P-glycoprotein protein expression

As mentioned above (section 5.3.2.2), no P-gp was detected in 5 x 10^5 $CD4^+$, $CD56^+$ or $CD8^+$ lymphocytes of MMT subjects when using the Western blot assay described in section 5.2.5. Using larger lymphocyte samples (1.6-3.0 x 10^6 cells), P-gp protein expression was detected in $CD4^+$ cells of subjects S2-S6, but not S1 (Figure 5-24). Normalised P-gp expression (P-gp/calnexin) values for subjects S2-S6 were 0.79, 0.82, 0.74, 0.83 and 0.87, respectively. When compared to Western blots of healthy volunteer samples performed during assay development (see Figure 5-13), there was noticeably more non-specific staining of MMT subject samples, making it difficult to distinguish separate 170 and 150 kDa P-gp bands. There was also large variability in total protein content between samples (Figure 5-24).

The relationship between *ABCB1* mRNA expression and P-gp protein expression in $CD4^+$ lymphocytes is shown in Figure 5-25. $CD4^+$ P-gp protein expression was lowest in the subject homozygous for the AGC**TT** haplotype (0.74), as compared to the homozygous AGC**T**C subject (0.82), and AGCGC / AG**TTT** subjects (0.79, 0.83 and 0.87).

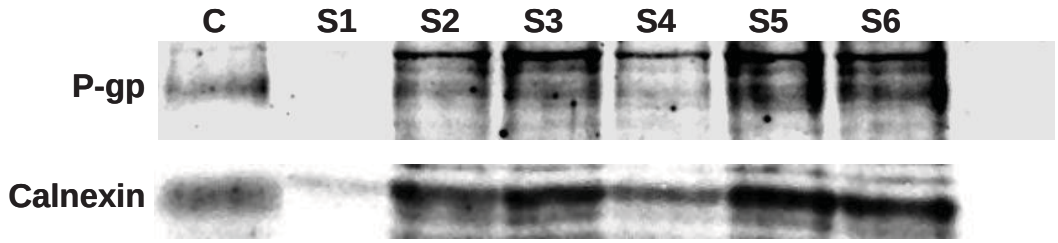

Figure 5-24. Western blot detection of P-gp (and calnexin loading control) in CD4$^+$ lymphocytes of MMT subjects.

P-gp: P-glycoprotein. **C:** Positive control (6 μg of healthy non-opioid-dependent control CD4$^+$ lymphocyte lysate spiked with 1 μg of LLC-PK1-*MDR1* lysate). **S1-6:** MMT subject samples.

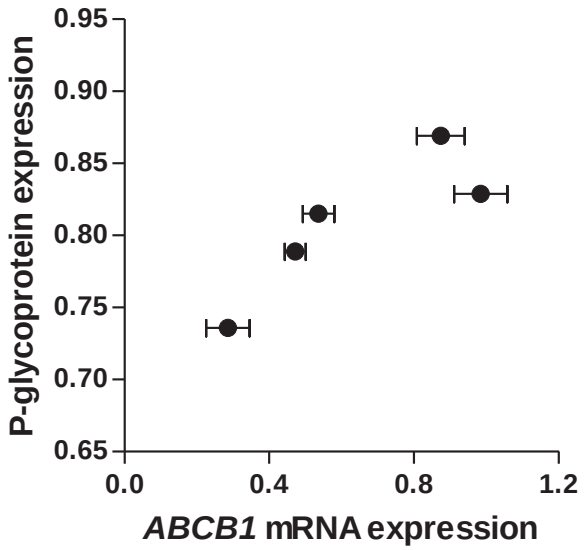

Figure 5-25. Relationship between *ABCB1* mRNA[a] and P-gp[b] expression in CD4$^+$ lymphocytes of MMT subjects (r_s = 0.90, P = 0.08).

[a]*ABCB1* mRNA expression (normalised to *GAPDH*) relative to CD4$^+$ lymphocytes of a healthy non-opioid-dependent control. [b]P-gp protein expression normalised to calnexin loading control. mRNA expression data are mean ± range for each subject. P-gp protein expression was a single measurement.

The relationships between P-gp protein expression in CD4$^+$ cells and both MMT dose requirements and (R)-methadone C_{trough} are shown in Figure 5-26.

Unfortunately, the remaining CD56$^+$ lymphocytes (originally for the functional assay) were lost during the initial cell washing step (see section 5.3.2.2) due to the use of 20X concentrated PBS mistakenly provided by another member of the laboratory (instead of 1X

PBS). The Western blot for $CD8^+$ lymphocytes failed, with no P-gp bands detected for positive control.

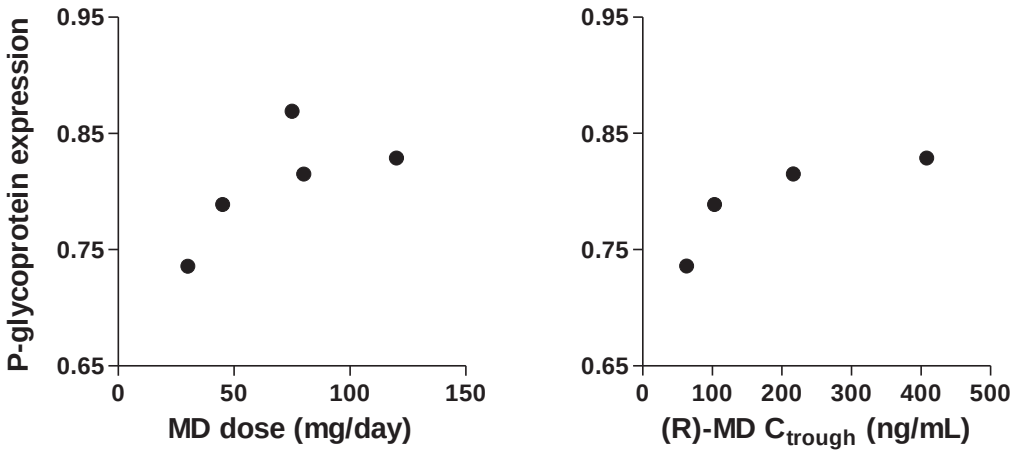

Figure 5-26. Relationship between $CD4^+$ lymphocyte P-gp expression[a] and MMT dose requirements (r_s = 0.70, P = 0.2) and (R)-methadone C_{trough} (r_s = 1.00, P = 0.08).

[a]Normalised to calnexin loading control.

5.3.4. Discussion

5.3.4.1. Protocol performance in opioid-dependent subjects

Based on findings during assay development (using healthy volunteer lymphocytes), target cell numbers for performing the qRT-PCR, Western blot and functional assays were set at 1 x 10^5, 5 x 10^5 and (at least) 0.75 x 10^6 cells, respectively. Using 12-16 mL of blood, these targets were achieved for $CD4^+$ and $CD8^+$ lymphocytes of all MMT subjects, whilst 5 out of 6 subjects had enough lower-abundance $CD56^+$ cells for all three assays. This was despite the relative recoveries of PBMCs from opioid-dependent subjects being around half that of the healthy volunteers tested during assay development (0.8-1.9 x 10^6 versus 1.6-3.1 x 10^6 cells per mL of blood). The purity of $CD4^+$ and $CD8^+$ fractions was confirmed by qualitative reverse transcription PCR. Whilst very slight CD8 PCR bands were detected in some $CD56^+$ samples, this likely reflects the small proportion of $CD56^+/CD8^+$ lymphocytes previously observed in this fraction (see section 5.2.3.2.2.1), rather than contamination with $CD8^+/CD56^-$ cells. For the $CD56^+$ sample from subject S2 that displayed CD4 amplification, closer

inspection of laboratory notes indicated there was miscalculation of CD56 microbead requirements when isolating this sample. As such, the contamination in this sample is likely a result of a poor isolation of $CD56^+$ cells due to an experimental error. Therefore, it can be concluded that (in the absence of experimental error) the magnetic isolation procedure was effective in isolating pure fractions of $CD4^+$, $CD56^+$ and $CD8^+$ lymphocytes from opioid-dependent subjects.

CD4 and CD56 PCR also confirmed that subject mRNA samples were free from genomic DNA contamination (after DNase treatment). Whilst this method of detecting genomic DNA was sufficient for this pilot study, including minus reverse transcriptase reactions (for each mRNA sample) during cDNA synthesis is a standard control for detecting background contamination, and would be recommended in future studies.

With regards to the qRT-PCR assay, large variability in mRNA yield was initially observed between subject samples (as evidenced by large variability in *GAPDH* C_T values). However, this variability was drastically reduced by retrospectively adjusting starting mRNA and/or cDNA volumes and re-performing the qRT-PCR analysis. In fact, this method was so effective in normalising cDNA input into the qRT-PCR reaction, that the between-subject CVs after volume adjustments were equivalent to (for $CD4^+$ and $CD8^+$ samples), or only slightly greater than (for $CD56^+$ samples), the CVs for within-subject triplicates. Therefore, from only a small fraction of cells, the optimised mRNA isolation and quantification protocols were able to accurately quantify *ABCB1* mRNA expression in $CD4^+$, $CD56^+$ and $CD8^+$ lymphocytes of opioid-dependent subjects.

Unfortunately, the number of lymphocytes originally designated for Western blot analysis proved to be insufficient for detecting P-gp protein expression in opioid-dependent subject samples. One possible explanation for this may have been a lower P-gp expression in MMT subjects when compared to the healthy volunteers used during assay development. Indeed, in

qRT-PCR experiments, $CD4^+$ *ABCB1* mRNA expression in opioid-dependent subjects was found to be, on average, 37% lower than in the $CD4^+$ control sample. However, even when the number of cells used for Western blot analysis was increased by up to 3-fold, detection of P-gp bands was still problematic and inconsistent. As such, future studies should consider alternative methods for quantifying P-gp protein expression. For example, the analysis of membrane fractions as opposed to whole cell lysates may aid in reducing the significant background staining observed in opioid-dependent subject samples. Alternatively, flow cytometric methods have now been developed which allow truly quantitative measurement of P-gp surface expression, as well as function (Chinn et al., 2007), and may provide a viable alternative to conducting separate Western blot and functional assays. In either case, the number of lymphocytes required for quantifying P-gp protein expression may need to be re-evaluated prior to conducting future studies.

5.3.4.2. Pilot study findings

Since this was a pilot study conducted in only 6 subjects, it is not possible to make any strong conclusions from the data. However, the observation of lowest $CD4^+$ lymphocyte *ABCB1* mRNA and P-gp protein expression in the AGC**TT**/AGC**TT** subject is congruent with the main findings of Chapter 3, where carriers of this variant haplotype had significantly lower methadone requirements than other subjects. As such, it can be hypothesised that the AGC**TT** haplotype causes decreased P-gp expression, resulting in greater CNS exposure to methadone (due to decreased BBB efflux), and hence lower dose and C_{trough} requirements. However, this interesting observation needs to be confirmed in a larger study, and it is still unclear whether the AGC**TT** haplotype also affects P-gp's methadone transport function.

The results of this pilot study also indicate that $CD4^+$ lymphocyte *ABCB1* and P-gp expression may be related to methadone dose and (R)-methadone C_{trough} in MMT subjects. Although the correlations were not statistically significant, both *ABCB1* mRNA and P-gp protein

expression displayed clear positive associations with both dose and C_{trough} requirements. Unfortunately, since all opioid-dependent subjects were already stabilised in methadone treatment, it is not possible to conclude whether differences in P-gp expression were the cause (representing efflux at the BBB), or the consequence (through P-gp induction by methadone), of variability in methadone requirements. Further investigations employing the original study design (see section 5.3.1) will be able to address this.

In line with previous studies (Klimecki et al., 1994), $CD56^+$ and $CD8^+$ lymphocytes had 2- to 7-fold higher *ABCB1* mRNA expression than $CD4^+$ lymphocytes. Whilst the associations of $CD56^+$ and $CD8^+$ mRNA expression with *ABCB1* genetic variability and methadone exposure were less clear than for $CD4^+$ cells, the low number of samples for this pilot study preclude any conclusion regarding potential lymphocyte subset differences in the *ABCB1* genetic variability-expression-methadone exposure relationship.

5.4. Conclusions

In conclusion, the *ex vivo* protocol developed here was an effective and relatively non-invasive method for studying *ABCB1* mRNA and P-gp protein expression, and potentially P-gp function, in healthy volunteers. However, the methods employed for determining P-gp protein expression, and also possibly function, need to be revised before conducting further studies in opioid-dependent subjects. Nonetheless, this pilot study provided the first evidence of an association between *ABCB1*/P-gp expression and methadone exposure in the opioid-dependent MMT population. These findings justify further investigation (employing the original study design) to establish whether differences in expression are the cause or consequence of methadone exposure, and to determine the degree to which *ABCB1* genetic variability plays a role in this relationship.

Chapter 6. In vitro P-glycoprotein transport of opioids

6.1. Introduction

When evaluating the potential impact of P-gp transport variability on opioid distribution, it is important not only to initially identify those opioids that are actually P-gp substrates, but also to subsequently determine the ability of P-gp to influence their membrane permeability. This is particularly important since, as discussed in Chapter 1 (section 1.5.2.1), P-gp's impact on transcellular permeability can vary significantly between substrates, depending on their intrinsic membrane permeability, and can also be influenced by the size and direction of any substrate concentration gradient. Therefore, to aid in the evaluation and interpretation of the potential impact of *ABCB1* pharmacogenetics on opioid therapies, their P-gp transport (and potentially inhibitory) characteristics must first be clearly established.

As discussed in Chapter 1, numerous opioids, including morphine, have been clearly identified *in vitro* and/or *in vivo* in animals as P-gp substrates. For methadone, whilst it has been found to display P-gp substrate characteristics in the rat everted intestinal sac (Bouer et al., 1999), this was not observed in a human Caco-2 cell model (Stormer et al., 2001). Although, the concentration of methadone (10 μM) tested by Stormer and colleagues (2001) was nearly 7-fold higher than the C_{max} typically observed in MMT patients (~3500 ng/mL versus ~500 ng/mL (even less unbound) (Foster et al., 2000; Mitchell et al., 2004)). As such, P-gp transport (or lack thereof) in this model may have reflected the potential for intestinal methadone transport, but not P-gp transport at the BBB where the concentration gradient is not so extreme. Alternatively, though rare, species-dependency in transport has been observed, with some compounds displaying P-gp activity in mouse, but not human, cell lines (Yamazaki et al., 2001). This phenomenon may also be important for β-endorphin, which has been identified as a P-gp substrate in rodent P-gp inhibition and gene knockout models, but, like methadone, has yet to be confirmed as a substrate of human P-gp. As such, one aim of

this study was to confirm the status of β-endorphin and methadone as substrates (and/or inhibitors) of human P-gp specifically, and at concentrations more relevant for BBB transport (for methadone).

In addition, prior to commencing this thesis, the active transport of buprenorphine and norbuprenorphine had yet to be investigated. Therefore, this study also aimed to examine whether these compounds are also substrates of human P-gp.

6.2. Transport assay development and validation

6.2.1. Introduction

Epithelial/endothelial cell monolayers are one of the most commonly used *in vitro* models for assessing P-gp transport. The cell lines employed in these models differentiate in culture to form confluent cell monolayers, complete with tight intercellular junctions similar to those observed in epithelial/endothelial barriers *in vivo*. Importantly, once differentiated, these monolayers are functionally polarised, expressing P-gp only on the apical surface of the membrane (Figure 6-1). As such, they provide a good *in vitro* model for P-gp transport of compounds across cell monolayer barriers, and allow the assessment of P-gp's ability to both efflux (that is, facilitate basal to apical elimination), as well as protect (that is, limit apical to basal permeability/absorption).

In the 'classical' technique employed for *in vitro* monolayer P-gp transport studies, test compounds are added to either the basal or apical compartment (donor) of the transport system (see Figure 6-1), and the concentrations of substrate appearing in the opposite (receiver) compartment is measured over time, usually a few hours. From these experiments, the substrate permeability in the basal-to-apical (B>A) and apical-to-basal (A>B) directions can be determined and compared. Since P-gp transport occurs in the B>A direction, P-gp substrates can be expected to have a high B>A:A>B permeability ratio. The experiments

should then be repeated in the presence of a P-gp inhibitor, which will reduce the B>A permeability and/or increase A>B permeability, lowering the B>A:A>B ratio, to confirm that transport is due to P-gp (see Figure 6-2). Alternatively, this basic protocol can be adapted to evaluate test compounds as P-gp inhibitors, simply by measuring the permeability of a known P-gp substrate in the presence and absence of the test inhibitor.

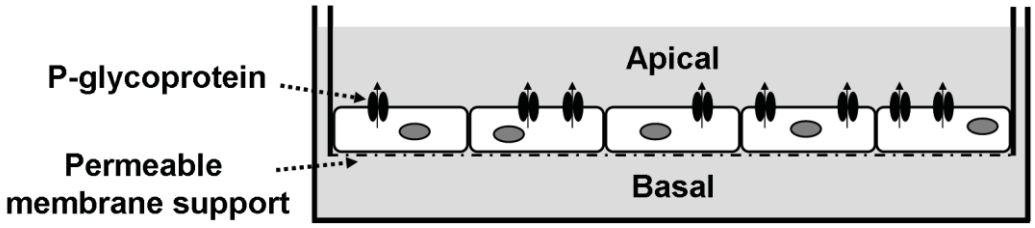

Figure 6-1. Example of P-gp apical expression in a confluent monolayer of polarised epithelial/endothelial cells.

For transport studies, cells are cultured on a permeable membrane support to allow passage of drug between the monolayer and the basal compartment. Note the tight extracellular junctions that act to limit paracellular transport.

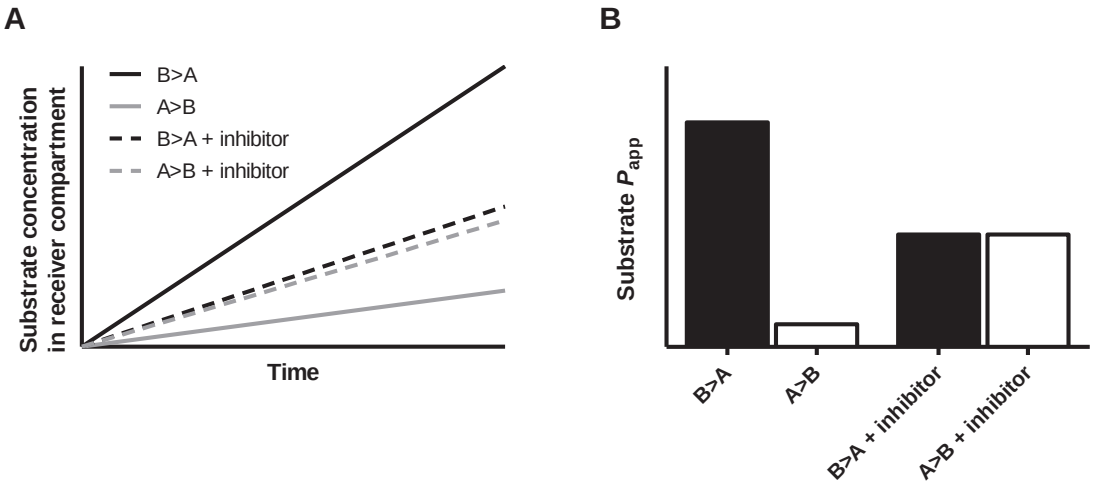

Figure 6-2. Example of typical results from a 'classical' cell monolayer transport study.

A: Relationship of substrate concentration in the receiver compartment (opposite of donor/loading compartment) versus time indicates substrate passage across the monolayer is faster in the B>A compared to A>B direction, presumably due to active B>A transport. In the presence of an inhibitor, active P-gp transport is abolished, resulting in approximately equal rates of B>A and A>B passage. **B:** These relationships are often also expressed in the form of substrate apparent permeability (P_{app}), which represents the rate of substrate flux adjusted for monolayer surface area and substrate concentration in the donor compartment (see section 6.2.2.7).

One drawback of this 'classical' technique is that at least eight separate cell monolayers are required to determine whether a test compound is a P-gp substrate and/or inhibitor. As such, alternative methods for the simultaneous determination of P-gp substrate and inhibitor characteristics have been developed. One such protocol developed by Balimane and Chong (2005) is outlined in Figure 6-3.

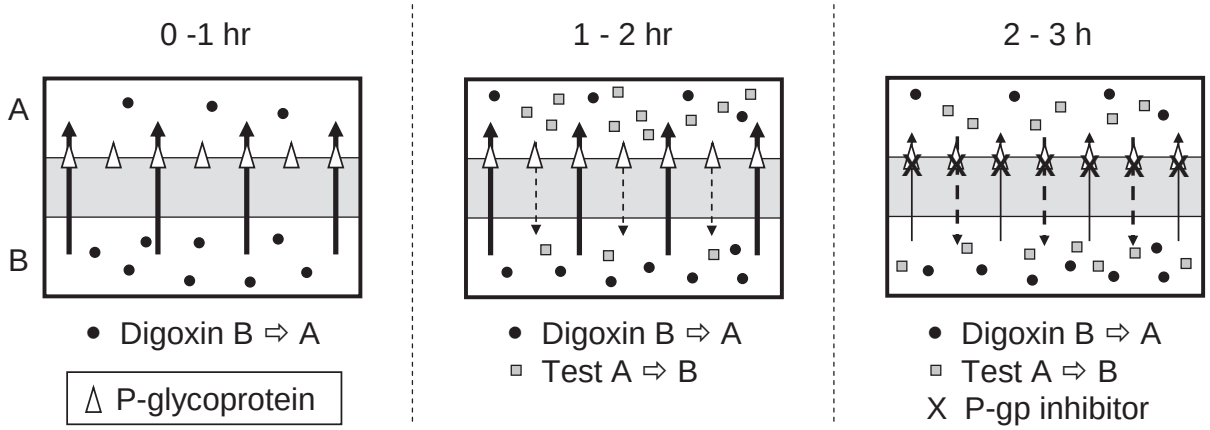

Figure 6-3. Outline of the combined P-gp substrate and inhibitor assay described by Balimane and Chong (2005).

The experiment is performed in a single monolayer continuously over 3 x 1-hour phases. 0-1 hour phase: B>A permeability of digoxin (known P-gp substrate). 1-2 hour phase: A>B transport of test compound, and inhibition of digoxin B>A by the test compound. 2-3 hour phase: inhibition of test compound A>B and digoxin B>A by known P-gp inhibitor.

If a reduction of digoxin B>A is observed between 0-1 and 1-2 hour phases, then the test compound is likely to be a P-gp inhibitor, and comparisons between digoxin B>A in 1-2 and 2-3 hour phases can give an indication of the inhibitory potency (relative to the known P-gp inhibitor used in the 2-3 hour phase). If the known P-gp inhibitor increases the A>B permeability of the test compound between the 1-2 and 2-3 hour phases, then the compound is a P-gp substrate. As such, a test compound can be evaluated as a P-gp substrate and inhibitor in just three hours, using only a single monolayer. Thus this method requires less time for replicate experiments, and provides a more efficient model for testing numerous compounds at different concentrations.

Both the 'classical' and the Balimane and Chong (2005) techniques were trialled during assay development.

With regard to the specific cell lines used, one of the best characterised *in vitro* models for studying P-gp transport is the human colon carcinoma cell line, Caco-2. In addition to expressing human P-gp, differentiated Caco-2 cells also express other human drug transporters common to epithelial barriers (unlike commonly used *ABCB1*-transfected animal cell models) (Audus et al., 1990; Hunter et al., 1993a; Hunter et al., 1993b; Walle et al., 1999a; Walle et al., 1999b). As such, they can be expected to provide a transport model more akin to the human *in vivo* context, where multiple transporters are often working in tandem (or potentially in opposition) to facilitate or limit drug permeability. Indeed, a good correlation ($r^2 = 0.96$) between *in vitro* Caco-2 permeability values and human *in vivo* AUC data has been demonstrated for various compounds (Fliszar et al., 2007). Caco-2 cells were therefore chosen as the cell line to use in this study.

6.2.2. Methods

6.2.2.1. Materials

Sodium bicarbonate, digoxin (unlabelled), verapamil, FITC-conjugated inulin, bovine serum albumin (BSA), and dimethylsulfoxide (DMSO) were purchased from Sigma-Aldrich (Castle Hill, Australia). Sterile solutions of L-glutamine, sodium pyruvate, non-essential amino acids, penicillin-G / streptomycin and trypsin-EDTA were purchased from the Central Services Unit of the School of Molecular and Biomedical Science, University of Adelaide (Adelaide, SA, Australia), as was heat-inactivated fetal bovine serum (FCS). Minimal essential medium with Earl's salts (MEM), Hank's buffered salt solution (HBSS) and HEPES buffer were purchased from Invitrogen (Mulgrave, Vic, Australia). Radiolabelled [H^3]-digoxin (23.4 Ci/μmol) was purchased from Perkin Elmer (Boston, MA, USA). "EcoLite" liquid scintillation fluid was purchased from ICN Biomedicals Australia (Seven Hills, NSW, Australia).

6.2.2.2. Cell culture

Caco-2 cells (passage #17) were obtained from the American Type Culture Collection (Rockville, MD, USA). Cells were cultured at 37°C (5% CO_2 atmosphere) in 75 cm^2 vented BD Falcon™ flasks (distributed by the Central Services Unit of the School of Molecular and Biomedical Science, University of Adelaide) containing MEM adjusted to 2 mM L-glutamine, 1 mM sodium pyruvate, 0.1 mM non-essential amino acids, 1.5 g/L sodium bicarbonate, 100 U/mL penicillin-G, 100 μg/mL streptomycin and 10% FCS (pH 7.5). Cells were subcultured up to passage #30 by growing to ~80% confluency then performing trypsin-EDTA treatment to detach and disperse the differentiated cells. Half of the cells in each flask were then transferred to 2-4 new flasks, and the remaining half at each passage cryopreserved in freezing medium (culturing medium + 5% DMSO, placed in a Nalgene 'Mr Frosty' isopropanol bath (In Vitro Technologies Pty Ltd, Noble Park, VIC, Australia) overnight at -70°C then transferred to liquid nitrogen).

For transport experiments, Caco-2 cells (passage #20-28) were seeded onto 12-well plates of Corning Transwell® filter membranes (distributed by Crown Scientific, Minto, NSW, Australia) at 60,000 cells/cm^2. Monolayers were cultured in complete medium for 21-28 days, changing media every 2-3 days. Prior to conducting transport experiments, monolayer integrities were checked by measuring transepithelial electrical resistance (TEER) with an EVOM epithelial voltohmmeter (World Precision Instruments, Sarasota FL, USA). Only monolayers with TEER values greater than 400 Ωcm^2, and good monolayer morphology (by microscopic inspection), were used for transport experiments.

6.2.2.3. Balimane and Chong (2005) method

For the Balimane and Chong technique to be valid, a consistent digoxin transport over the entire assay period must be established. As such, the following experiments were performed.

Prior to conducting all transport experiments using the Balimane and Chong technique, confluent monolayers were washed twice for 15 minutes with blank transport buffer (HBSS + 10 mM HEPES, pH 7.4), in both compartments, to remove components of the complete medium. Digoxin B>A transport was then assessed by adding 0.8 mL of transport buffer to the apical compartment, and adding 1.5 mL of transport buffer containing 0.033, 1 or 5 μM digoxin (33 nM [H^3]-digoxin supplemented with unlabelled digoxin when required) to the basal compartment. Monolayers were then incubated at 37°C. Every hour, up to 4 hours, 50 μL samples were taken from both the apical and basal compartments and frozen at -20°C for later quantification of [H^3]-digoxin (see section 6.2.2.5).

In addition to control experiments with digoxin alone, B>A transport of digoxin was assessed in the presence of 1, 5, 10, 25, 50, 100 or 500 μM of verapamil (P-gp inhibitor) added to the apical compartment at 0, 1, 2 or 3 hours.

For all experiments, 15 μL of 1 mg/mL FITC-inulin was added to the apical compartment at commencement of transport, and a 50 μL sample taken from the basal compartment every hour to measure any paracellular leakage (see sections 6.2.2.6 and 6.2.2.7). TEER measurements were also taken every hour as additional confirmation of monolayer integrity.

All samples taken were replaced by an equal volume of blank transport buffer.

6.2.2.4. 'Classical' method

6.2.2.4.1. Original protocol

Based on existing published methods (Fromm et al., 1999; Wandel et al., 1999; Balimane & Chong, 2005), the original protocol for the 'classical' transport assay was as follows.

Confluent monolayers were first washed twice for 15 minutes with blank transport buffer. Then, 1 μM of digoxin (33 nM [H^3]-digoxin supplemented with unlabelled digoxin) in

transport buffer was added to the basal compartment (1.5 mL) for B>A transport, or the apical compartment (0.8 mL) for A>B transport. Blank transport buffer was then added to the receiver compartments. For some experiments, 10 or 100 μM of verapamil was added to the apical compartment.

Fifteen microlitres of 1 mg/mL FITC-inulin was then added to the apical compartment for the determination of paracellular leakage, TEER measurements taken, and the monolayers incubated at 37°C.

Every hour (up to 4 hours), 100 μL samples were taken from both the apical and basal compartments (for measuring digoxin and FITC-inulin), and replaced with 100 μL of blank transport buffer. TEER was also measured every hour.

6.2.2.4.2. Optimised protocol

Based on the findings of trial experiments using the basic protocol (see section 6.2.3.3), an optimised protocol was adapted. The most significant protocol change was the inclusion of a monolayer pre-treatment with 1 μM of digoxin (in complete medium) for 48 hours prior to conducting transport experiments, with the aim of inducing P-gp expression. In addition, 5% BSA was added to the second 15 minute wash with transport buffer prior to initiating the transport experiment, with the aim of reducing non-specific binding of digoxin to transwell apparatus. Equal volumes (0.8 mL) were used in both the apical and basal compartments and, for inhibition experiments, 100 μM of verapamil was added to both the apical and basal compartments, with the aim of limiting, as much as possible, variability between compartments. Finally, monolayers were gently rocked during the incubation periods to ensure adequate mixing of compounds.

6.2.2.5. Quantification of radiolabelled [H^3]-digoxin

Fifty microlitres of sample, [H^3]-digoxin standard (6, 22, 50, 100, 222, 500, 778 or 1000 nM, at 0.8 Ci/μmol), or blank transport buffer was added to 3 mL of liquid scintillation fluid in a 6 mL scintillation vial (Kartell Labware, Silverwater, NSW, Australia), vortexed and left overnight at room temperature. Each sample was counted for 3 minutes in a liquid scintillation counter (model LS5801, Beckman Coulter Australia Pty Ltd, Gladesville, NSW, Australia). An example of a [H^3]-digoxin liquid scintillation standard curve is shown in Figure 6-4. Sample digoxin concentrations were interpolated from the standard curve using non-linear regression (3rd-order polynomial with $1/Y^2$ weighting). The presence of verapamil had no effect on liquid scintillation counting.

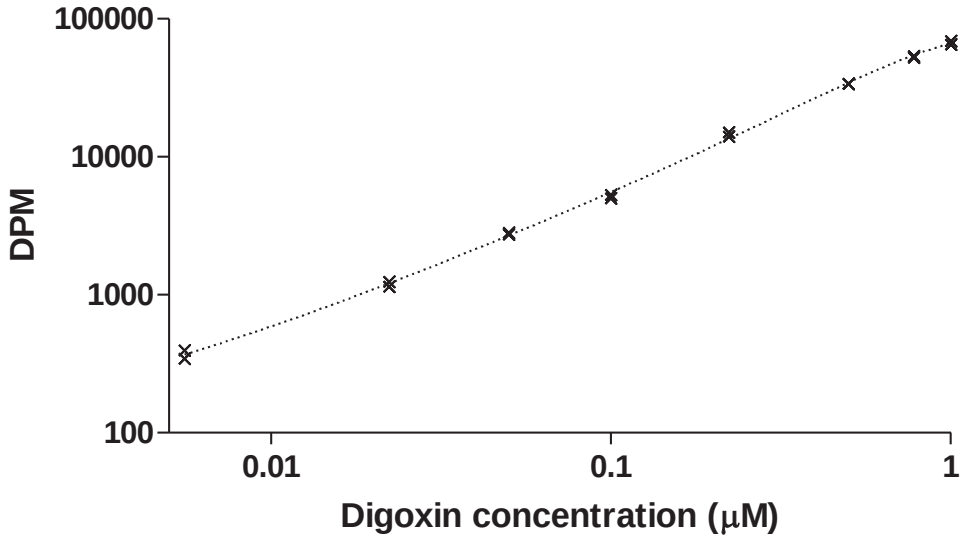

Figure 6-4. Example of a [H^3]-digoxin standard curve determined by liquid scintillation counting.

Digoxin standard concentrations (duplicates) were 6, 22, 50, 100, 222, 500, 778 and 1000 nM (at 0.8 Ci/μmol). Line is 3rd-order polynomial best fit with $1/Y^2$ weighting (r^2 = 0.998). DPM: disintegrations per minute.

6.2.2.6. Quantification of FITC-inulin

Fifty microlitres of each sample, FITC-inulin standard (25, 50, 100, 500, 1,000, 5,000 and 10,000 ng/mL) (duplicates), and blank transport buffer, was loaded onto a white 96-well

microplate (Nunc™, Rochester, NY, USA, distributed by In Vitro Technologies) and fluorescence measured on a microplate reader (BMG Lab Technologies, Offenburg, Germany) using 485 nm excitation and 525 nm emission filters. An example of a FITC-inulin standard curve is shown in Figure 6-5. Sample FITC-inulin concentrations were interpolated from the standard curve using linear regression.

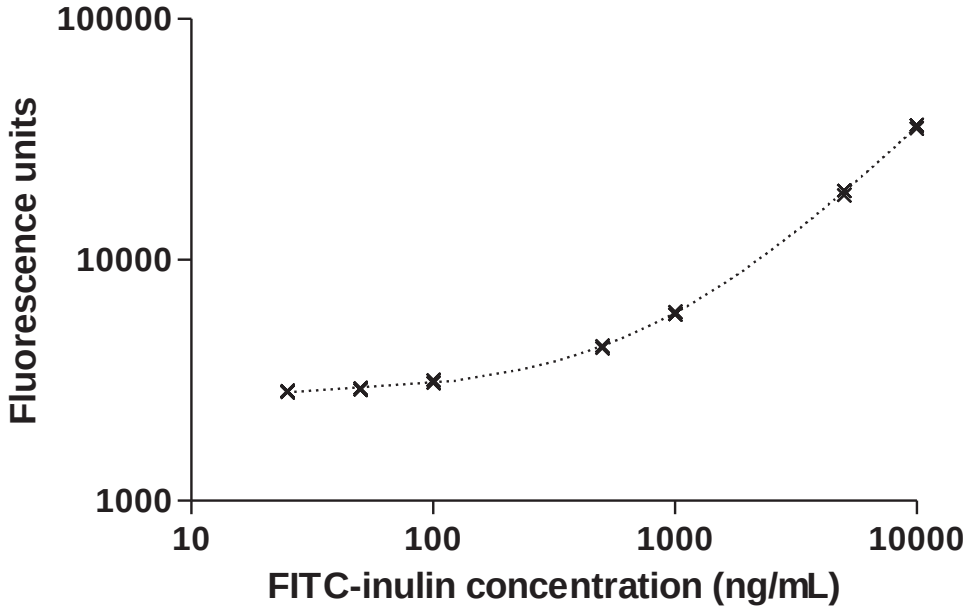

Figure 6-5. Example standard curve of FITC-inulin fluorescence.

Standard concentrations (duplicates) are 25, 50, 100, 500, 1,000, 5,000 and 10,000 ng/mL. Line is linear regression best-fit ($r^2 = 0.999$).

6.2.2.7. Data analysis

Apparent permeability (P_{app}) is commonly defined using the following equation;

$$P_{app\ (cm/s)} = \frac{dA}{dt \times S \times C_0}$$

where dA/dt is the flux of the compound across the membrane in nmol per second (s), S is the surface area of the membrane (cm^2), and C_0 is the initial concentration in the donor compartment (μM).

To allow for the determination of P_{app} over consecutive time periods, with multiple sampling from both compartments, the following equation was devised that takes into account the loss of test compound in each compartment due to prior sampling;

$$P_{app\ (cm/s)} = \frac{C_{r(t)} \times V_r - [(C_{r(t-1)} \times V_r) - (C_{r(t-1)} \times V_{sr(t-1)})]}{t \times S \times [(C_{d(t-1)} \times V_d) - (C_{d(t-1)} \times V_{sd(t-1)})]}$$

where $C_{r(t)}$ is the concentration (nM) in the receiver compartment at time t (end of transport period); V_r is the volume (L) of the receiver compartment; $C_{r(t-1)}$ is the concentration (nM) in the receiver compartment prior to transport period; $V_{sr(t-1)}$ is the volume (L) sampled from the receiver compartment prior to transport period; *t* is the time-length (s) of the transport period; S is the surface area (cm^2) of the membrane; $C_{d(t-1)}$ is the concentration (μM) in the donor compartment prior to the transport period; V_d is the volume (L) of the donor compartment; and $V_{sd(t-1)}$ is the volume (L) sampled from the donor compartment prior to the transport period.

For ease of reference, digoxin and opioid P_{app} values are presented as nm/s. Differences in P_{app} between directions (B>A versus A>B) were examined by Mann-Whitney U test, whilst differences between treatment groups were examined with either Mann-Whitney U test or Kruskal-Wallis test (with Dunns post-hoc test) where appropriate.

Inulin paracellular leakage was calculated using the same equation, and monolayers with inulin P_{app} greater than 5×10^{-6} cm/s (~2 %/hour) were excluded from analysis (Hidalgo et al., 1989).

6.2.3. Results

6.2.3.1. Cell culture

For validation experiments, a total of 228 monolayers were cultured (19 x 12-well plates). However, over half of the monolayers (123) were destroyed during the course of the 21-day

culture periods, due to cross-contamination (primarily with yeast) as a result of sharing cell culture facilities with other investigators.

6.2.3.2. Balimane and Chong (2005) method

Of the 105 viable monolayers, 35 were used for experiments to validate the Balimane and Chong method (3 separate experiments in total). Unfortunately, neither of these experiments were able to demonstrate a consistent digoxin B>A transport, with P_{app} values ranging from 4.1 x 10^{-11} to 5.0 x 10^{-3} nm/s between the three experiments, and 2- to 12-fold variability in digoxin B>A P_{app} values over assay period within experiments. Furthermore, no consistent inhibition by any verapamil concentration was observed, in fact, in one experiment, 25 μM, 100 μM and 500μM verapamil caused 13-, 19-, and 33-fold *increases* in digoxin B>A P_{app}, respectively. As such, this method was abandoned in favour of the 'classical' method.

6.2.3.3. Classical method

As shown in Figure 6-6, when results were combined for all experiments performed using the original protocol (5 monolayers in each direction, 4 x 1-hour transport periods per monolayer), the overall digoxin B>A P_{app} (nm/s) was around 1.5-fold greater than A>B P_{app} (mean ± SD: 70.5 ± 27.1 versus 46.2 ± 32.3. P = 0.03). In addition, overall, co-treatment with both 10 μM (n = 2 monolayers in each direction, 4 x 1-hour periods each) and 100 μM (n = 4 monolayers in each direction, 4 x 1-hour periods each) verapamil appeared to decrease the B>A, and/or increase the A>B permeability of digoxin relative to digoxin alone ($P < 0.05$ for B>A versus B>A + 10 μM verapamil).

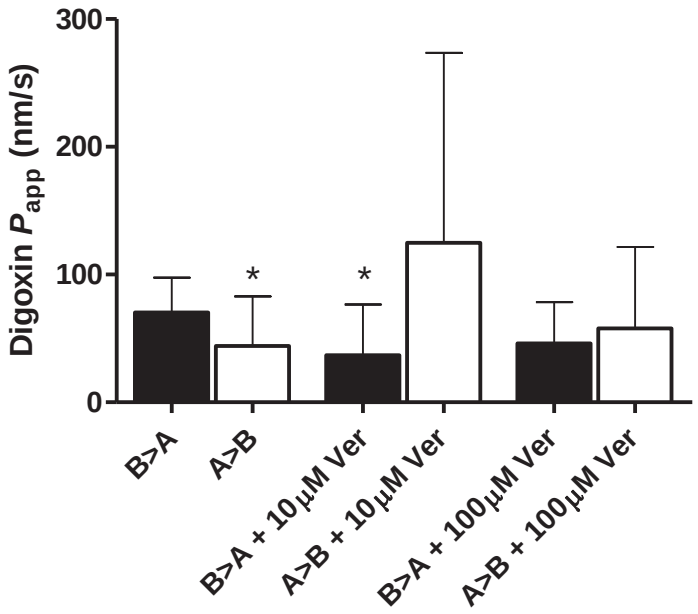

Figure 6-6. Average basal-to-apical (B>A) and apical-to-basal (A>B) digoxin permeability (P_{app}) alone (n = 5 monolayers (20 hours total) for each direction) and in the presence of 10 μM (n = 2 monolayers (8 hours total) for each direction) or 100 μM (n = 4 monolayers (16 hours total) for each direction) verapamil (Ver) using the basic protocol described in section 6.2.2.4.1.

Bars are mean + SD. *P < 0.05 versus B>A.

However, significant variability within treatment groups was observed both between experiments and, as shown in Figure 6-7, over the 4-hour time-course of experiments. Furthermore, taking into account final digoxin concentrations in both compartments, as well as the amount of digoxin removed in sampling, on average only around 30% of the total digoxin added at the beginning of the experiment could be accounted for. As such, adjustments to the basic protocol were made to produce more consistent results (see section 6.2.2.4.2).

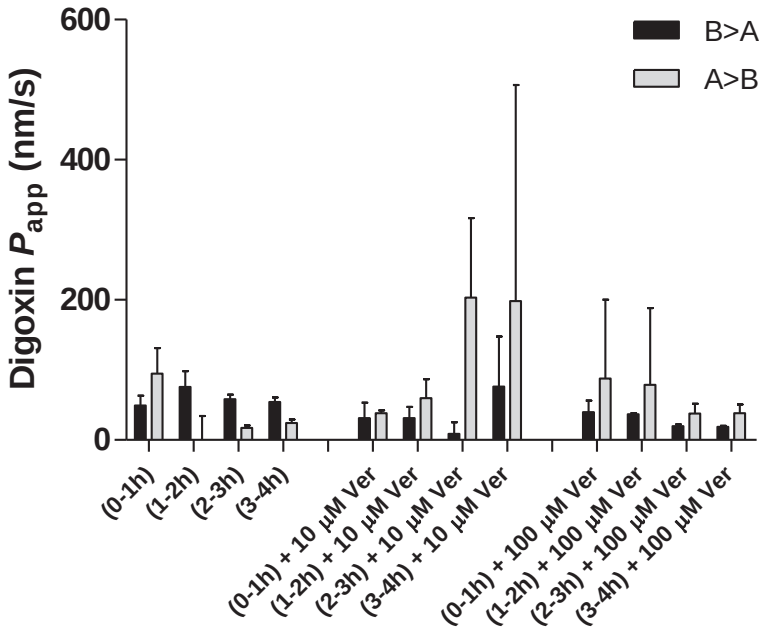

Figure 6-7. Example of significant variability in digoxin B>A and A>B permeability (P_{app}) within treatment groups (digoxin alone, n = 3 monolayers each; digoxin + 10 µM verapamil (Ver), n = 2 monolayers each; and digoxin + 100 µM verapamil, n = 3 monolayers each) over the course of a 4 hour experiment using the basic protocol (described in section 6.2.2.4.1.).

Bars are mean + SD for each 1-hour efflux period.

As shown in Figure 6-8, when results were combined for all experiments performed using the optimised protocol (10 monolayers in each direction, 3-4 x 1-hour transport periods per monolayer), the overall digoxin B>A P_{app} (nm/s) was around 4-fold greater than A>B (mean ± SD: 89.7 ± 22.4 versus 22.7 ± 7.2. $P < 0.0001$). In addition, overall, co-treatment with 100 µM of verapamil (n = 7 monolayers in each direction, 4 x 1-hour periods each) significantly decreased the B>A, and increased the A>B permeability of digoxin relative to digoxin alone ($P < 0.0001$ for both, Figure 6-8), reducing the B>A:A>B ratio to 1.1. Furthermore, as shown in Figure 6-9, digoxin P_{app} was relatively consistent over the entire experimental period.

Using the optimised protocol, around 70% of the digoxin originally loaded to the donor compartment could be accounted for (when considering final digoxin concentrations in both compartments, as well as the amount of digoxin removed in sampling).

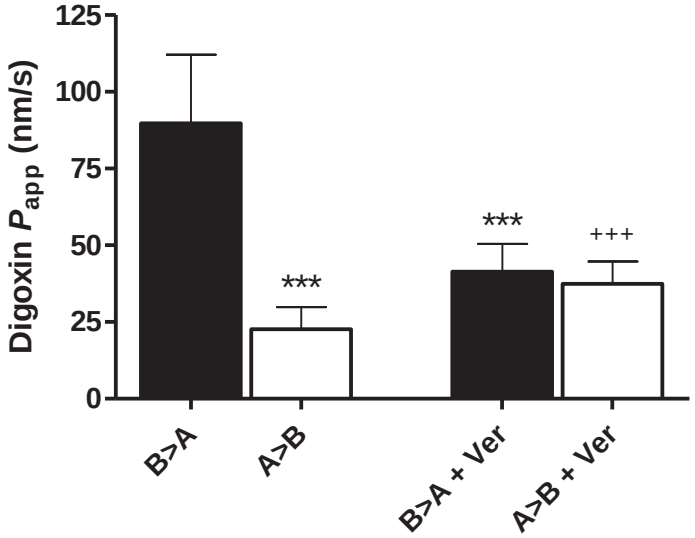

Figure 6-8. Average basal-to-apical (B>A) and apical-to-basal (A>B) digoxin permeability (P_{app}) alone (n = 10 monolayers (38 hours total) for each direction) and in the presence of 100 µM verapamil (Ver) (n = 7 monolayers (28 hours total) for each direction) using the optimised protocol described in section 6.2.2.4.2.

Bars are mean + SD. ***P < 0.0001 versus B>A. $^{+++}$P < 0.0001 versus A>B.

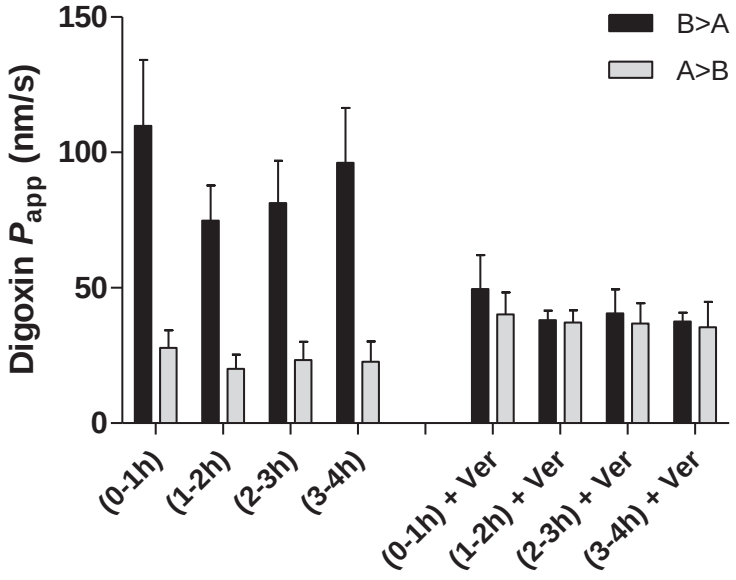

Figure 6-9. Digoxin basal-to-apical (B>A) and apical-to-basal (A>B) permeability (P_{app}) alone (n = 10 monolayers each) and in the presence of 100 µM verapamil (Ver) (n = 7 monolayers each) over the course of a 4-hour experiment when using the optimised protocol described in section 6.2.2.4.2.

Bars are mean + SD for each 1-hour efflux period.

6.2.4. Discussion

Whilst an attempt was made to replicate the combined P-gp substrate and inhibitor assay of Balimane and Chong (2005), the inability to produce a stable P-gp efflux over the 4-hour experimental procedure meant that this method was abandoned in favour of the simpler 'classical' approach to Caco-2 monolayer transport. However, even when employing a basic protocol, various problems were still encountered. For example, whilst the original 'classical' protocol was able to generate a greater B>A than A>B P_{app} for digoxin, the difference was only around 1.5-fold on average, there was a poor recovery of digoxin from the system (~30%), and significant variability was observed both between and within experiments, particularly among verapamil treated samples. As such, based on these observations, changes were made to the original protocol to enhance the polarity in digoxin transport (i.e. increase the digoxin B>A:A>B P_{app} ratio), and to produce more consistent results.

It was hypothesised that the relatively low digoxin B>A:A>B P_{app} ratio using the original protocol (1.5:1 compared to 6-11:1 in previous studies (Fromm et al., 1999; Wandel et al., 1999; Balimane & Chong, 2005)) may have been a result of low P-gp expression in the Caco-2 cells employed for this study. Indeed, significant variability in P-gp expression between Caco-2 batches and passages has previously been reported (Walter & Kissel, 1995). As such, a 48-hour monolayer pre-treatment with unlabelled digoxin was employed to induce P-gp expression in the monolayers (Takara et al., 2002), and was successful in increasing the digoxin B>A:A>B P_{app} ratio to around 4:1.

The inclusion of BSA in pre-washes appeared to decrease the non-specific binding of digoxin, as indicated by an increase in the total mass recovery (not taking into account intracellular digoxin accumulation) from 30 to 70% (presumably due to the blocking of non-specific binding sites on the transwell insert surface). This in combination with the use of equal basal and apical compartment volumes, the addition of verapamil to both compartments when

required, and the mixing of monolayers during efflux, was found to be effective in significantly reducing variability in digoxin P_{app} both between and within experiments and treatment groups.

Importantly, using the optimised protocol, treatment with 100 μM verapamil effectively (and consistently) abolished the 4-fold difference between B>A and A>B P_{app} for digoxin, resulting in a B>A:A>B P_{app} ratio of approximately 1:1. As such, this optimised protocol was deemed suitable for the subsequent evaluation of opioid P-gp efflux of opioids, as well as determining the effects of opioids on digoxin transport.

6.3. *In vitro* transport of opioids

Having developed a reliable assay for measuring P-gp transport across Caco-2 cell monolayers with the prototypic P-gp substrate digoxin, the aim was to test (R)- and (S)-methadone, buprenorphine, norbuprenorphine and β-endorphin as both substrates of P-gp, and inhibitors of P-gp-mediated digoxin transport.

6.3.1. Methods

Seven 12-well transwell plates were seeded, each on a different day, using the standard procedure. The plan was to use 5 plates for determining P-gp transport of test opioids in duplicate, with one positive control digoxin panel and two test compound panels per plate (each panel consisting of 4 monolayers: B>A, A>B, B>A + verapamil, A>B + verapamil). The remaining 2 plates were to be used to characterise opioid inhibition of digoxin transport.

Employing the optimised protocol, the first 12 monolayers were used to determine the B>A and A>B P_{app} of 1 μM digoxin (positive control), 200 ng/mL buprenorphine and 500 ng/mL (R)-methadone, in the absence and presence of 100 μM verapamil. The next 4 plates were destroyed as a result of the incubator door being left open by another user, whilst a further plate was lost to bacterial cross-contamination. The final plate was used to determine the B>A

and A>B P_{app} of 1 μM digoxin (positive control), 500 ng/mL buprenorphine and 500 ng/mL norbuprenorphine, in the absence and presence of 100 μM verapamil. However, analysis of inulin paracellular passage in this plate revealed a P_{app} greater than 1 x 10^{-5} cm/s for all monolayers over the course of the experiment. As such, the samples from this plate were not analysed.

No experiments could be performed for β-endorphin due to limited monolayer availability.

Digoxin and FITC-inulin were quantified and their P_{app} determined as described in sections 6.2.2.5 and 6.2.2.6. Monolayers with TEER less than 400 Ωcm^2, or inulin P_{app} greater than 5 x 10^{-6} cm/s (~2 %/hour), were excluded from analysis.

6.3.1.1. (R)-methadone quantification

Fifty microlitre samples were quantified for (R)-methadone using an established stereoselective high performance liquid chromatography (HPLC) - atmospheric pressure chemical ionization mass-spectrometry assay (described in (Foster et al., 2006)).

6.3.1.2. Buprenorphine quantification

Buprenorphine concentrations were determined using a HPLC method originally developed by Andrew Menelaou of the Department of Clinical and Experimental Pharmacology, University of Adelaide.

In preparation for HPLC quantification, 50 μL of sample and 50 μL of 1 μM imipramine internal standard were transferred to a 10 mL tube containing 400 μL of saturated sodium bicarbonate solution. Four millilitres of 70:30 hexane:ether was then added to the tubes and mixed for 20 minutes on a rotary mixer. After centrifuging for 10 minutes at 1800 x g, the organic layer was transferred to a new 10 mL tube containing 100 μL of 5 mM hydrochloric acid, and mixed for 20 minutes. After centrifuging again for 10 minutes at 1800 x g, the upper

organic layer was aspirated, leaving a 100 µL acid bubble, of which 50 µL was subsequently injected onto the HPLC system.

The HPLC system comprised a SIL-10A autoinjector, LC-10AS pump, SPD-10A VP UV-Vis detector (210 nm) and a SCL-10A VP system controller (Shimadzu, Kyoto, Japan). The stationary phase was a LUNA C5 (150 x 4.6 mm) column (Phenomenex, Lane Cove, NSW, Australia) with an Alumina C18 (10 x 5 mm) pre-column (Alltech, Baulkham Hills, NSW, Australia). The original mobile phase consisted of 48% acetonitrile with 20 mM potassium hydrogen phosphate adjusted to pH 6.6. However, at pH 6.6, injection of verapamil revealed a broad peak at the same retention time as buprenorphine (10 minutes), which was not completely removed in the extraction process. As such, the mobile phase pH was increased in increments of 0.2 until, at pH 7.4, the buprenorphine (~24 minutes), verapamil (7-7.5 minutes) and imipramine (13-14 minutes) peaks could be clearly distinguished from one another (Figure 6-10).

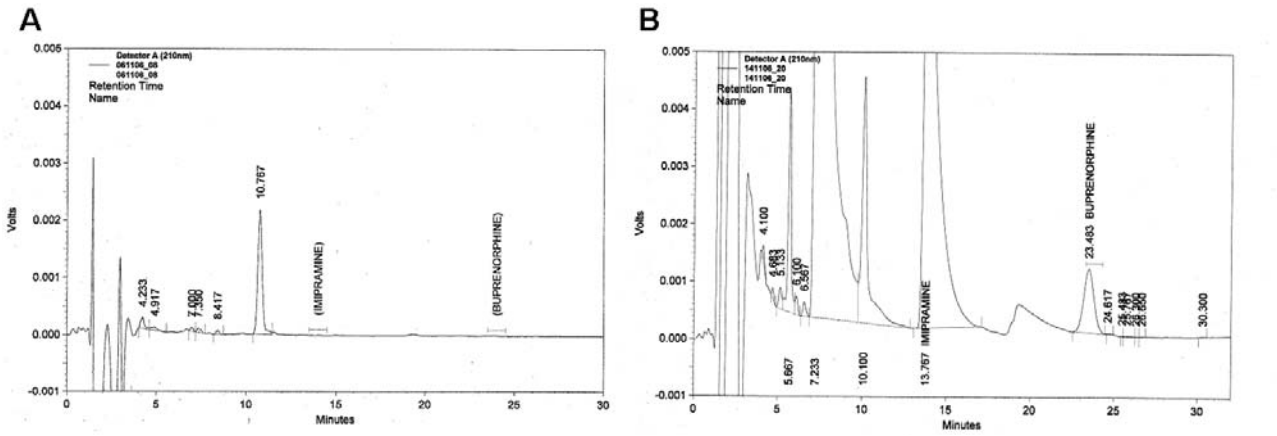

Figure 6-10. Example of HPLC chromatograms for detection of buprenorphine.

A: Transport buffer blank extraction chromatogram. **B:** Transport assay sample (with verapamil) extraction chromatogram showing peaks for verapamil (7.2 minutes), imipramine (13.8 minutes), and buprenorphine (~92 ng/mL) (23.4 minutes).

A buprenorphine standard curve (Figure 6-11) was generated using final standard concentrations of 20, 40, 100, 200, 400, 1000 and 2000 ng/mL (i.e. 50 μL extractions of 40, 80, 200, 400, 2000 and 4000 ng/mL buprenorphine in transport buffer). Sample buprenorphine concentrations were interpolated from the standard curve of buprenorphine peak area ratios (buprenorphine peak area / imipramine internal standard peak area) using linear regression ($1/Y^2$ weighting).

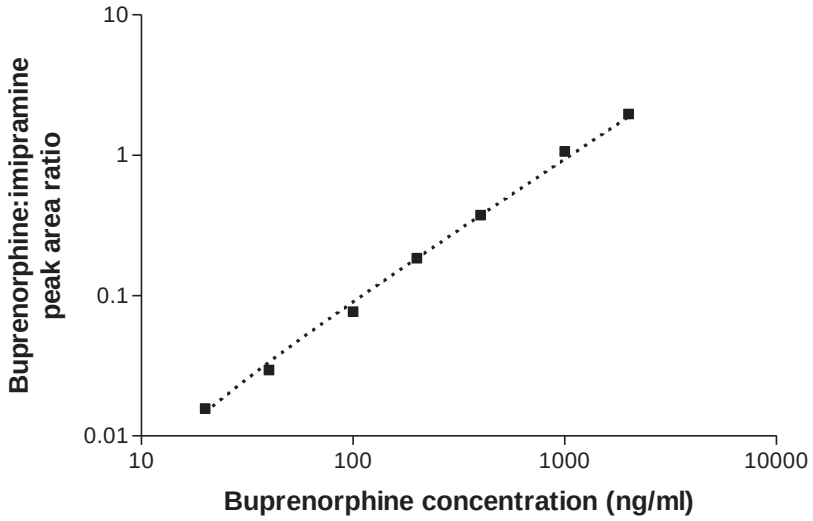

Figure 6-11. Example standard curve of buprenorphine by HPLC detection.
Final standard concentrations are 20, 40, 100, 200, 400, 1,000 and 2,000 ng/mL. Line is linear regression best-fit ($1/Y^2$ weighting) ($r^2 = 0.993$).

Unfortunately, buprenorphine concentrations in the receiver compartments were all just below the limit of quantification using this HPLC assay. As such, for each buprenorphine transport monolayer, P_{app} was determined using the decrease in buprenorphine in the donor compartment (instead of the increase in the receiver compartment), and the average P_{app} over the entire assay duration calculated (due to significant variability between transport periods).

6.3.2. Results

The digoxin positive control monolayers demonstrated a 6-fold greater B>A P_{app} than A>B, which was abolished with verapamil treatment.

As shown in Figure 6-12, methadone permeability was high (> 130 nm/s) in both directions, with no apparent B>A polarity of transport (average B>A:A>B ratio = 0.81). With verapamil treatment however, there was a slight decrease in B>A, and slight increase in A>B, which was most apparent during the final hour of the transport experiment (Figure 6-12B), resulting in an average B>A:A>B ratio of 0.60. As such, the methadone B>A:A>B ratio was nearly 1.4-fold higher in the absence of verapamil.

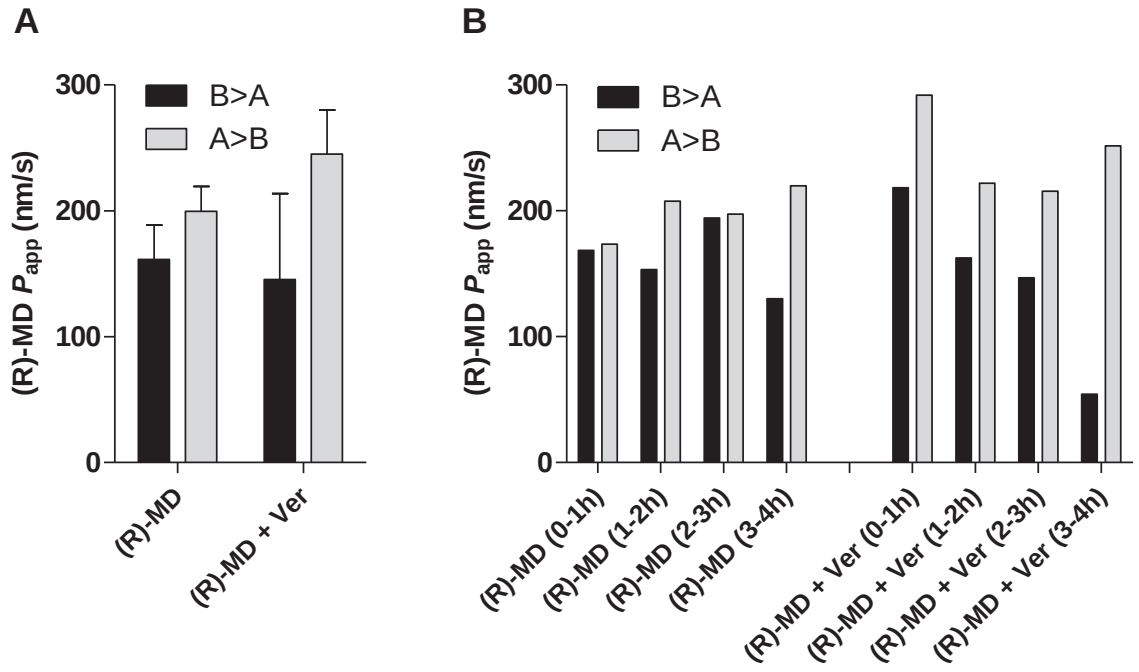

Figure 6-12. (R)-methadone ((R)-MD, 500 ng/mL) apparent permeability (P_{app}) across Caco-2 cell monolayers in the absence and presence of 100 µM verapamil (Ver).

A: Average (+ SD) P_{app} for the entire 4-hour transport experiment. **B:** Time-dependent changes in (R)-methadone P_{app} over the 4 x 1-hour transport periods.

In the absence of verapamil, buprenorphine displayed very high and variable membrane permeability in both the B>A (266-423 nm/s) and A>B (357-915 nm/s) directions (Figure 6-13) (average B>A:A>B ratio = 0.54). Verapamil treatment more than halved the average buprenorphine B>A P_{app} (down to 127 nm/s), but had little effect on A>B permeability (442-677 nm/s with verapamil), resulting in an average B>A:A>B ratio of 0.23. As such, the buprenorphine B>A:A>B ratio was nearly 2.4-fold higher in the absence of verapamil.

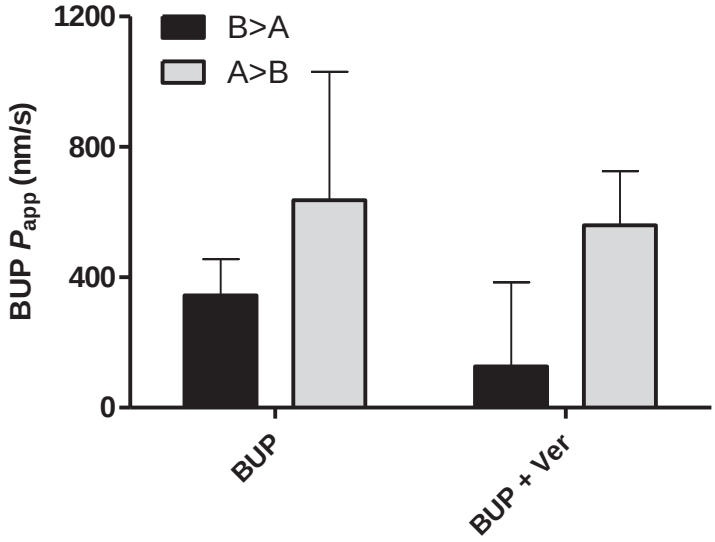

Figure 6-13. Mean (+SD) buprenorphine (BUP, 200 ng/mL) apparent permeability (P_{app}) across Caco-2 cell monolayers in the absence and presence of 100 µM verapamil (Ver) over 4 hours.

6.3.3. Discussion

As with the previous study by Stormer and colleagues (2001) using racemic methadone, no polarity in (R)-methadone permeability was observed, this was despite a significant decrease in the concentration used in this study (3500 ng/mL racemic versus 500 ng/mL (R)-methadone). Interestingly however, verapamil was found to decrease (R)-methadone B>A, and increase A>B permeability, revealing that the methadone B>A:A>B ratio was around 1.4-fold higher in the presence of P-gp transport. This indicates that in this assay, P-gp may still be influencing (R)-methadone permeability across the Caco-2 cell monolayers, but is being counteracted by the actions of an A>B transporter, which is revealed upon P-gp inhibition. As discussed previously, Caco-2 cells are known to express numerous human transporters, and the presence of a human A>B methadone transporter in this model could explain the observed species differences in methadone polarised transport. However, no strong conclusion can be made without replication of this experiment and identification of the other transporter involved. Nonetheless, the findings of this study (in light of the subsequent studies by others

confirming methadone as a human P-gp substrate, see below), indicate that P-gp substrates do not necessarily always display polarized transport across monolayers. This may have important implications when applying cell monolayer models, without appropriate inhibitor controls, for the screening of compounds as P-gp substrates.

Similarly to methadone, buprenorphine did not display the polarised B>A transport across Caco-2 monolayers expected of P-gp substrates, but its B>A P_{app} did appear to be greatly reduced in the presence of verapamil, again suggesting some P-gp transport activity. Indeed, the buprenorphine B>A:A>B ratio was, on average, 2.4-fold higher in the presence of P-gp transport. However, the observed buprenorphine P_{app} in both directions was highly variable over the experimental period, making interpretation difficult. In addition, the P_{app} for buprenorphine was also very high (266-915 nm/s), when compared to methadone (130-220 nm/s) and digoxin (~90 nm/s), but very similar to the B>A and A>B P_{app} values recently reported by Hassan and colleagues (2009) also in Caco-2 cells (562 and 447 nm/s, respectively). This suggests that burpenorphine's membrane permeability may not be limited to a great extent by P-gp activity, probably due to its high lipophilicity (n-octanol/pH 7.4 buffer partition coefficient (logD) = 3.93 (Avdeef et al., 1996; Jensen et al., 2007)).

Whether this high bi-directional permeability of buprenorphine is concentration-dependent (potentially leaving a role for P-gp at lower, clinically relevant, concentrations), or perhaps also facilitated by the activity of other transporters, requires further investigation.

Unfortunately, due to time constraints compounded by continuing difficulties in maintaining healthy and viable cell culture (due to shared facilities), further transport experiments (i.e. replication and other planned experiments outlined in section 6.3.1) were abandoned in favour of the clinical studies described in the previous chapters. However, numerous studies examining human P-gp transport of opioids have subsequently been conducted by other researchers.

With regards to methadone, Hassan and colleagues (2009) recently demonstrated a 2.5-fold greater B>A permeability for racemic methadone in Caco-2 cells, which was reduced to 1.45-fold in the presence of verapamil. However, the effect of P-gp on methadone transport appeared minor when compared to the 83-fold B>A polarity in paclitaxel transport observed in the same study. Another study in human-*ABCB1*-transfected HEK293 (human kidney) cells also reported a modest 1.9-fold higher B>A permeability for racemic methadone, which was not observed in breast cancer resistance protein *ABCG2*-transfected cells (Tournier et al., 2009). These 1.7- and 1.9-fold increases in methadone B>A:A>B ratio in the presence of P-gp activity are similar to the 1.4-fold increase observed in this study. As such, there is mounting evidence that methadone is a substrate for human P-gp. However, P-gp's effects on methadone membrane permeability appear modest when compared to its influence on other well-known P-gp substrates such as digoxin and paclitaxel. To my knowledge, with the exception of ABCG2 (see above), the influence of other drug transporters on methadone membrane permeability has yet to be investigated.

Apart from a single study reporting a 50% increase in buprenorphine brain distribution due to P-gp inhibition in rats (Suzuki et al., 2007), all other research employing a variety of models, including ATPase activation (Hassan et al. 2009), *in vitro* human cell monolayers (Hassan et al., 2009; Tournier et al., 2009), *ex vivo* perfusion of mouse (Coles et al., 2009) and human (Nekhayeva et al., 2006) placenta, and P-gp knockout in mice (Hassan et al. 2009), has indicated that buprenorphine is not a P-gp substrate. Alternatively, norbuprenorphine, which is more than 500-fold less lipophilic than buprenorphine (Jensen et al., 2007), has demonstrated an 11-fold B>A efflux ratio across human *ABCB1*-transfected HEK293 cell monolayers, which was significantly greater than the 1.9-fold difference for methadone measured in the same study (Tournier et al. 2009). Furthermore, in studies of cerebral kinetics in sheep, norbuprenorphine demonstrated slow entry across the BBB and, unlike buprenorphine, did not display significant retention within the brain compartment, indicating

a greater *in vivo* potential for P-gp modulation than its parent (Jensen et al., 2007). As such, as discussed in Chapter 3, any influence of P-gp variability on buprenorphine response seems likely to be an indirect consequence of changes in the pharmacokinetics of norbuprenorphine.

6.4. Conclusion

In conclusion, a Caco-2 cell monolayer assay for the investigation of P-gp substrates and inhibitors was successfully developed. Difficulties in establishing and validating this method, as well as the failed attempt to replicate the combined assay described by Balimane and Chong (2006), reflect the significant inter-laboratory variability commonly observed when employing cell monolayer models (Walter & Kissel, 1995), and highlight the importance of optimising and validating monolayer models with known P-gp substrates before proceeding with the assessment of test compounds.

Results from the methadone transport experiment, in combination with those of more recent studies, provide further *in vitro* support for methadone as a substrate of human P-gp. Whilst the influence of P-gp on methadone's transcellular permeability seems relatively small when compared to other known P-gp substrates, these *in vitro* findings lend support to the idea that P-gp is most likely to affect methadone distribution at the BBB, where conditions are most favourable for limiting drug passage (see Chapter 1, section 1.5.2).

Few conclusions could be drawn from this study regarding P-gp transport of buprenorphine, due largely to the high and significantly variable P_{app} observed. However, the vast majority of evidence generated by other groups since completing this study indicates that buprenorphine is not a physiologically relevant P-gp substrate. Despite this, there is still evidence to suggest that P-gp activity may influence buprenorphine response by altering the distribution and/or elimination of its active metabolite, norbuprenorphine.

Further studies are still required to determine whether β-endorphin is a human P-gp substrate.

Chapter 7. Discussion

The P-gp efflux transporter has been identified as potentially influencing the intestinal absorption and CNS distribution of various opioids. As such, it was hypothesised that genetic variability in the *ABCB1* gene (encoding P-gp) could play a major role in the interindividual variability in opioid response. Therefore, the major aims of this thesis were to investigate the impact of *ABCB1* genetic variability on maintenance treatment opioid requirements, maintenance treatment response, and the risk of illicit opioid dependence, as well as develop new methods for investigating dynamic interactions between *ABCB1* genetic variability, P-gp expression/function and maintenance opioid exposure.

7.1. New methods

In order to fulfil the aims of this thesis, several new and adapted methods first had to be established and validated.

Firstly, for the retrospective clinical studies of Chapters 3 and 4, a new robust and reproducible PCR-RFLP method was successfully developed and validated for the identification of the C1236T SNP of *ABCB1*.

Secondly, as no methods for estimating haplotype phase had previously been used in our laboratory, new protocols for predicting haplotypes from *ABCB1* SNP data were required. Therefore, an existing, freely available, statistical program (PHASE) was extensively validated by me (both within the software, and by confirmation of expected linkage disequilibrium), both in a smaller validation set of subject samples and in the final subject populations, as an accurate and robust tool for the estimation of *ABCB1* haplotypes from complete genotype data. With the exception of a small number of subjects with missing genotype data or rare haplotype combinations (who were subsequently excluded from haplotype analyses), the PHASE estimated haplotypes could be said, with a high level of

confidence, to represent the true haplotype configurations of subjects. The establishment of this protocol for accurately determining the phase of *ABCB1* genotype combinations enabled a more informative haplotype approach to investigating *ABCB1* pharmacogenetics (as opposed to individual genotype analysis).

Thirdly, a new magnetic isolation procedure was successfully developed for the isolation of pure fractions of $CD4^+$, $CD56^+$ and $CD8^+$ lymphocytes from human whole PBMCs. Protocols for the quantitative real-time PCR (qRT-PCR) analysis of *ABCB1* mRNA expression, and the Western blot analysis of P-gp protein expression, in healthy subject lymphocytes were also successfully developed. The magnetic separation and qRT-PCR protocols were successfully applied for analysis of MMT subject samples as part of the *ex vivo* pilot study (Chapter 5). However, Western blot detection of P-gp proved significantly more difficult in the opioid-dependent subject samples. Nonetheless, subject to further development of P-gp protein expression and functional assays (see recommendations in Chapter 5, section 5.2.3.3), the new *ex vivo* lymphocyte procedure described in this thesis provides a good model for the relatively non-invasive investigation *ABCB1* mRNA and P-gp protein expression and P-gp function in human subjects.

7.2. *ABCB1* genetic variability as a determinant of substitution opioid requirements

The primary goal of this thesis was to investigate the relationship between *ABCB1* genetic variability and maintenance treatment opioid requirements. More specifically, the main focus was to evaluate *ABCB1* genetic variability as a potential clinical optimisation tool for predicting daily dose requirements, or potentially individualised target plasma concentrations that could be incorporated as part of therapeutic drug monitoring. To this end, the retrospective study presented in Chapter 3 identified significant associations between *ABCB1* haplotypes and both methadone and buprenorphine maintenance dose requirements.

For standard dose MMT subjects (15-180 mg/day), the most significant findings related to the AGC**TT** variant haplotype of *ABCB1*. Carriers of this haplotype had lower methadone maintenance doses and lower (R)-methadone C_{trough} requirements, with no change in C_{trough}/dose. As such, AGC**TT** carriers appear to have decreased P-gp activity at the BBB (as opposed to increased intestinal absorption or decreased renal clearance), resulting in increased CNS methadone exposure for a given dose. Support for these findings was provided by the *ex vivo* pilot study (Chapter 5), which found that $CD4^+$ lymphocyte *ABCB1* mRNA and P-gp protein expression was lowest in the subject homozygous for this AGC**TT** haplotype, thus potentially providing mechanistic support for the link between the AGC**TT** haplotype and low MMT dose requirements. It was also found that standard MMT subjects homozygous for the wild-type AGCGC haplotype required higher MMT doses than heterozygous carriers and non-carriers, presumably due to higher P-gp activity than subjects carrying variant haplotypes.

In the clinical context, the observed haplotype effects seem relatively moderate, equating to changes of only 38-70% within a 12-fold range of doses. Indeed, there was significant overlap between haplotype groups, reflecting not only that multiple factors govern dose requirements (see below), but also that the influence of P-gp on methadone's transcellular permeability, and thus the impact of *ABCB1* genetic variability, is relatively small when compared to other known P-gp substrates (as indicated by *in vitro* experiments in Chapter 6). Nonetheless, the results of Chapter 3 provided the first evidence that identification of *ABCB1* genetic variability in opioid-dependent patients may contribute to individualizing MMT, and that the examination of *ABCB1* haplotypes has greater utility than analysing SNPs independently.

One of the other major findings of this thesis however, was that these *ABCB1* haplotypes did not associate with methadone requirements in the high dose (180-300 mg/day) MMT population (Chapter 4). As such, based on the findings of Chapter 4 and other international studies in similar subject groups, it appears that two distinct MMT populations may exist with

regards to *ABCB1* pharmacogenetics, the first being standard dose MMT (< 150-200 mg/day) where *ABCB1* haplotypes significantly influence methadone requirements, and the second being high dose MMT (> 150-200 mg/day) where they do not. As a consequence, as was shown in Chapter 4, Figure 4-2, in treatment populations where methadone doses are not heavily restricted by government legislation or clinic policy, *ABCB1* genetic variability alone is a poor predictor of methadone requirements and unlikely to be of clinical utility (see Chapter 4 Discussion).

Due to the small number of BMT subjects available, it is difficult to make comment on the clinical utility of *ABCB1* genotyping for predicting BMT dose requirements. However, results from Chapter 3 indicated a relationship between *ABCB1* haplotypes (AGCGC and AGC**TT**) and dose requirements, similar to those observed in standard dose MMT subjects, particularly amongst BMT subjects with successful treatment outcomes. Interestingly, results from the *in vitro* study described in Chapter 6 and subsequent transport studies by other researchers indicate that buprenorphine is not actually a P-gp substrate. However, genotype differences in both buprenorphine and norbuprenorphine pharmacokinetics were also observed in Chapter 3. As such, it is possible that *ABCB1* genetic variability may affect BMT dose requirements via changes in norbuprenorphine transport influencing its biliary excretion.

7.2.1. Confounding factors

One major confounding factor encompassing the *ABCB1* pharmacogenetics of both MMT and BMT is the highly heterogeneous nature of the opioid-dependent and maintenance treatment populations being studied. In addition to the numerous environmental factors already known to contribute to variability in response to both heroin and maintenance opioids, as well as variability in P-gp expression and function (see Chapter 1, sections 1.4 and 1.5.4), the findings of this thesis indicate that prior heroin use, sex, dose range and time in treatment may also modulate the impact of *ABCB1* genetic variability on substitution opioid requirements.

Furthermore, more recent studies have identified multiple genes other than *ABCB1*, such as *OPRM1* and *DRD2*, that may also be involved in determining MMT dose requirements and response. Finally, in addition to these multiple environmental and genetic factors, that are summarised in Figure 4-3 of Chapter 4, the *in vitro* study in Chapter 6 has suggested the presence of another transporter other than P-gp that could influence methadone membrane permeability, and may represent an additional, previously unknown, variable when investigating MMT pharmacogenetics.

Therefore, whilst the impact of some confounding factors (such as CYP450 metabolism) can be eliminated by measuring plasma concentrations, the examination of *ABCB1* genetic variability alone is unlikely to adequately describe the variability in substitution opioid requirements. Thus larger multi-centre prospective trials are still required to determine whether *ABCB1* haplotypes, along with other genetic and environmental factors, are likely to contribute to a clinically useful model for optimising opioid maintenance treatment.

7.3. Secondary findings

7.3.1. *ABCB1* genetic variability and maintenance treatment response

In addition to identifying associations between *ABCB1* genetic variants and methadone requirements, a secondary aim of this thesis was to investigate the role of *ABCB1* genetic variability in influencing maintenance treatment response.

As described in Chapter 3, C1236T variant frequencies were higher among poor treatment outcome subjects and those subjects reporting in-treatment withdrawal. Interestingly though, these poor treatment outcome subjects reported adverse events associated with both over- and under-dosing. As such, it appears that the association between the C1236T variant and poor treatment response is due to an overall unpleasant treatment experience encompassing both withdrawal and adverse opioid effects. Therefore, it is unclear whether this SNP is influencing

methadone distribution, or perhaps endogenous components of the stress, reward and addiction systems (such as β-endorphin) affecting general treatment response.

Whilst these effects on treatment response act to further complicate the relationship between *ABCB1* variants and dose requirements, if these associations can be confirmed prospectively, they could provide a genomic marker for poor treatment response, and thus potentially a decision support tool for determining optimal treatment approaches, and the requirement for in-treatment monitoring and/or an increased provision of ancillary services.

7.3.2. Methadone requirements/exposure and *ex vivo* P-gp expression

In addition to providing some mechanistic support for the association between the AGC**TT** haplotype and substitution opioid requirements (see above), the *ex vivo* pilot study (Chapter 5) provided the first evidence of a positive association between *ABCB1*/P-gp expression and methadone exposure in the opioid-dependent MMT population. Unfortunately, it was not possible to conclude whether differences in P-gp expression were the cause (representing efflux at the BBB), or the consequence (through P-gp induction by methadone), of variability in methadone requirements. However, if they are the cause of variable dose requirements, then determination of lymphocyte P-gp expression could provide an effective dose optimisation tool. Alternatively, if methadone exposure is determining P-gp expression, it could potentially reduce the impact of *ABCB1* genetic variability on P-gp activity (and hence methadone requirements) at high doses or after prolonged treatment, or eliminate its role altogether. As such, these findings justify further investigation.

7.3.3. *ABCB1* genetic variability and opioid dependence

Due to its potential influence on the CNS distribution of morphine and opioid peptides of the endogenous reward system, *ABCB1* genetic variability was also investigated as a genetic basis for individual differences in risk and severity of opioid dependence. However, no significant

differences in haplotype distributions were observed between opioid-dependent and control subject populations, nor did any haplotype appear to affect the age of onset of regular heroin use. A potential association between *ABCB1* haplotypes and levels of prior heroin use was also investigated, but revealed no significant relationship between the two. As such, my research has indicated that *ABCB1* genetic variability, at least in the treatment-seeking population, is not associated with the risk of opioid-dependence or prior heroin use.

7.4. Summary

In light of the current findings, a revision of the hypothesised mechanisms (originally outlined in Chapter 1, Figure 1-5) for the impact of *ABCB1* genetic variability on opioid dependence and substitution opioid response is shown in Figure 7-1.

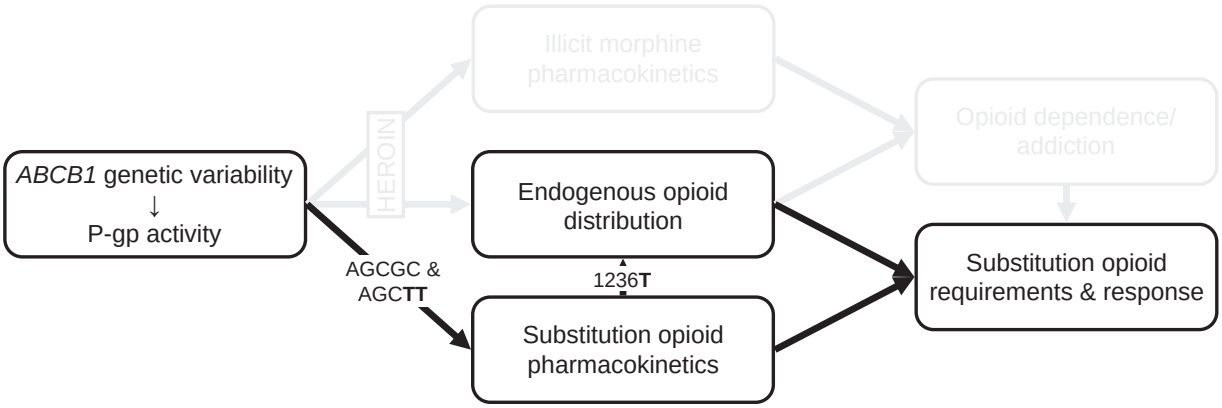

Figure 7-1. Revised summary of the mechanisms behind the impact of *ABCB1* genetic variability on opioid substitution treatment based on thesis findings.

The AGCGC and AGC**TT** haplotypes are associated with altered substitution opioid distribution, resulting in higher and lower substitution opioid requirements, respectively. The 1236**T** variant is associated with poor treatment response, unrelated to substitution opioid exposure, but possibly due to altered endogenous opioid distribution.

7.5. Conclusion

In conclusion, this thesis has generated sufficient evidence to justify further prospective investigation of *ABCB1* haplotypes as a potential tool for optimising buprenorphine and standard dose methadone substitution treatment. However, *ABCB1* genetic variability should not be considered alone, and a combined interpretation of multiple genetic and environmental factors will be required to provide a more complete picture of the factors governing the successful treatment of opioid dependence. Whilst the heterogeneous nature of the opioid-dependent treatment population represents a significant barrier, it is hoped this knowledge might one day provide clinicians with an additional clinical tool for establishing the individualized target doses and/or plasma concentrations required for efficacious opioid substitution therapy.

Chapter 8. References

Aarnoudse AL, van Schaik RH, Dieleman J, Molokhia M, van Riemsdijk MM, Ligthelm RJ, Overbosch D, van der Heiden IP and Stricker BH (2006) MDR1 gene polymorphisms are associated with neuropsychiatric adverse effects of mefloquine. *Clin Pharmacol Ther* **80:**367-374.

ABCI (1997) *Australian Illicit Drug Report 1996-97*, Australian Bureau of Criminal Intelligence, Canberra.

AIHW (2007) *Statistics on drug use in Australia 2006, in: Drug Statistics Series No. 18. Cat. no. PHE 80.*, Australian Institute of Health and Welfare, Canberra.

AIHW (2009) *National Opioid Pharmacotherapy Statistics Annual Data collection: 2008 report.* Bulletin no. 72. Cat. no. AUS 115., Australian Institute of Health and Welfare, Canberra.

Alderman CP and Allcroft PD (1997) Digoxin-itraconazole interaction: possible mechanisms. *Ann Pharmacother* **31:**438-440.

Amato L, Davoli M, C AP, Ferri M, Faggiano F and R PM (2005) An overview of systematic reviews of the effectiveness of opiate maintenance therapies: available evidence to inform clinical practice and research. *J Subst Abuse Treat* **28:**321-329.

Ambudkar SV, Kimchi-Sarfaty C, Sauna ZE and Gottesman MM (2003) P-glycoprotein: from genomics to mechanism. *Oncogene* **22:**7468-7485.

Ameyaw MM, Regateiro F, Li T, Liu X, Tariq M, Mobarek A, Thornton N, Folayan GO, Githang'a J, Indalo A, Ofori-Adjei D, Price-Evans DA and McLeod HL (2001) *MDR1* pharmacogenetics: frequency of the C3435T mutation in exon 26 is significantly influenced by ethnicity. *Pharmacogenetics* **11:**217-221.

Angelin B, Arvidsson A, Dahlqvist R, Hedman A and Schenck-Gustafsson K (1987) Quinidine reduces biliary clearance of digoxin in man. *Eur J Clin Invest* **17:**262-265.

Anggard E, Gunne LM, Homstrand J, McMahon RE, Sandberg CG and Sullivan HR (1975) Disposition of methadone in methadone maintenance. *Clin Pharmacol Ther* **17:**258-266.

Aquilante CL, Letrent SP, Pollack GM and Brouwer KL (2000) Increased brain P-glycoprotein in morphine tolerant rats. *Life Sci* **66:**PL47-51.

Arrese M and Trauner M (2003) Molecular aspects of bile formation and cholestasis. *Trends Mol Med* **9:**558-564.

Aubrun F, Langeron O, Quesnel C, Coriat P and Riou B (2003) Relationships between measurement of pain using visual analog score and morphine requirements during postoperative intravenous morphine titration. *Anesthesiology* **98:**1415-1421.

Audus KL, Bartel RL, Hidalgo IJ and Borchardt RT (1990) The use of cultured epithelial and endothelial cells for drug transport and metabolism studies. *Pharm Res* **7:**435-451.

Avdeef A, Barrett DA, Shaw PN, Knaggs RD and Davis SS (1996) Octanol-, chloroform-, and propylene glycol dipelargonat-water partitioning of morphine-6-glucuronide and other related opiates. *J Med Chem* **39:**4377-4381.

Balimane PV and Chong S (2005) A combined cell based approach to identify P-glycoprotein substrates and inhibitors in a single assay. *Int J Pharm* **301:**80-88.

Ball D and Collier D (2002) Substance misuse, in: *Psychiatric genetics and genomics* (McGuffin P, Owen MJ and Gottesman IL eds), Oxford University Press, Oxford.

Bament D, Cooke R, Weekley J and Ali R (2004) *Treatment outcomes at 12 months post admission to drug treatment: the third report of the South Australian component of the Australian Treatment Outcomes Study – Heroin.* DASC Monograph No 16 Research Series, Adelaide.

Barnes MR (2007) *Bioinformatics for geneticists: A bioinformatics primer for the analysis of genetic data, 2nd Edition*. John Wiley & Sons, New York.

Barratt C, Lai T, Nashef L, Valentin A, Fisniku L, Moran N, Asherson P and Makoff A (2006) No association of single nucleotide polymorphisms in the micro-opioid receptor subunit gene with idiopathic generalized epilepsy. *Epilepsia* **47:**1728-1731.

Bauer B, Yang X, Hartz AM, Olson ER, Zhao R, Kalvass JC, Pollack GM and Miller DS (2006) In vivo activation of human pregnane X receptor tightens the blood-brain barrier to methadone through P-glycoprotein up-regulation. *Mol Pharmacol* **70:**1212-1219.

Becquemont L, Camus M, Eschwege V, Barbu V, Rey E, Funck-Brentano C and Jaillon P (2000) Lymphocyte P-glycoprotein expression and activity before and after rifampicin in man. *Fundam Clin Pharmacol* **14:**519-525.

Bell J, Burrell T, Indig D and Gilmour S (2006) Cycling in and out of treatment; participation in methadone treatment in NSW, 1990-2002. *Drug and Alcohol Dependence* **81:**55-61.

Bell J, Chan J and Kuk A (1995) Investigating the influence of treatment philosophy on outcome of methadone maintenance. *Addiction* **90:**823-830.

Bell JR, Butler B, Lawrance A, Batey R and Salmelainen P (2009) Comparing overdose mortality associated with methadone and buprenorphine treatment. *Drug Alcohol Depend* **104:**73-77.

Bendayan R, Ronaldson PT, Gingras D and Bendayan M (2006) In situ localization of P-glycoprotein (ABCB1) in human and rat brain. *J Histochem Cytochem* **54:**1159-1167.

Besse D, Lombard MC, Zajac JM, Roques BP and Besson JM (1990) Pre- and postsynaptic distribution of mu, delta and kappa opioid receptors in the superficial layers of the cervical dorsal horn of the rat spinal cord. *Brain Res* **521:**15-22.

Booth CL, Brouwer KR and Brouwer KL (1998) Effect of multidrug resistance modulators on the hepatobiliary disposition of doxorubicin in the isolated perfused rat liver. *Cancer Res* **58:**3641-3648.

Borowsky SA and Lieber CS (1978) Interaction of methadone and ethanol metabolism. *Journal of Pharmacology and Experimental Therapeutics* **207:**123-129.

Borst P and Elferink RO (2002) Mammalian ABC transporters in health and disease. *Annu Rev Biochem* **71:**537-592.

Bouer R, Barthe L, Philibert C, Tournaire C, Woodley J and Houin G (1999) The roles of P-glycoprotein and intracellular metabolism in the intestinal absorption of methadone: in vitro studies using the rat everted intestinal sac. *Fundam Clin Pharmacol* **13:**494-500.

Boulton DW, Arnaud P and DeVane CL (2001) Pharmacokinetics and pharmacodynamics of methadone enantiomers after a single oral dose of racemate. *Clinical Pharmacology and Therapeutics* **70:**48-57.

Britt MD and Wise RA (1981) Opiate rewarding action: independence of the cells of the lateral hypothalamus. *Brain Res* **222:**213-217.

Brown LS, Jr., Kritz S, Chu M and Madray C (2006) Safety, efficacy, and tolerability of nelfinavir-containing antiretroviral therapy for patients coinfected with HIV and hepatitis C undergoing methadone maintenance. *J Subst Abuse Treat* **30:**331-335.

Brunner M, Langer O, Sunder-Plassmann R, Dobrozemsky G, Muller U, Wadsak W, Krcal A, Karch R, Mannhalter C, Dudczak R, Kletter K, Steiner I, Baumgartner C and Muller M (2005) Influence of functional haplotypes in the drug transporter gene ABCB1 on central nervous system drug distribution in humans. *Clin Pharmacol Ther* **78:**182-190.

Callen DF, Baker E, Simmers RN, Seshadri R and Roninson IB (1987) Localization of the human multiple drug resistance gene, MDR1, to 7q21.1. *Hum Genet* **77:**142-144.

Calvo R, Lukas JC, Rodriguez M, Carlos MA and Suarez E (2002) Pharmacokinetics of methadone in HIV-positive patients receiving the non-nucleoside reverse transcriptase efavirenz. *Br J Clin Pharmacol* **53:**212-214.

Campa D, Gioia A, Tomei A, Poli P and Barale R (2008) Association of ABCB1/MDR1 and OPRM1 gene polymorphisms with morphine pain relief. *Clin Pharmacol Ther* **83:**559-566.

Canaparo R, Nordmark A, Finnstrom N, Lundgren S, Seidegard J, Jeppsson B, Edwards RJ, Boobis AR and Rane A (2007) Expression of cytochromes P450 3A and P-glycoprotein in human large intestine in paired tumour and normal samples. *Basic Clin Pharmacol Toxicol* **100:**240-248.

Caplehorn JR, Dalton MS, Cluff MC and Petrenas AM (1994) Retention in methadone maintenance and heroin addicts' risk of death. *Addiction* **89:**203-209.

Caplehorn JR, Dalton MS, Haldar F, Petrenas AM and Nisbet JG (1996) Methadone maintenance and addicts' risk of fatal heroin overdose. *Subst Use Misuse* **31:**177-196.

Caplehorn JR, Lumley TS and Irwig L (1998) Staff attitudes and retention of patients in methadone maintenance programs. *Drug Alcohol Depend* **52:**57-61.

Cascorbi I, Gerloff T, Johne A, Meisel C, Hoffmeyer S, Schwab M, Schaeffeler E, Eichelbaum M, Brinkmann U and Roots I (2001) Frequency of single nucleotide polymorphisms in the P-glycoprotein drug transporter *MDR1* gene in white subjects. *Clin Pharmacol Ther* **69:**169-174.

Chan HS and Ling V (1997) Anti-P-glycoprotein antibody C219 cross-reactivity with c-erbB2 protein: diagnostic and clinical implications. *J Natl Cancer Inst* **89:**1473-1476.

Chandler B, Detsika M, Khoo SH, Williams J, Back DJ and Owen A (2007) Factors impacting the expression of membrane-bound proteins in lymphocytes from HIV-positive subjects. *J Antimicrob Chemother* **60:**685-9.

Chang G, Chen L and Mao J (2007) Opioid tolerance and hyperalgesia. *Med Clin North Am* **91:**199-211.

Chaudhary PM, Mechetner EB and Roninson IB (1992) Expression and activity of the multidrug resistance P-glycoprotein in human peripheral blood lymphocytes. *Blood* **80:**2735-2739.

Chen CJ, Clark D, Ueda K, Pastan I, Gottesman MM and Roninson IB (1990) Genomic organization of the human multidrug resistance (MDR1) gene and origin of P-glycoproteins. *J Biol Chem* **265:**506-514.

Chinn LW, Gow JM, Tse MM, Becker SL and Kroetz DL (2007) Interindividual variability in the effect of atazanavir and saquinavir on the expression of lymphocyte P-glycoprotein. *J Antimicrob Chemother* **60:**61-67.

Choo EF, Kurnik D, Muszkat M, Ohkubo T, Shay SD, Higginbotham JN, Glaeser H, Kim RB, Wood AJ and Wilkinson GR (2006) Differential in vivo sensitivity to inhibition of P-glycoprotein located in lymphocytes, testes, and the blood-brain barrier. *J Pharmacol Exp Ther* **317:**1012-1018.

Choo EF, Leake B, Wandel C, Imamura H, Wood AJ, Wilkinson GR and Kim RB (2000) Pharmacological inhibition of P-glycoprotein transport enhances the distribution of HIV-1 protease inhibitors into brain and testes. *Drug Metab Dispos* **28:**655-660.

Choudhuri S and Klaassen CD (2006) Structure, function, expression, genomic organization, and single nucleotide polymorphisms of human ABCB1 (MDR1), ABCC (MRP), and ABCG2 (BCRP) efflux transporters. *Int J Toxicol* **25:**231-259.

Chowbay B, Li H, David M, Bun Cheung Y and Lee EJ (2005) Meta-analysis of the influence of MDR1 C3435T polymorphism on digoxin pharmacokinetics and MDR1 gene expression. *Br J Clin Pharmacol* **60:**159-171.

Chu TM, Lin TH and Kawinski E (1994) Detection of soluble P-glycoprotein in culture media and extracellular fluids. *Biochem Biophys Res Commun* **203:**506-512.

Coles LD, Lee IJ, Hassan HE and Eddington ND (2009) Distribution of saquinavir, methadone, and buprenorphine in maternal brain, placenta, and fetus during two different gestational stages of pregnancy in mice. *J Pharm Sci* **98:**2832-2846.

Coller JK, Barratt DT, Dahlen K, Loennechen MH and Somogyi AA (2006) ABCB1 genetic variability and methadone dosage requirements in opioid-dependent individuals. *Clin Pharmacol Ther* **80:**682-690.

Comets E, Verstuyft C, Lavielle M, Jaillon P, Becquemont L and Mentre F (2007) Modelling the influence of MDR1 polymorphism on digoxin pharmacokinetic parameters. *Eur J Clin Pharmacol* **63:**437-449.

Connor JP, Young RM, Saunders JB, Lawford BR, Ho R, Ritchie TL and Noble EP (2008) The A1 allele of the D2 dopamine receptor gene region, alcohol expectancies and drinking refusal self-efficacy are associated with alcohol dependence severity. *Psychiatry Res* **160:**94-105.

Corrigall WA and Vaccarino FJ (1988) Antagonist treatment in nucleus accumbens or periaqueductal grey affects heroin self-administration. *Pharmacol Biochem Behav* **30:**443-450.

Coulbault L, Beaussier M, Verstuyft C, Weickmans H, Dubert L, Tregouet D, Descot C, Parc Y, Lienhart A, Jaillon P and Becquemont L (2006) Environmental and genetic factors associated with morphine response in the postoperative period. *Clin Pharmacol Ther* **79:**316-324.

Cowan A, Friderichs E, Straßburger W and Raffa RB (2005) Basic pharmacology of buprenorphine, in: *Buprenorphine – the unique opioid analgesic* (Budd K and Raffa RB eds), pp 92-101, Thieme Verlag KG, Stuttgart.

Craddock SG, Rounds-Bryant JL, Flynn PM and Hubbard RL (1997) Characteristics and pretreatment behaviors of clients entering drug abuse treatment: 1969 to 1993. *Am J Drug Alcohol Abuse* **23:**43-59.

Crettol S, Besson J, Croquette-Krokar M, Hammig R, Gothuey I, Monnat M, Deglon JJ, Preisig M and Eap CB (2008a) Association of dopamine and opioid receptor genetic polymorphisms with response to methadone maintenance treatment. *Prog Neuropsychopharmacol Biol Psychiatry* **32:**1722-1727.

Crettol S, Deglon JJ, Besson J, Croquette-Krokar M, Hammig R, Gothuey I, Monnat M and Eap CB (2006) ABCB1 and cytochrome P450 genotypes and phenotypes: influence on methadone plasma levels and response to treatment. *Clin Pharmacol Ther* **80:**668-681.

Crettol S, Deglon JJ, Besson J, Croquette-Krokar M, Hammig R, Gothuey I, Monnat M and Eap CB (2008b) No influence of ABCB1 haplotypes on methadone dosage requirement. *Clin Pharmacol Ther* **83:**668-669; author reply 669-670.

Crettol S, Deglon JJ, Besson J, Croquette-Krokkar M, Gothuey I, Hammig R, Monnat M, Huttemann H, Baumann P and Eap CB (2005) Methadone enantiomer plasma levels, CYP2B6, CYP2C19, and CYP2C9 genotypes, and response to treatment. *Clin Pharmacol Ther* **78:**593-604.

Crettol S, Digon P, Golay KP, Brawand M and Eap CB (2007) In vitro P-glycoprotein-mediated transport of (R)-, (S)-, (R,S)-methadone, LAAM and their main metabolites. *Pharmacology* **80:**304-311.

Dagenais C, Graff CL and Pollack GM (2004) Variable modulation of opioid brain uptake by P-glycoprotein in mice. *Biochemical Pharmacology* **67:**269-276.

Dagenais C, Zong J, Ducharme J and Pollack GM (2001) Effect of mdr1a P-glycoprotein gene disruption, gender, and substrate concentration on brain uptake of selected compounds. *Pharm Res* **18:**957-963.

Dahan A, Yassen A, Bijl H, Romberg R, Sarton E, Teppema L, Olofsen E and Danhof M (2005) Comparison of the respiratory effects of intravenous buprenorphine and fentanyl in humans and rats. *Br J Anaesth* **94:**825-834.

Darke S, Hall W, Wodak A, Heather N and Ward J (1992) Development and validation of a multidimensional instrument for assessing outcome of treatment among opiate users: the Opiate Treatment Index. *British Journal of Addiction* **87:**733-742.

Darke S, Hetherington K, Ross J, Lynskey M and Teesson M (2004) Non-injecting routes of administration among entrants to three treatment modalities for heroin dependence. *Drug Alcohol Rev* **23:**177-183.

Darke S, Ross J and Hall W (1996) Prevalence and correlates of the injection of methadone syrup in Sydney, Australia. *Drug Alcohol Depend* **43:**191-198.

Darke S, Topp L and Ross J (2002) The injection of methadone and benzodiazepines among Sydney injecting drug users 1996-2000: 5-year monitoring of trends from the Illicit Drug Reporting System. *Drug Alcohol Rev* **21:**27-32.

DASC (2002) *Illicit drug use in South Australia 2002: a statistical overview*, Drug & Alcohol Services Council, Adelaide.

Dauchy S, Dutheil F, Weaver RJ, Chassoux F, Daumas-Duport C, Couraud PO, Scherrmann JM, De Waziers I and Decleves X (2008) ABC transporters, cytochromes P450 and their main transcription factors: expression at the human blood-brain barrier. *J Neurochem* **107:**1518-1528.

Davit B, Reynolds K, Yuan R, Ajayi F, Conner D, Fadiran E, Gillespie B, Sahajwalla C, Huang SM and Lesko LJ (1999) FDA evaluations using in vitro metabolism to predict and interpret in vivo metabolic drug-drug interactions: impact on labeling. *J Clin Pharmacol* **39:**899-910.

Degenhardt L, Black E, Breen C, Bruno R, Kinner S, Roxburgh A, Fry C, Jenkinson R, Ward J, Fetherston J, Weekley J and Fischer J (2006) Trends in morphine prescriptions, illicit morphine use and associated harms among regular injecting drug users in Australia. *Drug Alcohol Rev* **25:**403-412.

Dhawan BN, Cesselin F, Raghubir R, Reisine T, Bradley PB, Portoghese PS and Hamon M (1996) International Union of Pharmacology. XII. Classification of opioid receptors. *Pharmacol Rev* **48:**567-592.

Di Chiara G and Imperato A (1988) Drugs abused by humans preferentially increase synaptic dopamine concentrations in the mesolimbic system of freely moving rats. *Proc Natl Acad Sci U S A* **85:**5274-5278.

Doehring A, Hentig N, Graff J, Salamat S, Schmidt M, Geisslinger G, Harder S and Lotsch J (2009) Genetic variants altering dopamine D2 receptor expression or function modulate the risk of opiate addiction and the dosage requirements of methadone substitution. *Pharmacogenet Genomics* **19:**407-414.

Doering W (1979) Quinidine-digoxin interaction: Pharmacokinetics, underlying mechanism and clinical implications. *N Engl J Med* **301:**400-404.

Dole VP and Nyswander M (1965) A Medical Treatment for Diacetylmorphine (Heroin) Addiction. A Clinical Trial with Methadone Hydrochloride. *JAMA* **193:**646-650.

Donny EC, Brasser SM, Bigelow GE, Stitzer ML and Walsh SL (2005) Methadone doses of 100 mg or greater are more effective than lower doses at suppressing heroin self-administration in opioid-dependent volunteers. *Addiction* **100:**1496-1509.

Donny EC, Walsh SL, Bigelow GE, Eissenberg T and Stitzer ML (2002) High-dose methadone produces superior opioid blockade and comparable withdrawal suppression to lower doses in opioid-dependent humans. *Psychopharmacology (Berl)* **161:**202-212.

Doran CM, Shanahan M, Mattick RP, Ali R, White J and Bell J (2003) Buprenorphine versus methadone maintenance: a cost-effectiveness analysis. *Drug Alcohol Depend* **71:**295-302.

Doverty M, Somogyi AA, White JM, Bochner F, Beare CH, Menelaou A and Ling W (2001) Methadone maintenance patients are cross-tolerant to the antinociceptive effects of morphine. *Pain* **93:**155-163.

Drescher S, Glaeser H, Murdter T, Hitzl M, Eichelbaum M and Fromm MF (2003) P-glycoprotein-mediated intestinal and biliary digoxin transport in humans. *Clin Pharmacol Ther* **73:**223-231.

Drewe J, Ball HA, Beglinger C, Peng B, Kemmler A, Schächinger H and Haefeli WE (2000) Effect of P-glycoprotein modulation on the clinical pharmacokinetics and adverse effects of morphine. *Br J Clin Pharmacol* **50:**237-246.

Drewe J, Gutmann H, Fricker G, Torok M, Beglinger C and Huwyler J (1999) HIV protease inhibitor ritonavir: a more potent inhibitor of P-glycoprotein than the cyclosporine analog SDZ PSC 833. *Biochem Pharmacol* **57:**1147-1152.

DuPen A, Shen D and Ersek M (2007) Mechanisms of opioid-induced tolerance and hyperalgesia. *Pain Manag Nurs* **8:**113-121.

Dyer KR, Foster DJ, White JM, Somogyi AA, Menelaou A and Bochner F (1999) Steady-state pharmacokinetics and pharmacodynamics in methadone maintenance patients: comparison of those who do and do not experience withdrawal and concentration-effect relationships. *Clinical Pharmacology and Therapeutics* **65:**685-694.

Dyer KR and White JM (1997) Patterns of symptom complaints in methadone maintenance patients. *Addiction* **92:**1445-1455.

Eap CB, Bondolfi G, Zullino D, Bryois C, Fuciec M, Savary L, Jonzier-Perey M and Baumann P (2001) Pharmacokinetic drug interaction potential of risperidone with cytochrome p450 isozymes as assessed by the dextromethorphan, the caffeine, and the mephenytoin test. *Ther Drug Monit* **23:**228-231.

Eap CB, Bourquin M, Martin J, Spagnoli J, Livoti S, Powell K, Baumann P and Deglon J (2000) Plasma concentrations of the enantiomers of methadone and therapeutic response in methadone maintenance treatment. *Drug Alcohol Depend* **61:**47-54.

Eap CB, Buclin T and Baumann P (2002) Interindividual variability of the clinical pharmacokinetics of methadone: implications for the treatment of opioid dependence. *Clin Pharmacokinet* **41:**1153-1193.

Eich-Hochli D, Oppliger R, Golay KP, Baumann P and Eap CB (2003) Methadone maintenance treatment and St. John's Wort - a case report. *Pharmacopsychiatry* **36:**35-37.

Elkader AK, Brands B, Callaghan R and Sproule BA (2009a) Exploring the relationship between perceived inter-dose opioid withdrawal and patient characteristics in methadone maintenance treatment. *Drug Alcohol Depend* **105:**209-214.

Elkader AK, Brands B, Dunn E, Selby P and Sproule BA (2009b) Major depressive disorder and patient satisfaction in relation to methadone pharmacokinetics and pharmacodynamics in stabilized methadone maintenance patients. *J Clin Psychopharmacol* **29:**77-81.

EWGEAPC (1996) Expert Working Group of the European Association for Palliative Care Fortnightly Review: Morphine in cancer pain: modes of administration, in: *BMJ*, pp 823-826.

Excoffier L, Laval G and Schneider S (2005) Arlequin (version 3.0): An integrated software package for population genetics data analysis. *Evol Bioinform Online* **1:**47-50.

Faggiano F, Vigna-Taglianti F, Versino E and Lemma P (2003) Methadone maintenance at different dosages for opioid dependence. *Cochrane Database Syst Rev***:**CD002208.

Fliszar KA, Hill BT and Foster N (2007) Predicting human drug pharmacokinetics from in vitro permeability using an absorption-disposition model. *J Pharm Sci* **96:**2161-2170.

Fojo AT, Ueda K, Slamon DJ, Poplack DG, Gottesman MM and Pastan I (1987) Expression of a multidrug-resistance gene in human tumors and tissues. *Proc Natl Acad Sci U S A* **84:**265-269.

Ford J, Hoggard PG, Owen A, Khoo SH and Back DJ (2003) A simplified approach to determining P-glycoprotein expression in peripheral blood mononuclear cell subsets. *J Immunol Methods* **274:**129-137.

Foster DJ, Morton EB, Heinkele G, Murdter TE and Somogyi AA (2006) Stereoselective quantification of methadone and a d(6)-labeled isotopomer using high performance liquid chromatography-atmospheric pressure chemical ionization mass-spectrometry: application to a pharmacokinetic study in a methadone maintained subject. *Ther Drug Monit* **28:**559-567.

Foster DJ, Somogyi AA and Bochner F (1999) Methadone N-demethylation in human liver microsomes: lack of stereoselectivity and involvement of CYP3A4. *Br J Clin Pharmacol* **47:**403-412.

Foster DJ, Somogyi AA, Dyer KR, White JM and Bochner F (2000) Steady-state pharmacokinetics of (R)- and (S)-methadone in methadone maintenance patients. *Br J Clin Pharmacol* **50:**427-440.

Foster DJR, Somogyi AA, White JM and Bochner F (2004) Population pharmacokinetics of (R)-, (S)- and rac-methadone in methadone maintenance patients. *Br J Clin Pharmacol* **57:**742-755.

Frohlich M, Albermann N, Sauer A, Walter-Sack I, Haefeli WE and Weiss J (2004) In vitro and ex vivo evidence for modulation of P-glycoprotein activity by progestins. *Biochem Pharmacol* **68:**2409-2416.

Fromm MF, Kim RB, Stein CM, Wilkinson GR and Roden DM (1999) Inhibition of P-glycoprotein-mediated drug transport: A unifying mechanism to explain the interaction between digoxin and quinidine [seecomments]. *Circulation* **99:**552-557.

Ganapathy V and Miyauchi S (2005) Transport systems for opioid peptides in mammalian tissues. *Aaps J* **7:**E852-856.

Garrigos M, Mir LM and Orlowski S (1997) Competitive and non-competitive inhibition of the multidrug-resistance-associated P-glycoprotein ATPase--further experimental evidence for a multisite model. *Eur J Biochem* **244:**664-673.

Gaughwin M, Solomon P and Ali R (1998) Correlates of retention on the South Australian Methadone Program 1981-91. *Aust N Z J Public Health* **22:**771-776.

Gerloff T, Schaefer M, Johne A, Oselin K, Meisel C, Cascorbi I and Roots I (2002) *MDR1* genotypes do not influence the absorption of a single oral dose of 1 mg digoxin in healthy white males. *British Journal of Clinical Pharmacology* **54:**610-616.

Germann UA (1997) Detection of expressed recombinant protein based on multidrug resistance: P-glycoprotein, in: *Recombinant Protein Protocols: Detection and Isolation* (Tuan RS ed), pp 139-160, Humana Press, Totowa.

Gomella LG (2002) *Clinician's Pocket Reference*. McGraw-Hill Professional, New York.

Gottesman MM and Pastan I (1988) The multidrug transporter, a double-edged sword. *J Biol Chem* **263:**12163-12166.

Gow JM, Hodges LM, Chinn LW and Kroetz DL (2008) Substrate-dependent effects of human ABCB1 coding polymorphisms. *J Pharmacol Exp Ther* **325:**435-442.

Gramatte T and Oertel R (1999) Intestinal secretion of intravenous talinolol is inhibited by luminal R-verapamil. *Clin Pharmacol Ther* **66:**239-245.

Greenwald MK, Johanson CE, Moody DE, Woods JH, Kilbourn MR, Koeppe RA, Schuster CR and Zubieta JK (2003) Effects of buprenorphine maintenance dose on mu-opioid receptor availability, plasma concentrations, and antagonist blockade in heroin-dependent volunteers. *Neuropsychopharmacology* **28:**2000-2009.

Greiner B, Eichelbaum M, Fritz P, Kreichgauer HP, von Richter O, Zundler J and Kroemer HK (1999) The role of intestinal P-glycoprotein in the interaction of digoxin and rifampin. *J Clin Invest* **104:**147-153.

Grub S, Bryson H, Goggin T, Ludin E and Jorga K (2001) The interaction of saquinavir (soft gelatin capsule) with ketoconazole, erythromycin and rifampicin: comparison of the effect in healthy volunteers and in HIV-infected patients. *Eur J Clin Pharmacol* **57:**115-121.

Haas DW, Clough LA, Johnson BW, Harris VL, Spearman P, Wilkinson GR, Fletcher CV, Fiscus S, Raffanti S, Donlon R, McKinsey J, Nicotera J, Schmidt D, Shoup RE, Kates RE, Lloyd RM, Jr. and Larder B (2000) Evidence of a source of HIV type 1 within the central nervous system by ultraintensive sampling of cerebrospinal fluid and plasma. *AIDS Res Hum Retroviruses* **16:**1491-1502.

Hall W, Madden P and Lynskey M (2002) The genetics of tobacco use: methods, findings and policy implications. *Tob Control* **11:**119-124.

Hallinan R, Ray J, Byrne A, Agho K and Attia J (2006) Therapeutic thresholds in methadone maintenance treatment: a receiver operating characteristic analysis. *Drug Alcohol Depend* **81:**129-136.

Hamabe W, Maeda T, Fukazawa Y, Kumamoto K, Shang LQ, Yamamoto A, Yamamoto C, Tokuyama S and Kishioka S (2006) P-glycoprotein ATPase activating effect of opioid analgesics and their P-glycoprotein-dependent antinociception in mice. *Pharmacol Biochem Behav* **85:**629-636.

Hamabe W, Maeda T, Kiguchi N, Yamamoto C, Tokuyama S and Kishioka S (2007) Negative relationship between morphine analgesia and P-glycoprotein expression levels in the brain. *J Pharmacol Sci* **105:**353-360.

Hanna J, Foster DJ, Salter A, Somogyi AA, White JM and Bochner F (2005) Within- and between-subject variability in methadone pharmacokinetics and pharmacodynamics in methadone maintenance subjects. *Br J Clin Pharmacol* **60:**404-413.

Hassan HE, Myers AL, Coop A and Eddington ND (2009) Differential involvement of P-glycoprotein (ABCB1) in permeability, tissue distribution, and antinociceptive activity of methadone, buprenorphine, and diprenorphine: in vitro and in vivo evaluation. *J Pharm Sci* **98:**4928-4940.

Hassan HE, Myers AL, Lee IJ, Coop A and Eddington ND (2007) Oxycodone induces overexpression of P-glycoprotein (ABCB1) and affects paclitaxel's tissue distribution in Sprague Dawley rats. *J Pharm Sci* **96:**2494-2506.

Hawkins KN, Knapp RJ, Gehlert DR, Lui GK, Yamamura MS, Roeske LC, Hruby VJ and Yamamura HI (1988) Quantitative autoradiography of [3H]CTOP binding to mu opioid receptors in rat brain. *Life Sci* **42:**2541-2551.

Hedrick PW (2005) *Genetics of populations*. Jones and Bartlett Publishers International, London.

Heinrichs SC, Menzaghi F, Schulteis G, Koob GF and Stinus L (1995) Suppression of corticotropin-releasing factor in the amygdala attenuates aversive consequences of morphine withdrawal. *Behav Pharmacol* **6:**74-80.

Henry-Edwards SM, Gowing L, White J, Ali R, Bell J, Brough R, Lintzeris N, Ritter A and Quigley A (2003) Clinical guidelines and procedures for the use of methadone in the maintenance treatment of opioid dependence, National Drug Strategy, Australian Government Department of Health and Ageing, Canberra.

Hidalgo IJ, Raub TJ and Borchardt RT (1989) Characterization of the human colon carcinoma cell line (Caco-2) as a model system for intestinal epithelial permeability. *Gastroenterology* **96:**736-749.

Hirano T, Onda K, Toma T, Miyaoka M, Moriyasu F and Oka K (2004) MDR1 mRNA expressions in peripheral blood mononuclear cells of patients with ulcerative colitis in relation to glucocorticoid administration. *J Clin Pharmacol* **44:**481-6.

Hitzl M, Schaeffeler E, Hocher B, Slowinski T, Halle H, Eichelbaum M, Kaufmann P, Fritz P, Fromm MF and Schwab M (2004) Variable expression of P-glycoprotein in the human placenta and

its association with mutations of the multidrug resistance 1 gene (MDR1, ABCB1). *Pharmacogenetics* **14:**309-318.

Hoffmeyer S, Burk O, von Richter O, Arnold HP, Brockmöller J, Johne A, Cascorbi I, Gerloff T, Roots I, Eichelbaum M and Brinkmann U (2000) Functional polymorphisms of the human multidrug-resistance gene: multiple sequence variations and correlation of one allele with P-glycoprotein expression and activity *in vivo*. *Proceedings of the National Academy of Sciences of the United States of America* **97:**3473-3478.

Hsyu PH, Lillibridge J, Daniels E and Kerr BM (2006) Pharmacokinetic interaction of nelfinavir and methadone in intravenous drug users. *Biopharm Drug Dispos* **27:**61-68.

Hulse GK, English DR, Milne E and Holman CD (1999) The quantification of mortality resulting from the regular use of illicit opiates. *Addiction* **94:**221-229.

Hung CC, Chen CC, Lin CJ and Liou HH (2008) Functional evaluation of polymorphisms in the human ABCB1 gene and the impact on clinical responses of antiepileptic drugs. *Pharmacogenet Genomics* **18:**390-402.

Hunter J, Hirst BH and Simmons NL (1993a) Drug absorption limited by P-glycoprotein-mediated secretory drug transport in human intestinal epithelial Caco-2 cell layers. *Pharm Res* **10:**743-749.

Hunter J, Jepson MA, Tsuruo T, Simmons NL and Hirst BH (1993b) Functional expression of P-glycoprotein in apical membranes of human intestinal Caco-2 cells. Kinetics of vinblastine secretion and interaction with modulators. *J Biol Chem* **268:**14991-14997.

Hurley M, White J, Chadderton T, Banner L, Anderson G, Hurley E and Angelos P (2004) Guide for Pharmacists: Addiction treatment and maintenance pharmacotherapy (methadone and buprenorphine) programs in South Australia, Drug & Alcohol Services South Australia, Adelaide.

Hutchinson MR, Bland ST, Johnson KW, Rice KC, Maier SF and Watkins LR (2007) Opioid-induced glial activation: mechanisms of activation and implications for opioid analgesia, dependence, and reward. *ScientificWorldJournal* **7:**98-111.

Iribarne C, Berthou F, Baird S, Dreano Y, Picart D, Bail JP, Beaune P and Menez JF (1996) Involvement of cytochrome P450 3A4 enzyme in the N-demethylation of methadone in human liver microsomes. *Chem Res Toxicol* **9:**365-373.

Iribarne C, Berthou F, Carlhant D, Dreano Y, Picart D, Lohezic F and Riche C (1998) Inhibition of methadone and buprenorphine N-dealkylations by three HIV-1 protease inhibitors. *Drug Metab Dispos* **26:**257-260.

Isbell H and Eisenman AJ (1948) The addiction liability of some drugs of the methadon series. *J Pharmacol Exp Ther* **93:**305-313.

Jasinski DR, Pevnick JS and Griffith JD (1978) Human pharmacology and abuse potential of the analgesic buprenorphine: a potential agent for treating narcotic addiction. *Arch Gen Psychiatry* **35:**501-516.

Jenkinson RA, Clark NC, Fry CL and Dobbin M (2005) Buprenorphine diversion and injection in Melbourne, Australia: an emerging issue? *Addiction* **100:**197-205.

Jensen ML, Foster D, Upton R, Grant C, Martinez A and Somogyi A (2007) Comparison of cerebral pharmacokinetics of buprenorphine and norbuprenorphine in an in vivo sheep model. *Xenobiotica* **37:**441-457.

Johne A, Köpke K, Gerloff T, Mai I, Rietbrock S, Meisel C, Hoffmeyer S, Kerb R, Fromm MF, Brinkmann U, Eichelbaum M, Brockmöller J, Cascorbi I and Roots I (2002) Modulation of steady-state kinetics of digoxin by haplotypes of the P-glycoprotein *MDR1* gene. *Clinical Pharmacology and Therapeutics* **72:**584-594.

Johnson SW and North RA (1992) Opioids excite dopamine neurons by hyperpolarization of local interneurons. *Journal of Neuroscience* **12:**483-488.

Jonker JW, Wagenaar E, van Deemter L, Gottschlich R, Bender HM, Dasenbrock J and Schinkel AH (1999) Role of blood-brain barrier P-glycoprotein in limiting brain accumulation and sedative side-effects of asimadoline, a peripherally acting analgaesic drug. *British Journal of Pharmacology* **127:**43-50.

Kajinami K, Brousseau ME, Ordovas JM and Schaefer EJ (2004) Polymorphisms in the multidrug resistance-1 (MDR1) gene influence the response to atorvastatin treatment in a gender-specific manner. *Am J Cardiol* **93:**1046-1050.

Kalvass JC, Olson ER and Pollack GM (2007) Pharmacokinetics and pharmacodynamics of alfentanil in P-glycoprotein-competent and P-glycoprotein-deficient mice: P-glycoprotein efflux alters alfentanil brain disposition and antinociception. *Drug Metab Dispos* **35:**455-459.

Khaliq Y, Gallicano K, Venance S, Kravcik S and Cameron DW (2000) Effect of ketoconazole on ritonavir and saquinavir concentrations in plasma and cerebrospinal fluid from patients infected with human immunodeficiency virus. *Clin Pharmacol Ther* **68:**637-646.

Kharasch E, Whittington D, Hoffer C, Altuntas T and Sheffels P (2003a) Role of P-glycoprotein in the intestinal absorption of morphine, fentanyl and methadone. *Clinical Pharmacology & Therapeutics* **73:**P58.

Kharasch ED, Hoffer C and Whittington D (2004a) The effect of quinidine, used as a probe for the involvement of P-glycoprotein, on the intestinal absorption and pharmacodynamics of methadone. *British Journal of Clinical Pharmacology* **57:**600-610.

Kharasch ED, Hoffer C, Whittington D and Sheffels P (2003b) Role of P-glycoprotein in the intestinal absorption and clinical effects of morphine. *Clinical Pharmacology and Therapeutics* **74:**543-554.

Kharasch ED, Hoffer C, Whittington D and Sheffels P (2004b) Role of hepatic and intestinal cytochrome P450 3A and 2B6 in the metabolism, disposition, and miotic effects of methadone. *Clin Pharmacol Ther* **76:**250-269.

Kharasch ED, Hoffer C, Whittington D, Walker A and Bedynek PS (2009a) Methadone pharmacokinetics are independent of cytochrome P4503A (CYP3A) activity and gastrointestinal drug transport: insights from methadone interactions with ritonavir/indinavir. *Anesthesiology* **110:**660-672.

Kharasch ED, Walker A, Whittington D, Hoffer C and Bedynek PS (2009b) Methadone metabolism and clearance are induced by nelfinavir despite inhibition of cytochrome P4503A (CYP3A) activity. *Drug Alcohol Depend* **101:**158-168.

Kim RB, Leake BF, Choo EF, Dresser GK, Kubba SV, Schwarz UI, Taylor A, Xie HG, McKinsey J, Zhou S, Lan LB, Schuetz JD, Schuetz EG and Wilkinson GR (2001) Identification of functionally variant *MDR1* alleles among European Americans and African Americans. *Clinical Pharmacology and Therapeutics* **70:**189-199.

Kimchi-Sarfaty C, Gribar JJ and Gottesman MM (2002) Functional characterization of coding polymorphisms in the human *MDR1* gene using a vaccinia virus expression system. *Molecular Pharmacology* **62:**1-6.

Kimchi-Sarfaty C, Oh JM, Kim IW, Sauna ZE, Calcagno AM, Ambudkar SV and Gottesman MM (2007) A "silent" polymorphism in the MDR1 gene changes substrate specificity. *Science* **315:**525-528.

King M, Su W, Chang A, Zuckerman A and Pasternak GW (2001) Transport of opioids from the brain to the periphery by P-glycoprotein: peripheral actions of central drugs. *Nat Neurosci* **4:**268-274.

Kioka N, Tsubota J, Kakehi Y, Komano T, Gottesman MM, Pastan I and Ueda K (1989) P-glycoprotein gene (MDR1) cDNA from human adrenal: normal P-glycoprotein carries Gly185 with an altered pattern of multidrug resistance. *Biochem Biophys Res Commun* **162:**224-231.

Kitchen I, Slowe SJ, Matthes HW and Kieffer B (1997) Quantitative autoradiographic mapping of mu-, delta- and kappa-opioid receptors in knockout mice lacking the mu-opioid receptor gene. *Brain Res* **778:**73-88.

Klein HO, Lang R, Weiss E, Di Segni E, Libhaber C, Guerrero J and Kaplinsky E (1982) The influence of verapamil on serum digoxin concentration. *Circulation* **65:**998-1003.

Klimecki WT, Futscher BW, Grogan TM and Dalton WS (1994) P-glycoprotein expression and function in circulating blood cells from normal volunteers. *Blood* **83:**2451-2458.

Koob GF (2005) The neurocircuitry of addiction: Implications for treatment. *Clinical Neuroscience Research* **5:**89-101.

Kreek MJ (1984) Opioid interactions with alcohol. *Adv Alcohol Subst Abuse* **3:**35-46.

Kreek MJ (1996) Opiates, opioids and addiction. *Molecular Psychiatry* **1:**232-254.

Kreek MJ (1997) Opiate and cocaine addictions: challenge for pharmacotherapies. *Pharmacol Biochem Behav* **57:**551-569.

Kreek MJ, Bencsath FA, Fanizza A and Field FH (1983) Effects of liver disease on fecal excretion of methadone and its unconjugated metabolites in maintenance patients. Quantitation by direct probe chemical ionization mass spectrometry. *Biomed Mass Spectrom* **10:**544-549.

Kreek MJ, Garfield JW, Gutjahr CL and Giusti LM (1976a) Rifampin-induced methadone withdrawal. *N Engl J Med* **294:**1104-1106.

Kreek MJ, Gutjahr CL, Garfield JW, Bowen DV and Field FH (1976b) Drug interactions with methadone. *Ann N Y Acad Sci* **281:**350-371.

Kreek MJ and Koob GF (1998) Drug dependence: stress and dysregulation of brain reward pathways. *Drug Alcohol Depend* **51:**23-47.

Kristensen K, Blemmer T, Angelo HR, Christrup LL, Drenck NE, Rasmussen SN and Sjogren P (1996) Stereoselective pharmacokinetics of methadone in chronic pain patients. *Ther Drug Monit* **18:**221-227.

Kristensen K, Christensen CB and Christrup LL (1995) The mu1, mu2, delta, kappa opioid receptor binding profiles of methadone stereoisomers and morphine. *Life Sci* **56:**PL45-50.

Kroetz DL, Pauli-Magnus C, Hodges LM, Huang CC, Kawamoto M, Johns SJ, Stryke D, Ferrin TE, DeYoung J, Taylor T, Carlson EJ, Herskowitz I, Giacomini KM and Clark AG (2003) Sequence diversity and haplotype structure in the human ABCB1 (MDR1, multidrug resistance transporter) gene. *Pharmacogenetics* **13:**481-494.

Kuhlman JJ, Jr., Levine B, Johnson RE, Fudala PJ and Cone EJ (1998) Relationship of plasma buprenorphine and norbuprenorphine to withdrawal symptoms during dose induction, maintenance and withdrawal from sublingual buprenorphine. *Addiction* **93:**549-559.

Kusuhara H and Sugiyama Y (2001) Efflux transport systems for drugs at the blood-brain barrier and blood-cerebrospinal fluid barrier (Part 2). *Drug Discov Today* **6:**206-212.

Kuwano M, Oda Y, Izumi H, Yang SJ, Uchiumi T, Iwamoto Y, Toi M, Fujii T, Yamana H, Kinoshita H, Kamura T, Tsuneyoshi M, Yasumoto K and Kohno K (2004) The role of nuclear Y-box binding protein 1 as a global marker in drug resistance. *Mol Cancer Ther* **3:**1485-1492.

Lamba JK, Lin YS, Schuetz EG and Thummel KE (2002) Genetic contribution to variable human CYP3A-mediated metabolism. *Adv Drug Deliv Rev* **54:**1271-1294.

Lawford BR, Young RM, Noble EP, Sargent J, Rowell J, Shadforth S, Zhang X and Ritchie T (2000) The D_2 dopamine receptor A_1 allele and opioid dependence: association with heroin use and response to methadone treatment. *Am J Med Genet (Neuropsychiatr Genet)* **96:**592-598.

Ledoux S, Yang R, Friedlander G and Laouari D (2003) Glucose depletion enhances P-glycoprotein expression in hepatoma cells: role of endoplasmic reticulum stress response. *Cancer Res* **63:**7284-7290.

Letrent SP, Pollack GM, Brouwer KR and Brouwer KL (1998) Effect of GF120918, a potent P-glycoprotein inhibitor, on morphine pharmacokinetics and pharmacodynamics in the rat. *Pharm Res* **15:**599-605.

Letrent SP, Pollack GM, Brouwer KR and Brouwer KL (1999a) Effects of a potent and specific P-glycoprotein inhibitor on the blood-brain barrier distribution and antinociceptive effect of morphine in the rat. *Drug Metab Dispos* **27:**827-834.

Letrent SP, Polli JW, Humphreys JE, Pollack GM, Brouwer KR and Brouwer KL (1999b) P-glycoprotein-mediated transport of morphine in brain capillary endothelial cells. *Biochem Pharmacol* **58:**951-957.

Levran O, O'Hara K, Peles E, Li D, Barral S, Ray B, Borg L, Ott J, Adelson M and Kreek MJ (2008) ABCB1 (MDR1) genetic variants are associated with methadone doses required for effective treatment of heroin dependence. *Hum Mol Genet* **17:**2219-2227.

Lin JH and Yamazaki M (2003a) Clinical relevance of P-glycoprotein in drug therapy. *Drug Metabolism Reviews* **35:**417-454.

Lin JH and Yamazaki M (2003b) Role of P-glycoprotein in pharmacokinetics: clinical implications. *Clinical Pharmacokinetics* **42:**59-98.

Ling W, Wesson DR, Charuvastra C and Klett CJ (1996) A controlled trial comparing buprenorphine and methadone maintenance in opioid dependence. *Archives of General Psychiatry* **53:**401-407.

Lintzeris N, Clark N, Winstock A, Dunlop A, Muhleisen P, Gowing L, Ali R, Ritter A, Bell J, Quigley A, Mattick R, Monheit B and White J (2006) National clinical guidelines and procedures for the use of buprenorphine in the treatment of opioid dependence, National Drug Strategy, Australian Government Department of Health and Ageing, Canberra.

Lintzeris N, Lenne M and Ritter A (1999) Methadone injecting in Australia: a tale of two cities. *Addiction* **94:**1175-1178.

Liu B, Sun D, Xia W, Hung MC and Yu D (1997) Cross-reactivity of C219 anti-p170(mdr-1) antibody with p185(c-erbB2) in breast cancer cells: cautions on evaluating p170(mdr-1). *J Natl Cancer Inst* **89:**1524-1529.

Livak KJ and Schmittgen TD (2001) Analysis of relative gene expression data using real-time quantitative PCR and the 2(-Delta Delta C(T)) Method. *Methods* **25**:402-408.

Lockridge O, Mottershaw-Jackson N, Eckerson HW and La Du BN (1980) Hydrolysis of diacetylmorphine (heroin) by human serum cholinesterase. *J Pharmacol Exp Ther* **215:**1-8.

Lopatko OV, White JM, Huber A and Ling W (2003) Opioid effects and opioid withdrawal during a 24 h dosing interval in patients maintained on buprenorphine. *Drug Alcohol Depend* **69:**317-322.

Lötsch J, Skarke C, Wieting J, Oertel BG, Schmidt H, Brockmoller J and Geisslinger G (2006) Modulation of the central nervous effects of levomethadone by genetic polymorphisms potentially affecting its metabolism, distribution, and drug action. *Clin Pharmacol Ther* **79:**72-89.

Lown KS, Thummel KE, Benedict PE, Shen DD, Turgeon DK, Berent S and Watkins PB (1995) The erythromycin breath test predicts the clearance of midazolam. *Clin Pharmacol Ther* **57:**16-24.

Magura S, Nwakeze PC and Demsky SY (1998) Pre- and in-treatment predictors of retention in methadone treatment using survival analysis. *Addiction* **93:**51-60.

Magura S, Nwakeze PC, Kang SY and Demsky S (1999) Program quality effects on patient outcomes during methadone maintenance: a study of 17 clinics. *Subst Use Misuse* **34:**1299-1324.

Maldonado R (1997) Participation of noradrenergic pathways in the expression of opiate withdrawal: biochemical and pharmacological evidence. *Neurosci Biobehav Rev* **21:**91-104.

Mansour A, Khachaturian H, Lewis ME, Akil H and Watson SJ (1987) Autoradiographic differentiation of mu, delta, and kappa opioid receptors in the rat forebrain and midbrain. *J Neurosci* **7:**2445-2464.

Martin-Facklam M, Burhenne J, Ding R, Fricker R, Mikus G, Walter-Sack I and Haefeli WE (2002) Dose-dependent increase of saquinavir bioavailability by the pharmaceutic aid cremophor EL. *Br J Clin Pharmacol* **53:**576-581.

Martin C, Berridge G, Higgins CF and Callaghan R (1997) The multi-drug resistance reversal agent SR33557 and modulation of vinca alkaloid binding to P-glycoprotein by an allosteric interaction. *Br J Pharmacol* **122:**765-771.

Marzolini C, Paus E, Buclin T and Kim RB (2004) Polymorphisms in human MDR1 (P-glycoprotein): recent advances and clinical relevance. *Clin Pharmacol Ther* **75:**13-33.

Mattick R, Digiusto E, Doran C, O'Brien S, Shanahan M, Kimber J, Henderson N, Breen C, Shearer J, Gates J, Shakeshaft A and Investigators NT (2001) National Evaluation of Pharmacotherapies for Opioid Dependence: Report of Results and Recommendations, National Drug and Alcohol Research Centre, Sydney.

Mattick R, Kimber J, Breen C and Davoli M (2004) Buprenorphine maintenance versus placebo or methadone maintenance for opioid dependence. *Cochrane Database of Systemic Reviews* **3:**CD002207.

Mattick RP, Ali R, White JM, O'Brien S, Wolk S and Danz C (2003) Buprenorphine versus methadone maintenance therapy: a randomized double-blind trial with 405 opioid-dependent patients. *Addiction* **98:**441-452.

Maxwell DL, Gilmour-White SK and Hall MR (1989) Digoxin toxicity due to interaction of digoxin with erythromycin. *Bmj* **298:**572.

McCance-Katz EF, Farber S, Selwyn PA and O'Connor A (2000) Decrease in methodone levels with nelfinavir mesylate. *Am J Psychiatry* **157:**481.

McCance-Katz EF, Rainey PM, Smith P, Morse G, Friedland G, Gourevitch M and Jatlow P (2004) Drug interactions between opioids and antiretroviral medications: interaction between methadone, LAAM, and nelfinavir. *Am J Addict* **13:**163-180.

Meier Y, Pauli-Magnus C, Zanger UM, Klein K, Schaeffeler E, Nussler AK, Nussler N, Eichelbaum M, Meier PJ and Stieger B (2006) Interindividual variability of canalicular ATP-binding-cassette (ABC)-transporter expression in human liver. *Hepatology* **44:**62-74.

Meineke I, Freudenthaler S, Hofmann U, Schaeffeler E, Mikus G, Schwab M, Prange HW, Gleiter CH and Brockmoller J (2002) Pharmacokinetic modelling of morphine, morphine-3-glucuronide and morphine-6-glucuronide in plasma and cerebrospinal fluid of neurosurgical patients after short-term infusion of morphine. *Br J Clin Pharmacol* **54:**592-603.

Meissner K, Jedlitschky G, Meyer zu Schwabedissen H, Dazert P, Eckel L, Vogelgesang S, Warzok RW, Bohm M, Lehmann C, Wendt M, Cascorbi I and Kroemer HK (2004) Modulation of multidrug resistance P-glycoprotein 1 (ABCB1) expression in human heart by hereditary polymorphisms. *Pharmacogenetics* **14:**381-385.

Meresaar U, Nilsson MI, Holmstrand J and Anggard E (1981) Single dose pharmacokinetics and bioavailability of methadone in man studied with a stable isotope method. *Eur J Clin Pharmacol* **20:**473-478.

Merry C, Barry MG, Mulcahy F, Ryan M, Heavey J, Tjia JF, Gibbons SE, Breckenridge AM and Back DJ (1997) Saquinavir pharmacokinetics alone and in combination with ritonavir in HIV-infected patients. *Aids* **11:**F29-33.

Mitchell TB, Dyer KR, Newcombe D, Salter A, Somogyi AA, Bochner F and White JM (2004) Subjective and physiological responses among racemic-methadone maintenance patients in relation to relative (S)- vs. (R)-methadone exposure. *Br J Clin Pharmacol* **58:**609-617.

Moody DE, Alburges ME, Parker RJ, Collins JM and Strong JM (1997) The involvement of cytochrome P450 3A4 in the N-demethylation of L-alpha-acetylmethadol (LAAM), norLAAM, and methadone. *Drug Metab Dispos* **25:**1347-1353.

Moore TJ, Ritter A and Caulkins JP (2007) The costs and consequences of three policy options for reducing heroin dependency. *Drug Alcohol Rev* **26:**369-378.

Morton EB (2007) The clinical pharmacology of methadone induction, in: *School of Medical Sciences, Discipline of Pharmacology*, University of Adelaide, Adelaide.

Nair MP, Laing TJ and Schwartz SA (1986) Decreased natural and antibody-dependent cellular cytotoxic activities in intravenous drug abusers. *Clin Immunol Immunopathol* **38:**68-78.

NCBI (2010) Single Nucleotide Polymorphism Database (dbSNP) of Nucleotide Sequence Variation (Build 130) of the National Center for Biotechnology Information. URL: http://www.ncbi.nlm.nih.gov/projects/SNP/snp_ref.cgi?locusId=5243. Last accessed January 2010.

Nekhayeva IA, Nanovskaya TN, Hankins GD and Ahmed MS (2006) Role of human placental efflux transporter P-glycoprotein in the transfer of buprenorphine, levo-alpha-acetylmethadol, and paclitaxel. *Am J Perinatol* **23:**423-430.

NHMRC (2001) *Australian Alcohol Guidelines: Health Risks and Benefits*. National Helath and Medical Research Council, Canberra.

Nilsson MI, Anggard E, Holmstrand J and Gunne LM (1982) Pharmacokinetics of methadone during maintenance treatment: adaptive changes during the induction phase. *Eur J Clin Pharmacol* **22:**343-349.

NSW Department of Health (2006) New South Wales Opioid Treatment Program: Clinical guidelines for methadone and buprenorphine treatment of opioid dependence. Mental Health and Drug & Alcohol Office, NSW Department of Health, North Sydney.

Ohkawa T, Seki S, Dobashi H, Koike Y, Habu Y, Ami K, Hiraide H and Sekine I (2001) Systematic characterization of human CD8+ T cells with natural killer cell markers in comparison with natural killer cells and normal CD8+ T cells. *Immunology* **103:**281-290.

Ohtani M, Kotaki H, Sawada Y and Iga T (1995) Comparative analysis of buprenorphine- and norbuprenorphine-induced analgesic effects based on pharmacokinetic-pharmacodynamic modeling. *J Pharmacol Exp Ther* **272:**505-510.

Okura T, Morita Y, Ito Y, Kagawa Y and Yamada S (2009) Effects of quinidine on antinociception and pharmacokinetics of morphine in rats. *J Pharm Pharmacol* **61:**593-597.

Oldendorf WH, Hyman S, Braun L and Oldendorf SZ (1972) Blood-brain barrier: penetration of morphine, codeine, heroin, and methadone after carotid injection. *Science* **178:**984-986.

Olds ME (1982) Reinforcing effects of morphine in the nucleus accumbens. *Brain Res* **237:**429-440.

Ortega I, Rodriguez M, Suarez E, Perez-Ruixo JJ and Calvo R (2007) Modeling methadone pharmacokinetics in rats in presence of P-glycoprotein inhibitor valspodar. *Pharm Res* **24:**1299-1308.

Ouyang H, Andersen TE, Chen W, Nofsinger R, Steffansen B and Borchardt RT (2009) A comparison of the effects of p-glycoprotein inhibitors on the blood-brain barrier permeation of cyclic prodrugs of an opioid peptide (DADLE). *J Pharm Sci* **98:**2227-2236.

Owen A, Chandler B, Back DJ and Khoo SH (2004a) Expression of pregnane-X-receptor transcript in peripheral blood mononuclear cells and correlation with *MDR1* mRNA. *Antivir Ther* **9:**819-21.

Owen A, Chandler B, Bray PG, Ward SA, Hart CA, Back DJ and Khoo SH (2004b) Functional correlation of P-glycoprotein expression and genotype with expression of the human immunodeficiency virus type 1 coreceptor CXCR4. *J Virol* 78:12022-9.

Owen A, Goldring C, Morgan P, Chadwick D, Park BK and Pirmohamed M (2005) Relationship between the C3435T and G2677T(A) polymorphisms in the *ABCB1* gene and P-glycoprotein expression in human liver. *British Journal of Clinical Pharmacology* **59:**365-370.

Park SW, Lomri N, Simeoni LA, Fruehauf JP and Mechetner E (2003) Analysis of P-glycoprotein-mediated membrane transport in human peripheral blood lymphocytes using the UIC2 shift assay. *Cytometry A* **53:**67-78.

Pattinson KT (2008) Opioids and the control of respiration. *Br J Anaesth* **100:**747-758.

Pauli-Magnus C, Feiner J, Brett C, Lin E and Kroetz DL (2003) No effect of *MDR1* C3435T variant on loperamide disposition and central nervous system effects. *Clinical Pharmacology and Therapeutics* **74:**487-498.

Polli JW, Jarrett JL, Studenberg SD, Humphreys JE, Dennis SW, Brouwer KR and Woolley JL (1999) Role of P-glycoprotein on the CNS disposition of amprenavir (141W94), an HIV protease inhibitor. *Pharm Res* **16:**1206-1212.

Polli JW, Wring SA, Humphreys JE, Huang L, Morgan JB, Webster LO and Serabjit-Singh CS (2001) Rational use of in vitro P-glycoprotein assays in drug discovery. *J Pharmacol Exp Ther* **299:**620-628.

Pontieri FE, Tanda G and Di Chiara G (1995) Intravenous cocaine, morphine, and amphetamine preferentially increase extracellular dopamine in the "shell" as compared with the "core" of the rat nucleus accumbens. *Proc Natl Acad Sci U S A* **92:**12304-12308.

Quinn DI, Wodak A and Day RO (1997) Pharmacokinetic and pharmacodynamic principles of illicit drug use and treatment of illicit drug users. *Clin Pharmacokinet* **33:**344-400.

Rahi M, Heikkinen T, Hakkola J, Hakala K, Wallerman O, Wadelius M, Wadelius C and Laine K (2008) Influence of adenosine triphosphate and ABCB1 (MDR1) genotype on the P-glycoprotein-dependent transfer of saquinavir in the dually perfused human placenta. *Hum Exp Toxicol* **27:**65-71.

Rang HP, Dale MM and Ritter JM (1999) *Pharmacology*. Churchill Livingstone, Sydney.

Rang HP, Dale MM, Ritter JM and Moore PK (2003) *Pharmacology*. Churchill Livingstone, Sydney.

Raymond M and Rousset F (1995) An exact test for population differentiation. *Evolution* **49:**1280-1283.

Reckitt-Benckiser (2005) Buprenorphine monograph [online] Available from URL: http://www.fda.gov/cder/foi/label/2002/20732lbl.pdf. [Accessed 2005 May 17].

Redmond DE, Jr. and Krystal JH (1984) Multiple mechanisms of withdrawal from opioid drugs. *Annu Rev Neurosci* **7:**443-478.

Rhoades HM, Creson D, Elk R, Schmitz J and Grabowski J (1998) Retention, HIV risk, and illicit drug use during treatment: methadone dose and visit frequency. *Am J Public Health* **88:**34-39.

Riddell S, Shanahan M, Degenhardt L and Roxburgh A (2008) Estimating the costs of drug-related hospital separations in Australia. *Aust N Z J Public Health* **32:**156-161.

Riley J, Styles J, Verschoyle RD, Stanley LA, White IN and Gant TW (2000) Association of tamoxifen biliary excretion rate with prior tamoxifen exposure and increased mdr1b expression. *Biochem Pharmacol* **60:**233-239.

Rodriguez M, Ortega I, Soengas I, Suarez E, Lukas JC and Calvo R (2004) Effect of P-glycoprotein inhibition on methadone analgesia and brain distribution in the rat. *Journal of Pharmacy and Pharmacology* **56:**367-374.

Rook EJ, Huitema AD, van den Brink W, van Ree JM and Beijnen JH (2006) Pharmacokinetics and pharmacokinetic variability of heroin and its metabolites: review of the literature. *Curr Clin Pharmacol* **1:**109-118.

Ross J, Teesson M, Darke S, Lynskey M, Ali R, Ritter A and Cooke R (2005) The characteristics of heroin users entering treatment: findings from the Australian treatment outcome study (ATOS). *Drug Alcohol Rev* **24:**411-418.

Ross JR, Riley J, Taegetmeyer AB, Sato H, Gretton S, du Bois RM and Welsh KI (2008) Genetic variation and response to morphine in cancer patients: catechol-O-methyltransferase and multidrug resistance-1 gene polymorphisms are associated with central side effects. *Cancer* **112:**1390-1403.

Roth-Deri I, Green-Sadan T and Yadid G (2008) Beta-endorphin and drug-induced reward and reinforcement. *Prog Neurobiol* **86:**1-21.

Sadeque AJ, Wandel C, He H, Shah S and Wood AJ (2000) Increased drug delivery to the brain by P-glycoprotein inhibition. *Clinical Pharmacology and Therapeutics* **68:**231-237.

Sakurai A, Onishi Y, Hirano H, Seigneuret M, Obanayama K, Kim G, Liew EL, Sakaeda T, Yoshiura K, Niikawa N, Sakurai M and Ishikawa T (2007) Quantitative structure--activity relationship analysis and molecular dynamics simulation to functionally validate nonsynonymous polymorphisms of human ABC transporter ABCB1 (P-glycoprotein/MDR1). *Biochemistry* **46:**7678-7693.

Salama NN, Yang Z, Bui T and Ho RJ (2006) MDR1 haplotypes significantly minimize intracellular uptake and transcellular P-gp substrate transport in recombinant LLC-PK1 cells. *J Pharm Sci* **95:**2293-2308.

Sasongko L, Link JM, Muzi M, Mankoff DA, Yang X, Collier AC, Shoner SC and Unadkat JD (2005) Imaging P-glycoprotein transport activity at the human blood-brain barrier with positron emission tomography. *Clin Pharmacol Ther* **77:**503-514.

Sauna ZE, Kimchi-Sarfaty C, Ambudkar SV and Gottesman MM (2007) The sounds of silence: synonymous mutations affect function. *Pharmacogenomics* **8:**527-532.

Schinkel AH, Mayer U, Wagenaar E, Mol CA, van Deemter L, Smit JJ, van der Valk MA, Voordouw AC, Spits H, van Tellingen O, Zijlmans JM, Fibbe WE and Borst P (1997) Normal viability and altered pharmacokinetics in mice lacking mdr1-type (drug-transporting) P-glycoproteins. *Proc Natl Acad Sci U S A* **94:**4028-4033.

Schinkel AH, Roelofs EM and Borst P (1991) Characterization of the human MDR3 P-glycoprotein and its recognition by P-glycoprotein-specific monoclonal antibodies. *Cancer Res* **51:**2628-2635.

Schinkel AH, Smit JJ, van Tellingen O, Beijnen JH, Wagenaar E, van Deemter L, Mol CA, van der Valk MA, Robanus-Maandag EC, te Riele HP and et al. (1994) Disruption of the mouse *mdr1a* P-glycoprotein gene leads to a deficiency in the blood-brain barrier and to increased sensitivity to drugs. *Cell* **77:**491-502.

Schinkel AH, Wagenaar E, van Deemter L, Mol CA and Borst P (1995) Absence of the mdr1a P-Glycoprotein in mice affects tissue distribution and pharmacokinetics of dexamethasone, digoxin, and cyclosporin A. *J Clin Invest* **96:**1698-1705.

Schuetz EG, Furuya KN and Schuetz JD (1995) Interindividual variation in expression of P-glycoprotein in normal human liver and secondary hepatic neoplasms. *J Pharmacol Exp Ther* **275:**1011-1018.

Schuh KJ, Walsh SL and Stitzer ML (1999) Onset, magnitude and duration of opioid blockade produced by buprenorphine and naltrexone in humans. *Psychopharmacology (Berl)* **145:**162-174.

Schwab D, Fischer H, Tabatabaei A, Poli S and Huwyler J (2003) Comparison of in vitro P-glycoprotein screening assays: recommendations for their use in drug discovery. *J Med Chem* **46:**1716-1725.

Schwarz UI, Gramatte T, Krappweis J, Oertel R and Kirch W (2000) P-glycoprotein inhibitor erythromycin increases oral bioavailability of talinolol in humans. *Int J Clin Pharmacol Ther* **38:**161-167.

Seelbach MJ, Brooks TA, Egleton RD and Davis TP (2007) Peripheral inflammatory hyperalgesia modulates morphine delivery to the brain: a role for P-glycoprotein. *J Neurochem* **102:**1677-1690.

Seelig A (1998) How does P-glycoprotein recognize its substrates? *Int J Clin Pharmacol Ther* **36:**50-54.

Shapiro AB, Fox K, Lam P and Ling V (1999) Stimulation of P-glycoprotein-mediated drug transport by prazosin and progesterone. Evidence for a third drug-binding site. *Eur J Biochem* **259:**841-850.

Sipe BE, Jones RJ and Bokhart GH (2003) Rhabdomyolysis causing AV blockade due to possible atorvastatin, esomeprazole, and clarithromycin interaction. *Ann Pharmacother* **37:**808-811.

Skarke C, Jarrar M, Erb K, Schmidt H, Geisslinger G and Lötsch J (2003a) Respiratory and miotic effects of morphine in healthy volunteers when P-glycoprotein is blocked by quinidine. *Clinical Pharmacology and Therapeutics* **74:**303-311.

Skarke C, Jarrar M, Schmidt H, Kauert G, Langer M, Geisslinger G and Lotsch J (2003b) Effects of ABCB1 (multidrug resistance transporter) gene mutations on disposition and central nervous effects of loperamide in healthy volunteers. *Pharmacogenetics* **13:**651-660.

Somogyi AA, Barratt DT and Coller JK (2007) Pharmacogenetics of opioids. *Clin Pharmacol Ther* **81:**429-444.

Somogyvari-Vigh A, Kastin AJ, Liao J, Zadina JE and Pan W (2004) Endomorphins exit the brain by a saturable efflux system at the basolateral surface of cerebral endothelial cells. *Exp Brain Res* **156:**224-230.

Sparreboom A, van Asperen J, Mayer U, Schinkel AH, Smit JW, Meijer DK, Borst P, Nooijen WJ, Beijnen JH and van Tellingen O (1997) Limited oral bioavailability and active epithelial excretion of paclitaxel (Taxol) caused by P-glycoprotein in the intestine. *Proc Natl Acad Sci U S A* **94:**2031-2035.

Stafford J and Burns L (2009) An overview of the 2009 IDRS: the Injecting Drug User survey preliminary findings, in: *Drug Trends Bulletin*, National Drug and Alcohol Research Centre, University of New South Wales, Sydney.

Stephens M and Donnely P (2003) A comparison of bayesian methods for haplotype reconstruction. *American Journal of Human Genetics* **73:**1162-1169.

Stephens M, Smith N and Donnely P (2001) A new statistical method for haplotype reconstruction from population data. *American Journal of Human Genetics* **68:**978-989.

Sternini C (2001) Receptors and transmission in the brain-gut axis: potential for novel therapies. III. Mu-opioid receptors in the enteric nervous system. *Am J Physiol Gastrointest Liver Physiol* **281:**G8-15.

Stevens KE, Shiotsu G and Stein L (1991) Hippocampal mu-receptors mediate opioid reinforcement in the CA3 region. *Brain Res* **545:**8-16.

Stormer E, Perloff MD, von Moltke LL and Greenblatt DJ (2001) Methadone inhibits rhodamine123 transport in Caco-2 cells. *Drug Metab Dispos* **29:**954-956.

Sudchada P, Oo-puthinan S, Kerdpin O and Saelim N (2010) *ABCB1* gene expression in peripheral blood mononuclear cells in healthy Thai males and females. *Genet Mol Res* **9:**1177-85.

Sullivan HR and Due SL (1973) Urinary metabolites of dl-methadone in maintenance subjects. *J Med Chem* **16:**909-913.

Sullivan HR, Due SL and McMahon RE (1972) The identification of three new metabolites of methadone in man and in the rat. *J Am Chem Soc* **94:**4050-4051.

Suzuki T, Zaima C, Moriki Y, Fukami T and Tomono K (2007) P-glycoprotein mediates brain-to-blood efflux transport of buprenorphine across the blood-brain barrier. *J Drug Target* **15:**67-74.

Swegle JM and Logemann C (2006) Management of common opioid-induced adverse effects. *Am Fam Physician* **74:**1347-1354.

Takano M, Yumoto R and Murakami T (2006) Expression and function of efflux drug transporters in the intestine. *Pharmacol Ther* **109:**137-161.

Takara K, Tsujimoto M, Ohnishi N and Yokoyama T (2002) Digoxin up-regulates MDR1 in human colon carcinoma Caco-2 cells. *Biochem Biophys Res Commun* **292:**190-194.

Tanabe M, Ieiri I, Nagata N, Inoue K, Ito S, Kanamori Y, Takahashi M, Kurata Y, Kigawa J, Higuchi S, Terakawa N and Otsubo K (2001) Expression of P-glycoprotein in human placenta: relation to genetic polymorphism of the multidrug resistance (MDR)-1 gene. *Journal of Pharmacology and Experimental Therapeutics* **297:**1137-1143.

Tanda G, Pontieri FE and Di Chiara G (1997) Cannabinoid and heroin activation of mesolimbic dopamine transmission by a common mu1 opioid receptor mechanism. *Science* **276:**2048-2050.

Tanigawara Y (2000) Role of P-glycoprotein in drug disposition. *Ther Drug Monit* **22:**137-140.

Teesson M, Ross J, Darke S, Lynskey M, Ali R, Ritter A and Cooke R (2006) One year outcomes for heroin dependence: findings from the Australian Treatment Outcome Study (ATOS). *Drug Alcohol Depend* **83:**174-180.

Tennant F, Shannon J, Nork J, Sagherian A and Berman M (1991) Abnormal adrenal gland metabolism in opioid addicts: implications for clinical treatment. *Journal of Psychoactive Drugs* **23:**135-149.

Theis JG, Chan HS, Greenberg ML, Malkin D, Karaskov V, Moncica I, Koren G and Doyle J (1998) Increased systemic toxicity of sarcoma chemotherapy due to combination with the P-glycoprotein inhibitor cyclosporin. *Int J Clin Pharmacol Ther* **36:**61-64.

Theodorou S and Haber PS (2005) The medical complications of heroin use. *Curr Opin Psychiatry* **18:**257-263.

Thiebaut F, Tsuruo T, Hamada H, Gottesman MM, Pastan I and Willingham MC (1987) Cellular localization of the multidrug-resistance gene product P-glycoprotein in normal human tissues. *Proceedings of the National Academy of Sciences of the United States of America* **84:**7735-7738.

Thiebaut F, Tsuruo T, Hamada H, Gottesman MM, Pastan I and Willingham MC (1989) Immunohistochemical localization in normal tissues of different epitopes in the multidrug transport protein P170: evidence for localization in brain capillaries and crossreactivity of one antibody with a muscle protein. *J Histochem Cytochem* **37:**159-164.

Thompson SJ, Koszdin K and Bernards CM (2000) Opiate-induced analgesia is increased and prolonged in mice lacking P-glycoprotein. *Anesthesiology* **92:**1392-1399.

Thorn M, Finnstrom N, Lundgren S, Rane A and Loof L (2005) Cytochromes P450 and MDR1 mRNA expression along the human gastrointestinal tract. *Br J Clin Pharmacol* **60:**54-60.

Thummel KE, O'Shea D, Paine MF, Shen DD, Kunze KL, Perkins JD and Wilkinson GR (1996) Oral first-pass elimination of midazolam involves both gastrointestinal and hepatic CYP3A-mediated metabolism. *Clin Pharmacol Ther* **59:**491-502.

Thummel KE, Shen DD, Podoll TD, Kunze KL, Trager WF, Bacchi CE, Marsh CL, McVicar JP, Barr DM, Perkins JD and et al. (1994a) Use of midazolam as a human cytochrome P450 3A probe: II. Characterization of inter- and intraindividual hepatic CYP3A variability after liver transplantation. *J Pharmacol Exp Ther* **271:**557-566.

Thummel KE, Shen DD, Podoll TD, Kunze KL, Trager WF, Hartwell PS, Raisys VA, Marsh CL, McVicar JP, Barr DM and et al. (1994b) Use of midazolam as a human cytochrome P450 3A probe: I. In vitro-in vivo correlations in liver transplant patients. *J Pharmacol Exp Ther* **271:**549-556.

Tournier N, Chevillard L, Megarbane B, Pirnay S, Scherrmann JM and Decleves X (2009) Interaction of drugs of abuse and maintenance treatments with human P-glycoprotein (ABCB1) and breast cancer resistance protein (ABCG2). *Int J Neuropsychopharmacol***:**1-11.

Trang T, Quirion R and Jhamandas K (2005) The spinal basis of opioid tolerance and physical dependence: Involvement of calcitonin gene-related peptide, substance P, and arachidonic acid-derived metabolites. *Peptides* **26:**1346-1355.

Trescot AM, Datta S, Lee M and Hansen H (2008) Opioid pharmacology. *Pain Physician* **11:**S133-153.

Troost J, Albermann N, Emil Haefeli W and Weiss J (2004) Cholesterol modulates P-glycoprotein activity in human peripheral blood mononuclear cells. *Biochem Biophys Res Commun* **316:**705-711.

True WR, Heath AC, Scherrer JF, Xian H, Lin N, Eisen SA, Lyons MJ, Goldberg J and Tsuang MT (1999a) Interrelationship of genetic and environmental influences on conduct disorder and alcohol and marijuana dependence symptoms. *Am J Med Genet* **88:**391-397.

True WR, Xian H, Scherrer JF, Madden PA, Bucholz KK, Heath AC, Eisen SA, Lyons MJ, Goldberg J and Tsuang M (1999b) Common genetic vulnerability for nicotine and alcohol dependence in men. *Arch Gen Psychiatry* **56:**655-661.

Ueda CT, Williamson BJ and Dzindzio BS (1976) Absolute quinidine bioavailability. *Clin Pharmacol Ther* **20:**260-265.

Umbricht A, Huestis MA, Cone EJ and Preston KL (2004) Effects of high-dose intravenous buprenorphine in experienced opioid abusers. *J Clin Psychopharmacol* **24:**479-487.

UNODC (2008) *Global Illicit Drug Trends 2008*, United Nations Office on Drugs and Crime, New York.

Vaclavikova R, Nordgard SH, Alnaes GI, Hubackova M, Kubala E, Kodet R, Mrhalova M, Novotny J, Gut I, Kristensen VN and Soucek P (2008) Single nucleotide polymorphisms in the multidrug resistance gene 1 (ABCB1): effects on its expression and clinicopathological characteristics in breast cancer patients. *Pharmacogenet Genomics* **18:**263-273.

Vallejo R, de Leon-Casasola O and Benyamin R (2004) Opioid therapy and immunosuppression: a review. *Am J Ther* **11:**354-365.

van Asperen J, van Tellingen O and Beijnen JH (2000) The role of mdr1a P-glycoprotein in the biliary and intestinal secretion of doxorubicin and vinblastine in mice. *Drug Metab Dispos* **28:**264-267.

van der Kooy D, Mucha RF, O'Shaughnessy M and Bucenieks P (1982) Reinforcing effects of brain microinjections of morphine revealed by conditioned place preference. *Brain Res* **243:**107-117.

Vandesompele J, De Preter K, Pattyn F, Poppe B, Van Roy N, De Paepe A and Speleman F (2002) Accurate normalization of real-time quantitative RT-PCR data by geometric averaging of multiple internal control genes. *Genome Biol* **3:**RESEARCH0034.

Verebely K, Volavka J, Mule S and Resnick R (1975) Methadone in man: pharmacokinetic and excretion studies in acute and chronic treatment. *Clin Pharmacol Ther* **18:**180-190.

Verster A and Buning E (2003) Information for policymakers on the effectiveness of substitution treatment for opiate dependence, EuroMethwork, Amsterdam.

Vogelgesang S, Cascorbi I, Schroeder E, Pahnke J, Kroemer HK, Siegmund W, Kunert-Keil C, Walker LC and Warzok RW (2002) Deposition of Alzheimer's beta-amyloid is inversely

correlated with P-glycoprotein expression in the brains of elderly non-demented humans. *Pharmacogenetics* **12:**535-541.

Vogelgesang S, Kunert-Keil C, Cascorbi I, Mosyagin I, Schroder E, Runge U, Jedlitschky G, Kroemer HK, Oertel J, Gaab MR, Pahnke J, Walker LC and Warzok RW (2004) Expression of multidrug transporters in dysembryoplastic neuroepithelial tumors causing intractable epilepsy. *Clin Neuropathol* **23:**223-231.

Volkow ND, Fowler JS and Wang GJ (2003) The addicted human brain: insights from imaging studies. *J Clin Invest* **111:**1444-1451.

WA Drug and Alcohol Office (2007) Western Australia clinical policies and procedures for the use of methadone and buprenorphine in the treatment of opioid dependence, WA Drug and Alcohol Office, Mt Lawley.

Wakasugi H, Yano I, Ito T, Hashida T, Futami T, Nohara R, Sasayama S and Inui K (1998) Effect of clarithromycin on renal excretion of digoxin: interaction with P-glycoprotein. *Clin Pharmacol Ther* **64:**123-128.

Walle UK, French KL, Walgren RA and Walle T (1999a) Transport of genistein-7-glucoside by human intestinal CACO-2 cells: potential role for MRP2. *Res Commun Mol Pathol Pharmacol* **103:**45-56.

Walle UK, Galijatovic A and Walle T (1999b) Transport of the flavonoid chrysin and its conjugated metabolites by the human intestinal cell line Caco-2. *Biochem Pharmacol* **58:**431-438.

Walsh SL, Preston KL, Bigelow GE and Stitzer ML (1995) Acute administration of buprenorphine in humans: partial agonist and blockade effects. *J Pharmacol Exp Ther* **274:**361-372.

Walter E and Kissel T (1995) Heterogeneity in the human intestinal cell line Caco-2 leads to differences in transepithelial transport. *European Journal of Pharmaceutical Sciences* **3:**230.

Wandel C, Kim RB, Kajiji S, Guengerich P, Wilkinson GR and Wood AJ (1999) P-glycoprotein and cytochrome P-450 3A inhibition: dissociation of inhibitory potencies. *Cancer Res* **59:**3944-3948.

Wang D, Johnson AD, Papp AC, Kroetz DL and Sadee W (2005) Multidrug resistance polypeptide 1 (*MDR1, ABCB1*) variant 3435C>T affects mRNA stability. *Pharmacogenet Genomics* **15:**693-704.

Wang D and Sadee W (2006) Searching for polymorphisms that affect gene expression and mRNA processing: example *ABCB1* (*MDR1*). *Aaps J* **8:**E515-520.

Wang JS, Ruan Y, Taylor RM, Donovan JL, Markowitz JS and DeVane CL (2004) Brain penetration of methadone (R)- and (S)-enantiomers is greatly increased by P-glycoprotein deficiency in the blood-brain barrier of Abcb1a gene knockout mice. *Psychopharmacology (Berl)* **173:**132-138.

Wang RB, Kuo CL, Lien LL and Lien EJ (2003) Structure-activity relationship: analyses of p-glycoprotein substrates and inhibitors. *J Clin Pharm Ther* **28:**203-228.

Ward J, Mattick RP and Hall W (1998) *Methadone Maintenance Treatment and Other Opioid Replacement Therapies*. Harwood Academic Publishers, Amsterdam.

Way EL, Loh HH and Shen FH (1969) Simultaneous quantitative assessment of morphine tolerance and physical dependence. *J Pharmacol Exp Ther* **167:**1-8.

Weiss J, Dormann SM, Martin-Facklam M, Kerpen CJ, Ketabi-Kiyanvash N and Haefeli WE (2003) Inhibition of P-glycoprotein by newer antidepressants. *J Pharmacol Exp Ther* **305:**197-204.

Wetterich U, Spahn-Langguth H, Mutschler E, Terhaag B, Rosch W and Langguth P (1996) Evidence for intestinal secretion as an additional clearance pathway of talinolol enantiomers: concentration- and dose-dependent absorption in vitro and in vivo. *Pharm Res* **13:**514-522.

White JM and Irvine RJ (1999) Mechanisms of fatal opioid overdose. *Addiction* **94:**961-972.

Whiteside TL and Herberman RB (1989) The role of natural killer cells in human disease. *Clin Immunol Immunopathol* **53:**1-23.

Wilson RC, Wei JQ, Cheng KC, Mercado AB and New MI (1995) Rapid deoxyribonucleic acid analysis by allele-specific polymerase chain reaction for detection of mutations in the steroid 21-hydroxylase gene. *J Clin Endocrinol Metab* **80:**1635-1640.

Wojnowski L (2004) Genetics of the variable expression of CYP3A in humans. *Ther Drug Monit* **26:**192-199.

Wojnowski L and Kamdem LK (2006) Clinical implications of CYP3A polymorphisms. *Expert Opin Drug Metab Toxicol* **2:**171-182.

Wolff K, Rostami-Hodjegan A, Hay AW, Raistrick D and Tucker G (2000) Population-based pharmacokinetic approach for methadone monitoring of opiate addicts: potential clinical utility. *Addiction* **95:**1771-1783.

Wolff K and Strang J (1999) Therapeutic drug monitoring for methadone: scanning the horizon. *Eur Addict Res* **5:**36-42.

Xie HG, Wood AJ, Kim RB, Stein CM and Wilkinson GR (2004) Genetic variability in CYP3A5 and its possible consequences. *Pharmacogenomics* **5:**243-272.

Xie R, Hammarlund-Udenaes M, de Boer AG and de Lange EC (1999) The role of P-glycoprotein in blood-brain barrier transport of morphine: transcortical microdialysis studies in mdr1a (-/-) and mdr1a (+/+) mice. *Br J Pharmacol* **128:**563-568.

Yamazaki M, Neway WE, Ohe T, Chen I, Rowe JF, Hochman JH, Chiba M and Lin JH (2001) *In vitro* substrate identification studies for p-glycoprotein-mediated transport: species difference and predictability of *in vivo* results. *Journal of Pharmacology and Experimental Therapeutics* **296:**723-735.

Yokogawa K, Takahashi M, Tamai I, Konishi H, Nomura M, Moritani S, Miyamoto K and Tsuji A (1999) P-glycoprotein-dependent disposition kinetics of tacrolimus: studies in mdr1a knockout mice. *Pharm Res* **16:**1213-1218.

Yousif S, Saubamea B, Cisternino S, Marie-Claire C, Dauchy S, Scherrmann JM and Decleves X (2008) Effect of chronic exposure to morphine on the rat blood-brain barrier: focus on the P-glycoprotein. *J Neurochem* **107:**647-657.

Zanger UM, Turpeinen M, Klein K and Schwab M (2008) Functional pharmacogenetics/genomics of human cytochromes P450 involved in drug biotransformation. *Anal Bioanal Chem* **392:**1093-1108.

Zanker B, Barth C, Stachowski J, Baldamus CA and Land W (1997) Multidrug resistance gene MDR1 expression: a gene transfection in vitro model and clinical analysis in cyclosporine-treated patients rejecting their renal grafts. *Transplant Proc* **29:**1507-8.

Zhang W, Ramamoorthy Y, Tyndale RF and Sellers EM (2003a) Interaction of buprenorphine and its metabolite norbuprenorphine with cytochromes p450 in vitro. *Drug Metab Dispos* **31:**768-772.

Zhang Z, Friedmann PD and Gerstein D (2003b) Does retention matter? Treatment duration and improvement in drug use. *Addiction* **98:**673-684.

Zhou SF (2008) Structure, function and regulation of P-glycoprotein and its clinical relevance in drug disposition. *Xenobiotica* **38:**802-832.

Appendix A: Supplementary tables

Table A-1. Clinically confirmed cytochrome P450-mediated drug-drug interactions affecting methadone pharmacokinetics.

Drug	Effect on [plasma]	Mechanism	Reference(s)
Efavirenz	Significant decrease	CYP3A4 &/or CYP2B6 induction	(Barry et al., 1999; Clarke & Mulcahy, 2000; Marzolini et al., 2000; Pinzani et al., 2000; Clarke et al., 2001; Boffito et al., 2002; Eap et al., 2002; McCance-Katz et al., 2002; Gerber et al., 2004)
Nevirapine	Significant decrease	CYP3A4 &/or CYP2B6 induction	(Staszewski et al., 1998; Altice et al., 1999; Heelon & Meade, 1999; Otero et al., 1999; Pinzani et al., 2000; Clarke et al., 2001; Eap et al., 2002; Gerber et al., 2004; Rotger et al., 2005)
Other antiretrovirals[a]	Moderate decrease	CYP450 induction	(Bart et al., 2001; Gourevitch, 2001; Eap et al., 2002; McCance-Katz et al., 2004; Brown et al., 2006; Hsyu et al., 2006; Cao et al., 2008; Jamois et al., 2009)
Phenobarbital	Significant decrease	CYP450 induction	(Alvares & Kappas, 1972; Liu & Wang, 1984; Faucette et al., 2004)
Phenytoin	Significant decrease	CYP3A4 &/or CYP2B6 induction	(Finelli, 1976; Tong et al., 1981; Kreek, 1986; Eap et al., 2002)
Carbamazepine	Significant decrease	CYP3A4 &/or CYP2B6 induction	(Preston et al., 1984; Kuhn et al., 1989)
Diazepam/midazolam	Significant increase	CYP3A4 inhibition	(Preston et al., 1984)
Ciprofloxacin	Significant increase	CYP1A2 & CYP3A4 inhibition	(Herrlin et al., 2000)
Rifampin (rifampicin)	Significant decrease	CYP450 induction	(Kreek et al., 1976; Bending & Skacel, 1977; Kreek, 1986; Holmes, 1990; Borg et al., 1995; Eap et al., 2002; Faucette et al., 2004)
Ketoconazole, fluconazole	Moderate increase	CYP3A4 inhibition	(Cobb et al., 1998; Katz, 1999; Gourevitch, 2001; Tarumi et al., 2002)
Paroxetine	Moderate increase	CYP2D6 inhibition	(Begre et al., 2002)
Sertraline	Moderate increase	CYP450 inhibition	(Hamilton et al., 2000)
Fluoxetine, fluvoxamine	Significant increase	CYP450 inhibition	(Eap et al., 1997)
Fusidic acid	Significant decrease	CYP450 induction	(Brockmeyer et al., 1991)
Grapefruit	Moderate increase	CYP3A4 inhibition	(Bailey et al., 1998; Dresser et al., 2000)

Moderate: alteration in plasma concentrations not generally requiring dose adjustment. Significant: large alteration in plasma concentrations requiring dose adjustment and/or precipitating opioid withdrawal. [a]Abacavir, amprenavir, didanosine, nelfinavir, ritonavir, indinavir, saquinavir and stavudine.

Table A-2. Summary of *in vitro* studies investigating the functional effects of *ABCB1* SNPs and haplotypes on P-glycoprotein expression and function.

			Phenotype		
SNP	**Cell line**	**Probe drug(s)**	**Expression**	**Function**	**Reference**
A61G	HeLa	Verapamil, daunorubicin, vinblastine, calcein-AM, prazosin, bisantrene, forskolin	No effect	No effect	(Kimchi-Sarfaty et al., 2002)
		Paclitaxel		A > G	
	HEK293T	Calcein	No effect	No effect	(Gow et al., 2008)
		Paclitaxel		No effect	
G1199A	HeLa	Verapamil, daunorubicin, vinblastine, calcein-AM, prazosin, bisantrene, forskolin	No effect	No effect	(Kimchi-Sarfaty et al., 2002)
		Paclitaxel		G > A	
	LLC-PK1	Rhodamine		G > A	
		Doxorubicin	No effect	No effect	(Woodahl et al., 2004)
		Vinblastine, vincristine		G < A	
	LLC-PK1	Amprenavir, indinavir, lopinavir, ritonavir, saquinavir	-	G < A	(Woodahl et al., 2005)
	HEK293T	Doxorubicin, paclitaxel, vinblastine, vincristine	-	G < A	(Crouthamel et al., 2006)
	HEK293T	Calcein	No effect	No effect	(Gow et al., 2008)
		Paclitaxel		No effect	
	Insect Sf9	Verapamil		G > A	
		Nicardipine	-	G ≥ A	(Sakurai et al., 2007)
		Vinblastine		No effect	
C1236T	LLC-PK1	Rhodamine, vinblastine, vincristine	-	C > T	(Salama et al., 2006)
	HeLa	Rhodamine, paclitaxel, verapamil, daunorubicin, vinblastine, calcein-AM	No effect	No effect	(Kimchi-Sarfaty et al., 2007)
G2677T	HEK293T	Digoxin	No effect	G < T	(Kim et al., 2001)
	HEK293T	Calcein	No effect	No effect	(Gow et al., 2008)

			Phenotype		
SNP	**Cell line**	**Probe drug(s)**	**Expression**	**Function**	**Reference**
		Paclitaxel		G > T	
	HeLa	Verapamil, daunorubicin, vinblastine, calcein-AM, prazosin, bisantrene, forskolin	No effect	No effect	(Kimchi-Sarfaty et al., 2002)
		Paclitaxel		G > T	
	HeLa	Calcein	-	No effect	(Kroetz et al., 2003)
	LLC-PK1	Verapamil, digoxin, vinblastine, cyclosporine	No effect	No effect	(Morita et al., 2003)
	LLC-PK1	Rhodamine, vinblastine, vincristine	-	G > T	(Salama et al., 2006)
	Insect HighFive	Vincristine	No effect	G > T	(Schaefer et al., 2006)
	Insect Sf9	Vasodilators[a], steroids[b], nicorandil, tacrolimus, paclitaxel	-	G > T	(Sakurai et al., 2007)
		Anticancer drugs[c] (except etoposide, actinomycin D & paclitaxel), pinacidil, quinidine, penicillin G, acetylsalicylic acid		No effect	
		NSAIDs[d] (except acetylsalicylic acid), etoposide, actinomycin D, p-aminohippuric acid, novobiocin		G < T	
	HeLa	Rhodamine, paclitaxel, verapamil, daunorubicin, vinblastine, calcein-AM	No effect	No effect	(Kimchi-Sarfaty et al., 2007)
	3T3 fibroblasts	Calcein	G > T	No effect	(Aird et al., 2008)
G2677A	HeLa	Verapamil, daunorubicin, vinblastine, calcein-AM, prazosin, bisantrene, forskolin	No effect	No effect	(Kimchi-Sarfaty et al., 2002)
		Paclitaxel		G > A	
	Insect HighFive	Vincristine	No effect	G > A	(Schaefer et al., 2006)
	Insect Sf9	Vasodilators[a] (except nifedipine), anticancer drugs[c], NSAIDs[d], betamethasone, prednisolone, pinacidil, quinidine, penicillin G, p-aminohippuric acid, novobiocin	-	G < A	(Sakurai et al., 2007)
		Dexamethasone, cortisone, nicorandil, tacrolimus, nifedipine		No effect	
	3T3 fibroblasts	Calcein	G > A	G > A	(Aird et al., 2008)
	HEK293T	Calcein	No effect	G < A	(Gow et al., 2008)
		Paclitaxel		No effect	

			Phenotype		
SNP	**Cell line**	**Probe drug(s)**	**Expression**	**Function**	**Reference**
C3435T	LLC-PK1	Verapamil, digoxin, vinblastine, cyclosporine	No effect	No effect	(Morita et al., 2003)
	LLC-PK1	Rhodamine, vinblastine, vincristine	-	C > T	(Salama et al., 2006)
	Liver	-	C > T	-	(Wang et al., 2005)
	HeLa	Rhodamine, paclitaxel, verapamil, daunorubicin, vinblastine, calcein-AM	No effect	No effect	(Kimchi-Sarfaty et al., 2007)
A61G/ G1199A	HeLa	Verapamil, daunorubicin, vinblastine, calcein-AM, prazosin, bisantrene, forskolin	No effect	No effect	(Kimchi-Sarfaty et al., 2002)
		Paclitaxel		AG > GA	
A61G/ G2677T	HeLa	Verapamil, daunorubicin, vinblastine, calcein-AM, prazosin, bisantrene, forskolin	No effect	No effect	(Kimchi-Sarfaty et al., 2002)
		Paclitaxel		AG > GT	
G1199A/ G2677T	HeLa	Verapamil, daunorubicin, vinblastine, calcein-AM, prazosin, bisantrene, forskolin	No effect	No effect	(Kimchi-Sarfaty et al., 2002)
		Paclitaxel		GG > AT	
C1236T/ G2677T	LLC-PK1	Rhodamine, vinblastine, vincristine	-	CG > TT	(Salama et al., 2006)
	HeLa	Rhodamine, paclitaxel, verapamil, daunorubicin, vinblastine, calcein-AM	No effect	No effect	(Kimchi-Sarfaty et al., 2007)
	3T3 fibroblasts	Calcein	CG > TT	CG > TT	(Aird et al., 2008)
C1236T/C 3435T	LLC-PK1	Rhodamine, vinblastine, vincristine	-	CC > TT	(Salama et al., 2006)
	HeLa	Rhodamine, paclitaxel, verapamil, daunorubicin, vinblastine, calcein-AM	No effect	No effect	(Kimchi-Sarfaty et al., 2007)
G2677T/ C3435T	LLC-PK1	Verapamil, digoxin, vinblastine, cyclosporine	No effect	No effect	(Morita et al., 2003)
	LLC-PK1	Rhodamine, vinblastine, vincristine	-	GC > TT	Salama et al. 2006
	HeLa	Rhodamine, paclitaxel, verapamil, daunorubicin, vinblastine, calcein-AM	No effect	No effect	(Kimchi-Sarfaty et al., 2007)
	3T3 fibroblasts	Calcein	GC > TT	GC ≥ TT	(Aird et al., 2008)

			Phenotype		
SNP	**Cell line**	**Probe drug(s)**	**Expression**	**Function**	**Reference**
C1236T/ G2677T/ C3435T	LLC-PK1	Rhodamine, vinblastine, vincristine	-	CGC > TTT	(Salama et al., 2006)
	HeLa	Rhodamine, paclitaxel, verapamil, daunorubicin, vinblastine, calcein-AM	No effect	No effect	(Kimchi-Sarfaty et al., 2007)
	3T3 fibroblasts	Calcein	CGC > TTT	CGC > TTT	(Aird et al., 2008)
	HEK293T	Calcein	No effect	No effect	(Gow et al., 2008)
		Paclitaxel		No effect	
A61G/ C1236T/ G2677T/ C3435T	HEK293T	Calcein	No effect	No effect	(Gow et al., 2008)
		Paclitaxel		ACGC > GTTT	

[a]Vasodilators = verapamil, nifedipine, diltiazem, bepridil, fendiline, prenylamine, nicardipine; [b]Steroids = Dexamethasone, betamethasone, prednisolone, cortisone; [c]Anticancer drugs = vinblastine, etoposide, actinomycin D, daunorubicin, paclitaxel, methotrexate, doxorubicin, 5-fluorouricil; [d]NSAIDs = Acetylsalicyclic acid, indomethacin, acemeticin, ibuprofen, naproxen, mepirizole.

Table A-3. Summary of the relationships between *ABCB1* genetic variability and P-gp *ex vivo* expression and function in healthy volunteers.

SNP / haplotype	Tissue / cell type	Expression	Function		Reference
			Probe	Result	
A61G	Duodenum	No effect	-	-	(Siegmund et al., 2002)
G1199A	Duodenum	No effect	-	-	(Siegmund et al., 2002)
C1236T	Duodenum	No effect	-	-	(Siegmund et al., 2002)
	PBMC	No effect	Rhodamine	No effect	(la Porte et al., 2007)
G2677T	Duodenum	No effect	-	-	(Siegmund et al., 2002)
	CD56+	-	Rhodamine	GG ≥ GT ≥ TT	(Drescher et al., 2002)
	CD56+ & CD4+	-	Rhodamine	No effect	(Oselin et al., 2003a)
	CD4+, CD8+, CD19+ & CD56+	No effect	-	-	(Oselin et al., 2003b)
	Liver	No effect	-	-	(Owen et al., 2005)
	PBMC	-	IL-2, IL-4, INF-γ, TNF-α IL-10, IL-6	GG > GT > TT No effect	(Pawlik et al., 2005)
	PBMC	No effect	Rhodamine	No effect	(la Porte et al., 2007)
C3435T	Duodenum	CC > CT > TT	-	-	(Hoffmeyer et al., 2000)
	CD56+	CC > CT > TT	Rhodamine	CC > CT > TT	(Hitzl et al., 2001)
	CD56+	CC ≥ TT	Rhodamine	CC > TT	(Drescher et al., 2002)
	Duodenum	No effect	-	-	(Siegmund et al., 2002)
	Renal parenchyma	CC > TT	-	-	(Siegsmund et al., 2002)
	CD56+ & CD4+	-	Rhodamine	No effect	(Oselin et al., 2003a)
	CD4+, CD8+, CD19+ & CD56+	No effect	-	-	(Oselin et al., 2003b)
	PBMC	-	IL-2, IL-4, INF-γ, TNF-α IL-10, IL-6	CC > CT > TT No effect	(Pawlik et al., 2005)
	Liver	No effect	-	-	(Owen et al., 2005)
	PBMC	No effect	Rhodamine	No effect	(la Porte et al., 2007)
G2677T/ C3435T	PBMC	-	IL-2, IL-4, INF-γ, TNF-α IL-10, IL-6	GC > TT No effect	(Pawlik et al., 2005)
	PBMC CD4+ & CD8+	No effect -	- Cyclosporine	- No effect	(Ansermot et al., 2008)
C1236T/ G2677T/ C3435T	PBMC	No effect	Rhodamine	No effect	(la Porte et al., 2007)
	Duodenum	CCC>TTT	-	-	(Schwarz et al., 2007)

Table A-4. Summary of *in vivo* clinical studies examining the impact of *ABCB1* genetic variants on probe substrate pharmacokinetics and pharmacodynamics in healthy volunteers.

SNP / haplotype	Probe drug	Variant phenotype	Reference
A61G	Talinolol	No effect	(Siegmund et al., 2002)
	Digoxin	No effect	(Johne et al., 2002)
	Digoxin	No effect	(Gerloff et al., 2002)
G1199A	Talinolol	No effect	(Siegmund et al., 2002)
C1236T	Talinolol	No effect	(Siegmund et al., 2002)
	Digoxin	No effect	(Johne et al., 2002)
	Midazolam	No effect	(Eap et al., 2004)
	Saquinavir	No effect	(la Porte et al., 2007)
	Mefloquine	Men: No effect	(Aarnoudse et al., 2006)
		Women: ↑ side effects	
G2677T	Talinolol	↑AUC	(Siegmund et al., 2002)
	Digoxin	No effect	(Johne et al., 2002)
	Digoxin	↑*AUC & Cmax*	(Verstuyft et al., 2003)
	Digoxin	No effect	(Gerloff et al., 2002)
	Digoxin	No effect	(Comets et al., 2007)
	Fexofenadine	↓*AUC*	(Kim et al., 2001)
	Midazolam	No effect	(Eap et al., 2004)
	Saquinavir	No effect	(la Porte et al., 2007)
	Mefloquine	Men: No effect	(Aarnoudse et al., 2006)
		Women: ↑ side effects	
	(R)-methadone	No effect	(Lötsch et al., 2006)
C3435T	Talinolol	No effect	(Siegmund et al., 2002)
	Digoxin	↑AUC, Cmax, Ctrough; ↓Tmax	(Johne et al., 2002)
	Digoxin	↑AUC & *Cmax*	(Verstuyft et al., 2003)
	Digoxin	↑AUC & Cmax	(Hoffmeyer et al., 2000)
	Digoxin	No effect	(Gerloff et al., 2002)
	Digoxin	No effect	(Becquemont et al., 2001)
	Digoxin	↓Vc/F	(Comets et al., 2007)
	Cyclosporine	↑*AUC & Cmax*	(Min & Ellingrod, 2002)
	Fexofenadine	No effect	(Drescher et al., 2002)
	Fexofenadine	↓AUC	(Kim et al., 2001)
	Loperamide	↑*AUC*	(Skarke et al., 2003)
	Loperamide	No effect	(Pauli-Magnus et al., 2003)
	Phenytoin	↑AUC	(Kerb et al., 2001)
	Midazolam	No effect	(Eap et al., 2004)
	Losartan	No effect	(Yasar et al., 2008)
	Saquinavir	No effect	(la Porte et al., 2007)
	Moxifloxacin	↓Tmax ; ↑*AUC, Cmax*	(Weiner et al., 2007)
	Mefloquine	Men: No effect	(Aarnoudse et al., 2006)
		Women: ↑ side effects	
	Ebastine metabolites	↓ urinary excretion	(Gervasini et al., 2006)
	(R)-methadone	No effect	(Lötsch et al., 2006)
	Dicloxacillin	No effect	(Putnam et al., 2005)

SNP / haplotype	Probe drug	Variant phenotype	Reference
2677T/ 3435T	Digoxin	↑AUC & Cmax	(Johne et al., 2002)
	Digoxin	No effect	(Gerloff et al., 2002)
	Cyclosporine	No effect	(Ansermot et al., 2008)
	Talinolol	No effect	(Bernsdorf et al., 2006)
	(R)-methadone	No effect	(Lötsch et al., 2006)
G2677/ 3435T	Loperamide	↑AUC	(Skarke et al., 2003)
1236T/ 2677T/ 3435T	Fexofenadine	↓AUC	(Kim et al., 2001)
	Loperamide	No effect	(Pauli-Magnus et al., 2003)
	Saquinavir	No effect	(la Porte et al., 2007)
	Mefloquine	Men: No effect	(Aarnoudse et al., 2006)
		Women: ↑ side effects	
	Verapamil	No effect	(Takano et al., 2006)

AUC: area under the concentration-time curve. C_{max}: maximum plasma concentration. C_{trough}: lowest plasma concentration. T_{max}: time to reach maximum plasma concentration. Vc/F: oral volume of distribution in the central compartment. Phenotypes in italics displayed clear trends but were not statistically significant.

Table A-5. Sex effects on relationships between MMT dose requirements and *ABCB1* genotypes and haplotypes.

	Two-way ANOVA factor effects % of total variation (P-value)		
SNP	Gene	Sex	Interaction
A61G	4.2 (0.1)[a]	0.1 (0.9)[a]	1.3 (0.4)[a]
G1199A	1.0 (0.4)	1.5 (0.4)	1.2 (0.4)
C1236T	3.5 (0.4)	0.4 (0.6)	10.5 (0.05)
G2677T	2.6 (0.4)	0.6 (0.6)	9.6 (0.06)
C3435T	5.3 (0.2)	0.5 (0.6)	8.8 (0.07)
Haplotype			
AGCGC	4.2 (0.1)[a]	0.4 (0.6)[a]	**8.4 (0.04)[a]***
AG**T**GC	1.4 (0.4)	0.1 (0.8)	0.8 (0.5)
AGC**TT**	**14.0 (0.02)***	0.07 (0.8)	0.2 (0.9)
AG**TTT**	2.4 (0.5)	0.4 (0.6)	4.5 (0.3)
GGTTT	6.3 (0.07)[a]	0.2 (0.8)[a]	0.2 (0.8)[a]

[a]Male homozygous variant subjects excluded from two-way ANOVA analysis. ***P < 0.05**. Variant haplotype loci are indicated bold.

Table A-6. Treatment outcome (successful versus poor) effects on relationships between MMT dose requirements and *ABCB1* genotypes and haplotypes.

	Two-way ANOVA factor effects % of total variation (P-value)		
SNP	Gene	Outcome	Interaction
A61G	2.2 (0.3)[a]	2.4 (0.2)[a]	0.2 (0.7)[a]
G1199A	0.1 (0.8)	2.9 (0.2)	0.6 (0.5)
C1236T	1.3 (0.7)	5.3 (0.09)	1.8 (0.6)
G2677T	0.5 (0.9)	6.3 (0.06)	5.3 (0.2)
C3435T	0.6 (0.8)	2.9 (0.2)	8.2 (0.08)
Haplotype			
AGCGC	0.6 (0.6)[a]	1.0 (0.5)[a]	1.6 (0.4)[a]
AGC**TT**	**8.6 (0.03)***	1.1 (0.4)	0.0 (0.9)
AG**TTT**	1.9 (0.6)	0.0 (0.9)	1.6 (0.6)
GGTTT	**14.7 (0.004)[a]****	4.9 (0.09)[a]	2.0 (0.3)[a]

[a]Successful outcome homozygous variant subjects excluded from two-way ANOVA analysis. ***P < 0.05, **P < 0.01**. Variant haplotype loci are indicated in bold.

Table A-7. Sex effects on relationships between (R)-methadone C_{trough} requirements and *ABCB1* genotypes and haplotypes.

	Two-way ANOVA factor effects % of total variation (P-value)		
SNP	Gene	Sex	Interaction
A61G	8.1 (0.1)[a]	3.0 (0.3)[a]	2.5 (0.4)[a]
G1199A	8.5 (0.09)	3.3 (0.3)	0.9 (0.6)
C1236T	**18.7 (0.02)***	51.3 (0.4)	**20.9 (0.01)***
G2677T	3.7 (0.5)	2.6 (0.3)	**28.2 (0.005)****
C3435T	**16.7 (0.02)[b]***	4.3 (0.2)[b]	**15.9 (0.02)[b]***
Haplotype			
AGCGC	8.7 (0.1)[a]	0.3 (0.8)[a]	12.7 (0.05)[a]
AGC**TT**	**14.7 (0.04)[a]****	0.0 (0.9)[a]	1.7 (0.5)[a]
AG**TTT**	9.8 (0.2)	0.5 (0.7)	10.1 (0.2)
GGTTT	12.5 (0.05)[a]	0.7 (0.6)[a]	0.3 (0.8)[a]

[a]Male homozygous variant subjects excluded from two-way ANOVA analysis. [b]Male homozygous wild-type subjects excluded from two-way ANOVA analysis. ***P < 0.05, **P < 0.01**. Variant haplotype loci are indicated in bold.

Table A-8. Treatment outcome (successful versus poor) effects on relationships between (R)-methadone C_{trough} requirements and *ABCB1* genotypes and haplotypes.

	Two-way ANOVA factor effects % of total variation (P-value)		
SNP	Gene	Outcome	Interaction
A61G	1.4 (0.5)[a]	0.5 (0.7)[a]	1.2 (0.5)[a]
C1236T	**17.4 (0.047)***	2.7 (0.3)	1.0 (0.8)
G2677T	1.9 (0.7)	0.5 (0.7)	0.7 (0.9)
C3435T	3.1 (0.6)	0.7 (0.6)	3.1 (0.6)
Haplotype			
AGCGC	1.2 (0.5)[a]	0.1 (0.9)[a]	0.4 (0.7)[a]
AGC**TT**	**13.0 (0.04)***	1.0 (0.6)	0.3 (0.8)
AG**TTT**	12.8 (0.06)	0.2 (0.8)	2.8 (0.4)

[a]Successful outcome homozygous variant subjects excluded from two-way ANOVA analysis.

***P < 0.05.** Variant haplotype loci are indicated in bold.

Table A-9. Relationships between (R)-methadone C_{trough}/dose and *ABCB1* genotypes and haplotypes.

SNP	Genotype	n	(R)-methadone C_{trough}/dose (median ± SD, $ng.mL^{-1}.mg^{-1}$)	P-value[a]
A61G	A/A	31	1.8 ± 0.6	
	A/G	4	1.9 ± 0.7	0.4
	G/G	2	1.4 ± 0.1	
G1199A	G/G	34	1.5 ± 0.6	0.6
	G/A	3	2.0 ± 0.9	
C1236T	C/C	9	1.6 ± 0.5	
	C/T	17	2.0 ± 0.6	0.2
	T/T	10	1.8 ± 0.6	
G2677T	G/G	5	2.2 ± 0.5	
	G/T	25	1.8 ± 0.6	1.0
	T/T	7	1.8 ± 0.8	
C3435T	C/C	4	1.8 ± 0.9	
	C/T	16	1.6 ± 0.5	0.5
	T/T	17	1.8 ± 0.6	
Haplotype	**Copy #**	**n**		
AGCGC	0	18	1.8 ± 0.6	
	1	14	1.8 ± 0.5	0.5
	2	1	1.4	
AGCG**T**	0	26	1.8 ± 0.5	0.4
	1	7	1.8 ± 0.7	
AG**T**GC	0	30	1.8 ± 0.6	0.6
	1	3	2.3 ± 0.5	
AGC**TT**	0	28	1.8 ± 0.6	
	1	4	1.7 ± 0.3	0.7
	2	1	2.2	
AG**TTT**	0	13	1.6 ± 0.5	
	1	17	1.8 ± 0.6	0.2
	2	3	2.4 ± 0.5	
GG**TTT**	0	29	1.8 ± 0.6	
	1	3	1.5 ± 0.5	0.6
	2	1	1.5	

[a]P-values are from Kruskal-Wallis test or Mann-Whitney U test where appropriate. Variant haplotype loci are bold. Copy # 0 = non-carriers; 1 = heterozygous carriers; 2 = homozygous carriers.

Table A-10. Sex effects on relationships between (R)-methadone C_{trough}/dose and *ABCB1* genotypes and haplotypes.

	Two-way ANOVA factor effects % of total variation (P-value)		
SNP	Gene	Sex	Interaction
A61G	2.2 (0.4)[a]	0.0 (0.9)[a]	0.9 (0.6)[a]
G1199A	7.5 (0.09)	**13.2 (0.03)***	**11.0 (0.04)***
C1236T	3.4 (0.5)	2.9 (0.3)	5.6 (0.4)
G2677T	0.7 (0.9)	4.0 (0.2)	8.1 (0.3)
C3435T	5.4 (0.2)[b]	2.4 (0.4)[b]	1.2 (0.6)[b]
Haplotype			
AGCGC	2.4 (0.4)[a]	0.4 (0.7)[a]	3.0 (0.4)[a]
AGC**TT**	3.1 (0.3)[a]	0.2 (0.8)[a]	2.6 (0.4)[a]
AG**TTT**	6.9 (0.3)	0.3 (0.7)	5.6 (0.4)
GGTTT	2.0 (0.4)[a]	0.1 (0.9)[a]	1.4 (0.5)[a]

[a]Male homozygous variant subjects excluded from two-way ANOVA analysis. [b]Male homozygous wild-type subjects excluded from two-way ANOVA analysis. ***P < 0.05**. Variant loci are bold.

Table A-11. Treatment outcome (successful versus poor) effects on relationships between BMT dose requirements and *ABCB1* genotypes.

	Two-way ANOVA factor effects % of total variation (P-value)		
SNP	Gene	Outcome	Interaction
A61G	7.5 (0.3)	5.5 (0.4)	6.2 (0.4)
C1236T	1.3 (0.7)	1.9 (0.6)	2.8 (0.6)
G2677T	12.9 (0.2)[a]	1.6 (0.6)[a]	3.0 (0.6)[a]
C3435T	16.2 (0.1)[a]	0.0 (1.0)[a]	6.2 (0.3)[a]

[a]Successful outcome homozygous wild-type subjects excluded from two-way ANOVA analysis.

Table A-12. Sex effects on relationships between BMT dose requirements and *ABCB1* genotypes and haplotypes.

	Two-way ANOVA factor effects % of total variation (P-value)		
SNP	Gene	Sex	Interaction
A61G	14.2 (0.2)	0.1 (0.9)	6.2 (0.3)
C1236T	0.6 (0.8)	4.5 (0.5)	2.1 (0.6)
G2677T	22.8 (0.09)[a]	10.5 (0.2)[a]	0.1 (0.9)[a]
C3435T	16.2 (0.08)	4.2 (0.4)	19.0 (0.06)
Haplotype			
AGCGC	23.2 (0.1)	6.1 (0.3)	3.4 (0.4)
AG**TTT**	16.1 (0.2)[b]	9.7 (0.3)[b]	0.2 (0.9)[b]

[a]Male homozygous wild-type subjects excluded from two-way ANOVA analysis. [b]Male homozygous variant subjects excluded from two-way ANOVA analysis. Variant haplotype loci are bold.

Table A-13. Relationship between buprenorphine and norbuprenorphine C_{trough} and *ABCB1* genotypes.

SNP	Genotype	n	Buprenorphine C_{trough} (median ± SD, ng/mL)	P-value[a]	Norbuprenorphine C_{trough} (median ± SD, ng/mL)	P-value[a]
A61G	A/A	10	0.60 ± 0.76	0.3	1.03 ± 1.19	0.5
	A/G	3	0.42 ± 0.06		0.76 ± 0.39	
C1236T	C/T	8	0.44 ± 0.77	0.5	0.65 ± 1.39	0.5
	T/T	5	0.55 ± 0.66		0.97 ± 0.37	
G2677T	G/G	2	0.28 ± 0.08	0.2	0.40 ± 0.25	0.2
	G/T	9	0.55 ± 0.69		0.97 ± 1.22	
	T/T	2	1.22 ± 1.08		1.15 ± 0.60	
C3435T	C/C	1	0.22	0.4	0.58	0.2
	C/T	6	0.83 ± 0.82		1.40 ± 1.36	
	T/T	6	0.46 ± 0.63		0.72 ± 0.45	

[a]P-value from Kruskal-Wallis test or Mann-Whitney U test where appropriate.

Table A-14. Relationship between buprenorphine and norbuprenorphine C_{trough} and *ABCB1* haplotypes.

Haplotype	Copy #	n	Buprenorphine C_{trough} (median ± SD, ng/mL)	P-value[a]	Norbuprenorphine C_{trough} (median ± SD, ng/mL)	P-value[a]
AGCGC	0	7	0.46 ± 0.58	0.9	0.72 ± 0.47	0.4
	1	5	1.11 ± 0.92		1.45 ± 1.57	
AG**T**GC	0	9	0.65 ± 0.79	0.3	0.72 ± 1.29	1.0
	1	3	0.42 ± 0.17		0.97 ± 0.38	
AG**TTT**	0	3	0.34 ± 0.10	0.1	0.58 ± 0.38	0.3
	1	8	0.60 ± 0.72		1.03 ± 1.30	
	2	1	1.98		1.57	

[a]P-value from Kruskal-Wallis test or Mann-Whitney U test where appropriate.

Copy # 0 = non-carriers; 1 = heterozygous carriers; 2 = homozygous carriers.

Table A-15. Relationship between buprenorphine and norbuprenorphine C_{trough}/dose and *ABCB1* genotypes/haplotypes.

SNP	Genotype	n	Buprenorphine C_{trough}/dose (median ± SD, pg.mL^{-1}.mg^{-1})	P-value[a]	Norbuprenorphine C_{trough}/dose (median ± SD, pg.mL^{-1}.mg^{-1})	P-value[a]
A61G	A/A	10	74 ± 116	0.6	107 ± 109	0.8
	A/G	3	150 ± 67		110 ± 147	
C1236T	C/T	8	74 ± 72	0.7	99 ± 105	0.4
	T/T	5	108 ± 146		118 ± 129	
G2677T	G/G	2	94 ± 107		79 ± 44	
	G/T	9	70 ± 40	0.09	96 ± 93	0.1
	T/T	2	313 ± 117		337 ± 33	
C3435T	C/C	1	18		48	
	C/T	6	67 ± 46	0.1	133 ± 108	0.3
	T/T	6	139 ± 130		114 ± 125	
Haplotype	**Copy #**					
AGCGC	0	7	150 ± 120	0.07	118 ± 128	0.1
	1	5	56 ± 40		75 ± 77	
AG**T**GC	0	9	108 ± 113	0.3	118 ± 107	0.7
	1	3	39 ± 71		96 ± 160	
AG**TTT**	0	3	150 ± 82		110 ± 157	
	1	8	74 ± 63	0.3	107 ± 100	0.6
	2	1	396		314	

[a]P-value from Kruskal-Wallis test or Mann-Whitney U test where appropriate.

Copy # 0 = non-carriers; 1 = heterozygous carriers; 2 = homozygous carriers.

Table A-16. Summary table of results from Fisher's Exact Tests comparing the frequency of *ABCB1* variant alleles between successful and poor BMT outcome subjects.

	Fisher's Exact Test		
SNP	**Odds Ratio**	**(95% CI)**	**P-value**
A61G	1.22	(0.10 to 15.12)	1.0
G1199A	1.92	(0.07 to 51.07)	1.0
C1236T	0.78	(0.15 to 3.93)	1.0
G2677T	0.71	(0.17 to 3.03)	0.7
C3435T	1.50	(0.31 to 7.21)	0.7

High Odds Ratio indicates higher variant allele frequency in successful versus poor treatment group. CI: Confidence Interval.

Table A-17. Summary table of results from Fisher's Exact Tests comparing the frequency of *ABCB1* variant alleles between BMT subjects who did or did not experience withdrawal ('withdrawal-ever'[a]).

	Fisher's Exact Test		
SNP	**Odds Ratio**	**(95% CI)**	**P-value**
A61G	0.21	(0.01 to 4.52)	0.5
G1199A	0.56	(0.02 to 14.94)	1.0
C1236T	1.54	(0.24 to 9.90)	1.0
G2677T	1.50	(0.31 to 7.19)	0.7
C3435T	0.90	(0.16 to 4.92)	1.0

High Odds Ratio indicates higher variant allele frequency in subjects experiencing withdrawal. CI: Confidence interval. [a]See definition in Chapter 3, section 3.3.4.1.

Table A-18. Primer sequences for the qualitative PCR detection of CD4, CD56 and CD8 cDNA.

Assay		**Sequence**	**References**
CD4	Forward	5'-TCA GGG AAA GAA AGT GGT GC-3'	(Habasque et al., 2002)
	Reverse	5'-AAG AAG GAG CCC TGA TTT CC-3'	
CD56	Forward	5'-CCG TGA TTG TGT GTG ATG TGG T-3'	(Ponnampalam et al., 2008)
	Reverse	5'-CGA GGT TGG CGG TGG CA-3'	
CD8	Forward	5'-CCC TGA GCA ACT CCA TCA TGT-3'	(Mocellin et al., 2003)
	Reverse	5'-GTG GGC TTC GCT GGC A-3'	

Additional references for Appendix A

Aarnoudse AL, van Schaik RH, Dieleman J, Molokhia M, van Riemsdijk MM, Ligthelm RJ, Overbosch D, van der Heiden IP and Stricker BH (2006) MDR1 gene polymorphisms are associated with neuropsychiatric adverse effects of mefloquine. *Clin Pharmacol Ther* **80:**367-374.

Aird RE, Thomson M, Macpherson JS, Thurston DE, Jodrell DI and Guichard SM (2008) ABCB1 genetic polymorphism influences the pharmacology of the new pyrrolobenzodiazepine derivative SJG-136. *Pharmacogenomics J* **8:**289-296.

Altice FL, Friedland GH and Cooney EL (1999) Nevirapine induced opiate withdrawal among injection drug users with HIV infection receiving methadone. *Aids* **13:**957-962.

Alvares AP and Kappas A (1972) Influence of phenobarbital on the metabolism and analgesic effect of methadone in rats. *J Lab Clin Med* **79:**439-451.

Ansermot N, Rebsamen M, Chabert J, Fathi M, Gex-Fabry M, Daali Y, Besson M, Rossier M, Rudaz S, Hochstrasser D, Dayer P and Desmeules J (2008) Influence of ABCB1 gene polymorphisms and P-glycoprotein activity on cyclosporine pharmacokinetics in peripheral blood mononuclear cells in healthy volunteers. *Drug Metab Lett* **2:**76-82.

Bailey DG, Malcolm J, Arnold O and Spence JD (1998) Grapefruit juice-drug interactions. *Br J Clin Pharmacol* **46:**101-110.

Barry M, Mulcahy F, Merry C, Gibbons S and Back D (1999) Pharmacokinetics and potential interactions amongst antiretroviral agents used to treat patients with HIV infection. *Clin Pharmacokinet* **36:**289-304.

Bart PA, Rizzardi PG, Gallant S, Golay KP, Baumann P, Pantaleo G and Eap CB (2001) Methadone blood concentrations are decreased by the administration of abacavir plus amprenavir. *Ther Drug Monit* **23:**553-555.

Becquemont L, Verstuyft C, Kerb R, Brinkmann U, Lebot M, Jaillon P and Funck-Brentano C (2001) Effect of grapefruit juice on digoxin pharmacokinetics in humans. *Clin Pharmacol Ther* **70:**311-316.

Begre S, von Bardeleben U, Ladewig D, Jaquet-Rochat S, Cosendai-Savary L, Golay KP, Kosel M, Baumann P and Eap CB (2002) Paroxetine increases steady-state concentrations of (R)-methadone in CYP2D6 extensive but not poor metabolizers. *J Clin Psychopharmacol* **22:**211-215.

Bending MR and Skacel PO (1977) Rifampicin and methadone withdrawal. *Lancet* **1:**1211.

Bernsdorf A, Giessmann T, Modess C, Wegner D, Igelbrink S, Hecker U, Haenisch S, Cascorbi I, Terhaag B and Siegmund W (2006) Simvastatin does not influence the intestinal P-glycoprotein and MPR2, and the disposition of talinolol after chronic medication in healthy subjects genotyped for the ABCB1, ABCC2 and SLCO1B1 polymorphisms. *Br J Clin Pharmacol* **61:**440-450.

Boffito M, Rossati A, Reynolds HE, Hoggard PG, Back DJ and Di Perri G (2002) Undefined duration of opiate withdrawal induced by efavirenz in drug users with HIV infection and undergoing chronic methadone treatment. *AIDS Res Hum Retroviruses* **18:**341-342.

Borg L, Ho A, Peters JE and Kreek MJ (1995) Availability of reliable serum methadone determination for management of symptomatic patients. *J Addict Dis* **14:**83-96.

Brockmeyer NH, Mertins L and Goos M (1991) Pharmacokinetic interaction of antimicrobial agents with levomethadon in drug-addicted AIDS patients. *Klin Wochenschr* **69:**16-18.

Brown LS, Jr., Kritz S, Chu M and Madray C (2006) Safety, efficacy, and tolerability of nelfinavir-containing antiretroviral therapy for patients coinfected with HIV and hepatitis C undergoing methadone maintenance. *J Subst Abuse Treat* **30:**331-335.

Cao YJ, Smith PF, Wire MB, Lou Y, Lancaster CT, Causon RC, Bigelow GE, Martinez E, Fuchs EJ, Radebaugh C, McCabe S and Hendrix CW (2008) Pharmacokinetics and pharmacodynamics of methadone enantiomers after coadministration with fosamprenavir-ritonavir in opioid-dependent subjects. *Pharmacotherapy* **28:**863-874.

Clarke SM and Mulcahy FM (2000) Efavirenz therapy in drug users. *HIV Med* **1 Suppl 1:**15-17.

Clarke SM, Mulcahy FM, Tjia J, Reynolds HE, Gibbons SE, Barry MG and Back DJ (2001) The pharmacokinetics of methadone in HIV-positive patients receiving the non-nucleoside reverse transcriptase inhibitor efavirenz. *Br J Clin Pharmacol* **51:**213-217.

Cobb MN, Desai J, Brown LS, Jr., Zannikos PN and Rainey PM (1998) The effect of fluconazole on the clinical pharmacokinetics of methadone. *Clin Pharmacol Ther* **63:**655-662.

Comets E, Verstuyft C, Lavielle M, Jaillon P, Becquemont L and Mentre F (2007) Modelling the influence of MDR1 polymorphism on digoxin pharmacokinetic parameters. *Eur J Clin Pharmacol* **63:**437-449.

Crouthamel MH, Wu D, Yang Z and Ho RJ (2006) A novel MDR1 G1199T variant alters drug resistance and efflux transport activity of P-glycoprotein in recombinant Hek cells. *J Pharm Sci* **95:**2767-2777.

Drescher S, Schaeffeler E, Hitzl M, Hofmann U, Schwab M, Brinkmann U, Eichelbaum M and Fromm MF (2002) *MDR1* gene polymorphisms and disposition of the P-glycoprotein substrate fexofenadine. *British Journal of Clinical Pharmacology* **53:**526-534.

Dresser GK, Spence JD and Bailey DG (2000) Pharmacokinetic-pharmacodynamic consequences and clinical relevance of cytochrome P450 3A4 inhibition. *Clin Pharmacokinet* **38:**41-57.

Eap CB, Bertschy G, Powell K and Baumann P (1997) Fluvoxamine and fluoxetine do not interact in the same way with the metabolism of the enantiomers of methadone. *J Clin Psychopharmacol* **17:**113-117.

Eap CB, Buclin T and Baumann P (2002) Interindividual variability of the clinical pharmacokinetics of methadone: implications for the treatment of opioid dependence. *Clin Pharmacokinet* **41:**1153-1193.

Eap CB, Fellay J, Buclin T, Bleiber G, Golay KP, Brocard M, Baumann P and Telenti A (2004) CYP3A activity measured by the midazolam test is not related to 3435 C >T polymorphism in the multiple drug resistance transporter gene. *Pharmacogenetics* **14:**255-260.

Faucette SR, Wang H, Hamilton GA, Jolley SL, Gilbert D, Lindley C, Yan B, Negishi M and LeCluyse EL (2004) Regulation of CYP2B6 in primary human hepatocytes by prototypical inducers. *Drug Metab Dispos* **32:**348-358.

Finelli PF (1976) Letter: Phenytoin and methadone tolerance. *N Engl J Med* **294:**227.

Gerber JG, Rhodes RJ and Gal J (2004) Stereoselective metabolism of methadone N-demethylation by cytochrome P4502B6 and 2C19. *Chirality* **16:**36-44.

Gerloff T, Schaefer M, Johne A, Oselin K, Meisel C, Cascorbi I and Roots I (2002) *MDR1* genotypes do not influence the absorption of a single oral dose of 1 mg digoxin in healthy white males. *British Journal of Clinical Pharmacology* **54:**610-616.

Gervasini G, Vizcaino S, Carrillo JA, Caballero MJ and Benitez J (2006) The effect of CYP2J2, CYP3A4, CYP3A5 and the MDR1 polymorphisms and gender on the urinary excretion of the metabolites of the H-receptor antihistamine ebastine: a pilot study. *Br J Clin Pharmacol* **62:**177-186.

Gourevitch MN (2001) Interactions between HIV-related medications and methadone: an overview. Updated March 2001. *Mt Sinai J Med* **68:**227-228.

Gow JM, Hodges LM, Chinn LW and Kroetz DL (2008) Substrate-dependent effects of human ABCB1 coding polymorphisms. *J Pharmacol Exp Ther* **325:**435-442.

Habasque C, Aubry F, Jegou B and Samson M (2002) Study of the HIV-1 receptors CD4, CXCR4, CCR5 and CCR3 in the human and rat testis. *Mol Hum Reprod* **8:**419-425.

Hamilton SP, Nunes EV, Janal M and Weber L (2000) The effect of sertraline on methadone plasma levels in methadone-maintenance patients. *Am J Addict* **9:**63-69.

Heelon MW and Meade LB (1999) Methadone withdrawal when starting an antiretroviral regimen including nevirapine. *Pharmacotherapy* **19:**471-472.

Herrlin K, Segerdahl M, Gustafsson LL and Kalso E (2000) Methadone, ciprofloxacin, and adverse drug reactions. *Lancet* **356:**2069-2070.

Hitzl M, Drescher S, van der Kuip H, Schaffeler E, Fischer J, Schwab M, Eichelbaum M and Fromm MF (2001) The C3435T mutation in the human *MDR1* gene is associated with altered efflux of the P-glycoprotein substrate rhodamine 123 from CD56+ natural killer cells. *Pharmacogenetics* **11:**293-298.

Hoffmeyer S, Burk O, von Richter O, Arnold HP, Brockmöller J, Johne A, Cascorbi I, Gerloff T, Roots I, Eichelbaum M and Brinkmann U (2000) Functional polymorphisms of the human multidrug-resistance gene: multiple sequence variations and correlation of one allele with P-glycoprotein expression and activity *in vivo*. *Proceedings of the National Academy of Sciences of the United States of America* **97:**3473-3478.

Holmes VF (1990) Rifampin-induced methadone withdrawal in AIDS. *J Clin Psychopharmacol* **10:**443-444.

Hsyu PH, Lillibridge J, Daniels E and Kerr BM (2006) Pharmacokinetic interaction of nelfinavir and methadone in intravenous drug users. *Biopharm Drug Dispos* **27:**61-68.

Jamois C, Smith P, Morrison R, Riek M, Patel A, Schmitt C, Morcos PN and Zhang X (2009) Effect of saquinavir/ritonavir (1000/100 mg bid) on the pharmacokinetics of methadone in opiate-dependent HIV-negative patients on stable methadone maintenance therapy. *Addict Biol* **14:**321-327.

Johne A, Köpke K, Gerloff T, Mai I, Rietbrock S, Meisel C, Hoffmeyer S, Kerb R, Fromm MF, Brinkmann U, Eichelbaum M, Brockmöller J, Cascorbi I and Roots I (2002) Modulation of steady-state kinetics of digoxin by haplotypes of the P-glycoprotein *MDR1* gene. *Clinical Pharmacology and Therapeutics* **72:**584-594.

Katz LY (1999) Methadone-induced hallucinations. *J Am Acad Child Adolesc Psychiatry* **38:**355-356.

Kerb R, Aynacioglu AS, Brockmoller J, Schlagenhaufer R, Bauer S, Szekeres T, Hamwi A, Fritzer-Szekeres M, Baumgartner C, Ongen HZ, Guzelbey P, Roots I and Brinkmann U (2001) The predictive value of MDR1, CYP2C9, and CYP2C19 polymorphisms for phenytoin plasma levels. *Pharmacogenomics J* **1:**204-210.

Kim RB, Leake BF, Choo EF, Dresser GK, Kubba SV, Schwarz UI, Taylor A, Xie HG, McKinsey J, Zhou S, Lan LB, Schuetz JD, Schuetz EG and Wilkinson GR (2001) Identification of functionally variant *MDR1* alleles among European Americans and African Americans. *Clinical Pharmacology and Therapeutics* **70:**189-199.

Kimchi-Sarfaty C, Gribar JJ and Gottesman MM (2002) Functional characterization of coding polymorphisms in the human *MDR1* gene using a vaccinia virus expression system. *Molecular Pharmacology* **62:**1-6.

Kimchi-Sarfaty C, Oh JM, Kim IW, Sauna ZE, Calcagno AM, Ambudkar SV and Gottesman MM (2007) A "silent" polymorphism in the MDR1 gene changes substrate specificity. *Science* **315:**525-528.

Kreek MJ (1986) Drug interactions with methadone in humans. *NIDA Res Monogr* **68:**193-225.

Kreek MJ, Garfield JW, Gutjahr CL and Giusti LM (1976) Rifampin-induced methadone withdrawal. *N Engl J Med* **294:**1104-1106.

Kroetz DL, Pauli-Magnus C, Hodges LM, Huang CC, Kawamoto M, Johns SJ, Stryke D, Ferrin TE, DeYoung J, Taylor T, Carlson EJ, Herskowitz I, Giacomini KM and Clark AG (2003) Sequence diversity and haplotype structure in the human ABCB1 (MDR1, multidrug resistance transporter) gene. *Pharmacogenetics* **13:**481-494.

Kuhn KL, Halikas JA and Kemp KD (1989) Carbamazepine treatment of cocaine dependence in methadone maintenance patients with dual opiate-cocaine addiction. *NIDA Res Monogr* **95:**316-317.

la Porte CJ, Li Y, Beique L, Foster BC, Chauhan B, Garber GE, Cameron DW and van Heeswijk RP (2007) The effect of ABCB1 polymorphism on the pharmacokinetics of saquinavir alone and in combination with ritonavir. *Clin Pharmacol Ther* **82:**389-395.

Liu SJ and Wang RI (1984) Case report of barbiturate-induced enhancement of methadone metabolism and withdrawal syndrome. *Am J Psychiatry* **141:**1287-1288.

Lötsch J, Skarke C, Wieting J, Oertel BG, Schmidt H, Brockmoller J and Geisslinger G (2006) Modulation of the central nervous effects of levomethadone by genetic polymorphisms potentially affecting its metabolism, distribution, and drug action. *Clin Pharmacol Ther* **79:**72-89.

Marzolini C, Troillet N, Telenti A, Baumann P, Decosterd LA and Eap CB (2000) Efavirenz decreases methadone blood concentrations. *Aids* **14:**1291-1292.

McCance-Katz EF, Gourevitch MN, Arnsten J, Sarlo J, Rainey P and Jatlow P (2002) Modified directly observed therapy (MDOT) for injection drug users with HIV disease. *Am J Addict* **11:**271-278.

McCance-Katz EF, Rainey PM, Smith P, Morse G, Friedland G, Gourevitch M and Jatlow P (2004) Drug interactions between opioids and antiretroviral medications: interaction between methadone, LAAM, and nelfinavir. *Am J Addict* **13:**163-180.

Min DI and Ellingrod VL (2002) C3435T mutation in exon 26 of the human *MDR1* gene and cyclosporine pharmacokinetics in healthy subjects. *Therapeutic Drug Monitoring* **24:**400-404.

Mocellin S, Provenzano M, Rossi CR, Pilati P, Nitti D and Lise M (2003) Use of quantitative real-time PCR to determine immune cell density and cytokine gene profile in the tumor microenvironment. *J Immunol Methods* **280:**1-11.

Morita N, Yasumori T and Nakayama K (2003) Human MDR1 polymorphism: G2677T/A and C3435T have no effect on MDR1 transport activities. *Biochem Pharmacol* **65:**1843-1852.

Oselin K, Gerloff T, Mrozikiewicz PM, Pahkla R and Roots I (2003a) *MDR1* polymorphisms G2677T in exon 21 and C3435T in exon 26 fail to affect rhodamine 123 efflux in peripheral blood lymphocytes. *Fundam Clin Pharmacol* **17:**463-469.

Oselin K, Nowakowski-Gashaw I, Mrozikiewicz PM, Wolbergs D, Pahkla R and Roots I (2003b) Quantitative determination of MDR1 mRNA expression in peripheral blood lymphocytes: a possible role of genetic polymorphisms in the MDR1 gene. *Eur J Clin Invest* **33:**261-267.

Otero MJ, Fuertes A, Sanchez R and Luna G (1999) Nevirapine-induced withdrawal symptoms in HIV patients on methadone maintenance programme: an alert. *Aids* **13:**1004-1005.

Owen A, Goldring C, Morgan P, Chadwick D, Park BK and Pirmohamed M (2005) Relationship between the C3435T and G2677T(A) polymorphisms in the ABCB1 gene and P-glycoprotein expression in human liver. *British Journal of Clinical Pharmacology* **59:**365-370.

Pauli-Magnus C, Feiner J, Brett C, Lin E and Kroetz DL (2003) No effect of *MDR1* C3435T variant on loperamide disposition and central nervous system effects. *Clinical Pharmacology and Therapeutics* **74:**487-498.

Pawlik A, Baskiewicz-Masiuk M, Machalinski B and Gawronska-Szklarz B (2005) Involvement of P-gp in the process of apoptosis in peripheral blood mononuclear cells. *Int Immunopharmacol* **5:**821-828.

Pinzani V, Faucherre V, Peyriere H and Blayac JP (2000) Methadone withdrawal symptoms with nevirapine and efavirenz. *Ann Pharmacother* **34:**405-407.

Ponnampalam AP, Gargett CE and Rogers PA (2008) Identification and hormonal regulation of a novel form of NKp30 in human endometrial epithelium. *Eur J Immunol* **38:**216-226.

Preston KL, Griffiths RR, Stitzer ML, Bigelow GE and Liebson IA (1984) Diazepam and methadone interactions in methadone maintenance. *Clin Pharmacol Ther* **36:**534-541.

Putnam WS, Woo JM, Huang Y and Benet LZ (2005) Effect of the MDR1 C3435T variant and P-glycoprotein induction on dicloxacillin pharmacokinetics. *J Clin Pharmacol* **45:**411-421.

Rotger M, Colombo S, Furrer H, Bleiber G, Buclin T, Lee BL, Keiser O, Biollaz J, Decosterd L and Telenti A (2005) Influence of CYP2B6 polymorphism on plasma and intracellular concentrations and toxicity of efavirenz and nevirapine in HIV-infected patients. *Pharmacogenet Genomics* **15:**1-5.

Sakurai A, Onishi Y, Hirano H, Seigneuret M, Obanayama K, Kim G, Liew EL, Sakaeda T, Yoshiura K, Niikawa N, Sakurai M and Ishikawa T (2007) Quantitative structure--activity relationship analysis and molecular dynamics simulation to functionally validate nonsynonymous polymorphisms of human ABC transporter ABCB1 (P-glycoprotein/MDR1). *Biochemistry* **46:**7678-7693.

Salama NN, Yang Z, Bui T and Ho RJ (2006) MDR1 haplotypes significantly minimize intracellular uptake and transcellular P-gp substrate transport in recombinant LLC-PK1 cells. *J Pharm Sci* **95:**2293-2308.

Schaefer M, Roots I and Gerloff T (2006) In-vitro transport characteristics discriminate wild-type ABCB1 (MDR1) from ALA893SER and ALA893THR polymorphisms. *Pharmacogenet Genomics* **16:**855-861.

Schwarz UI, Hanso H, Oertel R, Miehlke S, Kuhlisch E, Glaeser H, Hitzl M, Dresser GK, Kim RB and Kirch W (2007) Induction of intestinal P-glycoprotein by St John's wort reduces the oral bioavailability of talinolol. *Clin Pharmacol Ther* **81:**669-678.

Siegmund W, Ludwig K, Giessmann T, Dazert P, Schroeder E, Sperker B, Warzok R, Kroemer HK and Cascorbi I (2002) The effects of the human *MDR1* genotype on the expression of duodenal P-glycoprotein and disposition of the probe drug talinolol. *Clinical Pharmacology and Therapeutics* **72:**572-583.

Siegsmund M, Brinkmann U, Schaffeler E, Weirich G, Schwab M, Eichelbaum M, Fritz P, Burk O, Decker J, Alken P, Rothenpieler U, Kerb R, Hoffmeyer S and Brauch H (2002) Association of the P-glycoprotein transporter MDR1(C3435T) polymorphism with the susceptibility to renal epithelial tumors. *J Am Soc Nephrol* **13:**1847-1854.

Skarke C, Jarrar M, Schmidt H, Kauert G, Langer M, Geisslinger G and Lotsch J (2003) Effects of ABCB1 (multidrug resistance transporter) gene mutations on disposition and central nervous effects of loperamide in healthy volunteers. *Pharmacogenetics* **13:**651-660.

Staszewski S, Haberl A, Gute P, Nisius G, Miller V and Carlebach A (1998) Nevirapine/didanosine/lamivudine once daily in HIV-1-infected intravenous drug users. *Antivir Ther* **3 Suppl 4:**55-56.

Takano M, Yumoto R and Murakami T (2006) Expression and function of efflux drug transporters in the intestine. *Pharmacol Ther* **109:**137-161.

Tarumi Y, Pereira J and Watanabe S (2002) Methadone and fluconazole: respiratory depression by drug interaction. *J Pain Symptom Manage* **23:**148-153.

Tong TG, Pond SM, Kreek MJ, Jaffery NF and Benowitz NL (1981) Phenytoin-induced methadone withdrawal. *Ann Intern Med* **94:**349-351.

Verstuyft C, Schwab M, Schaeffeler E, Kerb R, Brinkmann U, Jaillon P, Funck-Brentano C and Becquemont L (2003) Digoxin pharmacokinetics and MDR1 genetic polymorphisms. *Eur J Clin Pharmacol* **58:**809-812.

Wang D, Johnson AD, Papp AC, Kroetz DL and Sadee W (2005) Multidrug resistance polypeptide 1 (MDR1, ABCB1) variant 3435C>T affects mRNA stability. *Pharmacogenet Genomics* **15:**693-704.

Weiner M, Burman W, Luo CC, Peloquin CA, Engle M, Goldberg S, Agarwal V and Vernon A (2007) Effects of rifampin and multidrug resistance gene polymorphism on concentrations of moxifloxacin. *Antimicrob Agents Chemother* **51:**2861-2866.

Woodahl EL, Yang Z, Bui T, Shen DD and Ho RJ (2004) Multidrug resistance gene G1199A polymorphism alters efflux transport activity of P-glycoprotein. *J Pharmacol Exp Ther* **310:**1199-1207.

Woodahl EL, Yang Z, Bui T, Shen DD and Ho RJ (2005) MDR1 G1199A polymorphism alters permeability of HIV protease inhibitors across P-glycoprotein-expressing epithelial cells. *Aids* **19:**1617-1625.

Yasar U, Babaoglu MO and Bozkurt A (2008) Disposition of a CYP2C9 phenotyping agent, losartan, is not influenced by the common 3435C > T variation of the drug transporter gene ABCB1 (MDR1). *Basic Clin Pharmacol Toxicol* **103:**176-179.

Appendix B: Supplementary figures

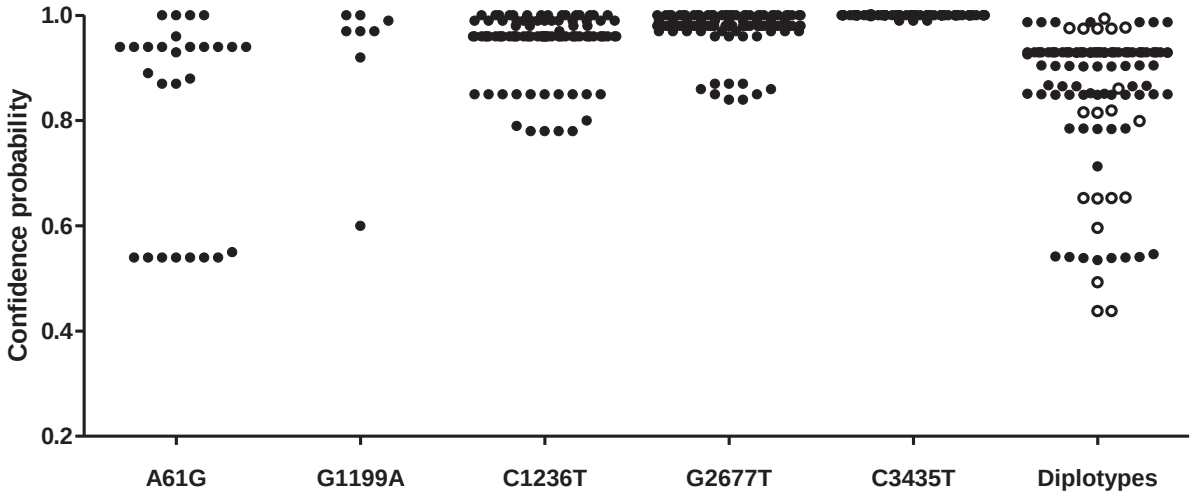

Figure B-1. Confidence probabilities of ambiguous phase calls made by PHASE for each individual locus, and for the overall diplotype predictions.

Each point represents a subject with ambiguous gametic phase. Hollow circles represent diplotype confidence probabilities for subjects with missing genotype data.

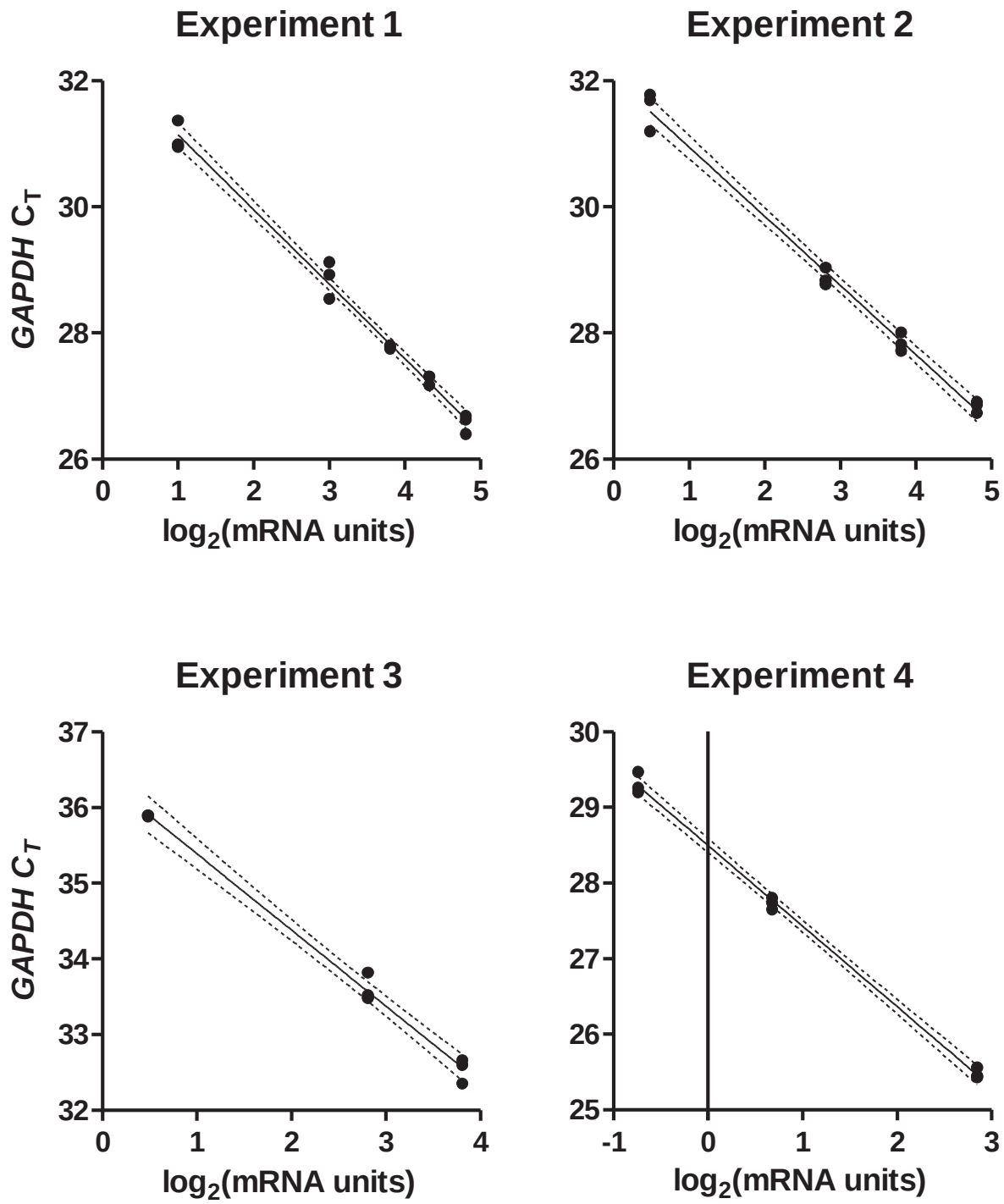

Figure B-2. Linear relationships between $\log_2$(mRNA concentration) and *GAPDH* C_T values over the range of 0.6 to 28 mRNA units in qRT-PCR validation experiments (Chapter 5, section 5.2.4.2).

Solid lines are linear regression best-fit (dotted lines are 95% confidence intervals). Slope (95% confidence intervals) for experiments 1-4 were: -1.18 (-1.28 to -1.11); -1.10 (-1.17 to -1.02); -1.01 (-1.11 to -0.91); -1.07 (-1.12 to -1.01). R^2 was greater than 0.98 for all four experiments.

Appendix C: Genomic locations, primer recognition sites and PCR product sequences for ABCB1 SNPs

The genomic locations, primer recognition sites and PCR product sequences for the A61G, G1199A and C1236T, G2677T and C3435T SNPs of the *ABCB1* gene are shown below. Numbers in brackets represent genomic distance (in nucleotides) from the transcription start site of the *ABCB1* gene. Underlined segments represent primer recognition sequences, bold nucleotides represent the amplified fragment(s), and shaded nucleotides represent SNP loci.

A61G

5′-(113,017)CCTGAGGCTCATGCATTTGGCTAATGAGCTGCGGTTTCTCTTCAGGTCGGAATGGATCTTGA

MDR-1b:5′-AGGAGCAAAGAAGAAGAACTTTTTTAAACTGAT-3′
ACCGCAATGGAGGAGCAAAGAAGAAGAACTTTTTTAAACTGAT**CAATAAAAGGTAACTAGCTTGTTTCATTTTCA**
3′-...TACCTCCTCGTTTCTTCTTCTTGAAAAAATTTGACTAGTTA...-5′

TAGTTTACATAGTTGCGAGATTTGAGTAATTTATTTCTAGCCTCCAGCTCTGAAATAAATGACATGTTGTTGTTT

TTAATTATTTTTAAGAAACGCAAGCTAGCCTTTGGAATCAATATCCCTGCTTAGAGCAGAAGTTTGTTGGCTGAG
3′-CGTTCGATCGGAAACCTTAG-5′:MDR-6

TGGAGCACAGCATATGCATTTTCCCTGTCTTTTTTGTTCTTTCTTTTAATGATACATAATATT(113,368)-3′

G1199A and C1236T

5′-(162,591)ACTTTATCCAGCTCTCCACAAAATATCACTAAAAGTAGTTATTGTAACCTAGTAATCTCTTAA

MDR-24:5′-CAGCTATTCGAAGAGTGGGC-3′
AATTTGATTCTGTTTAGAAGCCAAGTATTGACAGCTATTCGAAGAGTGGGC**ACAAACCAGATAATATTAAGGGAA**
3′-...AACTGTCGATAAGCTTCTCACCCGTGTT...-5′

ATTTGGAATTCAGAAATGTTCACTTCAGTTACCCATCTCGAAAAGAAGTTAAGGTACAGTGATAAATGATTAATC

AACAATTAATCTATTGAATGAAGAGTTTCTGATGTTTTCTTGTAGAGATTATAAAAAAGTGCATGTATATTTAAA

CCTAGTGAACAGTCAGTTCCTATATCCTGTGTCTGTGAATTGCCTTGAAGTTTTTTTCTCACGGGTCCTGGTAGA
3′-GGAACTTCAAAAAAAGAGTGAA-5′:MDR-25

TCTTGAAGGGCCTGAACCTGAAGGTGCAGAGTGGGCAGACGGTGGCCCTGGTTGGAAACAGTGGCTGTGGGAAGA

GCACAACAGTCCAGCTGATGCAGAGGCTCTATGACCCCACAGAGGGGATGGTGAGATGACCCATGCGAGCTAGAC

CCTGCGGTGATCAGCAGTCACATTGCACATCTTTCTGATGTTGCCCTTTCAATTACAAATGTATGAAAGTCACAC

TTACTTTTTATTCCAGGTCAGTGTTGATGGACAGGATATTAGGACCATAAATGTAAGGTTTCTACGGGAAATCAT
3′-CAGTCACAACTACCTGTCCTA-5′:C1236R

TGGTGTGGTGAGTCAGGAACCTGTATTGTTTGCCACCACGATAGCTGAAAACATTCGCTATGG(163,317)-3′

G2677T

5′-(181,656)TGAATATAGTCTCATGAAGGTGAGTTTTCAGAAAATAGAAGCATGAGTTGTGAAGATAATATT

MDR-9:5′-TGCAGGCTATAGGTTCCAGG-3′
TTTAAAATTTCTCTAATTTGTTTTGTTTTGCAGGCTATAGGTTCCAGG**CTTGCTGTAATTACCCAGAATATAGCA**
3′-...CAAAACGTCCGATATCCAAGGTCCGAAC...-5′

AATCTTGGGACAGGAATAATTATATCCTTCATCTATGGTTGGCAACTAACACTGTTACTCTTAGCAATTGTACCC

ATCATTGCAATAGCAGGAGTTGTTGAAATGAAAATGTTGTCTGGACAAGCACTGAAAGATAAGAAAGAACTAGAA

GGTGCTGGGAAGGTGAGTCAAACTAAATATGATTGATTAATTAAGTAGAGTAAAGTATTCTAATCAGTGTTATTT
3′-CCCTTCCACTCAGTTTGATTT-5′:MDR-10a
3′-CGACCCTTCCACTCAGTTTG-5′:G2677RWT
3′-AGACCCTTCCACTCAGTTTG-5′:G2677RV

TGTTACTCCCTACTGCTTACTATGCTCTAAGAATGTGTTTATAACCATTCCTCAAAGCAATCT(182,082)-3′

C3435T

5′-(203,663)ATCTCACAGTAACTTGGCAGTTTCAGTGTAAGAAATAAGATGTTAATTGTGCTACATTCAAAG

C3435TF:5′-TTGATGGCAAAGAAATAAAGC-3′
TGTGCTGGTCCTGAAGTTGATCTGTGAACTCTTGTTTTCAGCTGCTTGATGGCAAAGAAATAAAGC**GACTGAATG**
3′...GACGAACTACCGTTTCTTTATTTCGCTGA...5′

TTCAGTGGCTCCGAGCACACCTGGGCATCGTGTCCCAGGAGCCCATCCTGTTTGACTGCAGCATTGCTGAGAACA

TTGCCTATGGAGACAACAGCCGGGTGGTGTCACAGGAAGAGAGTGTGAGGGCAGCAAAGGAGGCCAACATACATG

CCTTCATCGAGTCGCTGCCTAATGTAAGTCTCTCTTCAAATAAACAGCCTGGGAGCATGTGGCAGCCTCTCTGGC
3′-GCTCAGCGACGGATTACATTC-5′:C3435TR

CTATAGTTTGATTTATAAGGGGCTGGTCTCCCAGAAGTGAAGAGAAATTAGCAACCAAATCA(204,088)-3′

Appendix D: Publications in support of this thesis

Coller, J., Barratt, D.T., Dahlen, K., Loennechen, M.H. and Somogyi, A.A. (2006) ABCB1 genetic variability and methadone dosage requirements in opioid-dependent individuals. *Clinical Pharmacology and Therapeutics, v.80 (6), pp. 682–690, December 2006*